



UNIVERSITÀ DEGLI STUDI DI SALERNO

Dipartimento di Ingegneria Civile

Dottorato di Ricerca

in

Ingegneria delle Strutture e del Recupero Edilizio e Urbano

XIII Ciclo N.S. (2012-2014)

**A CONCEPTUAL MODEL TO DESIGN
RECYCLED AGGREGATE CONCRETE
FOR STRUCTURAL APPLICATIONS**

Marco Pepe

Il Tutor

Prof. Dr. Enzo Martinelli

I Co-Tutor

*Prof. Dr. Eduardus A.B. Koenders
(TU Darmstadt - Germany)*

*Prof. Dr. Romildo Dias Toledo Filho
(UFRJ - Brazil)*

Il Coordinatore

Prof. Ciro Faella

*“Not everything that counts can be counted,
and not everything that can be counted counts”*

Albert Einstein

Acknowledgments

At the end of this PhD project, I would like to express my gratitude to all the people that have contributed to reach this achievement, so important for my professional and personal life.

First of all, I would like to express my deepest appreciation to my supervisors, Professors Enzo Martinelli, Eddy Koenders and Romildo Dias Toledo Filho for their guidance and the fruitful discussions we had during the period of the research. They represents my parents in research. Really thanks!!!

I am also grateful to Prof. Faella, Ph.D. Coordinator and head of our research group at University of Salerno. Moreover, I would like to extend my thanks to Antonio, Carmine and Gaetano for the nice atmosphere we created in our group and for the support I received from them.

Then, my acknowledgments go to all the research group of the NUMATS in Rio de Janeiro where I spent almost one year. They all contributed to make me feel at home. Especially, I would like to express my gratitude to my Brazilian “brothers” Visar, Saulo and Thiago for the nice moments we shared together during my stay in Rio de Janeiro.

I also acknowledge Calcestruzzi Irpini S.p.A., Colacem S.p.a., General Admixutes S.p.a. and Edil Cava S.r.l. for having supplied the materials for the experimental campaigns and Engineering S.r.l. and La.Sp.Ed. Tirreno s.r.l. for the support of some experimental tests performed on their laboratories.

Special thanks to my parents for having taught me to not give up to easy compromises and to privilege always the struggle that makes precious every achievement.

Thanks to Daniela, Alessia, my grandmother Lucia and my dear friend Francesco for their unconditional support that helps me to trust always in myself.

Finally to Marilena, the first of my heart, I would like to express my gratitude to her for the love, the patience, the support and the understanding that she always gave to me and that make special every moment together with her.

Table of Contents

Aims and scope of research	1
Organisation of the thesis	5
1. Introduction	7
1.1 Waste generation and environmental concerns	7
1.1.1 Construction and demolition waste	10
1.1.2 Concrete and construction industry: aggregates sources	12
1.1.3 Concrete and construction industry: cement production	14
1.2 Regulatory environment and guidelines	17
1.2.1 The Italian code for constructions	17
1.2.2 RILEM Recommendations	18
1.2.3 DAFStb Guidelines and DIN Standards	18
1.2.4 British Standards	19
1.2.5 Buildings Department of the Hong Kong	19
1.2.6 American Concrete Institute	20
1.2.7 Cement Concrete & Aggregates Australia	22
1.2.8 Main conclusions drawn from existing regulations and standards	23
2. Recycled Concrete Aggregates	27
2.1 State of the art for Recycled Concrete Aggregates (RCAs)	27
2.1.1 Processing procedures	27
2.1.2 Attached Mortar evaluation	30
2.1.3 Engineering properties of RCAs	31
2.2 Physical and mechanical characterisation of RCAs	32
2.2.1 Attached Mortar content	36
2.2.2 Porosity, water absorption and particle density	37
2.2.3 Mechanical strength	40
2.2.4 Bond strength between aggregates and cement paste	47
2.3 Alternative processing procedures for RCAs	50
3. Recycled Aggregate Concretes	57
3.1 Basic aspects about concrete mix design and technology	57
3.1.1 The role of aggregates in concrete mixture	58
3.1.2 Portland cement	59
3.1.3 Influence of moisture content and w/c ratio	60
3.1.4 Curing conditions	63

3.2 State of the art for Recycled Aggregate Concrete (RACs)	64
3.2.1 Workability	65
3.2.2 Compressive strength	67
3.2.3 Static modulus of elasticity	72
3.2.4 Tensile and flexural strength	73
3.2.5 Drying shrinkage	74
3.3 Experimental activities	75
3.3.1 Influence of alternative processing procedures on RCAs	76
3.3.2 Influence of the initial moisture condition of RCAs	81
3.3.3 Influence of the aggregate replacement and water to cement ratios	88
4. Insight into the influence of cement replacement in Recycled Aggregate Concrete	95
4.1 Fly Ash in Recycled Aggregate Concrete	95
4.1.1 Workability	96
4.1.2 Compressive strength	96
4.1.3 Alkali-silica reaction	99
4.1.4 Carbonation depth	100
4.1.5 Chloride ion penetration resistance	101
4.2 Experimental activities	104
4.2.1 Mix composition and experimental programme	104
4.2.2 Analysis of the results	111
4.3 Empirical relationships for compressive strength of RAC+fly ash	121
4.4 Conclusions	125
5. Modelling the hydration process and predicting the cement paste properties	127
5.1 Theoretical formulation	129
5.1.1 Adiabatic heat development of concrete	129
5.1.2 Heat flow and degree of hydration during setting and hardening	131
5.1.3 Development of the relevant mechanical properties	136
5.1.4 The “Maturity” concept	136
5.2 Numerical implementation	137
5.2.1 Finite difference solution of PDEs	138
5.2.2 Details about the proposed numerical “recipe”	141
5.3 Validation of the proposed heat-flow and hydration model	144
5.3.1 Outline of experimental test setups	144
5.3.2 Temperature experiments and numerical predictions	145
5.4 Hydration process and material properties	150

5.4.1 Correlation between degree of hydration and compressive strength	150
5.4.2 Correlation between maturity and compressive strength	152
5.5 Conclusions	152
6. Predicting the mechanical properties of RAC	155
6.1 Compressible packing model	156
6.1.1 Theoretical formulation	156
6.2 Application	163
6.3 Lattice Model	167
6.3.1 Theoretical formulation	167
6.3.2 Application	170
6.4 A proposed conceptual model for RACs	176
6.4.1 Theoretical approach	176
6.4.2 Proposed formulations for predicting the strength of RAC	178
6.4.3 Model validation	185
7. Mix design formulation for RAC	187
7.1 Conceptual Model flow chart	188
7.2 Conclusions	197
7.3 Future developments	197
References	199

Aims and scope of research

The construction sector is characterised by a significant demand for both energy and raw materials (Crow, 2008; Schneider et al., 2011) and, for this reason, the European Union has recently adopted a policy intended at promoting the use of recycled aggregates for concrete production, up to 70% for 2020 (EC, 2008), with the twofold aim of reducing the demand for natural sources and minimising the environmental impact of the concrete industry.

Therefore, several studies have been recently proposed for understanding the behaviour of concrete made with different types of recycled aggregates (Meyer, 2009), and, among them, a clear focus was placed on using aggregates derived from the demolition of concrete members and structures, generally referred to as Recycled Concrete Aggregates (RCAs) (McNeil & Kang, 2013). As a matter of fact, huge volumes of waste concrete can be derived from global construction demolition and rehabilitation projects, concrete testing laboratories, and from constructions damaged or collapsed as a results of human-induced actions or natural disasters, such as earthquakes (EDCW, 2014). Recycling these waste materials is an effective way for enhancing sustainability of both the concrete industry and the construction sector (Lima et al., 2013; Toledo Filho et al., 2013).

In fact, hardened concrete can be crushed and reused as coarse aggregate in the production of new concretes, leading to particular kinds of “green concretes” (fib, 2013) in which ordinary coarse aggregates are partially or totally replaced by RCAs, while at the same time reducing the so-called Construction and Demolition (C&D) waste (Behera et al., 2014). However, the definition of accurate relationships capable of predicting the relevant properties of concrete made out with these constituents, often referred to as Recycled Aggregates Concretes (RACs), is still considered an open issue. The lack of knowledge due to the fact that RCAs is characterised by a different composition with respect to the ordinary ones and, consequently, they have different engineering properties which can significantly affect the resulting mechanical performance of RACs (Florea & Brouwers, 2013), is the main reason for further investigating the physical and mechanical behaviour of RACs and its correlation with the relevant physical properties of RCAs.

As a matter of fact, RCAs can be schematised as a two phase composite of “original” Natural coarse Aggregates (NAs) and the adhering mortar (made of sand, hydration products and fractions of un-hydrated cement), the latter being generally referred to as Attached Mortar, AM (Belin et al., 2014; Abbas et al., 2009).

Several studies highlight that RCAs are significantly more porous than the corresponding NAs characterised by the same size grading (McNeil & Kang, 2013; Behera et al., 2014; Silva et al., 2014). This higher porosity of RCAs can be clearly attributed to the presence of AM that is characterised by a significantly higher percentage of capillary pores, micro cracks and, consequently, a more open structure (Guedes et al., 2013) which is accessible to water. The porosity of RCAs mainly depends on two variables: the composition of the original concrete mixture and the processing procedure performed for transforming concrete debris into aggregates for concrete (Pepe et al., 2014). Moreover, the presence of a constituent characterised by a higher porosity has a two-fold influence on the actual evolution of the concrete strength. On the one hand, the higher porosity of RCAs results in a higher water absorption capacity of aggregates which can affect the actual amount of free water in concrete mixes, hence, their effective water/cement ratio (Poon et al., 2004a; Choong et al., 2013; Mefteh et al., 2013) and, on the other hand, a porous constituent can represent the weaker “link” within the cementitious composite matrix (de Juan & Gutiérrez, 2009; González-Fonteboa et al., 2011; Liu et al., 2011; Folino & Xargay, 2014). Possible changes induced by using RCAs can alter the morphological nature and the physical and chemical bindings that lead to the formation of a robust concrete microstructure (Poon et al., 2004b). Therefore, controlling and predicting the resulting compressive strength of RACs are the main issues that should be addressed to make them a feasible solution for structural applications.

Besides this, a new vision is also required on defining the actual water content in RAC mixtures and the impact of the absorbed water absorbed by RCAs. Although a big deal of experimental results have been published in the last decades on investigating the mechanical behaviour of RACs, these results often propose merely empirical analyses for calibrating possible correlations between the concrete constituents and the resulting mechanical properties (Gomez-Soberon, 2002; Padmini et al., 2009; Duan & Poon, 2014). However, a recent article about a mix-design procedure intended at controlling the structural and durability-related properties of RACs being a possible exception to this prevailing trend (Fathifazl et al., 2009) is certainly worth of mention as a fundamental contribution to the subject under consideration.

Therefore, as a further step that goes beyond the usual experimental and empirical investigations, the research presented in the present thesis proposes a rational mix design method for predicting the compressive strength evolution of RACs by considering both the mixture composition and the key properties of RCAs (i.e.; the amount of the attached mortar and indirectly the water absorption capacity).

The formulations proposed in this thesis are based upon the results of several investigations carried out for characterising both RCAs and RACs. Several tests were performed on different kinds of recycled aggregates, taking into account their origin, the processing procedure adopted for crushing the concrete demolition debris and their resulting size grading. The analysis of the results obtained in such tests led to proposing a comprehensive conceptual formulation that links the main engineering properties of aggregates to the porosity, particle density and attached mortar content of RCAs. Moreover, several concrete batches were produced for investigating the influence that three key parameters (viz. aggregate replacement ratio, nominal water-to-cement ratio and initial moisture condition of aggregates) have on the relevant properties for structural concrete. The behaviour of structural concrete is then analysed at a “fundamental” level, with the aim of scrutinising the physical properties and the mechanical behaviour of RACs, taking into account the actual mixtures composition. Particularly, it is based on observing the hydration process developing inside RACs during the setting and hardening phase, and how these are influenced by the presence of RCAs (Koenders et al., 2014).

The activities described in this work were carried out at the laboratories of the University of Salerno (IT), the Federal University of Rio de Janeiro (BR), as part of the “EnCoRe” Project (FP7-PEOPLE-2011-IRSES n. 295283; www.encore-fp7.unisa.it) funded by the European Union within the Seventh Framework Programme, and Delft University of Technology (NL).

Organisation of the thesis

This Thesis is organised in seven chapters whose contents are summarised in the following.

Chapter 1 introduces the main issues related to the construction and demolition waste with a particular focus on the concrete waste generated by the demolition. Moreover, it reports a general overview of the actual guidelines and regulations dealing with to the use of recycled aggregate for concrete production.

Chapter 2 reports the main engineering properties of recycled concrete aggregates and then Chapter 3 analyses the influence of using these aggregates in the resulting mechanical performance of structural concrete. Both chapters are organised by reviewing the corresponding State-of-the-Art and the experimental activities performed during this PhD project.

Chapter 4 reports the results of a wide experimental campaign carried out on concretes made out with both recycled concrete aggregates (RCA) and fly-ash (FA) by investigating the influence of water-binder ratio such us aggregate and cement replacement on the resulting concrete performance.

Chapters 5 and 6 describe the proposed modelling approach for describing the chemical, physical and mechanical phenomena occurring when RCAs are employed for producing structural concrete. Particularly, a fundamental approach is proposed in Chapter 5 by modelling the hydration processes of cement paste through temperature measurements, while Chapter 6 describes the analytical and numerical formulations used for analysing the time evolution of the relevant mechanical properties of concrete.

The proposed experimental results and the theoretical models lead to a rational approach for controlling and predicting the compressive strength for RACs by taking into account both the processing procedure performed on RCAs, the relevant properties of constituents and the mixture composition: such formulations are summarised in Chapter 7.

Finally, the last sections of Chapter 7 report the main results achieved in the research, their impact on the current state of knowledge on structural concrete technology and the possible future developments of the present research.

1. Introduction

1.1 Waste generation and environmental concerns

In the second half of the last century, the world production of goods and services increased disproportionately, due to a strong demographic growth, expansion of urban areas and a great development of industrialization. Apart from undoubted benefits in terms of improved living standards, this phenomenon also resulted in an growing pressure on natural balances and resources of the Earth. However, the above mentioned process led to a remarkable increase in waste generation.

The origin of waste is manifold and there is no uniform and generally accepted classification across all countries. Nevertheless, the following classification is often adopted (Chalmin & Gaillochet, 2009):

- municipal waste, produced by individuals and economic activities;
- industrial waste, related to production processes;
- construction and demolition waste and waste from mining operations.

Moreover, regardless the previous classification, waste can also be defined as hazardous or non-hazardous, depending on their chemical composition and treatments for their disposal (AITEC, 2011).

Make a credible appraisal of the total waste production in the world is not an easy task, because of both the absence of reliable data in developing countries and the different waste classifications existing worldwide. However, according to recent researches (Chalmin & Gaillochet, 2009), about four billions of tons of solid industrial and municipal waste are produced worldwide every year. Slightly more than one half of such waste is collected and recycled: this is municipal waste (1,7 billion), including domestic and commercial ones, but also industrial waste, especially in manufacture industry (EEA, 2007).

Even though the recent global recession significantly affected the economy of Western countries leading to a drop in production, the significant growth of emerging countries, such as Brazil, Russia, China and India, kept the global demand for goods and services on an increasing trend. Thus, adopting a policy for a sustainable development at the global scale is more and more necessary, in order

to satisfy the socio-economic needs and safeguard the environmental resources at the same time.

In Europe, the contribution of each industrial sector to the generation of waste is well described by EEA (European Environment Agency), considering data from the first 15 Member States of the European Union. The percentages of waste production vary considerably among different sectors and waste categories, reflecting different socio-economic factors. It is interesting to note that the largest percentage (48%) corresponds to construction and demolition waste (C&D), whereas municipal waste, which probably better represents the idea of waste in the common way of thinking, is only about 12% (Figure 1.1).

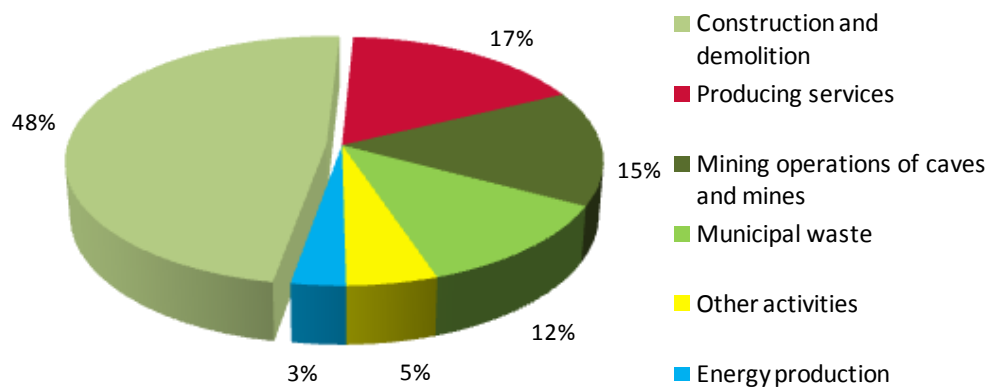


Figure 1.1: Total waste generation per sector in UE 15 (EEA, 2007).

Another remarkable consequence of industrialization and growth of production of goods and services is certainly the emission of carbon dioxide (CO₂) in the atmosphere. Since the XIX century, it was found that CO₂ emissions affect Earth's temperature through the so-called "global warming" or "greenhouse effect" (IEA, 2011). However, only in the '90s of the past century, a wide scientific debate was initiated for investigating the actual relationship between the so-called "greenhouse gas" emissions and the "global warming" effect.

Due to the growth of industrial activities in countries such as China, India, Russia and Brazil, which added to the steady industrial potential of Western Europe, Japan and United States, global warming has achieved warning levels (Figure 1.2). Therefore, in 1997, 160 countries signed the "Kyoto Protocol", an international treaty which commits industrialised countries in the period 2008-2012 to reduce greenhouse gas emissions not less than 5% compared to the emissions recorded in 1990, regarded as the base year. Particularly, the following compounds were considered as greenhouse gases: carbon dioxide (CO₂), methane (CH₄),

nitrous oxide (NO₂), hydrofluorocarbons (HFC), perfluorocarbons (PFC) and sulfur hexafluoride (SF₆).

However, United States backed off in 2001 after having ratified the protocol, while India, China and other developing countries were initially exempted from the requirements of the “Kyoto Protocol” because they were not among the major responsible of global emissions during in the last decades, when climate change become a major issue.

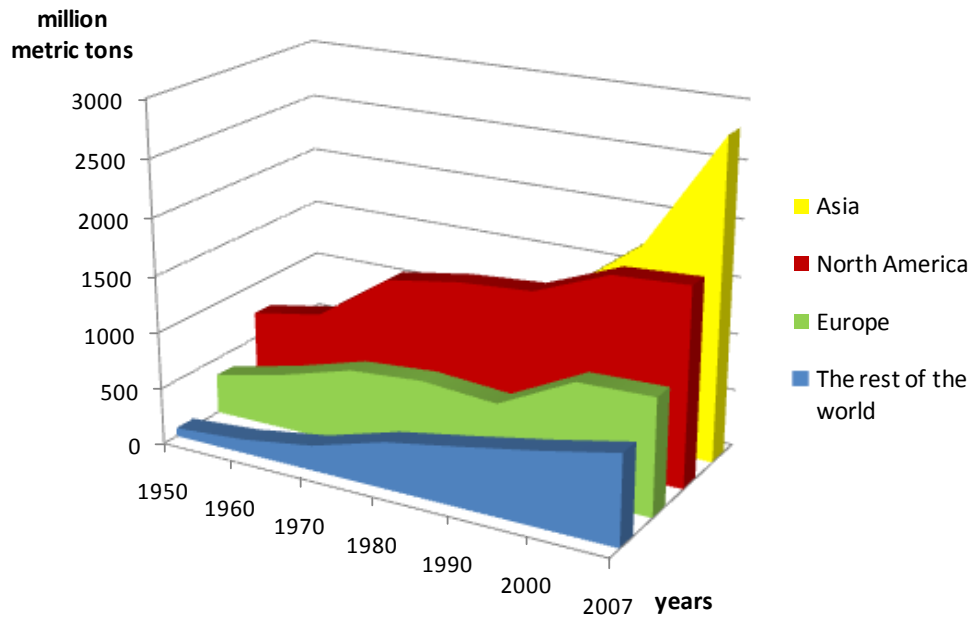


Figure 1.2: Total carbon emissions in the world since 1950 (Washington Post, 2009).

According to the most recent evaluations made by IEA (International Energy Agency), global greenhouse gas emissions achieved 30.6 billion tons in 2010. Since the time-line of the “Kyoto Protocol” was limited to 2012, the “2011 United Nations Climate Change Conference” was held in Durban (ZA) from 28 November to 11 December 2011, in order to establish a new treaty about carbon emissions limits. The conference agreed to a legally binding deal committing all countries, which will be prepared by 2015 and taking effect in 2020. The agreement, referred to as the “Durban platform”, was notable in that for the first time it included developing countries, such as China and India, as well as the United States which refused to accept the Kyoto Protocol.

Apart from water vapour, which is not related to industrialisation or human activities, carbon dioxide (CO₂) is generally considered as the major responsible

for greenhouse effect. Thus, it is useful to investigate how specific productive sectors contribute to its emission. Figure 1.3 shows that the cement industry contributes 5% of the global CO₂ emissions and, then, it is one of the most impacting sectors to be duly considered in any “green strategies”. Think for example of non-road transportation, which also produce the 5% of the total carbon dioxide emissions. Boeing, Airbus and Embraer, three world leaders in aviation industry, signed in March 2012 an agreement in order to produce bio-fuels and to halve the emissions by 2050, compared to the levels recorded in 2005 (www.boeingitaly.it, 2012). Consequently, a similar effort should be pursued to significantly reduce the environmental impact of concrete, with a particular emphasis on cement industry.

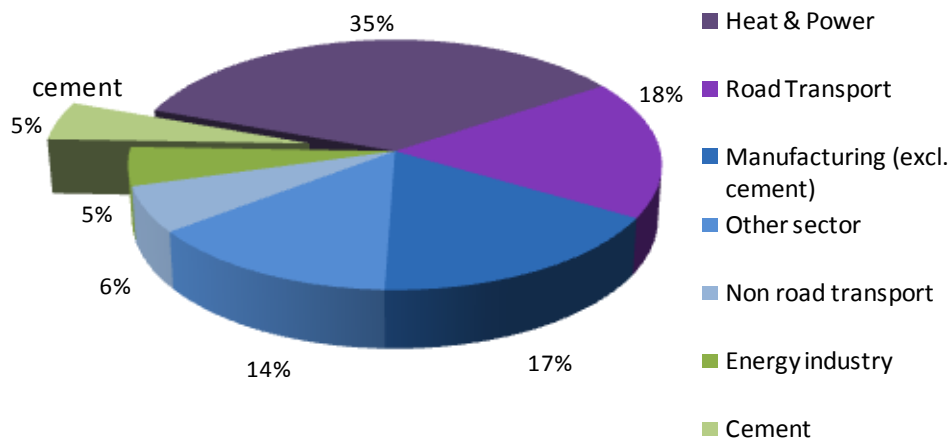


Figure 1.3: Global CO₂ production worldwide (WBCSD, 2012).

1.1.1 Construction and demolition waste

Construction and demolition waste (C&D) are defined as all waste that arises from construction, renovation and demolition activities; furthermore in some countries even materials from land levelling are included.

According to the European List of Waste (EC, 2000), C&D waste covers a very broad range of materials. Excluding non-hazardous waste, the most common categories identified are:

- concrete, bricks, tiles and ceramics;
- wood, glass and plastic;
- bituminous mixtures, coal tar and tarred products;
- metals;
- soil (including excavated soil from contaminated sites).

In Europe, about 850 million tons of these waste are generated every year, and this represents the 31% of the total waste generation (Figure 1.4). In recent years, several EU Member States have published results of analysis concerning the composition of C&D waste, and approximately one third of it consists of concrete (Böhmer et al., 2008).

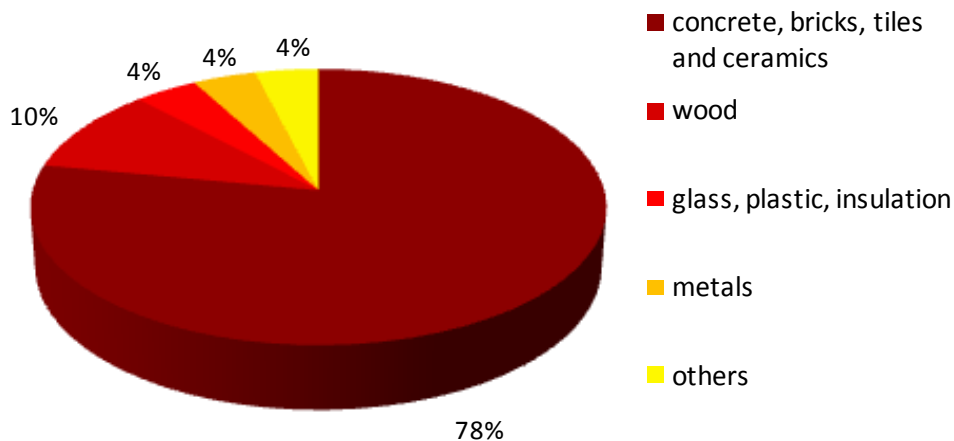


Figure 1.4: C&D waste materials (Fischer & Werge, 2009).

In order to compare C&D waste production among European countries, it is useful to refer to values per capita. Thus, considering data between 2004 and 2006, Luxembourg has the highest production per capita, with 15 tonnes, while any other country does not exceed the half of this value (Fischer & Werge, 2009). In 2004 France generated about 6 tons per capita, Finland 4 tons, while Germany showed a remarkable decrease of C&D waste production from 1995 to 2005, when less than 2 tons per capita were recorded. Finally, the large part of European countries, Italy included, generate between 1 and 2 tons.

According to Italian regulation, construction and demolition waste (C&D) are defined as “special waste”, and need to undergo “special procedures about the collection, storage, transport and final disposal” (D.lgs. n° 156/2006 Art. 185). However in Italy, as well as in many countries of the European Union, especially the Netherlands and Denmark, morphological and environmental conditions suggest to avoid the opening of new landfills, and, then, enhance the production of recycled aggregates from C&D waste.

Taking this point into account, it is interesting to integrate the previous data about C&D waste production, in order to offer an overall view. In fact, even if Italy, Denmark, Netherland and Estonia generate almost the same amount of C&D

waste per capita, Italy recycles only the 10% of its production (Legambiente, 2011), despite the remarkable results achieved by the other three mentioned countries, where the percentage of recycling is more than 90%. However also economic and industrial powers such as France and Germany seem to have understood the necessity to avoid landfilling, as they have 60% and 86%, respectively, of C&D waste recycling.

In recent years, both in order to limit the use of virgin materials in construction industry and to guarantee an environmental preservation, Europe adopted a policy to promote the reuse of recycled aggregate in concrete production. The European Directive n.98 of 19/11/2008 (EC, 2008) calls on member states to take the necessary measures to promote the reuse of products and the preparing measures for re-use activities, particularly by promoting the establishment of economic tools and criteria about tenders, quantitative targets or other measures". Moreover, art. 11 specifies that the preparing for reuse, recycling and other types of recovery of material, including construction and demolition waste, shall be at least increased to 70% (by weight) by 2020 (EDCW, 2014).

1.1.2 Concrete and construction industry: aggregates sources

According to the European Aggregates Association, aggregates are granular material used in construction, and it is possible to identify three different categories:

- natural aggregates, produced from mineral sources, such as quarries and gravel pits, and in some countries from sea-dredged material;
- secondary aggregates, produced from industrial processes;
- recycled aggregates, produced from processing material previously used in construction.

In 2008, the German Umweltbundesamt (Böhmer et al., 2008) published a very accurate report about production and utilization of aggregates in Europe. Even if in some cases data are not available, such as for Denmark which surely adopts green policy, it is possible to note how the use of recycled aggregates is still far from being competitive as compared with natural aggregates (Figure 1.5 and Figure 1.6).

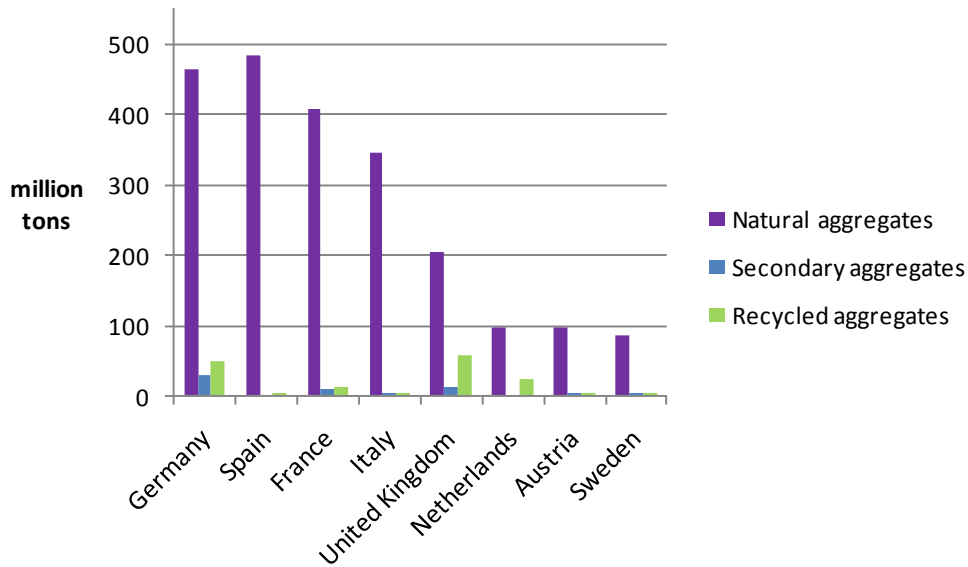


Figure 1.5: Aggregates production in Europe (Böhmer et al., 2008).

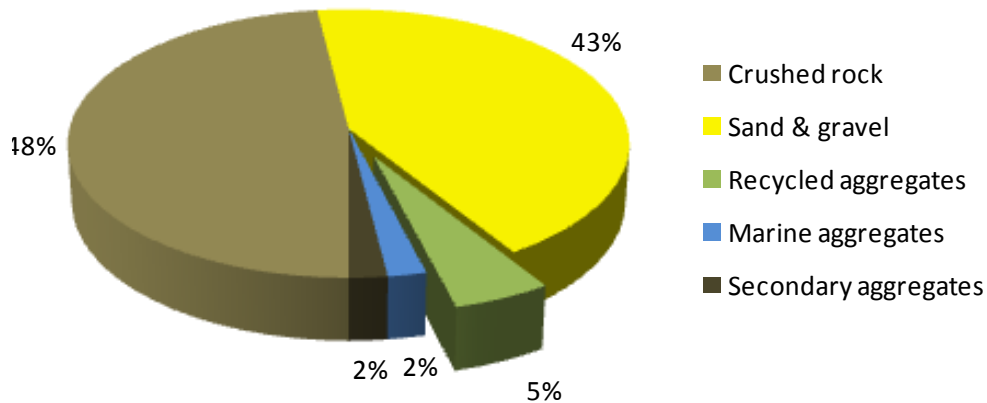


Figure 1.6: Source of aggregates in Europe (Böhmer et al., 2008).

In Italy the exploitation of natural aggregates is well described by Legambiente (2011). The active quarries are 5736, distributed throughout the peninsula, with more than 500 quarries in Sicily, Veneto and Lombardia. However it is worth to highlight that about 180 unauthorised quarries have been estimated only in Campania. Moreover, there are almost 15000 abandoned quarries, concentrated in Lombardia, Veneto, Trentino, Toscana, Marche and Campania (Figure 1.7).

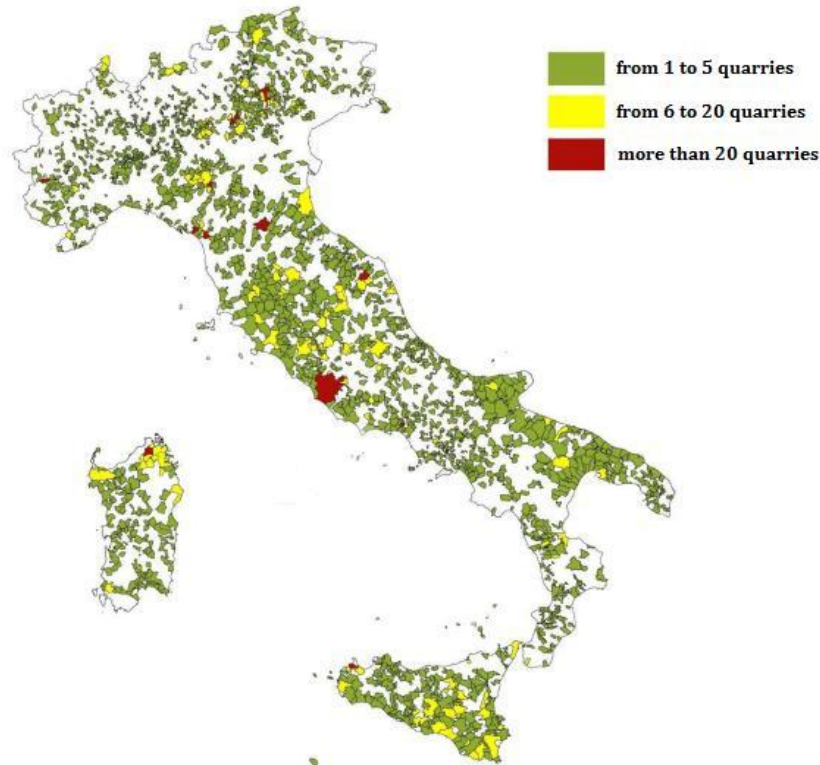


Figure 1.7: Distribution of active quarries in Italy (Legambiente, 2011).

Nevertheless, the most alarming aspect about natural aggregate management in Italy, is the regulatory framework, which is based upon a Royal Decree of 1927 (Legambiente, 2011). In fact, only some regions adopted a “Quarries Plan” in order to regulate the exploitation of natural resources, but generally all regional laws are very far from a modern management which takes into account the landscape and the environment.

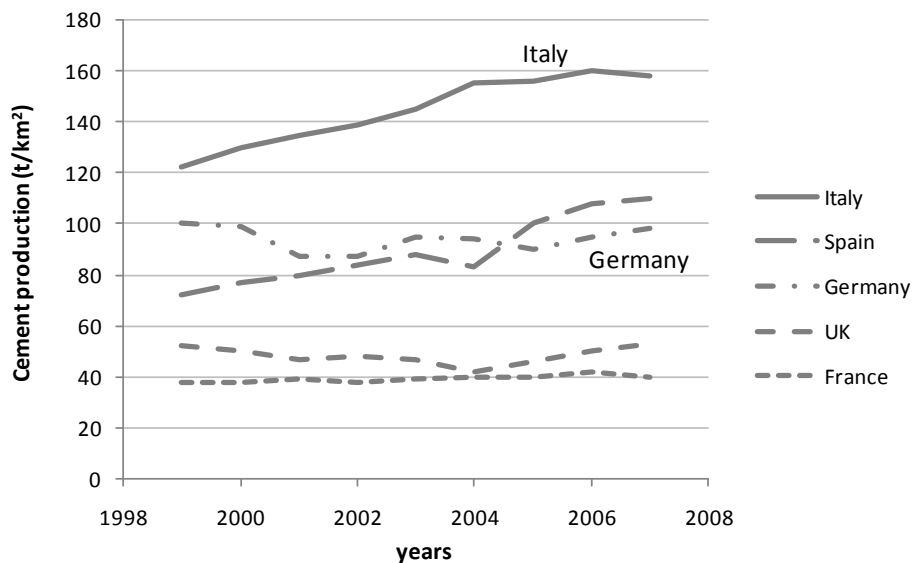
1.1.3 Concrete and construction industry: cement production

In 2010 the world production of hydraulic cement was 3,3 billion tons, with an increase of 7% on the preceding year (USGS, 2011). However, considering the infrastructure development in Asia and other emerging economies, such as Turkey and Brazil, cement production will further increase. China alone produces 1,8 billion tons of cement, which is 54% of the world total, followed by India at 7%, while the contribution of other major producers is no more than 2% for each one (Table 1.1).

Table 1.1: First ten cement producer countries in the world (USGS, 2011).

Country	Cement production [10 ⁶ metric tons]
China	1800
India	220
United States	63.5
Turkey	60
Brazil	59
Japan	56
Iran	55
Spain	50
Vietnam	50
Russia	49

In Europe, Spain is the first cement producer, with 50 million tons, followed by Italy and Germany, with 35 and 31 million tons, respectively. However, it is quite interesting to note how Italy denotes the greatest cement production per km² among European countries (Figure 1.8), and its production per capita is about 580 kg/inhabitant, that is almost three times higher than India (187 kg/inhabitant) or United States (206 kg/inhabitant).

Figure 1.8: Cement production per km² in Europe (AITEC, 2011).

As mentioned above, the cement industry produces about the 5% of global carbon dioxide emissions. Figure 1.9 shows the unit-based CO₂ emissions due to cement production by country and region. Higher numerical values characterise the

United States and the emerging Asian countries, while they are lower for countries, such as Japan, where energy efficient methods are widely adopted in the cement industry (ACF, 2008).

The production of carbon dioxide from a cement plant derives from two main stages of the cement production, namely combustion and calcination. Combustion accounts for approximately 40% and calcination for 50%, finally the remaining percentage is due to electricity and transport. The combustion-generated CO₂ emissions are related to fuel combustion, while CO₂ emissions due to calcination are formed when the raw materials (mostly limestone and clay) are heated to over 1500°C.

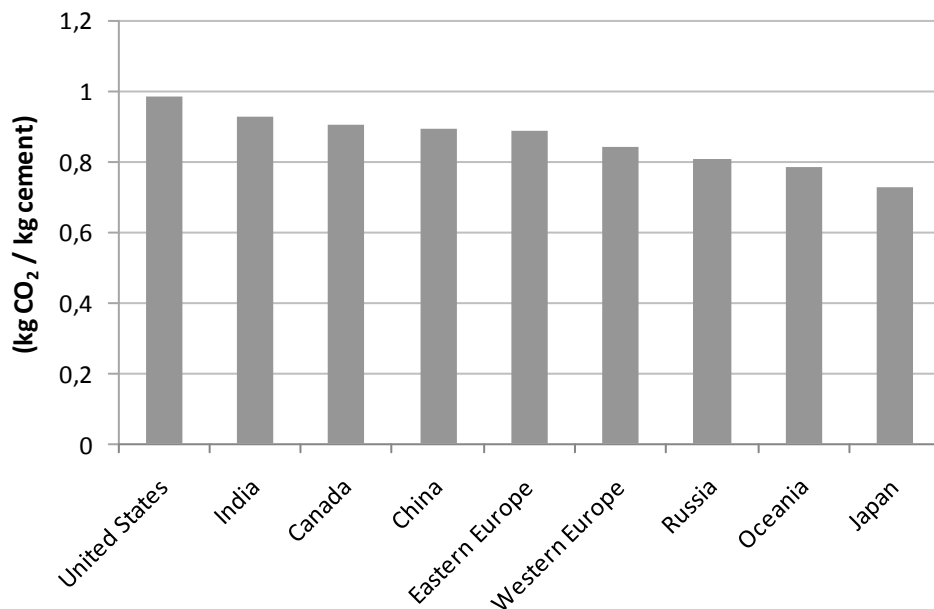


Figure 1.9: Unit-based CO₂ emission due to cement production by country and region (ACF, 2008).

According to a study realised by WWF and published in 2008, the world cement industry is able to reduce the emissions up to 90% by 2050, considering technologies available nowadays about production techniques (Müller & Harnisch, 2008). However, there is also a school of thought suggesting that it is essential to develop an innovative cement burning technology as well as the development of a new type of cement through material combinations (Sakai, 2005).

1.2 Regulatory environment and guidelines

The reuse C&D waste materials in the construction industry needs adequate technical means. Since C&D waste encompass a very broad range of materials characterised by significantly different relevant properties, it is useful to concentrate only on recycling of demolished concrete debris, which however represents approximately one third of total C&D waste generation in industrialised countries.

This section outlines existing standards, regulations and guidelines addressing the use of RCAs for the production of structural concrete. Particularly, the attention is focused on the Italian relevant code provisions, but also other regulations are considered. The most remarkable cases concern countries where waste disposal represents a crucial problem due to morphological and environmental conditions, such as Hong Kong and North European countries, or industrial counties which have promoted a new urbanisation process (e.g. Germany during the last few decades). However, also United States and Australia are mentioned as they show a growing interest about sustainable concrete waste reusing.

1.2.1 The Italian code for constructions

Italian current regulation allows the utilisation of recycled aggregates only as coarse fraction for new concrete production. The aggregates must be conform to EN 12620:2013 standards, specifying the source of material, the petrographic information and the particle size. Moreover, they must meet the requirements and limitations reported in Table 2.1.

Table 1.2: Recycled aggregates limitations (NTC, 2008).

Source of recycled material	Concrete grade	Percentage of utilization
Demolition of buildings (waste)	C8/10	up to 100 %
Demolition of concrete and reinforced concrete	\leq C30/37	\leq 30 %
	\leq C20/25	up to 60 %
From concrete > C45/55	\leq C45/55	up to 15 %
	Parent concrete	up to 5 %

A total replacement of natural aggregates, by recycled ones made of C&D waste, is allowed only for concrete to be employed in non-structural applications. In the case of structural concrete, the maximum allowed percentage of RCAs is

strongly limited for the usual compressive strength targets related to structural elements. Particularly, to achieve a compressive strength of 30 MPa (characteristic value for cylindrical specimens at 28-days of curing), corresponding to C30/37 grade, the maximum percentage of replacement of recycled coarse concrete aggregates is 30%. A higher percentage of replacement up to 60%, limits the concrete grade at C20/25.

However, Superior Council of Public Works aims to define a new ordinance, according to Ministry of Economic Development, accepting the most recent knowledge achieved about recycled concrete performance.

1.2.2 RILEM Recommendations

RILEM (*Réunion Internationale des Laboratoires et Experts des Matériaux, systèmes de construction et ouvrages*) is a technical association developing the knowledge of material properties and performance of structures, involving experts from different countries.

In 1994 RILEM (1994a) proposed some specifications for concrete with recycled coarse aggregates (> 4 mm), while the use of recycled sand was not recommended. RILEM Recommendations suggest a classification according to material composition: RCAC Type I is mainly constituted by crushed brick, RCAC Type II is made of crushed concrete, while RCAC Type III is recycled material from concrete and brick mixture containing up to 50% brick. Focusing the attention on RCAC Type II, it is allowed a total replacement of recycled coarse concrete aggregates and the maximum potential compressive grade strength is C50/60.

This value might seem too optimistic, considering the most part of results proposed by international standards, nevertheless RILEM Recommendation does not give any clarification about recycled concrete source and its original mechanical performance.

1.2.3 DAfStb Guidelines and DIN Standards

Recycled aggregates are classified into four types, depending on the material composition, in the German Standards, whereof DIN 4226-100 (2002) represents the final version. Type 1 and Type 2 derive both from concrete structures demolition, but the minimum content of concrete plus natural aggregate is 90% and 70% by mass, respectively; while other aggregate constituents may be clinker and calcium silicate bricks. Type 3 shall contain more than 80% dense brick, and it is found if pure brick masonry is demolished. Finally, Type 4 is a mixture of all mineral building materials without strict specification of the constituents.

In terms of applications and mechanical requirements, the best reference is the “Guideline of the German Committee for Reinforced Concrete (DAfStb, 1998)”. This document specifies that only aggregates > 2 mm belonging to Type 1 or Type 2, can be used for the production of structural concrete, moreover it proposes correlations between replacement percentage and mechanical performance of recycled aggregate concrete. So, except for particular cases, such as water resistance concrete or high freeze resistance concrete, it is allowed the production of concrete up to the strength class B35 (35 MPa), with a maximum percentage of recycled aggregate of 25% (in volume); an higher percentage of replacement as 35% can be employed for strength class concrete less than B25 (25 MPa).

1.2.4 British Standards

In United Kingdom, BS 8500-2 (2006) provides general requirements for coarse recycled aggregate. In accordance with the use of recycled concrete aggregate in new concrete production, it is allowed a maximum of 20% replacement of coarse aggregate and the relative compressive strength is fixed between 20 and 40 MPa. Moreover, it is specified that recycled aggregate concrete can be used for unreinforced concrete, internal concrete, and external concrete not exposed to chlorides or subject to de-icing salts. RAC also cannot be used in designated concrete for foundations or paving. Finally, it is useful to note that provisions for the use of fine recycled aggregates are not given in BS 8500-2, but it is not precluded their use.

1.2.5 Buildings Department of the Hong Kong

Buildings Department of the Hong Kong proposed in August 2003 one of the most detailed Guidelines related to the use of recycled concrete aggregates (HKBD, 2004). However, the big deal of publications released by the Hong Kong Polytechnic University showed a remarkable development of research in the use of RCA.

These Technical Guidelines are divided into two sections, considering two different percentages of replacement of recycled coarse concrete aggregate and the relative applications. Appendix A specifies that concrete with 100% of recycled coarse aggregates shall only be used for non-structural works, due to the relative grade strength of 20 MPa. A mix concrete design is also proposed, with the following specific composition:

- Ordinary Portland cement: 100 kg;
- Fine aggregates: 180 kg;

- 20 mm Coarse aggregate: 180 kg;
- 10 mm Coarse aggregate: 90 kg;

Appendix B of the same document refers to mix concrete with 20% recycled coarse aggregates. In this case the grade strength is between 25 and 35 MPa and, hence, this material is allowed for general applications, but it is not recommended for water retaining structures.

Both 100% and 20% recycled coarse aggregates analysed in these guidelines, shall be produced by crushing old concrete, and they shall meet the requirements reported in the following Table 1.3.

Table 1.3: Requirements for Recycled Coarse Concrete Aggregates (HKBD, 2004).

Mandatory requirements	Limits
Minimum dry particle density (kg/m ³)	2000
Maximum water absorption	10 %
Maximum content of wood and other material less dense than water	0.5 %
Maximum content of other foreign materials (e.g. metals, plastic, glass etc.)	1 %
Maximum fines	4 %
Maximum content of sand (< 4 mm)	5 %
Maximum content of sulphate	1 %
Flakiness index	40 %
10% fines test	100 kN

Finally, it is specified that under no circumstances it is allowed the utilisation of fine recycled aggregates from old concrete.

1.2.6 American Concrete Institute

The American Concrete Institute (ACI) highlights that using recycled aggregate in new concrete makes sense, because it reduces both waste production and natural aggregate demand. The source of recycled aggregate can be identified in concrete pavements, structures, sidewalks, curbs, and gutter that when are removed can be used in concrete production. Chapter 7 of ACI E-701 (2007) specifies that new concrete mixtures can contain both fine and coarse recycled aggregate. Although up to 100% of the coarse aggregate can be recycled material, the percentage of fine aggregate is usually limited to 10 to 20%, with the remainder being natural material. This is because of the high absorption of recycled fine aggregates. In fact, due to the cement mortar attached to the particles, the absorption of recycled aggregates is much higher than that of otherwise identical ordinary aggregates: typically 2 to 6% for coarse aggregate and higher for fine aggregate. This high absorption can make the resulting fresh concrete less workable. To offset this,

recycled aggregate should be sprinkled with water before the concrete is mixed, or extra water should be added to the mixture.

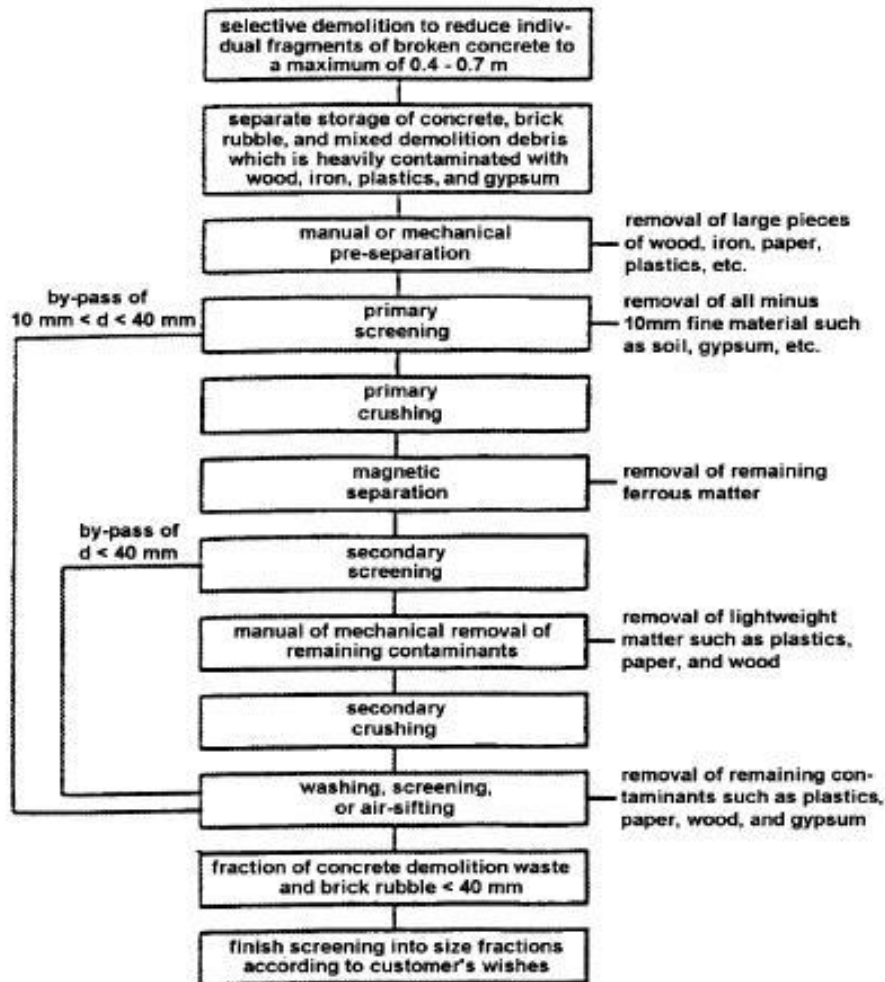


Figure 1.10: Processing procedure for building and demolition waste (ACI 555R-01).

Also ACI 555R-01 offers indications about production of new concrete from recycled one. The process to obtain recycled aggregate beginning at demolition site is well described, considering the several steps to select concrete waste and to treat it, in order to obtain an adequate material quality. In that respect, flow charts of typical plant for closed system production of recycled aggregate from concrete debris are presented (Figure 1.10). Furthermore the document refers to studies by Hansen (1986a) about properties of recycled concrete aggregate both coarse and fine. Hansen (1986a) concluded that the fine recycled aggregates are generally

coarser (Figure 1.11) and more angular than those needed to produce good quality concrete. Moreover, the results of his studies indicated that this coarseness and increased angularity were the reasons that concrete made with these materials tended to be somewhat harsh and unworkable.

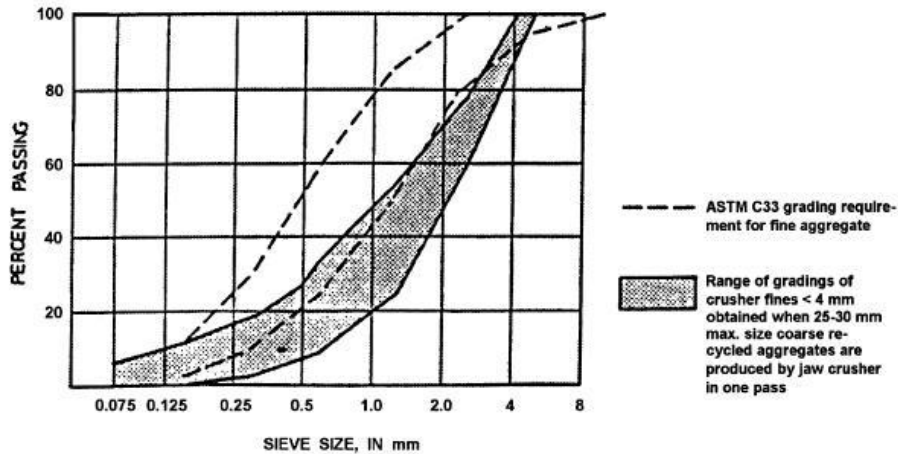


Figure 1.11: Range of gradings of crusher fines obtained when 33 mm maximum size coarse, recycled aggregates are produced by jaw crusher in one pass. (ACI 555R-01).

1.2.7 Cement Concrete & Aggregates Australia

Cement Concrete & Aggregates Australia (CCAA) is the main national body in Australia representing the interests of six billion dollar a year heavy construction materials industry. Recently, this organisation published an interesting document, a sort of Guidelines, fixing the current knowledge about the utilization of recycled aggregate in new concrete production (CCAA, 2008).

The most important references were Commonwealth Scientific and Industrial Research Organisation (CSIRO, 2002), and Concrete Institute of Australia Standards. Five types of recycled aggregates are identified and classified: Recycled Concrete Aggregate (RCA), Recycled Concrete and Masonry (RCM), Reclaimed Aggregate (RA), Reclaimed Asphalt Pavement (RAP) and Reclaimed Asphalt Aggregate (RAA). In this chapter only the first one will be taken into account, considering the present work's purpose and also because, in Australia, RCA is the most common construction and demolition waste used in concrete production.

Recycled Concrete Aggregate (RCA) is defined as crushed and clean waste concrete of at least 95% by weight of concrete with typical total contamination lower than 1% of the bulk mass. Other materials that may be present in RCA are gravel, crushed stone, hydraulic-cement concrete or a combination thereof deemed

suitable for premix concrete production. As CSIRO reported, Class 1A RCA, which is a good quality RCA with no greater than 0.5% brick content, had the potential for use in a wide range of applications, subject to appropriate test or performance requirements. Applications include partial replacement for virgin material in concrete production for non-structural work, such as kerbs and gutters.

It is emphasised that current field experience with the use of recycled concrete aggregates for structural applications is scarce, but on the other hand, the CSIRO (2002) “Guide to the use of recycled concrete and masonry materials”, clarifies the matter. In fact, it is possible to distinguish two different grades of recycled concrete aggregate, both belonging to Class 1A RCA:

- Grade 1 recycled aggregate concrete (RAC) is defined as concrete with up to 30% substitution level of Class 1A RCA recycled coarse concrete aggregate; it has a maximum specified strength limit of 40 MPa;
- Grade 2 recycled aggregate concrete (RAC) is allowed up to 100% substitution level of Class 1A RCA recycled coarse concrete aggregate and the maximum specified strength limit is 25 MPa.

Thus, for structural concrete, it is possible to fix that the maximum allowed percentage of replacement of recycled coarse concrete aggregate (RcCA) is 30%, while there was not any limitation about the use of RcCA for minor concrete.

1.2.8 Main conclusions drawn from existing regulations and standards

As the above mentioned recommendations show, the use of recycled concrete aggregate is intended mostly to replace the coarse virgin fraction in new concrete production. In fact, recycled fine aggregate from concrete exhibit deleterious characteristics that might compromise performance and workability of recycled concrete, especially if an accurate concrete mix it is not designed.

The requirements that aggregate shall meet in order to be used as RCA, seem to be almost the same for the documents proposed from different countries and institutions, and they are reported in Table 1.4. Even if the aggregate is defined as recycled concrete, a certain limited content of other “alien” materials, such as metals, plastics, clay lumps and glass, is allowed. In this respect, only ACI 555 R-01, among the current regulations, offer precise indications about a selective process of demolition intended at safeguarding the quality of RCAs. Conversely, the processing procedure implemented for producing recycled aggregates is generally designed by operator companies, according to their specific practices.

A total replacement of coarse natural aggregates is allowed only for non-structural concrete, due to the decrease of compressive strength that generally occurs considering the recycled material source. In this sense, it is useful to clarify

that RILEM Recommendations do not report the origin of recycled aggregates, so the relative maximum compressive strength value is referred to a very good quality of source material.

Table 1.4: Recycled concrete aggregate requirements: synoptic overview.

Institution (Country)	Material source	Maximum content of fine	Maximum content of other foreign materials
Italian Ministry of Infrastructure (NTC, 2008)	building demolition (for non structural concrete) and concrete demolition (for structural concrete)	-	-
RILEM (1994a)	-	5 %	1 %
DAfStB (1998)	demolished concrete structures	-	≤ 0,2 % (Type 1) ≤ 0,5 % (Type 2)
British Standard Institution (BS 8500-2, 2006)	crushing hard concrete	5 %	1 %
Building Department Hong Kong Government (HKBD, 2004)	crushing old concrete	4 %	1 %
American Concrete Institute (ACI E-701, 2007)	removed pavements, structures, sidewalks, curbs, and gutter	-	2 kg/m ³
Cement Concrete & Aggregates Australia (CCAA, 2008)	demolition waste of at least 95% concrete	-	-

Note: foreign materials are metals, plastics, clay lumps and glass.

Conversely, the replacement by recycled coarse concrete aggregate is strongly limited for structural applications, and the majority of international technical standards fix its value between 20% and 30%. Table 1.5 reports the main characteristics and limitations of RAC, as established by both current regulations and guidelines.

Table 1.5: Main characteristics of recycled concrete: synoptic overview.

Institution (Country)	Concrete application	Aggregate size	Maximum replacement percentage	Allowable compressive strength (28 days)
Italian Ministry of Infrastructure (NTC, 2008)	non-structural	coarse	100 %	10 MPa
	structural	coarse	30 %	37 MPa
			60 %	25 MPa
RILEM (1994a)	not specified	coarse	100 %	50 MPa
DAfStB (1998)	structural	coarse	35 %	25 MPa
			25 %	35 MPa
British Standard Institution (BS 8500-2, 2006)	not specified	coarse	20 %	20-40 MPa
Building Department Hong Kong Government (HKBD, 2004)	non-structural	coarse	100 %	20 MPa
	structural	coarse	20 %	25-30 MPa
American Concrete Institute (ACI E-701, 2007)	not specified	coarse fine	100 %	Not specified
			20 %	
Cement Concrete & Aggregates Australia (CCAA, 2008)	Grade 2 concrete	coarse	100 %	25 MPa
	Grade 1 concrete	coarse	30 %	40 MPa

2. Recycled Concrete Aggregates

This chapter describes the main features of recycled concrete aggregates (RCAs). An overview of the previous works available in literature is firstly presented. Then, the experimental activities performed on RCAs for the present research are described and discussed. The first part of the experimental activity report is aimed at evaluating the key physical and mechanical properties for RCA, such as water absorption, particle density and compressive strength. Moreover, in the last section an innovative alternative processing procedure for RCAs is proposed. The analysis of the experimental results available for RCA particles led to proposing some analytical formulations intended at correlating the main engineering properties of RCAs.

2.1 State of the art for Recycled Concrete Aggregates (RCAs)

The following sections present an overview of the processing procedures and the current state-of-the-art for recycled concrete aggregates (RCAs).

2.1.1 Processing procedures

This section reports the main alternative processes for producing recycled concrete aggregates from demolition waste. They can be mainly defined as follows:

- Demolition;
- Material separation;
- Material homogenisation;
- Size reduction;
- Sieving;
- Cleaning process.

Demolition

Demolition is obviously the starting stage of concrete recycling procedures. Several technical solutions are possibly available for demolishing existing concrete members and they can be adopted depending on various factors, such as the

building site and material and the demolition purpose. A fundamental classification can be adopted (HKBD, 2004; BS 6187:2011):

- general demolition;
- selective demolition.

In fact, general demolition is extended to the whole building, as all its components are dismantled and brought down to debris; as a result of this process, the generated waste is heterogeneously made out of several materials. Conversely, the selective demolition allows to better separate the materials for possible reuse and recycling.

From the practical point of view the demolition, either general or selective in nature, can be performed by adopting and/or combining several methods (HKBD, 2004):

- Top down method, manual or mechanical (Figure 2.1a);
- High reach arm (Figure 2.1b) or wrecking ball (Figure 2.1c);
- Implosion: using this method the building collapses on itself by a detonation.

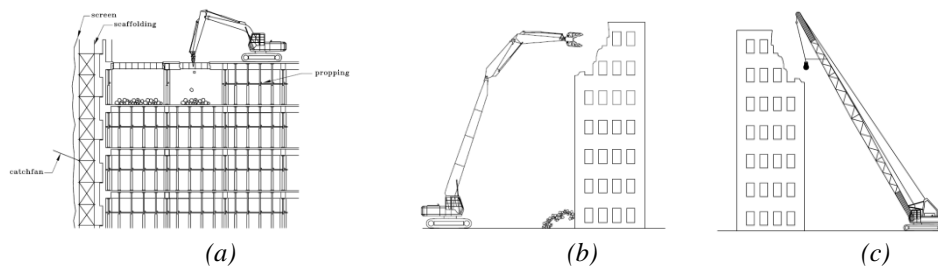


Figure 2.1: Alternative demolition methods (HKBD, 2004).

Material separation

This process is intended at separating the heterogeneous rubbles produced as a result of the demolition process, with the aim to select the materials which can be possibly recycled and/or reused.

As a matter of fact, material separation processes strictly depend on the type of demolition actually carried out. Particularly, if a general demolition process is adopted there is no initial separation of materials and consequently the separation stage is required for recycling the produced waste. In this case, the material separation can be performed based on the following criteria:

- visual inspection;
- division by colours;
- use specific machines for separate the various waste streams (i.e. wood, metal and plastic particles, bricks and concrete debris).

If the colour separation method is adopted, the red fraction can be usually denoted as the non-structural part made of clay brick and other ceramic-based (i.e. tiles) materials, while the gray fraction consists of particles mainly made of structural concrete (and, in a minor portion, mortar) debris (Pepe et al., 2014).

Conversely, if selective demolition is adopted, the different materials are demolished separately and consequently, wood, metal, plastic, non structural elements (i.e., ceramic based materials) and structural elements (i.e., cement based materials) are originally separated.

Material homogenisation

The homogenisation process is intended at reducing the heterogeneity of the selected waste in terms of both geometric (i.e. size distribution) and physical/mechanical characteristics. In principle, material homogenisation can be carried out by means of alternative methods whose choice depends on the waste fraction status (namely, bulk materials, solid rubbles or integer frame members).

For bulk materials (such as the concrete debris which are specifically addressed in this thesis), the material homogenisation stage can be implemented based on the so-called “cells process” method (homogenising process per unit cell). According to this method, various samples of materials are distributed on a plastic sheet in various different layers. Thus, the concrete particles are homogeneously distributed (in terms of geometric and physical characteristics) over the length of the sheet and can be subdivided in several sections throughout the length, called “cells” (Luz & Almeida, 2012).

Size reduction

This process is the key stage for turning demolition waste into concrete aggregates. It can be performed by using a crusher which transforms concrete debris in two fraction (EN 12620:2013):

- fine aggregates (nominal diameter less than 4.75 mm);
- coarse aggregates (nominal diameter bigger than 4.75 mm).

Relevant types of crushing equipment are jaw crushers, roll crushers, disc or gyrosphere crushers, gyratory crushers, cone crushers, rod mills, and impact-type crushers such as horizontal impactors (e.g., hammer mill) or vertical impactors (Alexander & Mindess, 2010).

Sieving

The sieving process is intended at subdividing the produced aggregates into size classes and removing the remaining powders, both produced at the particle size reduction stage (EN 12620:2013).

2.1.2 Attached Mortar evaluation

Concrete waste, resulting in RCAs, mainly contain two phases: natural aggregates (NA) and old attached mortar (AM).

The AM content is responsible for the changes of the key engineering properties for RCAs, mainly, water absorption and particle density (Butler, 2012). These peculiarity are responsible for possible influence on the mechanical performance of concrete made out with RACs. The amount of AM contents presents on RCAs depends on several factor such us processing procedures, original concrete mixture and particle size. Several authors demonstrated that when the steps of crushing processes increase, the total amount of AM is reduced (de Juan & Gutiérrez, 2009; Nagataki et al., 2004) and Etxeberria et al. (2007) declared that if an impact crusher is employed for RCAs production, a higher percentage of aggregates without AM could be achieved. The same authors, reported that the AM present in RCAs is lower in strength than the mortar produced in new concrete incorporating RCAs. As a result, they concluded that the weakest point in concrete produced with coarse RCA is governed by the strength of the RCA and their attached mortar.

The AM can represent between 25 and 60% (by volume) of the RCA. It is worth highlighting that the finer the aggregate, the higher the attached mortar content (Hansen & Narud, 1983; Tu et al., 2006; de Juan & Gutiérrez, 2009). The main problem is that it is not easy to determine the total amount of the Attached Mortar, neither a standard method has been defined for this measurement. Despite this, several different methods have been proposed in order to determine the percentage amount of attached mortar in RCAs.

Hansen and Narud (1983) prepared concrete cubes incorporating RCAs by using red-coloured cement. After being cut into slices and polished, the new red-coloured mortar and the attached old mortar on the RCA could be clearly distinguished.

Another common method used for determining the AM content is the treatment with a solution of hydrochloric acid (Gokce et al., 2004; Nagataki et al., 2004) or nitric acid (Movassaghi, 2006). This method focuses on the acid-dissolution of the cement paste as a way of separating the original aggregate from the old attached mortar and has produced acceptable results. However, as noted by de Juan & Gutiérrez (2009), this method cannot be used on RCAs containing original limestone as the acid also attacks the aggregate.

A combination of freeze-thaw and chemical breakdown has been another method used to determine the attached mortar content. Proposed by Abbas et al. (2008), the freeze-thaw treatment method combines ASTM standard C88-13 and

the MTO standard LS 614 (2001) to both mechanically and chemically breakdown the bond between the original aggregate and the attached mortar. The results of this test were validated by image analysis.

One of the most recent methods used involves subjecting the RCAs to a thermal treatment to separate the attached mortar (de Juan & Gutiérrez, 2009). Working on the principle that cement mortar begins to convert to quicklime at a temperature of 400°C, a muffle furnace is used to heat the aggregates and breakdown the attached mortar. To induce further thermal stresses, the aggregates are rapidly cooled in water. Table 2.1 presents and summarises the findings from previous researchers on the attached mortar content of coarse RCA.

Table 2.1: Summary from previous researchers on AM content for RCA (Butler, 2012).

Researcher	Method	AM content
Nagataki et al. (2004)	Hydrochloric acid dissolution	30.2 to 55.0%
Gokce et al. (2004)	Hydrochloric acid dissolution	32.4 to 55.7%
Fathifazl (2008)	Freeze-thaw + sulphate attack	23 to 41%
Movassaghi (2006)	Nitric acid dissolution	37.6 to 62.6%
Liu et al. (2011)	Image analysis	42.2 to 46.5%
de Juan and Gutiérrez (2009)	Thermal treatment	40 to 55%
Hansen & Narud (1983)	Linear traverse method	41 to 43%

2.1.3 Engineering properties of RCAs

The presence of attached mortar is greatly responsible for the higher water absorption capacity of RCAs compared with natural ones (McNeal & Kang, 2013; Behera et al., 2014). In fact, different authors report that the water absorption capacity of RCA is 2-3 times higher than natural aggregate and it may range up to 12% for coarse and fine RCA (Gómez-Soberón, 2002; Katz, 2003; Poon et al., 2004b). Poon et al. (2004b) in their study mentioned that it may vary up to 15%. Obviously, the water absorption capacity of RCA is higher for smaller particle size fraction, since the particles are characterised by a greater specific surface area (Hansen & Narud, 1983). Water absorption capacity of RCA varies depending on the amount of cement paste attached to the surface of the aggregate particles (Pepe et al., 2014). As a consequence, the higher water absorption capacity of RCA results in higher water absorption of RAC.

Another fundamental parameter characterising RCAs is represented by the particle density. As a matter of fact, the density of the attached mortar is quite less and accounts for the low specific gravity of RCA (Hansen, 1992; Nassar & Soroushian, 2012; Yang et al., 2008; Evangelista & de Brito, 2007; Sagoe-Crentsil

et al., 2001). Limbachiya et al. (2000), from the experimental investigation concluded that the relative density of RCA or surface saturated density (SSD) is approximately 7-9 % lower than natural aggregate. Moreover, the presence of higher porosity for RCA also determines its lower density (Khalaf & DeVenny, 2004).

RCA is generally poorly graded due to its poor particle size distribution (McNeal & Kang, 2013) It may be too coarse or too fine as a result of the processing and crushing through various types of crushers. The quantity of finer fractions in RCA is higher than in ordinary aggregates. It has an old interfacial transition zone (ITZ) due to the presence of the old attached mortar or cement paste surrounding it. This is weak in nature because of the presence of minute pores in the clinging mortar, continuous cracks and fissures developed inside the aggregate in consequence to the crushing process (Pepe et al., 2014).

RCAs are also characterised by lower mechanical properties, such as crushing strength, impact resistance and abrasion resistance, than natural aggregate (Limbachiya et al., 2000; Sagoe-Crentsil, 2001; López-Gayarre et al., 2009). Moreover, they can be contaminated with organic impurity such as textiles, fabrics, polymeric materials (Khalaf & DeVenny, 2004) and inorganic impurities due to the internal chemical reaction such as alkali aggregate reaction, high alumina cement, silt, clay, sulphate, chloride and increased quantity of dust particles (Ryu, 2003; Tam et al., 2005).

Although the potential for the use of RA has now been recognised, some factors still hinder the large use of RCAs in concrete as they affect the performance of the resulting materials in terms of workability, strength and durability. Thus, some salient properties of RA such as particle size distribution, shape and size of aggregate, porosity, absorption, toughness, hardness, strength and the impurity level, are necessarily to be assessed before its use in concrete. Therefore, the aforementioned inferior qualities and the weaknesses affecting RCAs hinder their use as constituents for concrete production and the lack of proper specification also discourages the recycling practice.

2.2 Physical and mechanical characterisation of RCAs

This section reports the main experimental activities performed on both natural and recycled concrete aggregates employed in this study with the aim of unveiling their key parameters that govern the physical properties and their behaviour inside concrete.

First of all, RCAs under investigation were received from different sources, such as demolished concrete structures and from some crushed concrete samples already tested in laboratory. As already reported in literature, the recycled aggregates differ from the natural ones both in term of morphology and composition. As a matter of fact, Figure 2.2 shows the results of an advanced 3D CT-scanning technique performed on natural (Figure 2.2a) and recycled aggregates (Figure 2.2b) used for characterising the internal morphology of the aggregates.

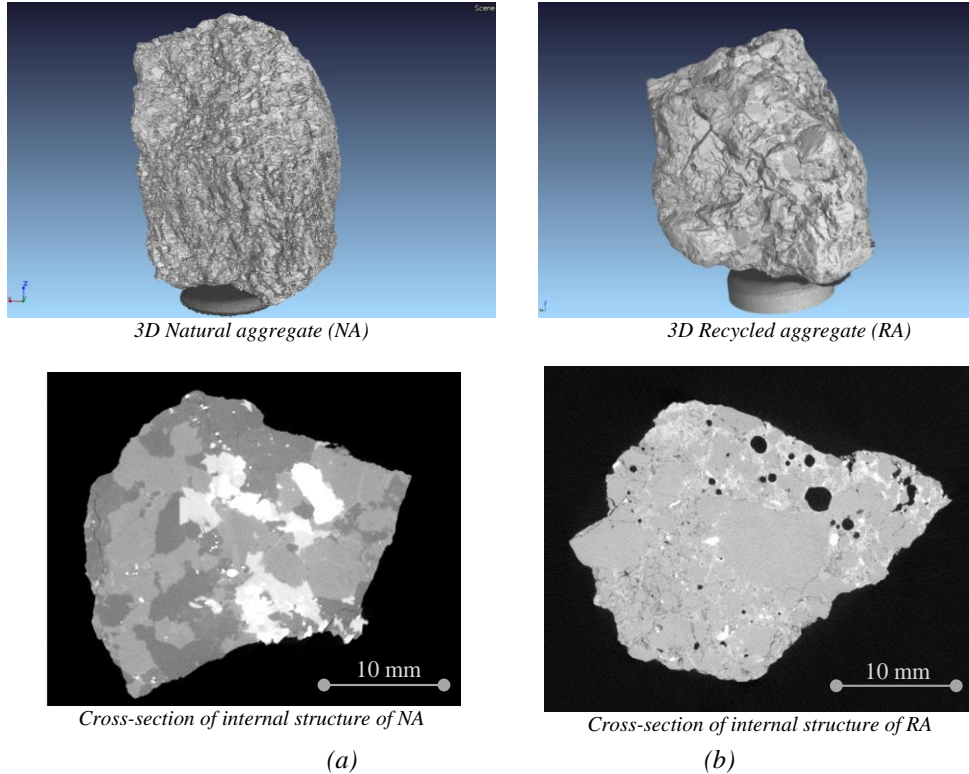


Figure 2.2: 3D scanner analysis of aggregates: (a) Natural, (b) Recycled.

The 3D scanner images clearly show the difference in surface texture as well as the internal morphology. Moreover, colour differences in the 2D cross-section show the internal density variations, i.e. ranging between the darker spots, representing high density and lighter spots of low density structures. The comparison between Figure 2.2a and Figure 2.2b emphasises the differences in internal structure of the recycled aggregates and the natural ones. In fact, recycled aggregates show a significantly higher percentage of porous spots and micro-cracks, caused by the porosity of the old mortar paste attached to the old natural aggregates. Moreover, besides this original feature of the original paste, the production and crushing process of the recycled aggregates (coming from

demolition waste) may also contribute to an additional disintegration and internal fracturing. For these reasons, recycled concrete aggregates may have significantly different properties compared with natural ones, depending on the amount of attached mortar still residing inside the recycled aggregates.

As already mentioned the research described herein comes out from a collaboration between UniSA (Italy) and UFRJ (Brazil). For this reason, the different aggregate sources employed in this study, have different origin, both from Italy and Brazil. The first column of Table 2.2 reports the original source of both natural and recycled aggregates employed in the research.

Table 2.2: Natural and Recycled aggregates.

Origin	Autogenous cleaning	Class	Label	Particle density [kg/m ³]	Water Absorption at 24h [%]
Natural from Italy	No	Sand	Sand_IT	2690	1.20
		C1	NA_{C1}_IT	2690	0.50
		C2	NA_{C2}_IT	2690	0.40
		C3	NA_{C3}_IT	2690	0.30
Natural from Brazil	No	Sand	Sand_BR	2668	1.40
		C1	NA_{C1}_BR	2547	1.28
		C2	NA_{C2}_BR	2634	3.39
Demolition waste from Brazil	No	C1	RCA_{1,C1}	1946	11.94
		C2	RCA_{1,C2}	2268	4.94
Demolition waste from Brazil	Yes	C1	RCA_{2,C1}	2261	5.56
		C2	RCA_{2,C2}	2328	4.09
Demolition waste from Italy	No	C1	RCA_{3,C1}	2127	8.70
		C2	RCA_{3,C2}	2290	6.60
Concrete samples from Italy	No	C2	RCA_{4,C2}	2008	8.29
Concrete samples from Brazil	No	C1	RCA_{5,C1}	2102	8.88
		C2	RCA_{5,C2}	2372	4.76
Demolition waste from Italy	No	Sand	RCA_{6,Sand}	2231	12.2
		C1	RCA_{6,C1}	2231	6.0
		C2	RCA_{6,C2}	2231	3.0
		C3	RCA_{6,C3}	2231	1.8

According to ASTM C33-13, three different size ranges were considered for the coarse aggregates: class 1 (C1, nominal diameter ranging between 4.75 mm and 9.5 mm) class 2 (C2, nominal diameter ranging between 9.5 and 19 mm) and class 3 (C3, nominal diameter ranging between 19 and 31 mm).

Moreover, with the aim of better understanding the influence of the processing procedure on the aggregate properties, an autogenous cleaning process was conceived and performed on the same employed particles (Pepe et al., 2014). More details about the autogenous cleaning process are reported in Section 2.3.

Several tests were performed both on single RCA particles and on representative samples taken from fractions, with the aim of determining the relevant physical properties of the RCAs and unveiling possible correlations of interest for the production of RACs.

The experimental campaigns performed on RCAs can be schematised by considering different aims:

- Evaluation of the Attached Mortar content on RCA;
- Determination of the key physical properties for RCA: water absorption and particle density;
- Evaluation of the mechanical strength of RACs particles;
- Evaluation of the bond strength between RCAs and cement mortar.

Particularly, the tests performed on the single aggregate particles are described below:

- Computer Tomography (CT) study and image analysis, performed according to ASTM E1570-11 for determining the amounts of Attached Mortar and Natural Aggregates;
- Mercury Intrusion Porosimetry (MIP), performed according to ASTM D4404-10 for determining the percentage of open porosity and the particle density.

Nine particles belonging to the C2 fraction were actually tested (Table 2.2):

- three samples of RCA₁: un-cleaned particles from a demolished structure in Brazil;
- three samples of RCA₂: cleaned particles from a demolished structure in Brazil;
- three samples of RCA₄: un-cleaned particles from tested concrete samples in Italy.

Meanwhile, for all kinds of aggregates (each class and origin reported in Table 2.2), the water absorption and particle density were measured by performing the standard test according to EN 1097-6:2013.

Finally, on some samples of C1 and C2 of recycled aggregates (RCA₁) the water absorption rate was evaluated by measuring the time evolution of their weight while they were completely immersed in water (oven dry condition at time zero).

2.2.1 Attached Mortar content

Generally, the physical properties of RCAs have a more complex nature than the ones characterising ordinary aggregates for concrete production. This complexity derives from the demolition and crushing techniques applied to produce the RCAs and is basically related to the fact that RCAs are composed of both ordinary aggregates and attached mortar (AM) fractions whose properties and interactions control the resulting physical properties of RCAs.

The amount of AM is one of the key parameters characterising the properties of RCAs and, consequently, their resulting concrete performance. In fact, the actual percentage of AM determines the relevant engineering properties of RCAs. However, measuring the amount of AM residing inside RCAs is not an easy task, and even a standard method to quantify this amount does not exist yet (Abbas et al., 2009; de Juan & Gutiérrez, 2009).

Based on the analysis of the experimental results obtained from this work, in the following sections, some analytical correlations between the actual AM content and the associating physical properties of RCAs, such as the water absorption (that represents the open porosity) and particle density, which properties are generally easy to be measured, is proposed.

As described in the previous subsection, the evaluation of the amount of the AM in RCAs was done by CT technique combined with image analysis and volume reconstruction, which allowed the author to determine the actual volume percentage of the phases present inside the RCA particles (i.e., natural aggregate fractions, attached mortar and voids).

Figure 2.3 reports an example of an image analysis performed on RCAs which shows the two identified types of materials, i.e. the clearer areas represent the “old” natural aggregates while the darker part is the AM, and the voids or closed porosity, i.e. represented by the black spots. The amount of AM, NA and closed porosity distributed inside the RCAs was determined by using the volume reconstruction technique (ASTM E1570-11). Then, these results were combined with the other tests performed on RCAs so that several correlations could be made, which are proposed in the next section for exploring the relations between the main engineering properties of recycled aggregates.

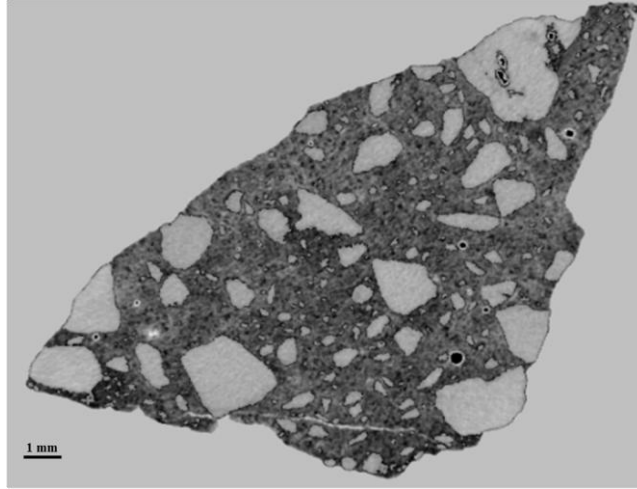


Figure 2.3: Mesoscopic view of a recycled concrete coarse aggregate.

Moreover, the details related to the evaluation of the AM content with CT scans technique are reported in the following Table 2.3.

Table 2.3: MIP and CT results.

Label	Sample	Nominal diameter (MIP) [mm]	Attached Mortar (CT) [%]	Open Porosity (MIP) [%]	Particle density (MIP) [kg/m ³]
RCA ₁	1	19.7	50.0	8.89	2161
	2	17.9	40.8	6.44	2374
	3	17.6	51.6	9.77	2242
RCA ₂	1	18.9	48.0	7.12	2403
	2	17.0	25.0	6.72	2400
	3	19.1	0.0	0.75	2585
RCA ₄	1	15.7	55.9	10.65	2202
	2	19.0	1.4	1.50	2659
	3	17.1	24.0	5.15	2457

2.2.2 Porosity, water absorption and particle density

Porosity (or void fraction) is defined as the volume fraction of empty voids over the total scanned RCA volume and, therefore, ranges between 0 and 1 (or 0 and 100%). Particularly, open porosity is of especially relevant for aggregates to be employed in concrete production: it represents a fraction of the total pore volume and allows additional water to accumulate and potentially being accessible by open

capillary pores, including dead-end pores and excluding closed pores (or non-connected cavities). The open porosity is directly related to the water absorption capacity that represents the maximum amount of water that the aggregates can absorb. The latter is calculated from the difference in weight between the saturated surface dry and oven dry states, expressed as a percentage of the oven dry weight (EN 1097-6:2013). Moreover, hereafter the “porosity” (identified by the symbol “p”) will be referred to the open porosity or, identically to the water absorption capacity. First of all, based upon the experimental results achieved from MIP test and CT examination (Table 2.3), a possible linear correlation is proposed for describing the variation of the porosity p as function of the Attached Mortar (AM) content and normalised by a nominal diameter (d_0) of 20 mm:

$$p = [p_{NA} \cdot (1 - AM) + p_{AM}(AM)] \cdot \frac{d_0}{d} \quad (2.1)$$

where “d” is the diameter of the aggregate expressed millimetres. This formulation can be interpreted as a liner combination of the two phases NA and AM. In fact, p_{NA} represents the porosity of a natural aggregate inside RCA, while p_M represents the porosity of the attached mortar residing to it (and was subjected to a crushing process). The calibration of equation (2.1) led to approximate values for p_{NA} and p_M equal to 0.45% and 15%, respectively. The agreement between the experimental data and the proposed analytical expression (2.1) is reported in Figure 2.4.

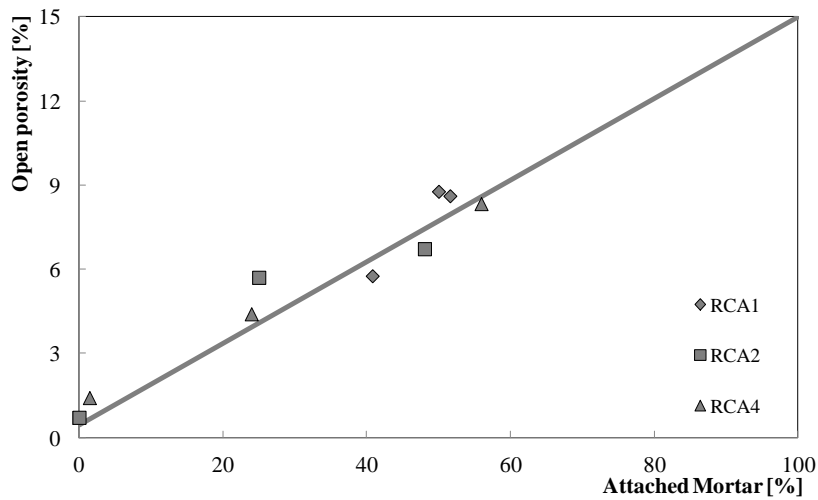


Figure 2.4: Experimental values of open porosity depending on attached mortar of RCA.

Nevertheless, even though the value of water absorption after 24h of soaking is generally assumed as a reference, the time evolution of the absorbed water can be a further relevant aspect for qualifying the key physical properties of the aggregates and, particularly, of RCAs. For this reason the absorption rate was measured for both classes C1 and C2 of recycled aggregates type RAC₁, as reported in Figure 2.5. Based on these results, an analytical expression between the water absorbing time t and the corresponding amount of absorbed water $Abs(t)$ can be proposed as:

$$\frac{Abs(t)}{p} = \left(1 - e^{-t \cdot k_1}\right)^{k_2} \quad (2.2)$$

where $Abs(t)$, in percentage, is the amount of absorbed water in a certain time t (expressed in hours), p is the above defined porosity (i.e., open porosity or capable of absorbing water) and k_1 and k_2 are two constants equal to 0.01 and 0.1, respectively.

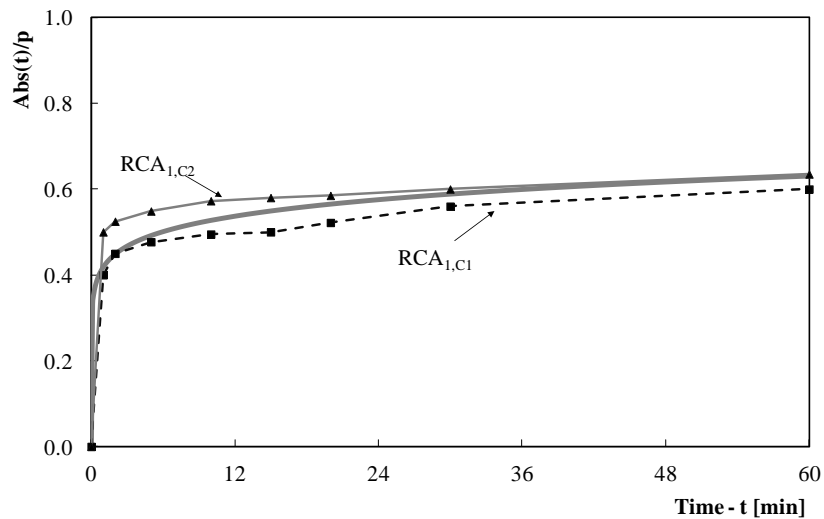


Figure 2.5: Experimental measurements of water absorption rate for different aggregates.

The particle density, defined as the actual oven-dried mass of an aggregate relative to ratio of the volume it occupies in water including the volume of any internally embedded voids and the volume occupies with water accessible voids only (EN 1097-6:2013), represents a fundamental parameter to be determined for the mix design of RAC mixtures. The results reported in Table 2.3 highlight the particle density and complies with the general trend that its value tends to decrease with an enhancing open porosity. As a first order approximation; the following

correlation can be proposed for the relationship between the particle density and the open porosity:

$$\gamma = \gamma_0 \cdot (1 - p)^2 \quad (2.3)$$

where γ_0 (equal to 2700 kg/m^3), representing the particle density of a fictive aggregate in which the open porosity is equal to zero. The results discussed in this subsection are also reported in Figure 2.6 which shows both the experimental data of the MIP tests and the result of the proposed formula (2.3).

Moreover, it is worth mentioning that although the proposed formulations are calibrated on experimental data achieved from tests performed on single particles (i.e., MIP and CT tests), they can be easily extended to a bigger sample of aggregates. In fact, the open porosity of aggregates can be measured through their water absorption capacity as well as the particle density that can be determined by performing the standard procedures (EN 1097-6:2013).

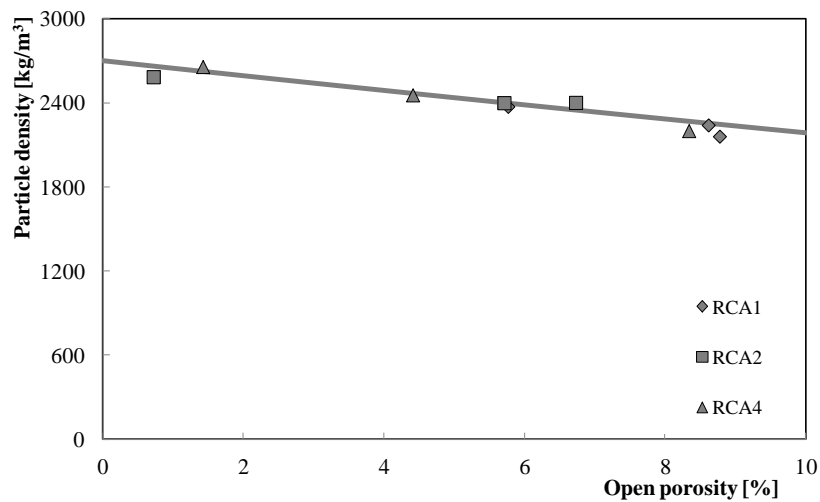


Figure 2.6: Experimental values of particle density of RCA depending of the open porosity.

2.2.3 Mechanical strength

Once having defined the key physical properties of RCAs, this section presents the experimental activity carried out on recycled concrete aggregates with the aim of unveiling their mechanical behaviour. Since the particles do not have a regular shapes, it is not easy to define a standard test methodology for determining, for example, their compressive strength or elastic modulus. In literature, several tests

method are available for determining, in a direct or indirect way, the mechanical behaviour of aggregate particles (Tavares, 2007).

Another fundamental aspect is related with the fact the particles in concrete are involved inside a mixture and for this reason their behaviour is influenced by the presence of the other particles and the others bulk phases (i.e., sand and cement). For these reasons, the possible test methods that can be performed on aggregate particles can be related to one single particle or to the bulk of aggregates.

In this research, the mechanical behaviour of RCAs has been evaluated by performing the compressive strength test on single particles. Moreover, it is worth highlighting that the results presented in this section are not aimed at determining an absolute value of the mechanical performance of RCAs, but they are rather intended at comparing their behaviour with ordinary natural aggregates.

Compressive strength test on single particles: method

Figure 2.7, schematically, reports the compressive strength test performed on the single particles considered in this study.

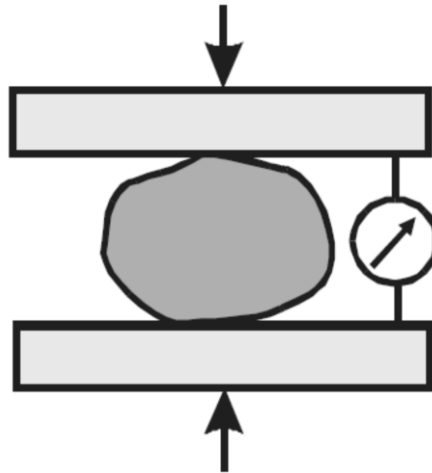


Figure 2.7: Compressive strength test on single particles (Tavares, 2007).

The stress distribution inside the aggregate particles during the compressive test cannot be directly determined as in the case of concrete cubes (EN 12390-3:2009) due to the irregular geometry. First of all, the contact load points can be no uniform for the various tested particles, but also for the same particle in the lower and the upper face. Despite this, it is possible to define the outset of particle breakage (Figure 2.8).

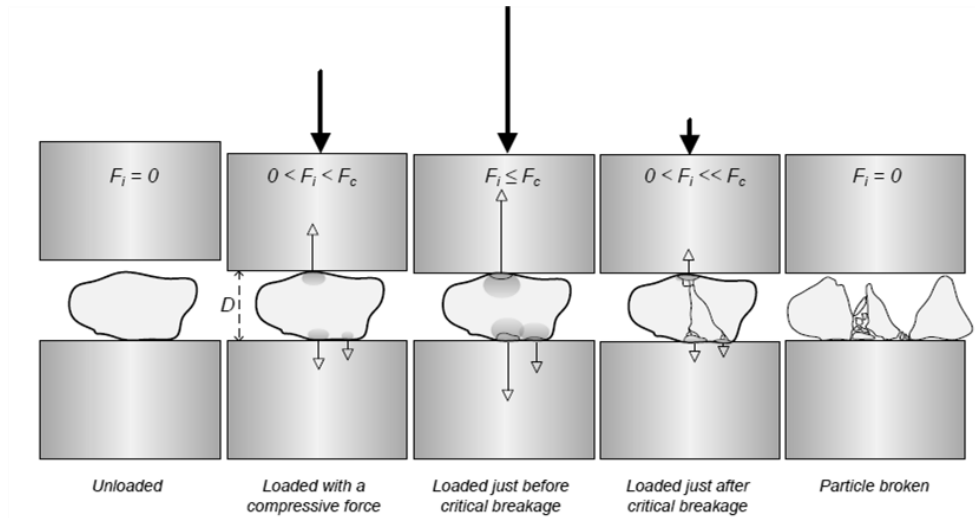


Figure 2.8: Schematic illustration of the different phases during a single particle compressive strength test (Quist, 2012).

Then, after reaching the critical force, a series of cracks occur in the particles up to its disintegration. This behaviour results in a discontinuous force-displacement diagram, as shown in Figure 2.9, where the point corresponding to the maximum force represent the critical phase (i.e., the particle breakage).

Then, additional peaks depends on further progressive breakage of the aggregate.

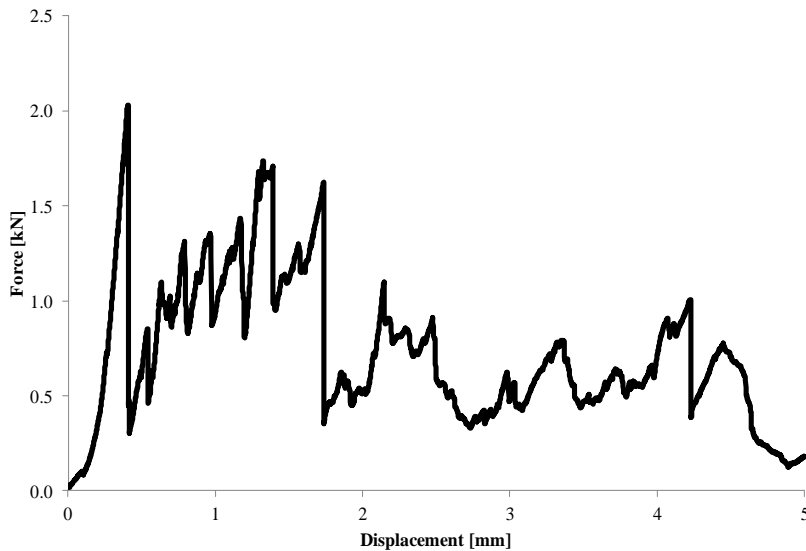


Figure 2.9: Typical force-deformation diagram from single particle compressive strength test.

In this research both natural and recycled aggregates were tested under compression. Particularly, NA_BR (see Table 2.2) particles for natural aggregates and RCA₁ and RCA₅ (see Table 2.2) were considered. For each aggregates type, two aggregate sizes were defined:

- Nominal diameter ranging from 12.5 mm and 16 mm;
- Nominal diameter ranging from 12.5 mm and 16 mm;

Moreover, for each group of particles, 50 tests were performed.

Compressive strength test on single particles: results

As above mentioned, due to the irregular shape of the particles it is not easy to define the maximum strength because, once define the maximum force it seems unrealistic to define the load contact area. Despite this, from literature (Tavares, 2007), it is possible to define the two following parameter for describing the mechanical behaviour of aggregate particles: the particle strength and the particle fracture energy.

The particle strength (σ_p) can be determined according to the following equation:

$$\sigma_p = \frac{2.8 \cdot F}{\pi \cdot d^2} \quad (2.4)$$

where F represents the critical force and d is the nominal diameter of the tested particles. In the same way, for each test, the particle fracture energy can be determined by evaluating the area under the force(F)-displacement(δ) diagram up to the point corresponding to the critical force:

$$E = \int_0^{\delta_c} F d\delta \cong \sum_i \frac{\Delta\delta_i \cdot \Delta F_i}{2} \quad (2.5)$$

Whenever the fracture characteristics of a single particles in a given size range of a certain material, are determined, a large scatter of data appears due to their heterogeneity. Such a variability, can be described by order statistics. In fact, the results can be order in ascending way and then assigning $i=1,2,\dots,n$ to the ranked observation, where n is the total number of the performed tests. So, the cumulative probability distribution (P) can be defined (Tavares, 2007):

$$P = \frac{n_i}{n_{TOT} + 1} \cdot 100 \quad (2.6)$$

Influence of nominal diameter

Figure 2.10 reports the particle strength distribution related to the particle size for natural aggregates. It shows that the particle strength distributions are affected by the nominal diameters of the particle in the case of natural aggregates. In fact, a decrease in the particle size results in a shift of the distributions to higher values.

This influence is commonly observed in brittle materials and is due to the fact that flaws, pores and grain boundaries are embodied in any solid material and in particular in geological materials (Tavares, 2007). The presence of this structural heterogeneity causes stress concentration that result in cracks. In the case of recycled concrete aggregates, this phenomenon is more evident. In fact, the comparison between the results reported in Figure 2.10 (i.e., natural aggregates) and Figure 2.11 (i.e., recycled concrete aggregate) highlights that the influence of the aggregates size is more relevant in the case of RCAs. The higher gap between small and big particles in the case of RCAs can be, probably, attributed to the higher percentage in terms of heterogeneity that causes the failure of the particle when it is loaded in compression.

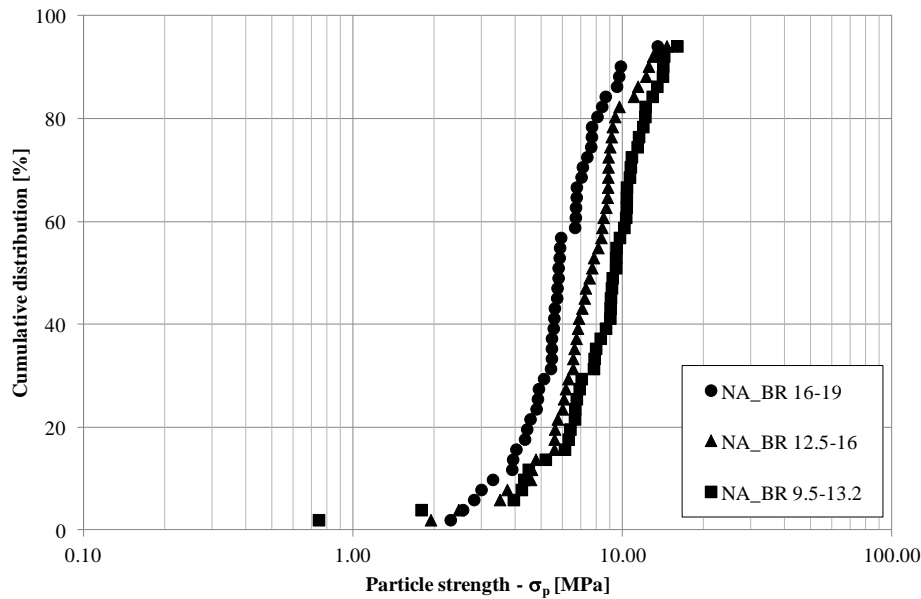


Figure 2.10: Particle strength, natural aggregates: influence of nominal diameter.

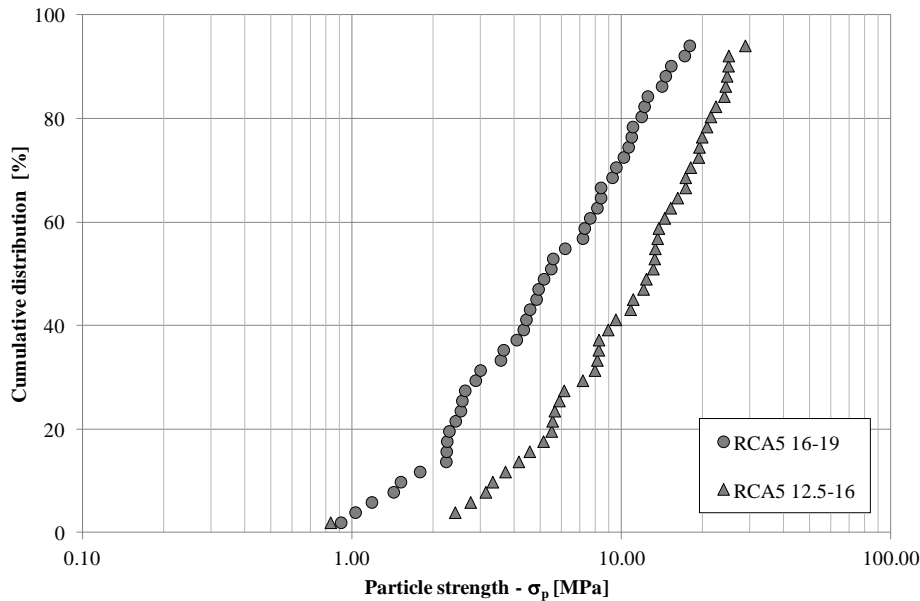


Figure 2.11: Particle strength, recycled concrete aggregates: influence of nominal diameter.

Influence of aggregate source

The analysis of the results reported in the following Figure 2.12 and Figure 2.13, led to unveiling the influence of the aggregates source on the mechanical properties of the particles both in terms of particle strength (Figure 2.12) and particle fracture energy (Figure 2.13). In fact, in both figures, the natural aggregates are characterised by a general trend of results with higher strength and energy in comparison with RCAs. In addition, the cumulative distribution of the results, in both figures, seems to have a more homogenous trend or at list the scatter between the results is lower than RCAs. In fact, the cumulative distribution, in the case of natural aggregates, results more “vertical”. This effect is due to the fact that the natural aggregates are more homogenous in nature compared with RCAs and for this, the internal structure of results more uniform between every particle. On the contrary, RCAs can be named as a three-phases material: AM, natural aggregates and the interfacial transition zone in between them (ITZ AM-Aggregate). This multiphase characteristic leads to a bigger scatter between the results of each batch. In fact the RCAs particles with higher values of strength and energy, are the particles with lower content of AM as their values are similar to the case of natural aggregates, while the lower strength values can be attribute to the presence of AM that, probably represents the weakest phase in the composite. This behaviour is also confirmed by the fact that the presence of AM content results in higher porosity for

RCAs. Under the physical point of view, the higher porosity leads to higher water absorption capacity, whereas from the mechanical standpoint, it results in lower values of strength.

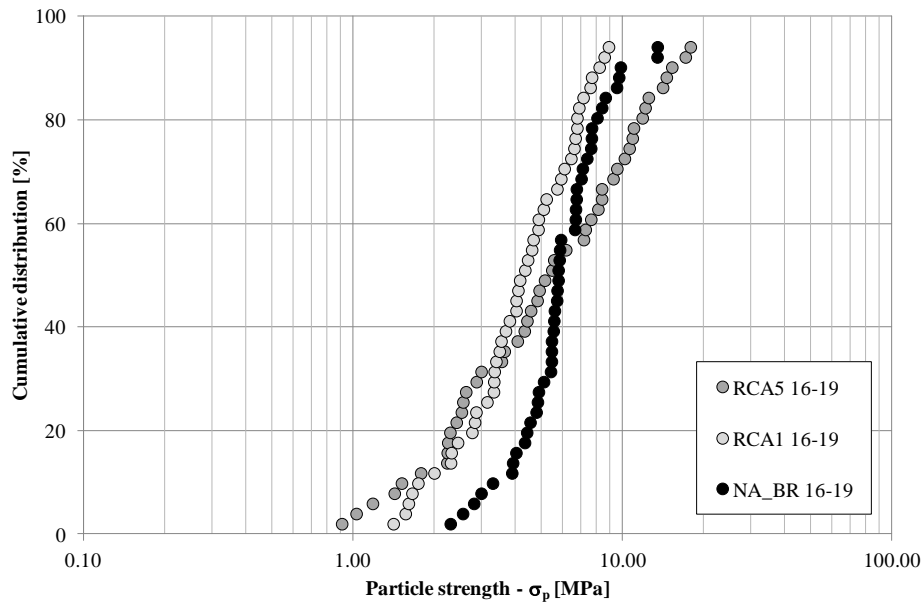


Figure 2.12: Particle strength: influence of aggregates source.

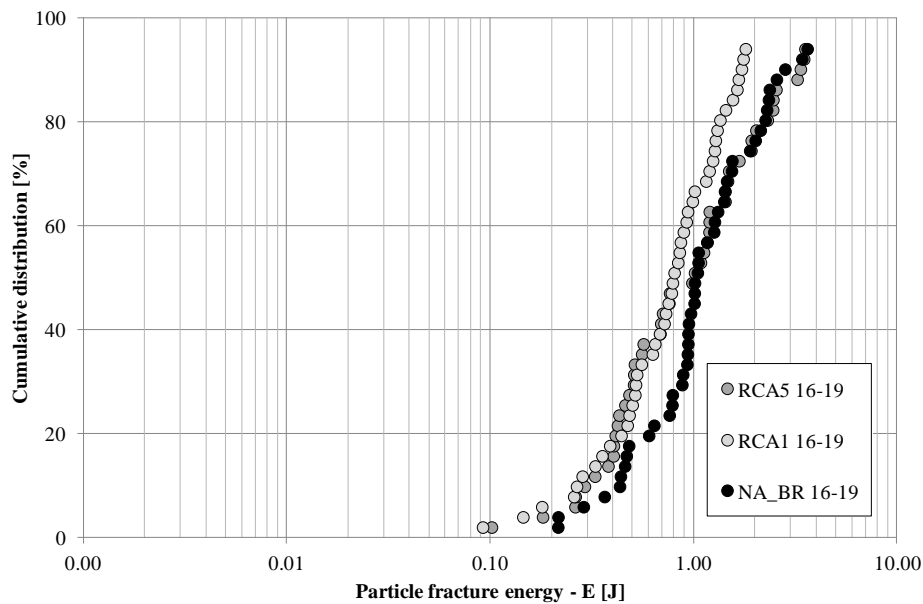


Figure 2.13: Particle fracture energy: influence of aggregates source.

2.2.4 Bond strength between aggregates and cement paste

The hardened “ordinary” concrete could be considered as a three-phase composite material consisting of cement paste, aggregate and interface (i.e., Interfacial Transition Zone, ITZ) between cement paste and aggregate. In the case of Recycle Concrete Aggregates some other phases must be introduced: Attached Mortar, ITZ between AM and cement paste and ITZ between AM and natural aggregates (Pepe et al., 2014). The load transfer mechanism between these phases depends on cement paste type, the surface characteristics of aggregate and adhesive bond developed at the interfaces (Struble et al., 1980). The ITZs bond results from some combination of mechanical interlocking of cement hydration products with the aggregate surface and chemical reaction between aggregate and cement paste (Scrivener et al., 2004).

As a matter of the fact, the interface zone is believed to play an important role in the cracking of concrete because its mechanical properties are essential in governing the cracks path propagation inside the concrete microstructure. Moreover, the relative values of the bond strength and stiffness with respect to the matrix and/or aggregate strength and stiffness are of major importance, rather than the absolute values of all these parameters. Several test method have been proposed in the literature for estimating the mechanical properties of the bond strength between the several phases present inside a concrete element but, despite this, it is not easy to evaluate the strength between aggregates and cement paste. In addition, when other phases can be defined (as in the case of RACs), the problem becomes more complicated.

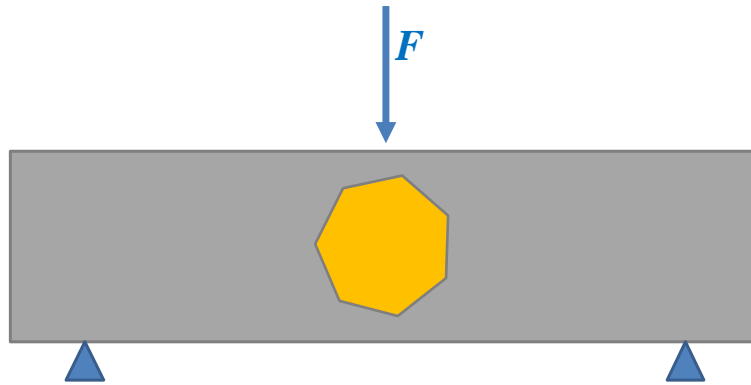


Figure 2.14: Bond strength test on single particles.

In this section, a new test methodology is proposed for the estimation of the bond strength between the phases preset in concrete. The test is similar to the three points bending test, generally performed on fiber reinforced concrete (fib, 2013), in

terms of load and boundary condition (see Figure 2.14). The main difference is the presence of one aggregate particle in the middle of the sample. Moreover, the aggregate presents a nominal diameter of 20 mm, the span is of 80 mm, the height of the “beam” is around 30 mm and the thickness is equal to 10 mm (Figure 2.14).

In order to make a comparison between ordinary and recycled aggregate concretes, several tests were performed on both natural and recycled concrete aggregates.

Particularly, the natural aggregates and the recycled ones were produced in Brazil. The natural aggregates employed for this analysis are defined as NA_BR in Table 2.2. Meanwhile, the recycled concrete aggregates were derived from both C&D waste and concrete samples already tested in laboratory (RCA₁ and RCA₅, respectively, in Table 2.2).

Figure 2.15 reports the results in terms of force-displacement diagram coming out from the proposed test methodology. For each particle type, ten tests were carried out.

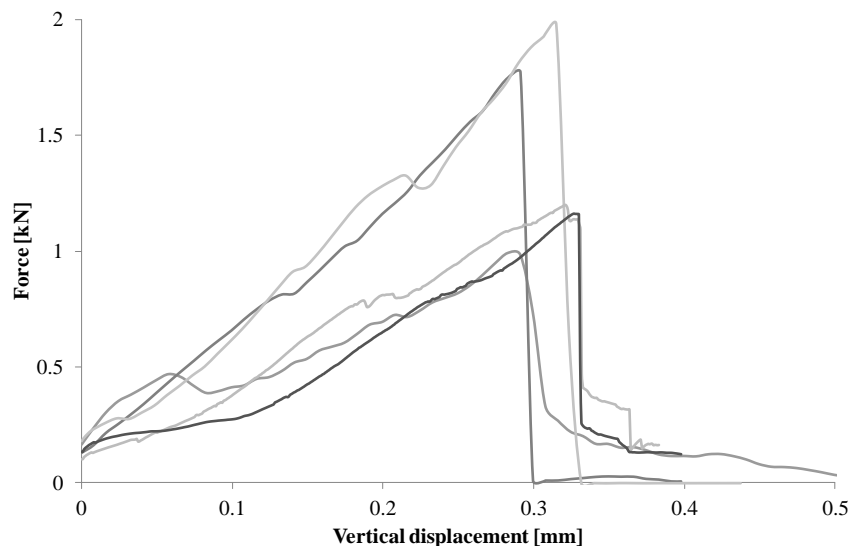


Figure 2.15: Typical force-deformation diagram from singular particle bond strength test.

Moreover, Figure 2.16 shows the possible failure mechanisms occurring during the tests. As a matter of fact, the two following failure cases were observed:

- Particle breakage (Figure 2.16a and Figure 2.16b);
- ITZ Aggregate – Paste (Figure 2.16c).

The particle breakage case can be subdivided in two other cases, in fact when recycled concrete aggregates are employed the weakest phase of the

composite can be the Attached Mortar (Figure 2.16a) or the ITZ between natural aggregate and Attached Mortar (Figure 2.16b).

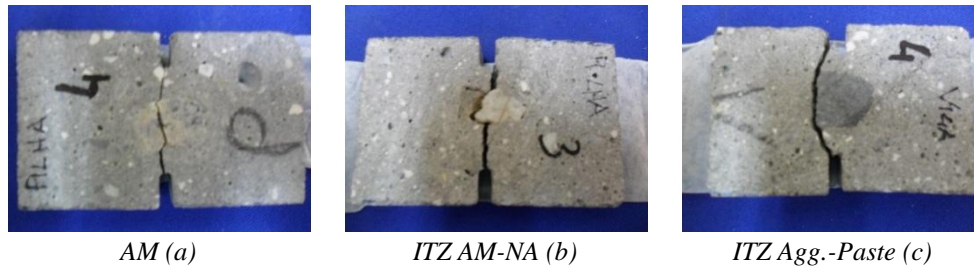


Figure 2.16: Failure mechanisms for bond strength test.

In Table 2.4 the results of the experimental test performed for the estimation of the bond strength between aggregates and paste, are reported. The average values of the maximum stresses registered during the tests, are estimated by dividing the maximum force reached during the test and the contact area between the particle and the cement paste. The evaluation of the contact area was determined by multiplying the perimeter of the bond (calculated by considering the average value of the aggregate nominal diameter) and the thickness of the beam (i.e., 10 mm).

Table 2.4: Experimental results of the bond strength test.

Aggregate type	Failure mechanism	Bond strength [MPa]
NA_BR	ITZ Aggregate – Paste	0.62
RCA ₁	Particle breakage	0.60
	ITZ Aggregate – Paste	0.80
RCA ₅	Particle breakage	0.40
	ITZ Aggregate – Paste	0.54

It is worth highlighting that in the case of RCAs, several specimens failed for particle breakage. This means that the bond strength between RCA and paste was stronger than the tensile strength of the particle. In fact, the RCAs are characterised by a more irregular shape compared with natural ones and for this reason the ITZ results stronger than its mechanical strength.

Certainly, in the future, more tests should be performed for better estimating the bond strength value of the aggregates in concrete, but the proposed methodology is a first step to define a standardised test for these measurements.

2.3 Alternative processing procedures for RCAs

The recycled concrete aggregates employed in this campaign were obtained from demolition of the hospital Clementino Fraga Filho in Rio de Janeiro – BR (Figure 2.17).



Figure 2.17: Demolition of hospital section, Ilha do Fundão, Rio de Janeiro, Brazil.

The recycled aggregates were selected and analysed by the university laboratory for construction materials LABEST (PEC/COPPE – UFRJ Rio de Janeiro), and were processed in the following steps:

- *Particle homogenisation*, with the objective to homogenise the demolition debris and remove residual wood, steel and plastic pieces;
- *Grinding and sieving*, aiming at transforming the demolition debris into aggregates of the appropriate size classes Class 2, Class 1 and Sand;
- *Autogenous cleaning*, intended at removing most of the “attached mortar” layers residing on the aggregate surfaces.

The first two processing steps are generally performed on Construction and Demolition waste to produce RCAs.

In addition, the third one was specifically carried out to possibly enhance the quality of RCAs and, with this, the mechanical properties of Recycled Aggregate Concrete (RAC).

The *particle homogenisation* carried out on the initial crushed concrete particles was based upon collecting and selecting such particles and debris by considering their predominant colour. Therefore, at the demolition site debris was selected and subdivided into the following two fractions:

- “grey”, consisting of particles mainly made of structural concrete (and, in a minor portion, mortar) debris;
- “red”, made of clay brick and other ceramic-based (i.e. tiles) materials.

This study focuses on demonstrating the recyclability of the “grey” fraction with emphasis on their mechanical performance of the resulting produced concrete. The homogenisation process was carried out by means of a so-called “cells process” (homogenising process per unit cell), in which the raw materials were distributed on a plastic sheet in different layers throughout the whole length of the sheet. Thus, the raw concrete particles are homogeneously distributed over the length of the sheet, and, starting from the middle section, layers of raw materials are subdivided in several sections called “cells”.



Figure 2.18: Homogenisation process.

Next, the homogenised material was then grinded with a crusher, jaw crusher type, model Queixada 200 produced by Vegedry (www.vegedry.com.br). During the grinding phase, the material was separated into two classes, namely fine and coarse aggregates. For each sample of the homogenised material, about 40% was obtained as coarse aggregates (nominal diameter bigger than 4.75 mm) and the rest was defined as fine aggregates (sand) (< 4.75 mm).



Figure 2.19: Grinding process with crusher.

After grinding, the recycled aggregates were sieved and divided into the three size classes already defined before in section 2.2.

With the aim of reducing the amount of fine materials attached to the surface of recycled aggregates (mainly debris from cement paste and sand, generally referred to as the AM defined above), an *autogenous cleaning* process was conceived and performed. With this process RCAs are placed in a rotating mill drum and collide against each other while removing pieces of attached mortar. The mill drum, 30 cm in diameter and 50 cm in depth (Figure 2.20), was filled up to 33% with “raw” recycled aggregates and the rotation rate was imposed to 60 rotations for minute. After the autogenous cleaning process, aggregates were cleaned with water and subsequently dried to remove all the produced fine remainings and impurities.

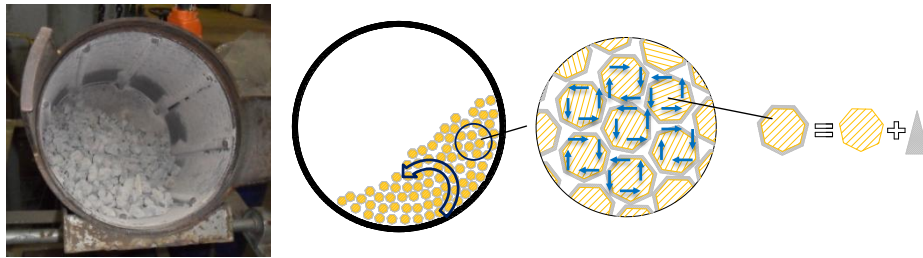


Figure 2.20: Autogenous cleaning process.

The efficiency of the autogenous cleaning process was analysed by investigating how it actually modified the key physical properties of the particles after applying different durations of cleaning (ranging from 2 to 15 minutes). To have a first measure of the cleaning capability and efficiency, some preliminary trials cases were performed on raw RCA particles (i.e., not homogenised). The effect of these trial procedures was “measured” by determining the water absorption capacity of the same particles before and after various “cleaning” durations. The results of autogenous cleaning, for both Class 1 and Class 2, showed a progressive decrease of the water absorption capacity, with increasing durations from 2 to 10 or 15 minutes. Based on these preliminary findings, the final choice for the duration of autogenous cleaning of the homogenised particles used in the experimental program is 10 and 15 minutes.

As part of the experimental programme, several tests were performed on both natural and recycled aggregate samples while aiming at comparing their key mechanical and physical properties like water absorption, specific mass, grain size distribution, thermal treatment for evaluating the attached mortar and image analysis using photographs.

The mass of the attached mortar (AM) that was removed from the outer layers of the recycled concrete aggregates (RCAs) was measured by a thermal treatment test. This method was used because a standard procedure for evaluating the attached mortar content of recycled aggregates is still lacking, and this thermal treatment test has been proposed by several authors (de Juan & Gutiérrez, 2009; Fathifazl et al., 2009). According them, the method represents most accurate results for evaluating the attached mortar content in RCAs. The procedure for evaluating the AM content develops in the following steps:

- Weighing a certain amount of dried recycled aggregates with initial mass m_i ;
- Immerging the dry aggregates in water for two hours. In this way the old mortar paste can saturate with water (and the old (solid) natural aggregates do not);
- Heating the saturated aggregates for two hours at a constant temperature of 500°C;
- Suddenly immerging of the aggregates in water at room temperature (20°C). The thermal shock will cause internal stresses and stimulate debonding and unleash of the attached mortar paste from the natural aggregate surface
- Removing (either manually or through a a rubber hammer) the particles of attached mortar that are possibly still adhered to the outer layer of the aggregate;
- Drying the resulting coarse aggregates (i.e., nominal diameter above 4 mm) up to 100°C to reach a constant mass (i.e., final mass, m_f);
- Defining the attached mortar as: $AM\% = \frac{m_i - m_f}{m_f}$.

The first tests performed to assess the efficiency of autogenous cleaning of the recycled concrete particles were carried out by determining the water absorption capacity and specific mass, performed according to NBR NM 53:2009 for coarse aggregates (i.e., Class 1 and Class 2). Figure 2.21 reports the results of the water absorption tests. It can be seen that the thorough cleaning (e.g. 15 minutes) leads to a significant reduction in water absorption, while this effect will be less for shorter durations of cleaning. As a result of this, the attached mortar is the parameter that determines the water absorption on the one hand and the implicit void percentage on the other. In fact, the results highlight that after the autogenous cleaning, the amount of absorbed water was reduced by 50% and 20% for Class 1 and Class 2, respectively.

Moreover, the above observations were also confirmed by measurements on the specific weight of the processed particle samples. Figure 2.22 provides an overview of the potential of autogenous cleaning as considered in this study, to transform crushed concrete particles into cleaned recycled concrete aggregates.

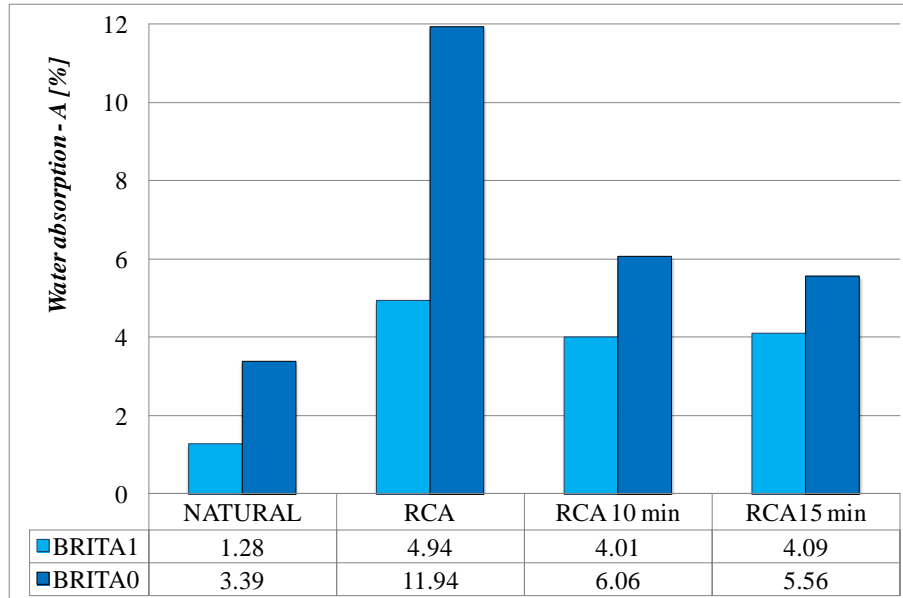


Figure 2.21: Water absorption at 24h of aggregates.

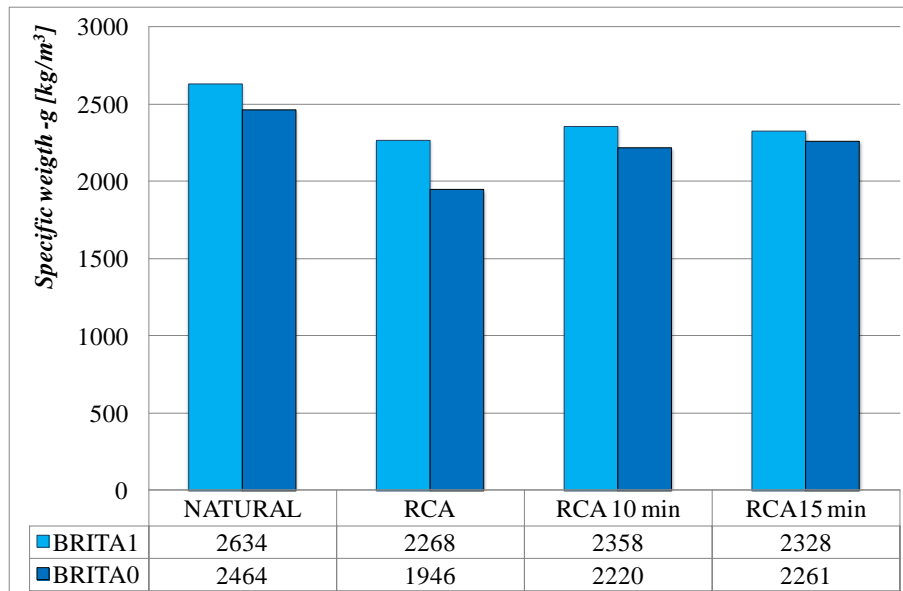


Figure 2.22: Particle density.

Another interesting evidence of the autogenous cleaning efficiency was obtained by analysing the resulting grain size distribution, throughout the sieving process realised in accordance with NBR NM 248:2003. In fact, the cleaning process led to an increasing amount of fine particles (Figure 2.23). Thus, it confirms the results of the previous tests, pointing out that a significant part of the outer layers of the crushed concrete particles were actually removed and transformed into much smaller particles, which could possibly be employed to improve the aggregate particle packing of RAC mixtures (De Larrard, 2005).

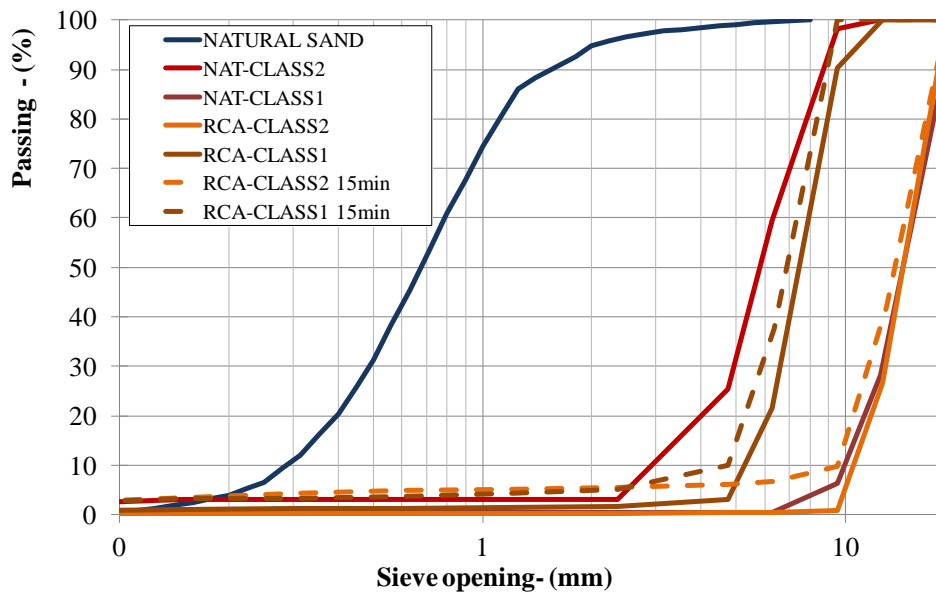


Figure 2.23: Grain size distribution of coarse and natural aggregates.

The thermal treatment method performed on the recycled aggregates further highlights the effectiveness of autogenous cleaning. In fact, uncleaned recycled aggregates show an AM content equal of $\cong 30\%$ while the cleaned aggregates, let to a decrease of the attached mortar up to $\cong 15\%$. Even though, the above reported values cannot represent the exact content of the old mortar paste attached to the aggregates (note that this procedure does not follow a regulated standard), comparison between the two cases (i.e., cleaned and uncleaned aggregates), confirms the above presented results for RCAs in terms of water absorption, specific weight and grain size distribution variation (see Figure 2.21, Figure 2.22 and Figure 2.23).

A final assessment of the actual effectiveness of autogenous cleaning can be obtained through a comparative visual analysis. Photos of concrete particles are taken after three different durations of cleaning and reported in Figure 2.24. The pictures show that autogenous cleaning not only removes the cement paste residuals possibly attached at the aggregate surface, but also modifies the final shape of recycled aggregates. Particularly, Figure 2.24 shows that the change in particle surface colour, roughness and shape evolved as a result of the autogenous cleaning procedure, with a clear modification of these properties after 15 minutes.



Figure 2.24: Image analysis using photographs.

The experimental results reported in this campaign show the effect of alternative processing procedures for RCAs on the physical and mechanical properties of RACs. In particular, the autogenous cleaning implemented at the laboratory scale led to interesting results in terms of enhancement of properties of crushed concrete particles, especially in terms of reduction of the attached mortar content on RCA surfaces and, consequently, on their water absorption capacity.

Finally, based upon the results discussed in this subsection, an analytical expression is proposed for evaluating the actual open porosity, p , as a function of the “autogenous cleaning time” t , expressed in minutes:

$$p(t) = \left(1 - \frac{a \cdot t}{b + t}\right) \cdot p_{t=0} \quad (2.7)$$

where $p_{t=0}$ represents the initial open porosity of the aggregates without autogenous cleaning, a is a constant equal to 0.6 for class C1 and 0.2 for the class C2 aggregates, while b is equal to 2 in both cases.

3. Recycled Aggregate Concretes

This chapter aims at reporting the main information about the mechanical properties of concrete made with recycled concrete aggregates: in the following this material will be referred to as Recycled Aggregate Concrete and identified by the acronym RAC.

The first section proposes an overview about concrete technology and summarises well known rules and practices currently adopted in the field of concrete technology.

The second section proposes a summary of the State-of-the-Art knowledge about RAC: it summarises the main findings of the big deal of researches mainly developed in the last decades and highlights the most relevant open issues to which are specifically addressed in this thesis.

Finally, all the applied research methodology and the performed experimental activities are described. Several key parameters of relevance of defining the RAC mixture composition are considered in this study, such as the original source and the processing procedures of RCAs, the aggregate replacement ratio, the water to cement ratio and the initial moisture condition for coarse aggregates.

3.1 Basic aspects about concrete mix design and technology

Features of concrete technology are well known nowadays, due to a very large number of researches published since the XIX century and a wide application in construction field (Neville, 1981; Mehta, 1986). This section is aimed at describing the role of the key parameters on the resulting properties of concrete and, particularly, highlighting the possible consequences of using recycled concrete particles as aggregates. In fact, recycled concrete aggregate (RCA) both coarse (RcCA) and fine (RfCA) show different physical and chemical characteristics from natural ones. Therefore, specific devices may be necessary to design good quality recycled aggregate concrete (RAC).

3.1.1 The role of aggregates in concrete mixture

Before analysing the influence of recycled aggregates in concrete, it is useful to focus on the role that aggregates play in ordinary concrete. The main reasons that justify the employment of aggregates in concrete mix concern technical aspects. In fact, the shrinkage of cement paste decreases as the amount of aggregates increases, and durability of concrete can be improved replacing much of cement paste with a better enduring material, such as aggregate (Collepari et al., 2009).

Moreover there is also an economic advantage of using aggregates in concrete mixtures, as they are less expensive than cement past.

To produce a workable concrete with a relatively low cement content, it is preferable that the aggregate is well mixed with granules of various sizes (de Larrard, 1999). In this case, the experience has shown that parameters such as mechanical strength and durability are greater than those obtained by a monogranular conglomerate. Conversely, the minimization of voids and pores affects workability of concrete at the fresh state. Thus, the optimum grain size distribution of the aggregate can be chosen on the basis of a compromise, considering the following aims: the maximum density of the conglomerate with a minimum cement content, a good workability and minimal segregation of the fresh mixture.

Practical reasons suggest to combine two or more types of aggregate to reproduce a satisfactory particle size distribution, particularly using a coarse fraction and a fine one. The most remarkable studies about sieve analysis, were carried out by Fuller, Thompson and Bolomey (Collepari et al., 2009). Fuller & Thompson (1906) proposed an ideal grain size distribution curve described by the following equation:

$$p = 100 \cdot \sqrt{d/D} \quad (3.1)$$

where p is the percentage of material passing through the sieve with opening d , and D is the maximum dimension ("maximum diameter") of the coarsest grain.

Bolomey (1947) revised the Fuller and Thompson equation in order to consider the required workability of the mixture. Thus, the parameter A was introduced to consider the expected consistency class and the aggregate shape:

$$p = A + (100 - A) \cdot \sqrt{d/D} \quad (3.2)$$

All codes and guidelines currently adopted about sieve analysis in concrete technology are intended at controlling the aforementioned influence of aggregates on the resulting concrete properties at both fresh and hardened states. The American ASTM C33-13 is probably the most widely adopted standard in this

field. The various size fractions of aggregates are sieved separately. Particularly, the portion of aggregate passing the 4.75 mm sieve and predominantly retained by the 75 μm sieve is called “fine aggregate” or “sand,” while the bigger particles are generally defined as “coarse aggregate”.

All the standards worldwide, both for coarse and fine aggregates, indicate a lower and upper limit for grain size distribution curve, which still apply for recycled aggregates.

3.1.2 Portland cement

Portland cement is the most common type of cement used as binder in concrete production. It is a fine powder obtained by grinding clinker, a limited amount of calcium sulphate and other minor constituents as allowed by various regulations (Collepari et al., 2009). The two major standards for classification of Portland cement are the ASTM C150-12 used in U.S., but also in several parts of the world, and the European EN 197-1:2011. ASTM C150-12 Standards define five different types of Portland cement, whereof the first one (Type I) is commonly used for general construction, especially when concrete is not to be in contact with soils or ground water (Table 3.1).

Table 3.1: Cement classification (ASTM C150-12).

Cement type	C ₃ S [%]	C ₂ S [%]	C ₃ A [%]	C ₄ AF [%]	MgO [%]	SO ₃ [%]
Type I	55	19	10	7	2.8	2.9
Type II	51	24	6	11	2.9	2.5
Type III	57	19	10	7	3.0	3.1
Type IV	28	49	4	12	1.8	1.9
Type V	38	43	4	9	1.9	1.8

Moreover, considering various mineral admixtures to Portland cement, such as blast furnace slag, silica fume or pozzolanic material, the European EN 197-1:2011 defines five different classes of cement:

1. CEM I: with 95% of clinker at least;
2. CEM II: with clinker percentage between 65 and 94%, and mineral additions in fixed proportions, which lead to the following subtypes:
 - II A/S, II B/S with blast furnace slag (S);
 - II A/D with silica (D);
 - II A/P, II B/P, II A/Q, II B/Q with natural (P) or industrial (Q) pozzolanic materials;
 - II A/V, II B/V, II A/W, II B/W with silic (V) or calcic (W) fly ash;

- II A/T, II B/T with calcined shale (T);
 - II A/L, II B/L with limestone (L);
 - II A/M, II B/M obtained from all the mineral additions mentioned before;
3. CEM III: with clinker percentage between 5 and 64%, and a high percentage of blast furnace slag (up to 95%);
 4. CEM IV: with clinker percentage between 45 and 89%, and pozzolanic constituents (up to 55%);
 5. CEM V: with clinker percentage between 20 and 64%, and mineral additions such as blast furnace slag, pozzolana or silica fly ash.

Furthermore, EN 197-1:2011 completes the cement notation, introducing its minimum compressive strength target (32.5, 42.5 or 52.5 MPa), measured at 28 days and the type of the initial hardening (R for rapid, N for ordinary).

Finally, it is useful remarking that in EN 197 cement types CEM I, II, III, IV, and V do not correspond to the cement types similarly denoted in ASTM C150-12, as the American standards do not mention mineral admixtures in cement classification.

3.1.3 Influence of moisture content and w/c ratio

The parameter that has the greatest influence on concrete performance, in terms of strength and workability, is represented by the water content in the mixture. Its role, usually expressed through the water cement ratio (w/c), is rather complex and must also take into account the moisture able to saturate the porosity of the aggregate, defined as absorption.

Generally, it is possible to characterise four different conditions concerning aggregate moisture content (m.c.). Firstly, when all the pores of aggregate are filled with water and the grain surface is dry, it is said that the aggregates are at saturated surface-dried (SSD) conditions. To state the water content related to SSD conditions, the material is immersed in water for 24 hours, and after it is dried on surface, by removing the excess water. Then the aggregate is heated to 100 °C until its weight keeps unchanging. The percentage loss versus dry weight it is called absorption a:

$$a = \frac{b_{SSD} - b_0}{b_0} \quad (3.3)$$

where b_{SSD} is the bulk of the aggregate, first kept under water until its total saturation and then dried on the surface and b_0 is the completely dry aggregate's bulk.

This value is a property of aggregate at SSD condition, and depends only on the porosity of the aggregate. Whereas the actual moisture content is affected by environmental conditions, and it can be fixed by the following relation:

$$m.c. = \frac{b - b_0}{b_0} \quad (3.4)$$

where b is the aggregate's bulk as it is available.

Considering the above basic aspects, it is possible to define the other three possible aggregate states. If the aggregate at SSD condition is air-dried, part of water in pores evaporates, so that it becomes unsaturated ($m.c. < a$); while if $m.c. > a$, the aggregate is wet. Finally, when the moisture content is equal to zero ($m.c. = 0$) the aggregate is defined dry. The four conditions previously described are schematically depicted in Figure 3.1.

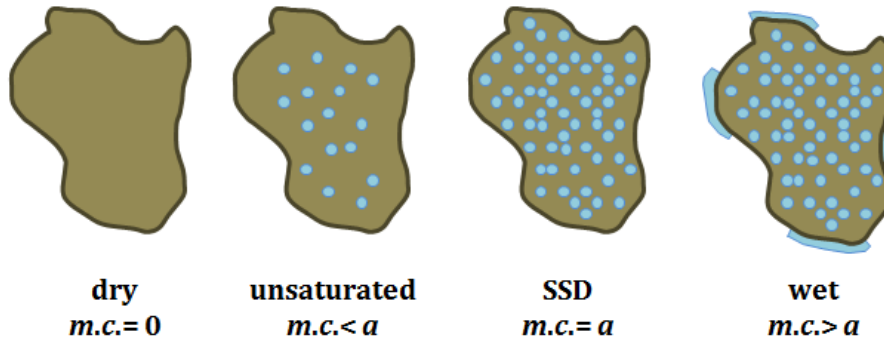


Figure 3.1: Different conditions related to moisture content (Collepari et al., 2009).

Therefore, the initial moisture condition of aggregates can have an influence on the actual amount of mixing water. On the one hand, unsaturated aggregates ($m.c. < a$, or even dry ones, $m.c. = 0$) can absorb part of the nominal mixing water by suction, with a consequent decrease of the effective mixing water. On the other hand, wet aggregates ($m.c. > a$) can release part of their absorbed water resulting in an increase of the total mixture water.

This matter becomes more complex when RCAs are used in concrete mixture, due to involved chemical and physical aspects. In fact, as reported in chapter 2, RCAs are characterised by the presence of AM consisting of both hydrated and unhydrated cement particles and the original fine aggregate (sand). For this reason, recycled aggregate has a significantly higher water absorption than the natural aggregate. Therefore, adding water is needed for obtaining the desired workability for concrete mixture with the aim of compensating the part of free water which would be absorbed by dry RCAs. Moreover, experience has showed

that this attached mortar is the main reason for the lower mechanical properties of recycled aggregates compared to natural ones.

All the authors who investigated the employment of RCA in concrete production, paid a great attention to this problem, and the water absorption of the aggregate was identified as a key parameter.

Table 3.2: Water absorption for both natural and recycled concrete aggregate.

Reference	Natural Aggregate	Water absorption (%)		
		RcCA	Natural Sand	RFCA
Xiaoa et al. (2005)	0.4	9.2		
Kou et al. (2008)	1.1	4.3		
Poon et al. (2004a)	1.2	6.3		
Yong & Teo (2009)	1.6	6.4		
Malešev et al. (2010)	0.4	2.4		
Limbachiya et al. (2012)	0.6	5.3		
Gomèz-Soberon (2002)	0.9	5.8	1.5	8.2
Lin et al. (2004)			2.2	11.9
Evangelista & de Brito (2007)			0.8	13.1
Corinaldesi & Moriconi (2009)	2.0	8.0	3.0	10.0

Table 3.2 shows the significant difference between natural and recycled aggregates in terms of water absorption. Particularly, such a difference is remarkable for the fine fraction, and this is the main reason why almost all international standards and regulations do not allow using recycled sand in concrete mixtures for structural applications.

Considering the increase in water absorption for RCA, many authors employed the aggregates at saturated surface-dried (SSD) conditions, in order to obtain both a good quality and an adequate workability for recycled concrete.

Malešev et al. (2010) found that the major changes in the quantity of absorbed water occur in the first 30 minutes, and also that the most remarkable changes in the consistency of ordinary concrete (without chemical admixtures) occur in the first 20–30 minutes. Taking into account these underlying attitudes, they suggested that the additional water amount can be calculated on the basis of the water absorption of recycled aggregate after 30 minutes, considered as reference time.

Consequently, mix proportions for RAC usually show a total w/c ratio and also an effective w/c ratio, lower than the previous one, because it does not consider the additional water necessary to saturate the particles. Nevertheless it is useful to specify that some researchers refer to DoE Method for concrete mix design (RRL, 1950), which mentions the free water content, instead of the effective one, but there is no significant difference with respect to the previous considerations. In fact, it is defined as the sum of the free mix water, the surface water of the aggregates and the water content of admixture less the water absorbed by the aggregate in the time between the mixing and the setting of the concrete.

3.1.4 Curing conditions

The word “curing” is used to describe the action taken to maintain moisture and temperature conditions in a freshly placed cementitious mixture to allow the hydraulic-cement hydration (ACI 308R-01), that is the series of chemical reactions that involve the mixing water and the binder particles and are responsible for the development of the mechanical properties of concrete.

Although analysing the specific reactions that govern the phenomenon is beyond the scopes of this thesis, remarking their essential features is useful for the following development of the work. Briefly, hydration regards aluminates and silicates, giving rise to the formation, respectively, of calcium aluminate hydrates (C-A-H), and calcium silicate hydrates (C-S-H) also known as cement gel. C-A-H compounds are responsible for the loss of workability, whereas C-S-H influence concrete hardening. Moreover, it should be specified that the hydration of tricalcium aluminate (C_3A) is so fast as to affect the plasticity of the mixture in a few minutes. For this reason, it is usually necessary to add gypsum, acting as a regulator of the setting, in order to slow down this process. Hydration reactions can proceed until all the cement reaches its maximum degree of hydration, or until all the space available for the hydration product is filled by cement gel, whichever limit is reached first.

Without an adequate supply of moisture, cementitious material in concrete cannot react to form good quality products. Moreover, the temperature is another important factor, since the rate of hydration is faster at higher temperatures (van Breugel, 1991). Among all the curing systems, it is possible to identify two most frequently used: water curing, which should provide a continuous cover of water on concrete surface, and steam curing, which allows to control the temperature of hydration. Generally, the increase in temperature results in a more rapid setting, accelerating the hydration of tricalcium aluminate (C_3A), while the influence on concrete hardening is more complex. Briefly, at early ages (1-7 days) the higher the

temperature the greater the compressive strength. At long curing ages (i.e., more than 28 days) the lower the temperature the greater the compressive strength. Thus, steam curing consists on a heat treatment, until a steady-state temperature is reached, followed by a short or long cooling, and it is widely applied for pre-cast concrete industry.

Kou et al. (2004) investigated the influence of curing conditions on concrete with RcCAs at different percentages, up to a total substitution of coarse natural fraction: each type of designed concrete mixture underwent water curing and steam curing regimes, and the relative compressive strength at different ages was measured (Table 3.3).

Table 3.3: Influence of curing condition on compressive strength (Kou et al., 2004).

Curing conditions	RcCAs [%]	Compressive strength [MPa]				
		1-day	4-day	7-day	28 day	90-day
Water curing	0	25.8	45.8	53.8	66.8	72.3
Steam curing	0	41.8	49.6	53.2	58.1	63.9
Water curing	20	23.6	43.2	51.2	62.4	68.0
Steam curing	20	41.9	47.9	50.3	57.4	65.9
Water curing	50	21.1	40.3	44.8	55.8	61.5
Steam curing	50	38.0	41.9	46.7	55.1	62.2
Water curing	100	15.5	26.8	36.2	42.0	50.2
Steam curing	100	28.1	32.1	35.7	41.4	48.4

The results showed that curing conditions affected concrete performance only in the early ages, and specimens which underwent steam curing showed higher compressive strength than those cured in water tank. For ages longer than 7 days, there was no significant influence of curing method. Moreover, any difference between water or steam regimes decreased as the percentage of RCAs increased.

3.2 State of the art for Recycled Aggregate Concrete (RACs)

Many experimental tests were carried out in several countries, in order to investigate the performance of concrete made with recycled concrete aggregate. The first studies about this matter started in 1970s in U.S., but only in the last ten years they greatly increased worldwide, due to the necessity to manage Construction and Demolition (C&D) waste, and achieved remarkable results.

A large number of researches investigated the possibility to employ any type of material from C&D waste, such as brick, asphalt pavement or glass cullet.

Anyway the present work will focus only on the use of recycled concrete as aggregate in new concrete production. This is related to two main reasons: first of all, old concrete is the largest part of the total C&D waste, moreover its employment showed better mechanical performance than other waste materials. The aim of this section is therefore to show what are the most remarkable results achieved by different researchers, about both fresh and hardened concrete properties. Moreover, as the investigation data make it possible, it is also proposed a comparison among the different experimental results, in order to define how recycled concrete aggregates generally affect concrete performance.

3.2.1 Workability

Glanville et al. (1947) defined workability as that property of concrete which determines the amount of useful internal work necessary to produce full compaction. Main factors that affect concrete workability are grading and shape of the aggregate, percentage of entrained air, quantity of water and admixture used.

Clearly if w/c ratio increases, concrete workability improves, but at the same time mechanical properties get worse, because excess water produces the formation of many capillary pores, which make material less dense and weaker.

As regards the aggregates, it is useful to focus that round sand gives greater workability than crushed one, while angular sand particles have an interlocking effect and less freedom of movement in the freshly mixed concrete than smooth rounded particles. As recycled aggregates are obtained by crushing structure, they are usually more angular than natural ones, so especially recycled fine concrete aggregates (RfCA) make fresh concrete quality worse. Nevertheless, the free water content is the key parameter controlling workability of fresh concrete. The higher water absorption of recycled aggregate implies that concrete made with RCA typically needs more water than conventional concrete, in order to obtain the same workability. Particularly, if recycled aggregates are employed in dry conditions, the concrete workability is greatly reduced due to their remarkable absorption capacity (Etxeberria et al., 2007). This property suggests that recycled aggregate shall be saturated before using.

The slump test with Abram's cone (EN 12350-2:2009) is the most commonly used method of measuring concrete workability. Yong & Teo (2009) investigated the influence of water absorption on concrete workability, by measuring slump values for different mixtures. According to DoE British Method (RRL, 1950), a control concrete (CC) was designed employing gravel as coarse aggregate and natural river sand as fine fraction. Keeping constant the total water/cement ratio (w/c= 0.41), two other mixes were produced by replacing,

respectively, 50% and 100% of recycled coarse concrete aggregate (RcCA). Finally, 100% of the same RcCAs was employed at SSD conditions, obtaining a fourth concrete mix. Results of slump test for each mix are showed in the following Table 3.4.

Table 3.4: Influence of water absorption of Recycled Concrete Aggregate on concrete workability (Yong & Teo, 2009).

Sample	Slump (mm)
Control Concrete (CC)	55
Recycled concrete (50% Replacement of RcCA)	10
Recycled concrete (100% Replacement of RcCA)	0
Recycled concrete (100% Replacement of SSD RcCA)	55

Increasing of percentage of RcCAs leads to slump values lower than those measured for concrete with natural aggregates, while concrete with 100% RcCAs exhibited negligible slump. This was caused by the high water absorption (6.4 %) of RcCAs, which absorbed water during the mixing process. In fact, only concrete made with recycled aggregates at SSD conditions showed competitive slump, compared to the concrete made with natural aggregates.

Furthermore, some researchers that investigated the performance of recycled concrete, not just employed recycled aggregates at SSD conditions but they also used chemical admixture such as super-plasticizers (SP). In fact, recycled concrete mixture can need low w/c ratio to reach competitive compressive strength; therefore, it is necessary the use of chemical admixtures in order to guarantee the required workability (Table 3.5).

Table 3.5: Required consistency class for different applications (EN 206:2013).

Consistency class	Slump (mm)	Application
S1	10 – 40	-
S2	50 – 90	-
S3	100 – 150	Unreinforced concrete structure
S4	160 – 210	Medium reinforced concrete structure
S5	> 220	Strongly reinforced concrete structure

Finally, it can be observed that increasing the fraction of coarse recycled aggregates in initial SSD conditions can also result in a significant increase of the slump: this can be explained by considering that part of the water absorbed by the soaked aggregates is released during mixing. In fact, this initial moisture content contributes more in enhancing the slump values for the mixtures made with RCA, than the ones made of natural aggregates (Limbachiya et al., 2012). Table 3.6 shows that the variation in slump is quite irregular, due to the other mentioned aspects which have influence on workability. However, it is interesting to note that

it is possible to obtain significant slump values if recycled concrete aggregates are saturated before mixing, even if no chemical admixture is used.

Table 3.6: Slump test results at different percentage of RcCA at SSD conditions.

Reference	RcCA (%)	RCA (%)	Effective w/c	Chemical Admixture	Slump (mm)
Limbachiya et al. (2012)	0	0	0.54		70
	30	20	0.54		60
	50	35	0.51		80
	100	70	0.48		120
Xiaoa et al. (2005)	0	0	0.43		42
	30	20	0.43		33
	50	35	0.43		41
	70	49	0.43		40
	100	70	0.43		44
Corinaldesi (2010)	0	0	0.40	SP	190 – 200
	50	29	0.40	SP	190 – 200
	0	0	0.50	SP	190 – 200
	50	29	0.50	SP	190 – 200
	0	0	0.60	SP	190 – 200
	50	29	0.60	SP	190 – 200
Malešev et al. (2010)	0	0	0.51		100
	50	34	0.51		85
	100	67	0.51		90
Kou et al. (2007)	0	0	0.45	SP	140
	20	12	0.45	SP	155
	50	30	0.45	SP	170
	100	60	0.45	SP	195
	0	0	0.55		150
	20	12	0.55		160
	50	30	0.55		170
	100	60	0.55		195

3.2.2 Compressive strength

Compressive strength is generally considered as the key mechanical property of structural concrete, as all other relevant parameters can be correlated to it. Moreover, the limitations fixed by regulations and guidelines about using recycled aggregates are also related to the target compressive strength.

For ordinary concrete, produced with natural aggregates, the parameters that most influence compressive strength are: w/c ratio, type of cement, type and quality of aggregate, and curing conditions. Obviously, when recycled concrete aggregates are employed, the replacement ratio, namely the part of natural aggregates which is replaced by recycled ones, becomes a fundamental additional parameter to take into account. Several experimental studies have been carried out

for investigating the influence of this parameter on the mechanical performance of concrete and, particularly, the decay in compressive strength and other relevant parameters with respect to the reference case of ordinary concrete. Most of these studies investigated the effect of replacing only the coarse fraction with recycled coarse concrete aggregates (RcCA) up to 100%, which corresponds to a total aggregate replacement ratio of around 60%.

Collecting several experimental studies, Figure 3.2 shows the reduction of compressive strength for recycled concrete at 28 days, as the replacement percentage of recycled coarse concrete aggregate (RcCA) increase. All results have been uniformed by considering the average values of compressive strength obtained on cubic specimens R_{cm} , while the reduction is calculated comparing the different performances, for each experimentation, to the corresponding $R_{cm,0}$ strength of the ordinary concrete, obtained without changing the other parameters (w/c, type of cement, curing conditions).

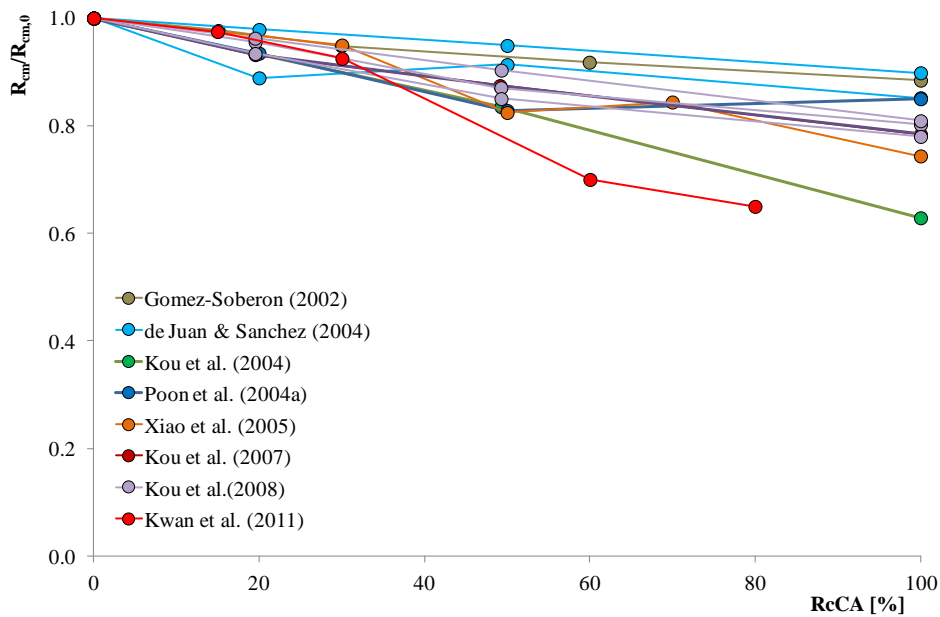


Figure 3.2: Compressive strength reduction at 28-days compared to ordinary concrete, due to the increase of RcCA replacement percentage.

The inverse relationship between the RCA content and compressive strength is due to the poor quality of attached mortar which has undergone the crushing process and which has created the zones of weakness in concrete (Kwan et al., 2012). It is interesting to note that up to 50% of replacement of natural coarse aggregates by recycled ones, the loss in compressive strength is constrained

between 5% and 20%, while the decay becomes much more significant for 100% RCA content. This scattering effect is mainly caused by two parameters: the origin of the concrete waste and the w/c ratio.

When RCAs are produced from original concretes of different qualities, the variation for compressive strength can be much larger than in the case of recycled aggregates derived by a unique source (Hansen, 1992). For instance, De Pauw (1981) found variations in 28-day compressive strength from 29.7 MPa to 49.1 MPa when concretes of identical mix proportions were produced with recycled aggregates from twelve 15-year old concretes of widely different quality. Table 3.7 summarises typical results reported by De Pauw (1981).

Table 3.7: Compressive strengths of recycled aggregate concrete produced from old concrete of various qualities (ACI 555R-01).

w/c of original concrete	Compressive strength of 15-year-old concrete (MPa)	w/c of recycled aggregate concrete	Compressive strength of recycled aggregate concrete at 28 days (MPa)
0.53	75.1	0.57	49.1
0.67	51.5	0.57	40.3
0.65	59.3	0.57	43.1
0.80	38.9	0.57	38.0
0.50	73.1	0.57	47.4
0.59	62.4	0.57	43.3
0.65	67.9	0.57	41.8
0.81	42.1	0.57	32.0
0.50	61.9	0.57	39.8
0.50	84.8	0.57	36.8
0.53	73.4	0.57	29.7
0.50	64.1	0.57	35.2

The variation in compressive strength for recycled concrete is also affected by the value of effective w/c ratio. In fact, when w/c ratio is kept constant at different percentages of RcCA, the compressive strength reduction, compared to an ordinary concrete, is higher for lower values of w/c. Nevertheless, about the role of the w/c ratio, it is more interesting to analyze how its variation affects the concrete performance at the same replacement percentage of RcCA. In order to show this point, several studies have been collected (Figure 3.3). All of them offer results of compressive strength after 28 days of water curing, both for ordinary concrete and RAC, employing ASTM Portland cement Type I. Data have been uniformed considering the average values for cubic specimens R_{cm} , and the effective w/c ratios.

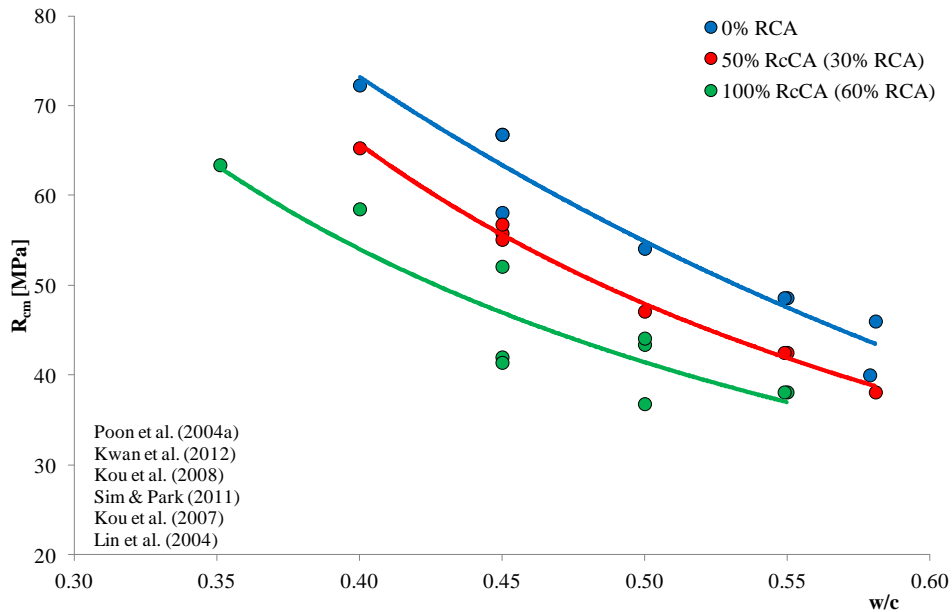


Figure 3.3: 28-days compressive strength for RCA with ASTM Portland cement Type I versus effective w/c ratio, at different RcCA percentage.

As the effective w/c ratio increases, the compressive strength decreases according to a trend quite similar compared to the ordinary concrete, while a high RCA content causes a compressive strength reduction as previous experimental results have showed. Anyway it is useful to clarify that data obtained from concrete with 100% of RcCA are strongly influenced by quality of the recycled aggregate and they result to be quite scattered.

As reported in chapters 2, several codes and guidelines for structural concrete restrict the replacement of ordinary coarse aggregates with recycled ones at a percentage of about 30%. Conversely, the results of the aforementioned researches figured out the possibility of extending this limit up to 50% or even to produce RAC with a total replacement of ordinary coarse aggregates. For example, it is interesting to compare the compressive strength obtained for ordinary concrete and RAC, obtained by using the same effective w/c ratio, the same type of cement, but with the 50% of recycled coarse concrete aggregates. In that respect, several experimental campaigns have been considered: in all of them, specimens underwent the same steps. Ordinary concrete was produced and tested at 28 days, after water curing conditions; then recycled aggregates, obtained from old concrete of different quality, were used to replace the 50% of coarse natural fraction. They were saturated before the mixing and they were employed to produce a recycled

aggregate concrete at same conditions of the ordinary one (the same type of cement was used and w/c ratio was kept constant).

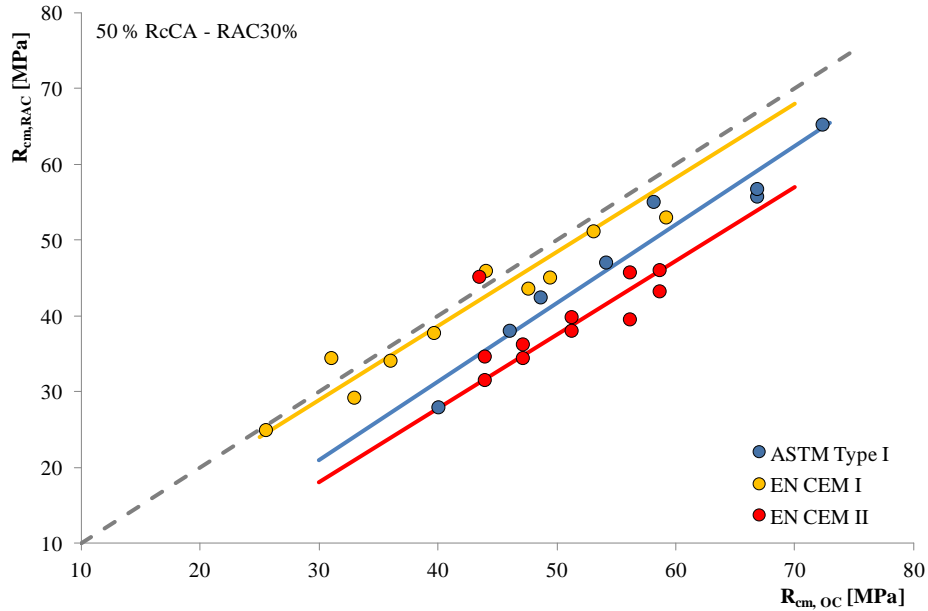


Figure 3.4: Relation between 28-days compressive strength for RAC with 50% of RcCA (30% RCA) and corresponding strength of ordinary concrete (OC).

From these data, as Figure 3.4 shows, it is possible to find a linear relation between the performance of ordinary concrete and corresponding RAC:

$$R_{cm}(RAC_{30}) = a \cdot R_{cm}(OC) + b \quad (3.5)$$

ASTM Type I: $a = 1.02$; $b = -9.22$

CEM I: $a = 0.90$; $b = 2.12$

CEM II: $a = 0.79$; $b = -1.70$

Moreover, the compressive strength ranges between almost 30 and 60 MPa, depending on the original concrete source. Hence, structural applications are feasible for RACs. A similar analysis could be proposed considering the recycled concrete obtained by a total substitution of natural coarse aggregate (100% RcCA), but in this case the large scatter of experimental results make not significant any comparison.

In all the experimental researches showed before, only coarse recycled aggregate have been employed, as this is the common position of most regulations and guidelines. Essentially fine recycled aggregates are not usually used due to their too high water absorption, which influences the water amount in the mixture. Moreover, a total replacement of natural aggregates with recycled ones affects the compressive strength too, leading to a remarkable worsening of mechanical performance for common values of w/c ratio.

Finally, only with a good quality of recycled concrete aggregate, combined with a very accurate mix-design, it is reasonable to produce a RAC with high percentage (more than 30%) of recycled aggregate, both coarse and fine, achieving adequate compressive strength performance for structural applications.

3.2.3 Static modulus of elasticity

The elastic properties of concrete are related to its main components. In the stress-strain plane, the curve for ordinary concrete is generally in-between the aggregate curve and cement paste's one. As ordinary aggregates have an elastic modulus of elasticity much greater than cement paste, concrete elastic modulus increases with the aggregate/cement paste ratio (Collepari et al., 2009).

Considering several researches carried out for investigating the performance RACs, it is possible to state that the elastic modulus generally decreases with an increase in the recycled aggregate content, while it increases with a decrease in w/c ratio or with an increase in the curing age.

Several researchers found different relations between static modulus of elasticity E for recycled concrete aggregate and the relative compressive strength at 28 days (Figure 3.5). Below some of them are reported, considering the accuracy of the experimental data, and they are compared to the relation proposed for ordinary concrete by current technical Italian standards (NTC, 2008):

- Ravindrarajah & Tam (1985) $E = 7770 \cdot R_{cm}^{0.33}$ (3.6);

- Kou et al.(2008) $E = 5775 \cdot R_{cm}^{0.408}$ (3.7);

- Corinaldesi (2010) $E = 18800 \cdot \sqrt[3]{\frac{0.83 \cdot R_{cm}}{10}}$ (3.8);

- NTC 2008 $E = 22000 \cdot \left(\frac{f_{cm}}{10}\right)^{0.3}$ (3.9).

The first three relationships derive from experimental studies on cubic specimens of RAC. Average compressive strength R_{cm} values at 28 days have been related to the chord static elastic modulus of elasticity E , interpolating experimental results. On the other hand, the last relation is taken from the Italian current regulation (NTC, 2008), in accordance with the European regulation EN 1992-1-1:2004, and it refers to ordinary concrete. In this case, the average value for cylindrical specimen f_{cm} at 28-days appears: thus, it is appropriate to convert it to the cubic compressive strength value, in order to offer a comparison with the previous experimental relations obtained for RAC.

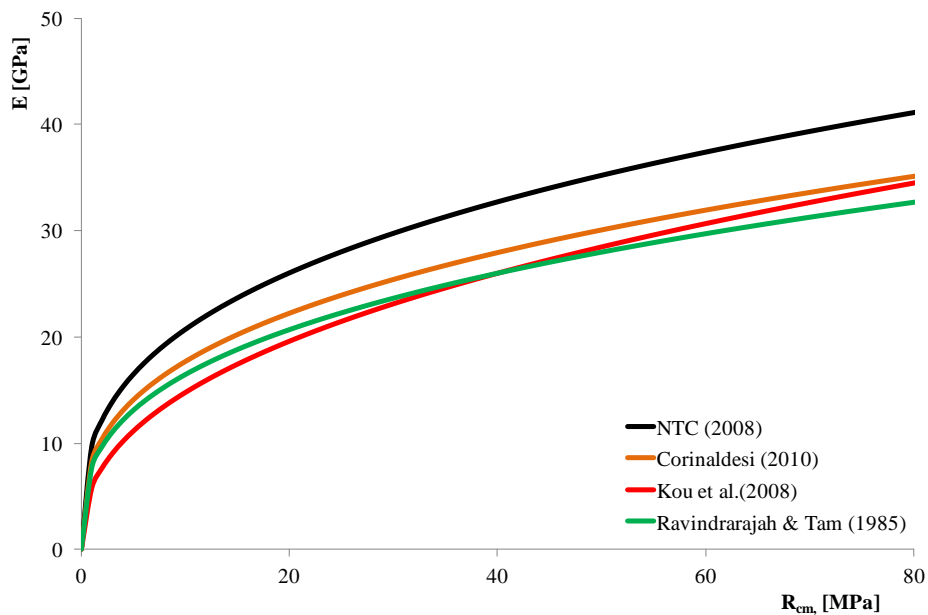


Figure 3.5: Relation between 28-days compressive strength and static elastic modulus.

The range defined by the experimental relationship is fairly narrow, while, as expected, the equation given for the ordinary concrete overestimates the elastic modulus of concrete prepared with recycled aggregate.

3.2.4 Tensile and flexural strength

Although the compressive strength is the key mechanical property, the values attained by both tensile and flexural concrete strength are also relevant as they control the serviceability conditions.

Flexural strength is usually determined by testing a concrete beam, with loadings at different points, according to specific standards (fib, 2013). All the

experimental researches about RAC showed that there is no remarkable difference between ordinary concrete and concrete with a percentage of recycled coarse aggregates up to 50%. However, the flexural strength can decrease as the coarse ordinary fraction is replaced by recycled aggregates, even if this reduction is usually between 20 and 40%. This is because the recycled aggregates tend to deform more compared to natural aggregates and the modulus of elasticity of recycled aggregates is lower than the modulus of natural aggregates (Yong & Teo, 2009).

The well known Brazilian test on cylindrical specimen is one of the most common methods for determining tensile strength. Also in this case, experimental studies show that an increase in the recycled aggregate content decreases the splitting tensile strength, especially for high percentage of replacement.

Finally, it is interesting to report what Kou et al. (2007) found in their experimental campaign. They highlighted that tensile splitting strength of the recycled aggregate concrete did not necessarily decrease when the w/c ratio increased, which apparently contradicted with common knowledge about ordinary concrete. Therefore, they concluded that as the tensile strength of concrete was significantly affected by the interfacial transition zone between the aggregate and the cement matrix, the variability of the surface texture of the recycled aggregate was probably the main reason which caused the paradoxical results (Kou et al., 2007).

3.2.5 Drying shrinkage

It is known that concrete shrinks when exposed to dry air, while it swells if it is under water. However, among these two types of deformation, drying shrinkage is the most significant one, due to its effect on the concrete behaviour. In fact, while the increase in volume induces compression on expansion restrained concrete members, drying shrinkage implies tensile stress and, then, it can result in cracks, due to the low tensile strength. Drying shrinkage develops during time and it is higher for lower values of relative humidity, but it is also affected by the water/cement ratio and the aggregate/cement ratio (Colleparidi et al., 2009). It increases due to a large amount of mixture water, while at same w/c ratio, high values of aggregate/cement ratio make the shrinkage lower.

Considering the role of these parameters, it is reasonable that RAC shows a higher drying shrinkage than the ordinary concrete (Table 3.8). This behaviour can be attributed to the supplementary water provided by recycled aggregate used. Furthermore, the old mortar attached on the RCA may also contribute in the increased shrinkage strains as the volume of cement paste increases as well

(Limbachiya et al., 2012). Experimental results available in the literature show that the partial replacement of coarse natural aggregates (up to 30%) with recycled ones, does not affect the shrinkage. Conversely, remarkable percentages of recycled coarse concrete aggregate (more than 50%), lead to higher values of drying shrinkage, due to the large amount of mixture water.

Table 3.8: Experimental results for Drying shrinkage.

Reference	RcCA (%)	Effective w/c	Aggregate/cement	Age (days)	R.H. (%)	Drying shrinkage ($\cdot 10^{-6}$)
Kou et al. (2008)	0	0.55	4.22	112		400
	20	0.55	4.22	112		450
	50	0.55	4.18	112		480
	100	0.55	4.14	112		550
Limbachiya et al. (2012)	0	0.66	6.85	91	60±5	290
	30	0.66	6.85	91	60±5	320
	50	0.61	6.32	91	60±5	450
	100	0.58	5.96	91	60±5	650
	0	0.54	5.55	91	60±5	340
	30	0.54	5.55	91	60±5	340
	50	0.51	5.08	91	60±5	520
	100	0.48	4.81	91	60±5	630
Gómez-Soberón (2002)	0	0.52	4.20	90	50	374
	15	0.52	4.20	90	50	376
	30	0.52	4.14	90	50	352
	60	0.52	4.04	90	50	410
	100	0.52	3.91	90	50	403
Malešev et al. (2010)	0	0.51	5.30	28		339
	50	0.51	5.19	28		306
	100	0.51	5.07	28		407

3.3 Experimental activities

The experimental activities carried out on Recycled Aggregate Concretes are aimed at understanding the role played by recycled aggregates in affecting the relevant properties of structural concrete. Particularly, several experimental campaigns were performed with the scope of investigating the influence on the concrete performance of the following parameters:

- Processing procedures for RCAs;

- Initial moisture condition of coarse aggregates;
- Aggregate replacement ratio;
- Nominal water-to-cement ratio.

In the following sections, details regarding the experimental activity carried out during the research are given.

3.3.1 Influence of alternative processing procedures on RCAs

The first experimental campaign described in this section is intended at investigating the influence of processing procedures proposed in Section 2.3 on the physical and mechanical performance of the resulting recycled aggregate concrete.

Materials and methods

All the mixtures were produced by using “high initial strength Portland cement”, indicated as CP V ARI RS, according to the National Brazilian Standard NBR 5733:1991, characterised by a specific mass of 3100 kg/m³, and having a chemical composition as reported in Table 3.9. The characteristic value of the compressive strength of the cement paste is 25 MPa after 3 days, with an expected rise to about 55 MPa after 60 days of hardening. The grain size distribution of the Portland cement showed that 95% of its particles are smaller than 50 µm and 50% of the particles are passing 15 µm. Moreover, a polycarboxilate superplasticizer, Glenium 51, was used for workability control, which is characterised by a specific mass of 1.07 kg/l and a solid concentration content of 30% (www.basf-cc.com.br).

Table 3.9: Chemical compounds of the CP V ARI RS cement.

Chemical components	%
CaO	67.697
SiO ₂	17.220
Al ₂ O ₃	5.537
SO ₃	4.678
Fe ₂ O ₃	3.431
TiO ₂	0.337
K ₂ O	0.337
MnO	0.269
SrO	0.256
BaO	0.153
Ag ₂ O	0.034
ZnO	0.033
CuO	0.019

Both natural and recycled aggregates were employed in this experimental campaign and, for natural aggregates, common crushed limestone were classified in three size classes according to the Brazilian standard: NA_BR (class2, class1 and sand according to Table 2.2). Meanwhile, the recycled concrete aggregates were obtained after the demolition of the hospital Clementino Fraga Filho in Rio de Janeiro (BR). The recycled aggregates were selected and analysed by the university laboratory for construction materials LABEST (PEC/COPPE – UFRJ Rio de Janeiro), and were processed as described in section 2.3. In particular, both RCA₁ and RCA₂ (see Table 2.2) were used in order to analyse the effect of processing procedures on the mechanical properties of the resulting recycled aggregate concrete.

Based on the results obtained so far, crushed concrete debris were processed to recycled aggregates, and three different mixtures were designed to analyse the different behaviour of concrete made with original (uncleaned) and cleaned recycled aggregates. The mix design of produced concrete, are reported in Table 3.10.

Table 3.10: Influence of alternative processing procedures on RCAs: Mix composition.

Aggregates and Cement												
Sand		Sand_BR										
Class1		NA _{C1} _BR			RCA _{1,C1}			RCA _{2,C1}				
Class2		NA _{C2} _BR			RCA _{1,C2}			RCA _{2,C2}				
Cement type		CP V ARI RS										
Mix composition												
Mix	CEM	w	ads.w	SP	w/c	Natural [kg/m ³]			RCA ₁ [kg/m ³]		RCA ₂ [kg/m ³]	
						Sand	C1	C2	C1	C2	C1	C2
REF	300	160	31.4	4.02	0.53	952.6	439.9	470.2				
RAC	300	160	71.8	4.02	0.53	950.4			346.6	404.0		
RAC CL	300	160	49.9	4.02	0.53	951.3					403.1	415.1

Particularly, a reference mixture, indicated as REF, was prepared with all natural components. Moreover, two additional mixtures, denoted as RAC and RAC CL, were designed with 50% (in volume) of the natural aggregates are replaced with recycled ones, with and without 15 minutes of autogenous cleaning, respectively.

All batches were produced with 300 kg/m³ cement and a w/c ratio of 0.53. To compensate the water absorption of both dry recycled and natural aggregates,

additional water was poured during mixing while taking into account the water absorption tests (see Table 2.2).

The aforementioned mixtures were produced according to the following procedure. First, sand, fine and coarse aggregates were added to the mixer and mixed for 90 seconds. Then, cement was added and mixed for another 90 seconds. In the following step, 70% of the total water was added to the aggregate blend before adding it to the mixture, then, this blend was mixed for one minute, and then added to the mixer. Finally, the superplasticizer and the rest of water was added to the mixer, and mixing proceeded for another 10 minutes.

A slump test was performed and concrete was cast (in three steps on a vibrating table for expelling the entrapped air) in steel cylinders. After one day, specimens were demoulded and the concrete was placed in a water curing room (21°C) up to the designated times for testing the compressive strength, elastic modulus and tensile splitting strength.

Results and analysis

This subsection reports a summary of the experimental results obtained from RAC samples produced as described in the previous subsection. As mentioned, three different mixtures were designed for analysing the effect of alternative processing procedure for RCAs on the mechanical properties of concretes made with them.

The fresh concrete properties were investigated through a slump test (EN 12350-2:2009). Results are reported in Figure 3.6 and clearly highlight the effect autogenous cleaning has on the mix rheology.

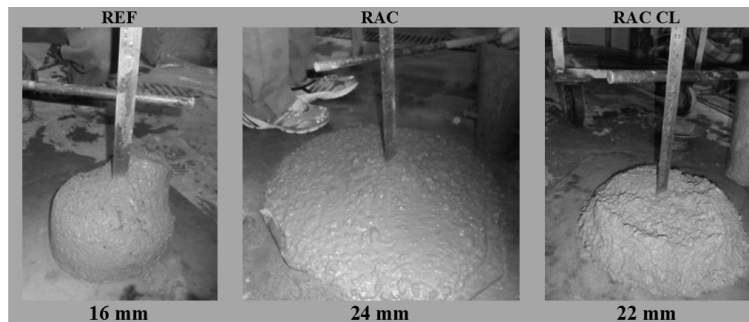


Figure 3.6: Slump test results.

First of all, it is worth mentioning that a higher slump value was observed for mixtures with uncleaned recycled aggregates (RAC) with respect to the corresponding reference mix (REF). This largely depends on the fact that the same amount of superplasticizer was added for all mixtures, whereas the absorption compensation water was added on the bases of water absorption tests carried out on

aggregates after 24 h of absorption time. As a matter of fact, recycled aggregates within the concrete mix cannot absorb such an amount of water in a short period time which is equal to the mixing time. Since the mixing process only takes 10 to 15 minutes which is much less than the absorption time used in the absorption tests (24 h), the remaining part of the water just modifies (increases) the water content in the mix (and the w/c ratio), leading to an increase in workability (and a decrease in compressive strength). Thus, such a higher amount of total mixing water available in the RAC mix, led to slump values significantly higher than those corresponding to the reference mix. Further investigations are needed to better understand the role of added water in RACs and, possibly, to achieve a sound definition of such a key parameter. The same effect is observed for the mix with cleaned aggregates (RAC CL), whose lower water absorption capacity required a lower amount of added compensation water and, led to lower slump values.

The effectiveness of autogenous cleaning of RCAs was also evaluated by conducting several compressive strength tests, elastic modulus tests and tensile splitting strength tests.

The compressive strength of concrete the three mixtures was determined at an age of 2, 7, 14, 28 and 60 days (five tests for each curing age) according to the NBR 5739:2007 on cylindrical specimens with a nominal diameter of 100 mm and a height of 200 mm.

Figure 3.7 provides the results of the compressive strength evolution. Samples of the REF mix show an average 28-day compressive strength of 33 MPa and, because of ongoing hydration, a compressive strength of 37 MPa was reached after 60 days of curing.

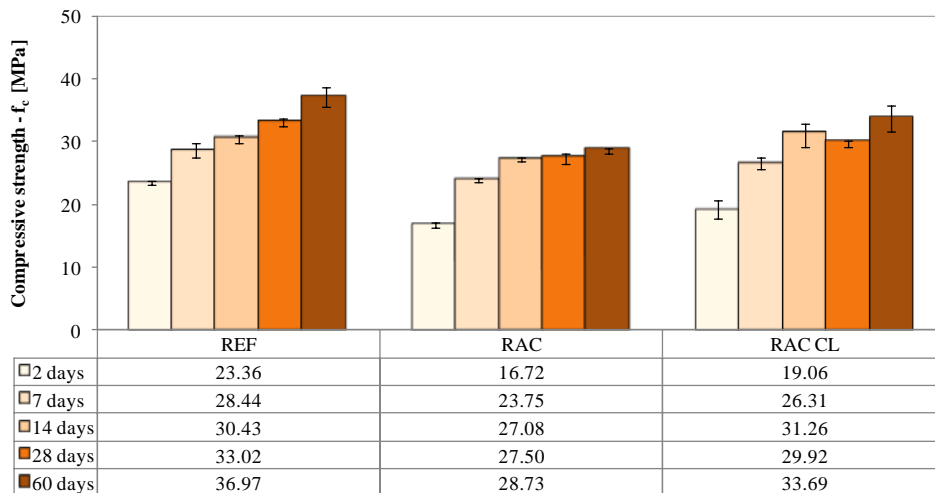


Figure 3.7: Compressive strength results.

As can be observed from the results presented in Figure 3.7, the compressive strength of RAC concrete reduced by about 20%. This is mainly due to a higher amount of water added for compensating absorption that increased the effective value of the w/c ratio. This effect and the change in the affective amount of free water was already observed before in terms of workability and rheological properties. However, the beneficial effect of autogenous cleaning clearly emerges when analysing the compressive strength results obtained for RAC CL, where a significantly smaller reduction was measured (8.9%).

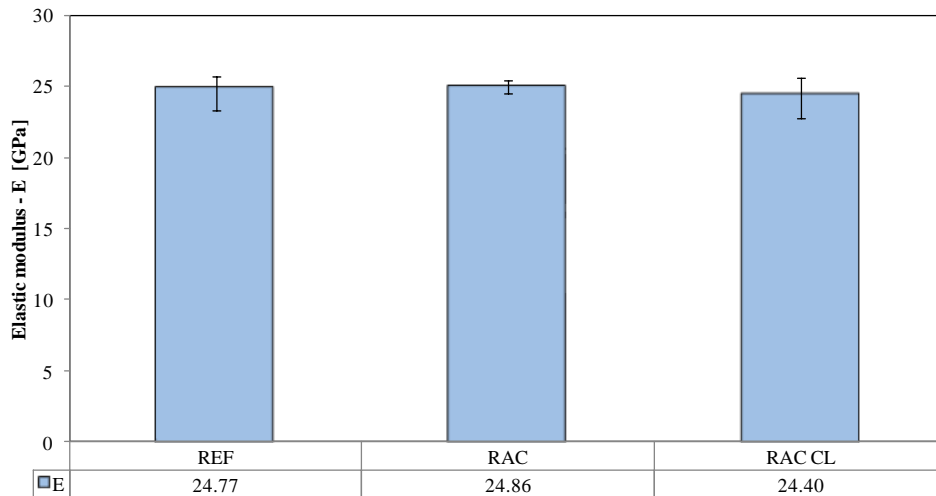


Figure 3.8: Elastic modulus.

The elastic modulus of concrete was determined in accordance with the Brazilian standard NBR 8522:2008 by using cylindrical specimens (nominal diameter equal to 100 mm and a height equal to 200 mm), tested after 28 days of water curing (three specimens for each batch). The elastic modulus of the concretes are determined from the load displacement graphs by connecting two points on the ascending branch of the stress-strain relationship with a straight line. These points represent a stress value equal to 0.50 MPa and a value equal to 30% of the maximum strength reached during compression of the test, respectively. The results presented in Figure 3.8 show that addition of cleaned or uncleaned aggregates does not significantly affect the elastic modulus. Values around 24 GPa were measured for the elastic modulus of all concrete batches considered in this study.

The Brazilian tensile splitting strength was determined from cylindrical specimens (ASTM C496-11) after 28 days of water curing (three specimens for each batch). The results show that the use of uncleaned recycled aggregates significantly reduces (i.e., around 13%) the tensile splitting strength, while

autogenous cleaning leads to higher tensile strength's and also led to a reduction in scatter (less than 4%) of the results obtained from the three tests performed on RAC CL samples (Figure 3.9).

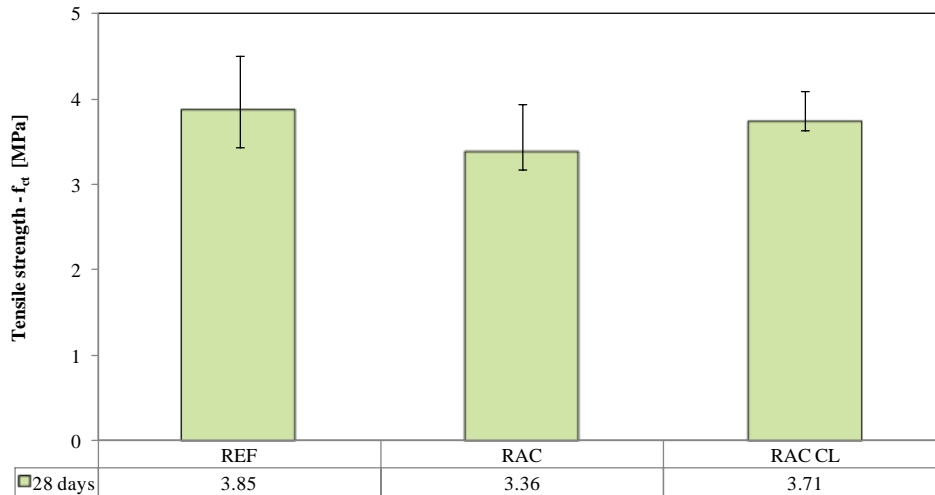


Figure 3.9: Tensile strength.

The experimental results reported in this section showed the effect of alternative processing procedures for RCAs on the physical and mechanical properties of RACs. Particularly, the accurate absorption tests carried out on the processed aggregates and the rheological characterisation of the resulting fresh concrete highlighted the actual influence of absorption water on the physical and mechanical properties of RACs. Moreover, the results obtained in terms of uniaxial compressive strength and tensile strength showed a positive effect of autogenous cleaning for the RAC samples tested in this experimental program.

Finally, it is worth mentioning that upscaling of the amount of particles and dimensions of the mill drum can have a significant effect on the actual effectiveness of the processing procedures investigated in this work. Experimental results reported in this section pointed out the potential of autogenous cleaning for RAC. A pilot application at industrial scale should be conducted to confirm similar effects.

3.3.2 Influence of the initial moisture condition of RCAs

As recycled aggregates are characterised by higher water absorption compared with natural ones, and (as described in the firsts sections of this chapter) the total amount of free water plays a key rule on the evolution of the physical and

mechanical properties at both hardened and fresh state for resulting concrete, the initial moisture condition of RCA employed in concrete is able to influence the total amount of free water available in the mixture.

For this reason, the following experimental campaign investigates the changes on mechanical and physical performance of RACs by considering the possible variation of the initial moisture condition for RCAs.

Materials and methods

Four different concrete mixtures with 30% recycled aggregate replacement are considered in the present study with emphasis on the relationship between the compressive strength development and the corresponding time evolution of the degree of hydration. Two key parameters, i.e. the water to cement ratio and the initial moisture condition of the recycled aggregates, respectively, are considered in this campaign and their impact on the final concrete quality is investigated. Particularly, their influence on both the hydration reaction and the evolution of the compressive strength of concretes made with recycled aggregates is investigated. Therefore, two mixtures are designed with a different nominal water/cement ratio, i.e. 0.45 and 0.60. Moreover, for the recycled aggregates two different initial moisture conditions were realised, according to the two following definitions:

- Dry condition (DRY): the coarse aggregates are dried for 24 hours in an oven with a constant temperature of 100°C;
- Saturated condition (SAT): the coarse aggregates are saturated for 24 hours in water and, before mixing, their surface was dried with a cloth.

As a matter of fact, natural aggregates used in ordinary concretes are generally characterised by a low water absorption capacity and their corresponding portion of “absorbed water” can easily be accounted for in the concrete mix design. On the contrary, a higher water absorption capacity of RCAs clearly depends on their production process. Particularly, internal damage and cracks due to demolition and crushing, results in a non-negligible influence of RCAs water absorption capacity on the concrete mix performance, in both the fresh state (in terms of actual workability and rheological properties) and the hardened state (in terms of mechanical properties). The processing of the RCAs as considered in this study has led to the following ranges of the grain sizes:

- C3, nominal size 19 - 31.5 mm;
- C2, nominal size 9.5 - 19 mm;
- C1, nominal size 4.75 – 9.5 mm;
- Sand, nominal size small than 4.75 mm.

Table 3.11 describes the actual composition of the four concrete mixtures considered and differentiates between the two aforementioned values of the nominal water to cement ratios and the two initial moisture conditions.

Table 3.11: Influence of the initial moisture condition of RCAs: Mix composition.

Aggregates and Cement									
Sand	Sand_IT								
Class1	NA _{C1_IT}				-				
Class2	NA _{C2_IT}				RCA _{6,C2}				
Class3	-				RCA _{6,C3}				
Cement type	CEM I 42.5 R								
Mix composition									
Mix	CEM	w	ads. w	w/c	Sand_IT	NA _{C1_IT}	NA _{C2_IT}	RCA _{6,C2}	RCA _{6,C3}
	[kg/m ³]				[kg/m ³]				
0.45DRY	410	185	0	0.45	760	130	300	100	400
0.45SAT	410	185	21	0.45	760	130	300	100	400
0.60DRY	310	185	0	0.60	850	130	300	100	400
0.60SAT	310	185	21	0,60	850	130	300	100	400

The amount of RCAs is kept constant to 30% of the total amount of aggregates, with a distribution over the different fractions, i.e. a total replacement of the coarse fraction, a partial replacement of the finer fraction, and no replacement of sand.

The volume of water absorbed by the saturated aggregates is not included in the calculation of the w/c ratio. The absorbed volumes are estimated by considering the amount of the various aggregate fractions and their respective water absorption capacity, which was determined on both the natural and recycled aggregates. Table 3.11 reports the amounts of water absorbed by recycled aggregate in saturated conditions, apart from the regular mixing water.

Finally, a common Portland cement, type CEM I 42.5 R (EN 197-1:2011), was used as a binder in all concrete mixes. For all four concrete mixtures tested, the hydration process was monitored by measuring the temperature evolution in the centre of a concrete cube during the first seven days after casting. To this end, a cubic sample of each concrete mix was cured in semi-adiabatic conditions with the aim of measuring the temperature evolution and to use this data as input for the proposed simulation model (described in chapter 5) to calculate the hydration process. For this purpose, such a concrete sample was cast within an insulated mould with a rib size of 150 mm (Figure 3.10).



Figure 3.10: Insulated mould inducing semi-adiabatic boundary conditions on the curing concrete sample.

Four out of the six side planes of the cubic sample border with a thick layer (about 100 mm) of insulation material, whereas two planes were insulated with a significantly thinner layer (of about 40 mm). Therefore, the heat produced by the hydration reaction was supposed to be mainly dissipated through the two faces bordering with the thinner layers of insulation material. Since these two faces are placed opposite from each other (namely, the top and bottom of the system depicted in Figure 3.10) a 1D heat flow was supposed to occur.



Figure 3.11: Temperature measurement inside insulated mould.

The evolving exothermic reaction under semi-adiabatic conditions leads to an temperature enhancement in the cube, which also affects the kinetics of the

cement hydration reaction. The evolution of the hydration temperature inside the cube was monitored with respect to the ambient temperature using two thermocouple wires (Figure 3.11).

Moreover, apart from the one cured within the insulated mould, ten other concrete samples of each mix were cast and cured in a water bath under isothermal conditions at a temperature T_R of 22° C. Couples of these samples were tested in compression (Figure 3.12) after 2, 3, 7, 14 and 28 days of hardening, with the aim of determining the average strength at the aforementioned curing ages.



Figure 3.12: Compression test.

Results and analysis

The time evolution of temperature is measured for the four concrete mixes described in Table 3.11. The different results obtained for such mixtures reveal the actual influence of the mix ingredients and moisture conditions of the recycled aggregates on the cement hydration reaction. Figure 3.13 shows the temperature development measured in the two concrete samples with a $w/c=0.45$. It can be observed that the sample with dry aggregates reaches the highest peak value for the temperature as well as a slightly higher rate of the hydration reaction for the ascending branch. This could likely be attributed to the relatively lower amount of water in this mix with dry aggregates. As a matter of fact, the role of the w/c ratio on the hydration process is well known and this observation is basically in line with this well-established knowledge (van Breugel, 1991). On the contrary, the sample with saturated recycled aggregates exhibited a slightly longer reaction period, which could likely be attributed to the higher amount of available water, and a slower temperature decay in the post-peak branch.

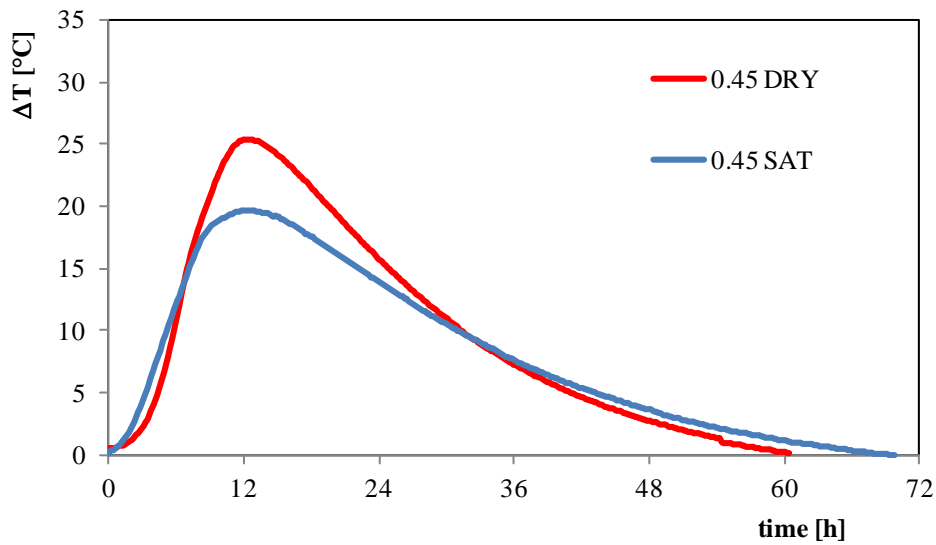


Figure 3.13: Time evolution of temperature on curing concrete samples ($w/c=0.45$).

Similar considerations can be drawn from Figure 3.14 for the two concrete mixtures with a w/c of 0.60. Higher peak values for the temperature were achieved in the concrete made with dry aggregates, but in this case the post-peak temperature decay observed in the two samples showed similar rates.

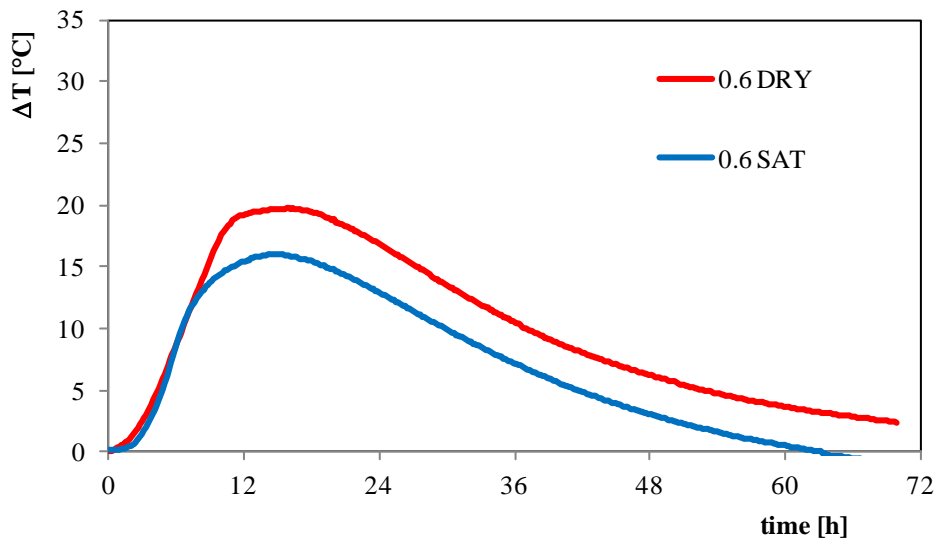


Figure 3.14: Time evolution of temperature on curing concrete samples ($w/c=0.60$).

For the compressive strength evolution, the influence of the two parameters under consideration, i.e. the w/c factor of the mix and the moisture condition of the recycled aggregates, on the hydration reaction of the four mixtures (Table 3.11) is expected to have a clear effect on the time evolution of the compressive strength.

Figure 3.15 shows the results of the compressive strength development in terms of average compressive cube strength R_{cm} , according to the procedure described in the previous subsection. The results confirm that the initial moisture content of the recycled aggregates plays an important role in the development of the compressive strength of concrete Figure 3.15. In this regard, dry aggregates lead to higher values of the R_{cm} over the investigated time span of 28 days, for both w/c ratios considered in this study. Moreover, the compressive strengths measured from the samples with recycled aggregates in dry condition and a w/c=0.6 (denoted as 0.60DRY) loose $\approx 60\%$ of their 28-day strength when applying saturated recycled aggregates. For the corresponding tests done for the w/c ratio of 0.45 with recycled aggregates under dry and saturated conditions this reduction is $\approx 50\%$. As a matter of fact, both mixtures made with saturated aggregates were characterised by a very low compressive strength, apparently as a result of the higher total amount of water (mixing water + absorbed water) which potentially led to a higher value of the actual (local) w/c ratio, depending on the possible release of the absorbed water from the aggregates into the mix.

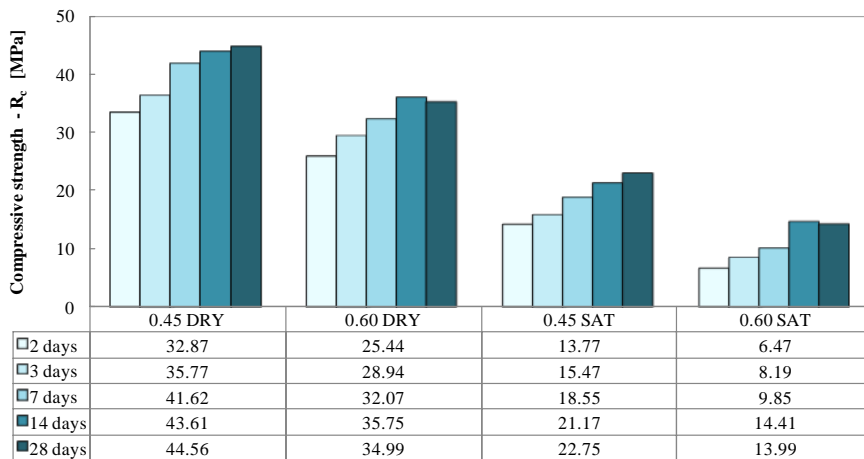


Figure 3.15: Time evolution of the average compressive strength on concrete samples.

The correlation between the hydration processes and the resulting compressive strength can be figured out by calculating the evolution of the degree of hydration from the temperature curves as presented in Figure 3.13 and Figure 3.14 and by comparing the results with the strength measurements reported in

Figure 3.15. A deeper investigation towards the quantitative relationship between these hydration-related measurements and the compressive strength is proposed in the following chapters 5 and 6.

3.3.3 Influence of the aggregate replacement and water to cement ratios

Once having defined the key role of the initial moisture condition of RCA on the resulting properties of RACs, it is important to understand how this parameter affects the nominal value of the water-to cement ratio. With this aim, the following experimental campaign considers the variation of the initial moisture condition by combining the possible variation of the aggregate replacement ratio and the water to cement ratio.

Materials and methods

This subsection describes the mix composition and mix procedure for the concrete batches considered in this campaign. All mixtures were produced by using a high initial strength cement, denominated as CEM I 52.5 R according to EN 197-1:2011. Meanwhile, three different size ranges were considered for the aggregates: sand (nominal diameter smaller than 4.75 mm) and coarse aggregates (C1 and C2 classes already defined in the previous sections).

Table 3.12: Influence of the aggregate replacement and water to cement ratios: Mix design.

Aggregates and Cement								
Sand	Sand_IT							
Class1	NA _{C1_IT}				RCA _{3,C1}			
Class2	NA _{C2_IT}				RCA _{3,C2}			
Cement type	CEM I 52.5 R							
Mix composition								
Mix	CEM	w	w/c	Sand_IT	NA _{C1_IT}	NA _{C2_IT}	RCA _{3,C1}	RCA _{3,C2}
	[kg/m ³]							
0.50NATDRY	344	172	0.5	742	554	554	-	-
0.50NATSAT	344	172	0.5	742	557	557	-	-
0.50RAC30DRY	344	172	0.5	742	554	-	-	474
0.50RAC30SAT	344	172	0.5	742	557	-	-	505
0.50RAC60DRY	344	172	0.5	742	-	-	440	474
0.50RAC60SAT	344	172	0.5	742	-	-	478	505
0.40RAC60DRY	430	172	0.4	712	-	-	422	454
0.40RAC60SAT	430	172	0.4	712	-	-	458	484
0.60RAC60DRY	287	172	0.6	762	-	-	452	487
0.60RAC60SAT	287	172	0.6	762	-	-	491	519

The first rows of Table 3.12 report the aggregate types employed for concrete production, while their main characteristics are summarised in Table 2.2.

It is worth highlighting that natural sand derived from cracking limestone rocks is employed in this study. In fact, no recycled sand is employed, as it would have been too porous and, then, it would have had a significantly detrimental effect on the resulting concrete properties (Lima et al., 2013). Conversely, in this campaign a combination of both NAs and RCAs were employed as coarse aggregates. Ten different concrete mixtures were produced for investigating, mainly, the influence of the three following parameters:

- (nominal) value of the water-to-cement ratio: 0.40, 0.50 and 0.60;
- RCAs-to-NAs replacement ratio ranging from 0 to 30 to 60 % relative to the total volume of fine and coarse aggregates (i.e. considering also the natural sand);
- initial moisture condition of the coarse aggregates (Koenders et al., 2014): oven-dried, realised by heating the aggregates for 24 hours at a temperature of $100\pm 5^\circ\text{C}$ (DRY), and saturated surface dry, obtained by submerging the aggregates in water for 24 hours (SAT).

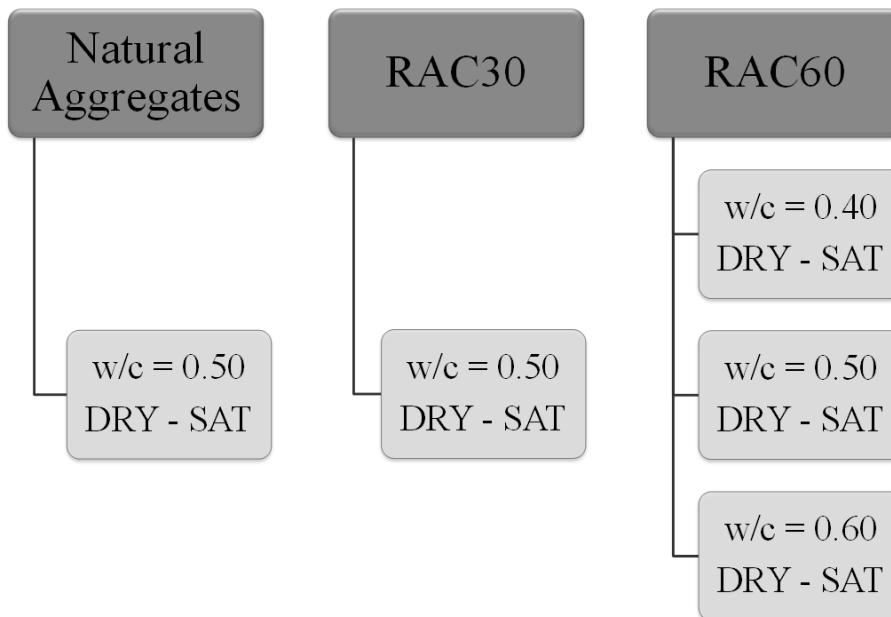


Figure 3.16: Experimental campaign.

Figure 3.16 shows a schematic representation of the mixtures produced for investigating the influence of recycled aggregates in the RACs, while Table 3.12

describes into detail the mix compositions. In all mixtures, the fine fractions (i.e., sand) represented 40% (in volume) of the total amount of aggregates, while the remaining 60% is equally divided into two fractions of coarse aggregates (i.e., C1 and C2).

The first two reference mixtures described in Table 3.12 were obtained with only natural aggregates (NAT in the mixture labels), a nominal water-cement ratio of 0.50 (also mentioned in the labels) and two alternative initial moisture conditions of the coarse aggregates (i.e., DRY and SAT).

Therefore, a RCAs-to-NAs coarse aggregate replacement of 30% was obtained via a complete replacement of the coarse fraction (namely class C2) with the corresponding ones made of RCAs, whereas 60% was achieved by replacing both fractions C1 and C2 of the NAs with the corresponding fractions of RCAs. Then, the two mixtures denoted as 0.50RAC30DRY and 0.50RAC30SAT were derived from 0.50NATDRY and 0.50NATSAT, by fully replacing the C2 fraction with an equal volume of RACs. Similarly, the two mixtures, denoted as 0.50RAC60DRY and 0.50RAC60SAT, were obtained from the reference ones by replacing all the coarse aggregates (i.e. classes C1 and C2).

Finally, the last four rows refer to the composition of the two mixtures obtained by either reducing to 0.40 or raising to 0.60 the nominal w/c ratio: the internal proportion between the various aggregate fractions were kept unchanged in all mixtures. For each mixture, nine compressive strength tests were conducted on cubic specimens according EN 12390-3:2009 after 1, 3 and 28 days of curing in a water bath under isothermal conditions at a temperature $20\pm 2^{\circ}\text{C}$. Moreover, the time development of temperature was measured in the center of the cubes, prepared for all concrete mixtures and cured in semi-adiabatic conditions so that an indirect monitoring of the hydration process could be registered and applied to the numerical procedure as recently proposed in the scientific literature (Martinelli et al., 2013). As a matter of fact, the concrete specimens prepared for compressive strength measurements were ordinarily cured in isothermal conditions at room temperature. However, due to the small size of such specimens and due to the quick dissipation of the reaction heat to the environment, no significant temperature enhancement could be measured that could be of use for a numerical hydration analysis (see chapter 5). Therefore, a special insulated mould was designed to measure the evolution of the hydration temperature inside a cube such that a significant temperature enhancement was monitored with respect to the room temperature, using two thermocouple wires (as already described in the previous section).

Results and analysis

The results obtained from the experimental campaign are analysed and discussed in this subsection. Particularly, Figure 3.17 and Figure 3.18 show the time evolution of compressive strength and temperature during the first 28 days of hardening.

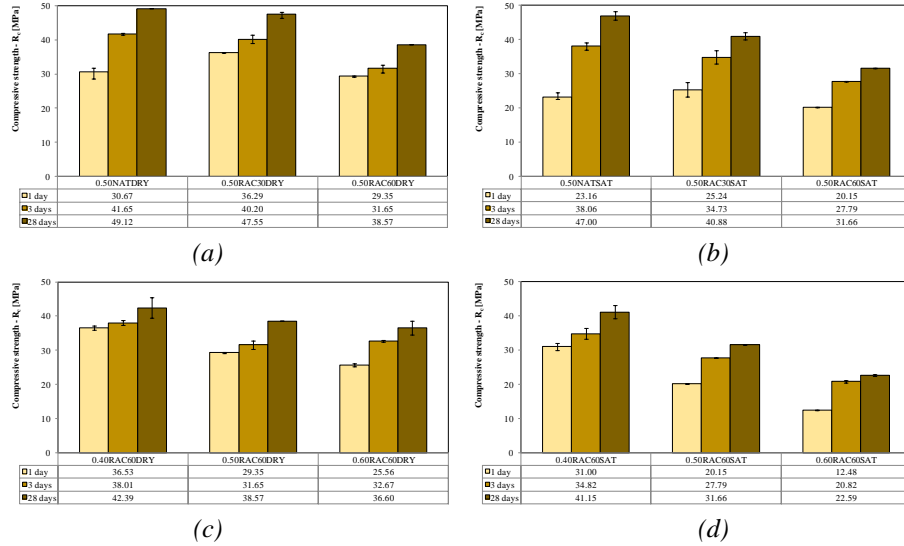


Figure 3.17: Compressive strength time-evolution.

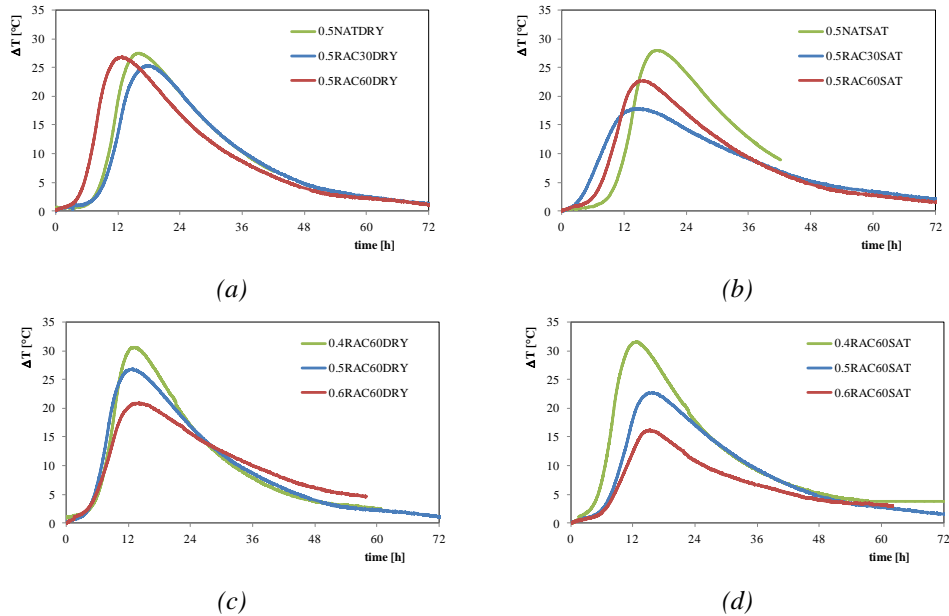


Figure 3.18: Temperature-time evolution.

The analysis of these results clearly show that the use of RCAs in concrete, as well as their initial moisture condition, influence the resulting concrete performance.

First, when comparing the compressive strength results of the concrete mixes characterised by the same nominal water-to-cement ratio and same initial moisture condition (i.e., $w/c=0.5$, DRY and SAT) it turns out that with enhancing aggregate replacement ratio, the 28 day compressive strength is decreasing. This effect becomes even more pronounced whenever employing saturated initial moisture conditions (SAT). This result can be explained by the higher porosity of recycled aggregates. In fact, when a SAT condition is employed, the aggregates tend to release accumulated water into the mixture and consequently to change the water-to-cement ratio. On the contrary, when DRY conditions are adopted, the aggregates tend to absorb part of the mixing water and, then, reduce the actual water-to-cement ratio. This phenomenon is less evident when natural aggregates are used because of their lower absorption capacity and, consequently, the amount of water, potentially released or absorbed into a mixture is negligible compared to the total amount of mixing water. On the other hand, analysis of the compressive strength results of those mixtures characterised by the same aggregate replacement ratio (i.e., RAC60), but with different nominal water-to-cement ratios (i.e., moving from 0.40 to 0.50 to 0.60), highlights the key impact of the w/c ratio on the final strength of concrete, as was already known from literature. It is worth mentioning that also in this case, the initial moisture condition plays an important role. In fact, with increasing nominal water-to-cement ratio, the gap between the DRY and SAT mixtures also increases (by comparing the 28 days compressive strength).

A more fundamental analysis can be performed by considering the differences of the temperature measurements in time, as reported in Figure 3.18. Experimental results highlight that a lower w/c ratio results in a faster acceleration of temperature. A similar effect was observed for enhancing aggregate replacement ratio or whenever applying DRY aggregate conditions.

Based on the above considerations and the analysis of results, it is clear that the initial moisture condition and the aggregate porosity tend to modify the water-to-cement ratio and, for this reason, an effective w/c ratio taking into account both the initial moisture condition and the aggregate porosity can be defined as follows:

$$\left(\frac{w}{c}\right)_{\text{eff}} = \frac{w}{c} + \frac{w_{\text{add}}}{c} - \delta \cdot \left(\sum_{i=1}^n \frac{P_i \cdot P_i}{c}\right) \quad (3.10)$$

where w/c is the nominal water-to-cement ratio, w_{add} is the extra water added to the mix from the (partially or totally) soaked the aggregates, p_i and P_i represent the absorption capacity and the weight in the mixture of the i -th aggregate fraction, and

δ is a parameter that takes into account the initial moisture condition of the aggregates and is zero in SAT conditions and 0.5 in DRY ones. The calibration $\delta=0.5$ for DRY condition is that during mixing and casting it turned out that the aggregates are able to absorb an amount of water equivalent to 50% of their 24-hour capacity (see chapter 2). Table 3.13 reports the values of the effective water-to-cement ratio calculated by equation (3.10) and later used as input values for modelling the time evolution of the degree of hydration (chapter 5).

Table 3.13: Effective water-to-cement ratio values.

Mix		nominal w/c	effective w/c
0.50NAT	DRY	0.50	0.50
	SAT	0.50	0.50
0.50RAC30	DRY	0.50	0.46
	SAT	0.50	0.50
0.50RAC60	DRY	0.50	0.39
	SAT	0.50	0.50
0.40RAC60	DRY	0.40	0.32
	SAT	0.40	0.40
0.60RAC60	DRY	0.60	0.47
	SAT	0.60	0.60

4. Insight into the influence of cement replacement in Recycled Aggregate Concrete

Since concrete is the most widely used construction material, several solutions are nowadays under investigation to reduce the environmental impact of its production processes. They often consist of partially replacing "natural" constituents with recycled ones, in view of the twofold objective of reducing both the demand of raw materials and the amount of waste to be disposed in landfills.

This chapter analyse the feasibility of producing structural concrete by combining both recycled concrete aggregates and fly ash. A brief overview on the influence of fly ash in concrete mixtures are outlined. Then, the results of a wide experimental campaign carried out on concrete samples made with both recycled concrete aggregates (RCAs) and fly-ash (FA), respectively in partial substitution of natural aggregates and cement, are proposed.

The reported results highlight the time evolution of compressive strength and the tensile strength value achieved at 28 days, along with some relevant physical properties, such as permeability and resistance to chloride ion penetration. These results clearly demonstrate the feasibility of producing structural concrete made with significant amounts of the aforementioned recycled constituents and industrial by-products clearly.

4.1 Fly Ash in Recycled Aggregate Concrete

Blast-furnace slag, fly and bottom ash and silica fume are the most used admixtures for concrete (Isaia et al., 2003). Fly ash usually derives from coal combustion in boilers of power plants, as a result of the reactions and transformations underwent by mineral impurities of coal (such as quartz, clay and pyrite). This non-combustible fraction is heated to over 1400 °C in the combustion chamber, then it melts and forms small droplets dragged by flue gas, which undergo a sudden cooling as they leave the boiler and, finally, solidify as glassy particles of spherical shape. The filters installed in power plants purifies fumes and separating ashes, which are finally sent to the storage silos (Beltz, 2009). The most interesting aspect about fly ashes concerns with their chemical characteristics: they are mainly

constituted by silica (SiO_2), alumina (Al_2O_3), and iron oxide (F_2O_3) and, hence, their composition is rather similar to natural pozzolana. Moreover, their microstructures are comparable, because fly ashes are constituted for more than 70% by amorphous glassy particles.

These important properties justify why fly ash is considered as concrete mixing material and, then, it is valued as an economic resource. In that respect, the most important power companies, e.g. AEP in the U.S., TEPCO in Japan or Enel in Italy, are investing in scientific research about fly ash applications in concrete production.

Since 1970s fly ash has been used in concrete as a mineral admixture, due its pozzolanic properties. However, only in recent years a big deal of research developed in order to investigate how it affects performance of recycled aggregate concrete. Although the use of recycled aggregate has a negative effect on the mechanical properties of the concrete, it was found that the addition of fly ash results in mitigating this detrimental effect and enhancing concrete durability. Considering that fly ash can be used as cement replacement or as an additional cementitious material in concrete, in the following subsections the main consequences of this by product on fresh and hardened state characteristics of RAC are outlined, based on some experimental results available in literature.

4.1.1 Workability

The high fineness (dimension between 1 and 100 microns) and spherical shape of fly ash particles remarkably improve workability of fresh concrete, both if fly ash is used as cement replacement or as a filler replacing the fine aggregate. Obviously this benefit is more evident as the percentage of fly ash used in concrete mixture increases, but usually guidelines or regulation allow for a maximum replacement in the range of 15 to 25%, due to its influence on strength development. Moreover, a better fluidity of fresh concrete can also take water/binder ratios lower for the same workability, getting better concrete mechanical performance.

4.1.2 Compressive strength

The contribution to the development of concrete strength due to fly ash is quite different with respect to the ordinary one provided by Portland cement, as the two constituents have distinctive chemical characteristics of pozzolanic materials. At earlier stages, the use of fly ash in concrete mixtures slows the hydration reactions down, because pozzolana gets involved only after cement hydration, as soon as a necessary amount of calcium hydroxide, able to react with silica ash, forms (Collepari et al., 2009).

In terms of mechanical performance, the main consequence is that fly ash concrete shows a lower compressive strength than cement concrete at early ages, but its strength development in the long term generally close this gap. This behaviour is emphasised as the percentage of fly ash increases, but, meanwhile, mechanical performance gets worse for high percentage of fly ash.

Since most of the experimental studies available on RAC consider the possibility to replace only the coarse ordinary aggregate fraction, it is interesting to realise how fly ash affects mechanical performance for concrete with 100% of RcCA. Therefore, some experimental results for RAC with ASTM Type I Portland Cement (ASTM C150/C150M-12) are analysed below, stating that all of them referred to water/binder ratio (w/b), following the ACI 318-11 approach.

The percentage of Class F fly ash used as partial cement replacement was usually between 15 and 30%, and as expected, at 28 days the compressive strength of RAC with fly ash was lower compared to Portland cement recycled concrete, but after long curing ages (50-60 days), both materials showed almost the same strength (Figure 4.1). However, although the chemical reaction of fly ash led to slightly higher values of strength after 60 days of curing, the mechanical performance was still far from the ordinary concrete. In order to highlight the similar behaviour of different experimental studies analysed, average values of compressive strength R_{cm} have been multiplied by w/b ratio.

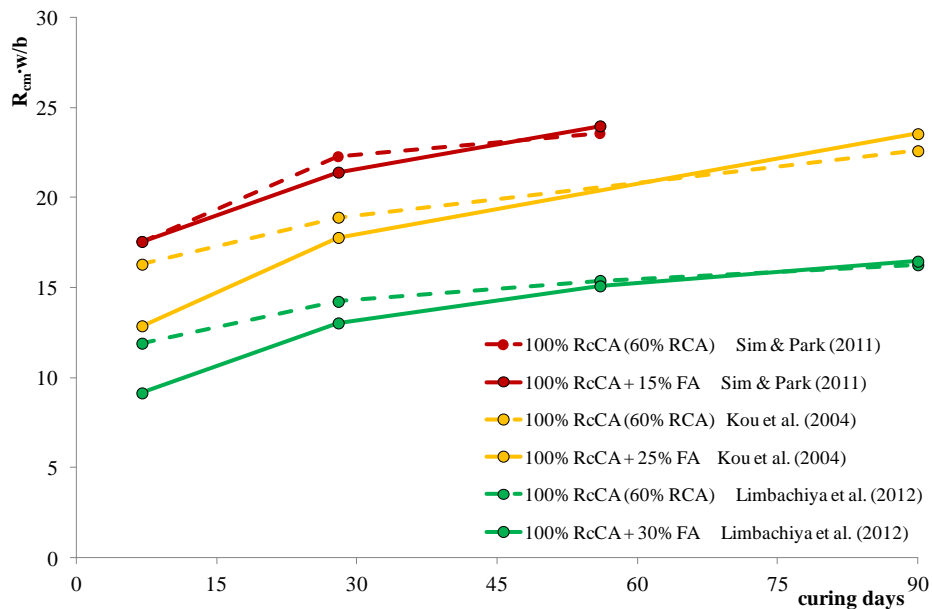


Figure 4.1: Compressive strength development using Class F Fly Ash as partial Portland cement for concrete with 100% RcCA.

On the other hand if fly ash is used as additional cementitious material, remarkable results may be obtained by partially replacing natural sand. In fact, the pore structure improves and, particularly, the volume of macro pores reduces, with favourable consequences in terms of mechanical performance (Lima et al., 2013). In these conditions the RAC compressive strength, even if only at long ages, is very similar compared to the ordinary concrete.

A significant example of this behaviour was proposed by Kou et al. (2008) in their experimental studies. Recycled aggregate concrete was designed with ASTM Type I cement (ASTM C150/C150M-12) and a replacement percentage of coarse natural aggregates up to 100%. Then, the same batches were obtained employing Class F fly ash as additional binder material. Compressive strength at different curing ages was measured and compared to an ordinary concrete, made with Portland cement and natural aggregate. Experimental results showed that RAC with fly ash (RAC+FA) achieved higher compressive strength than Portland Cement RAC since early ages. Moreover its mechanical performance was certainly competitive at 28 days, while it was even better at long ages. Compressive strength of RAC+FA obviously improved as w/b ratio decreased (Figure 4.2).

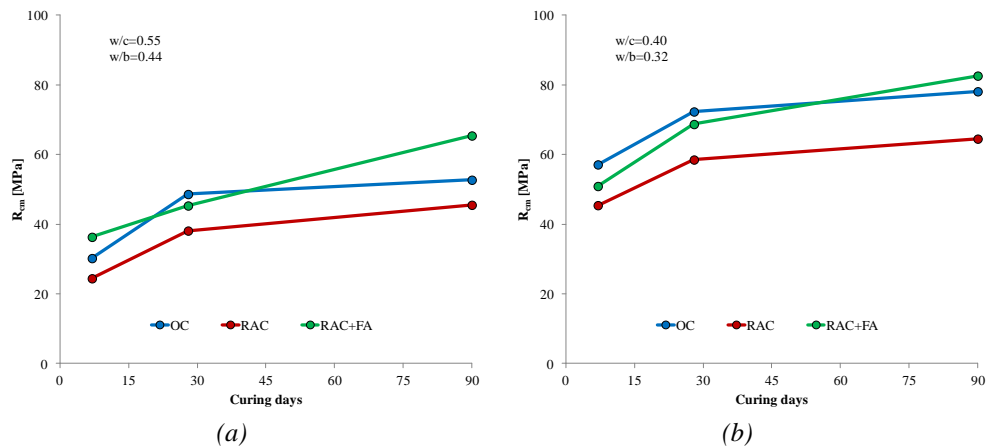


Figure 4.2: Compressive strength development using Class F Fly Ash in addition to Portland cement for concrete with 100% RcCA, at different w/b ratio (Kou et al., 2008).

These interesting results suggest that fly ash can be used not only as an example of sustainable building development, but also for a satisfactory performance in terms of compressive strength for recycled aggregate concrete.

4.1.3 Alkali-silica reaction

Among concrete deterioration causes referable to the aggregates, the alkali-silica reaction (ASR) is perhaps the most severe, due to the intensity of degradation and also for extension of phenomenon. However, this is an aspect of concrete chemistry which appears in most of the studies about the material durability.

Some forms of silica present within the aggregate can react with the alkali of cement (sodium and potassium) to form alkali silicate hydrates, which aim to expand and are strongly disruptive towards the surrounding cement paste. The consequences are the formation of cracks or localised material expulsions that can seriously affect the durability of concrete structures. ASR depends on content of alkali in concrete, reactivity degree of silica and moisture content of the environment. However, it occurs very slowly and it is accelerated by high temperatures. The pitfall of this phenomenon is essentially related to two characteristics. First, the reactive silica is not distributed uniformly: this involves the risk of not highlight its presence if aggregate specimen does not contain any particles of reactive silica, and to consider, therefore, acceptable an aggregate that should be discarded. Moreover, ASR occurs after some time, even after many years from concrete casting, when it is difficult any remedial action able to stop the phenomenon.

As regards RAC, experimental studies show that recycled aggregate concrete is usually free from alkali-silica reaction. In fact, in the case when it contains recycled aggregate that had been exposed to degradation by ASR, this reaction may not develop because it has been extinguished in the original concrete, or it could never develop because the ideal conditions to expand are not available. However, it could appear in the RAC if such conditions are present: for example, if recycled aggregate comes from a partial reactive concrete, or if cement and recycled aggregate alkalis may increase the pH in RAC thus becoming more aggressive than pH of ordinary concrete, where the cement is the only alkalis source (Barreto Santos et al., 2009).

The addition of fly ash, which also contains reactive silica, reveals paradoxically beneficial towards expansibility of alkali-silica gel, on condition that it does not exceed certain minimum dosage. In fact, the increase of reactive silica leads to a greater surface area of reactive material, and therefore to a lower alkali concentration for the unit area. Most recent studies agree on this beneficial effect provided by pozzolanic material in concrete. For example, Enel researches state that the use of ashes from coal, effectively allows to prevent the potential alkali-silica reaction, while American and Australian studies suggest also the percentages of employing in the mixture. CCAA reports that “a 20% cement replacement with

fly ash was found to control ASR expansion in the new concrete to safe levels” (CCAA, 2008). In accordance with this point, the American NRMCA published a study about fly ash effects, highlighting how “for adequate resistance to alkali silica reaction (ASR) with some types of aggregate and for sulfate resistance, more than 25% of fly ash frequently is required” (NRMCA, 2008).

4.1.4 Carbonation depth

The hydration of cement produces a certain amount of calcium hydroxide $\text{Ca}(\text{OH})_2$, which ensures that concrete pH is in the range of 12.5-13.5. In this highly alkaline environment steel rebar is passivated and protected from corrosion. Carbonation is the process that leads to the formation of calcium carbonate through the reaction of carbon dioxide in the air with calcium hydroxide or other constituents of concrete (silicates and aluminates), resulting in a reduction of the pH from around 12 to below 9.



Under such a value of pH, the steel rebar becomes active and the corrosion process is initiated affecting the interface steel-concrete and the loading carrying capacity of reinforced concrete element. This process starts at the surface, then slowly moves deeper and deeper into the concrete, so it is usually measured by carbonation depth (mm).

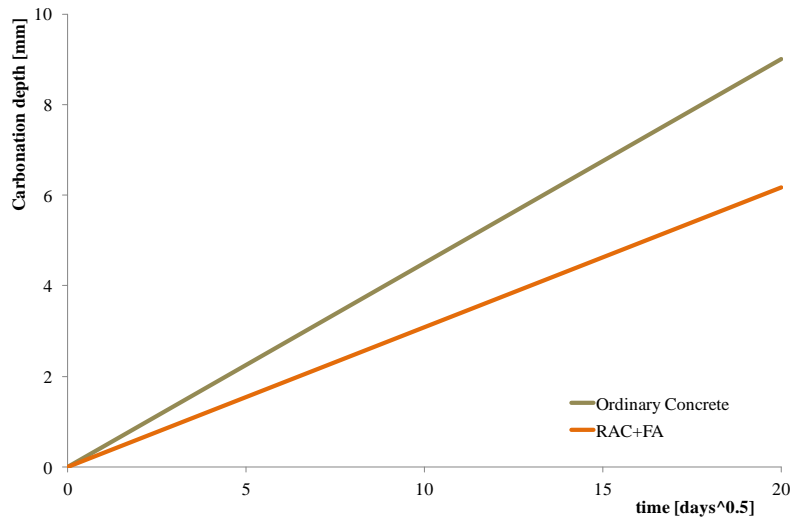


Figure 4.3: Carbonation depth for ordinary concrete and RAC+FA, as function of time of exposure (Corinaldesi & Moriconi, 2009).

Levy & Helene (2004) found that by using concrete recycled aggregates, with 100% replacement, the carbonation depth is lower when compared with ordinary concrete made by natural aggregates. In fact the higher alkaline reserve in RAC, due to the old mortar and calcium hydroxide particles, acts by protecting concrete surface against carbonation mechanisms (Corinaldesi & Moriconi, 2009).

Moreover, also the addition of fly ash proved to be very effective in reducing carbonation risk (Figure 4.3). Sim & Park (2011) noted that the more the amount of pozzolanic materials the deeper carbonation depth developed, because the calcium silicate hydrate formed from the pozzolanic reaction absorbed more alkali ions, hence lowering pH level in concrete. However, the same authors highlighted how the low carbonation resistance particularly at early ages was compensated with maturity and better microstructure by adding pozzolanic materials. In fact, the progress of carbonation process is governed by the pore network characteristics, so experimental results showed that the carbonation becomes limited because of the increasing difficulty for carbon dioxide to penetrate into the depth of the concrete pore network (Limbachiya et al., 2012).

Therefore it can be concluded that the recycled aggregate concrete with fly ash addition can provide sufficient resistance to the carbonation, increasing the service life of reinforced concrete structures.

4.1.5 Chloride ion penetration resistance

Permeability is a very important feature of reinforced concrete, as it generally controls its durability. Chloride attack can be due to the exposure to seawater, to de-icing salts or to other environmental and industrial conditions. Chloride ions penetrate in concrete by diffusion along water paths or open pores. Part of these chlorides can react with the cement hydrate products, mainly tricalcium-aluminates (C_3A), forming stable chloro-complexes. If the concentration of chloride ions exceeds the amount that could react with some components of hydrated cement paste, the remaining free chloride ions may lead to the initiation of corrosion process (Limbachiya et al., 2012).

The most common method used for assessing the chloride ion penetration resistance in concrete is the measurement of electrical charge passing in specimen, put into voltage cells and connected to sodium chloride solution. Experimental results show that the chloride ion penetration resistance becomes poorer as the amount of recycled concrete aggregate increases (Li, 2008), and this can be easily attributed to the higher porosity of that material. However, some researches (Limbachiya et al., 2012) specify that substituting 30% of natural coarse aggregates

by the recycled ones, has no significant effect on the chloride ions content compared to an ordinary concrete.

It is also interesting to examine the effect of fly ash content. The penetrability of concrete usually decreases with the addition of supplementary cementitious material such as fly ash (Figure 4.4). As pointed out above, part of the chlorides ions in the solution can react with some component of the cement such as the C_3A , while blended cement contains less C_3A than the Portland cement concrete. Nevertheless, it is also worth mentioning that fly ash contains higher proportions of active alumina compared to Portland cement (around 30% by weight), which is capable of binding and immobilizing chloride ions in solution. Moreover, fly ash is characterized by a slow reaction with portlandite to produce a secondary C–S–H that fill the coarser capillary pores, largely present in recycled concrete, and leads to a low porosity, improving resistance to permeability.

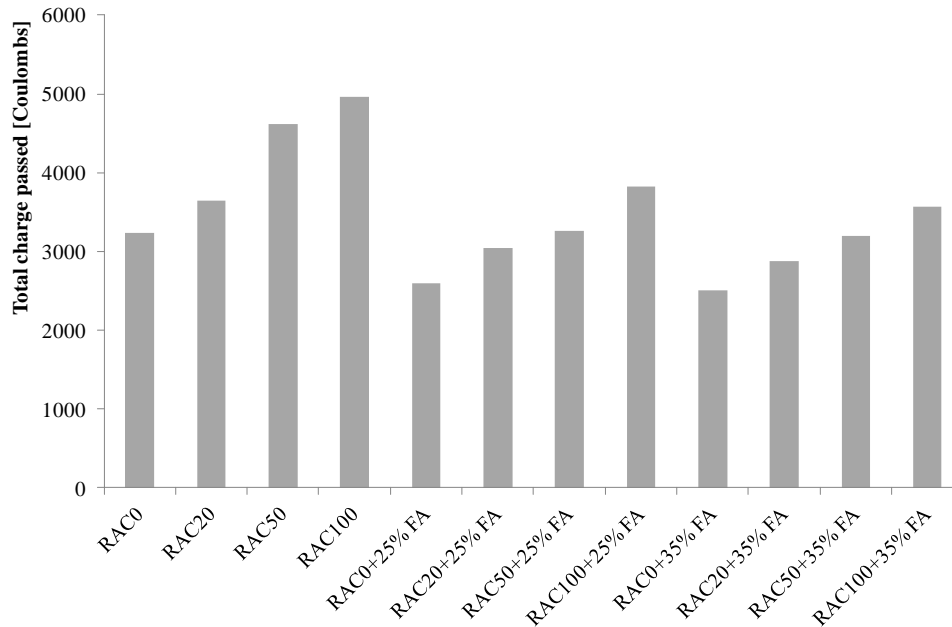


Figure 4.4: Chloride ion penetrability described in total charge passed measured at different percentage of fly ash after 28 days of curing (Kou et al., 2007).

However, Zhang & Gjorv (1991) assert that permeability of concrete is more affected by cementitious matrix than the lightweight aggregate porosity. In that respect it is interesting to focus on the relation between chloride ion resistance (in total charge passed) and fly ash content in concrete, as highlighted in a research developed by Valente et al. (2011), see Figure 4.5.

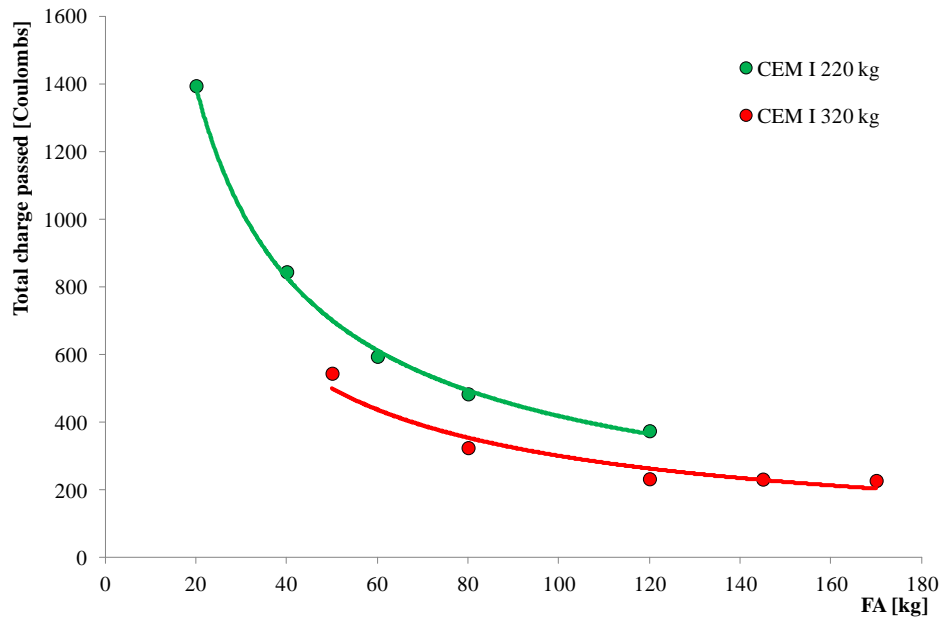


Figure 4.5: Relation between chloride ion penetrability and fly ash content in concrete mixture (Valente et al., 2011).

4.2 Experimental activities

4.2.1 Mix composition and experimental programme

The whole experimental programme discussed in the following subsections is aimed at investigating the possible influence of RCAs and FA on the key properties of the “eco-friendly” concretes under consideration. At this purpose, the behaviour of twelve different concretes made with the aforesaid recycled constituents has been studied. Moreover, a further mixture, assumed as a “control mix”, has been designed and realised with only natural aggregates and Portland cement.

The recycled concrete aggregates employed for this campaign were supplied by an Italian dealer company and certified according to the European standards (EN 12620:2013). They were obtained by crushing concrete rubbles coming from demolitions. Table 2.2 summarises the key results of the qualification tests carried out on RCAs.

Moreover, according to the European Codes and Standards, common crushed limestone particles were employed as natural aggregates (EN 12620:2013). Both recycled and natural aggregates were selected, cleaned and sieved in laboratory. Their maximum nominal diameter d_{\max} was 31.5 mm, and four size fractions were sorted:

- C3 fraction, ranging from 19 to 31.5 mm;
- C2 fraction, ranging from 9.5 to 19 mm;
- C1 fraction, ranging from 4.75 to 9.5 mm;
- Sand, having nominal diameter smaller than 4.75 mm.

Some of the most important physical properties of both recycled and natural aggregates, such as the mass density and the water absorption capacity, were measured for according to the ASTM C127-12, for coarse particles, and ASTM C128-12, for fine ones.

Table 2.2 reports such measures and highlights the lower mass density and the higher water absorption of RCAs with respect to the NAs. The table points out the higher water absorption of RCAs. As already mentioned in chapter 2, this is a well-known feature of RCAs, clearly deriving from the crushing process of demolished concrete debris needed to obtain particles to be employed as aggregates in concrete.

Common Portland cement, type CEM I 42.5 R (see the European classification EN 197-1:2011), was employed as a binder. It is basically made of clinker, without the addition of any binder or inert components.

The consequence of the partial replacement of cement with FA was also

investigated in this study. For this purpose, according to ASTM C618-05 specifications and in compliance with both European EN 450:2012 and EN 12620:2012 standards, a class F coal Fly Ash was considered. The chemical composition and some physical properties of both cement and fly ash are reported in Table 4.1.

Finally, an acrylic-based super-plasticizer was also used to control the workability of the fresh concrete mixes without modifying the water-to-cement (w/c) ratio.

Table 4.1: Chemical composition and physical properties of cement and fly ash.

Element	CEM I 42.5 R	Fly ash
CaO (%)	64.06	2.30
SiO ₂ (%)	18.90	46.90
Al ₂ O ₃ (%)	4.90	28.50
Fe ₂ O ₃ (%)	3.66	6.22
SO ₃ (%)	2.92	0.04
MgO (%)	0.82	1.23
Loss of Ignition (%)	3.18	6.20
Specific weight (kg/m ³)	3110	2100

As already mentioned, after a careful mix design, thirteen different concretes were produced by changing the percentage of substitution of natural aggregate with RCAs and by varying the amounts of cement and FA. Table 4.2 describes the composition of such mixes.

The first column of the table reports a label denoting the mixture and providing key information about the type of aggregates and the fly ash content. Particularly, the natural aggregate type is defined by letter “N”; conversely, with “R” the presence of a given percentage of recycled aggregates is indicated. This percentage is provided through a number following such letter, i.e. 30, 60 or 100. If any, a first letter denotes the content of fly ash (“L” for low content, “M” for medium-high, “H” for high). As an example, “LN” refers to a mix containing only natural aggregates and the lowest content of fly ash among those considered (i.e. 80 kg/m³); label “LR60”, instead, denotes a mix characterised by the same fly ash content, whereas the 60% of natural aggregates is replaced by an equivalent volume amount of recycled ones.

Other information reported in the table are: the mass per unit volume of cement (C) and of fly ash (FA) and their ratio (FA/C); the percentage of recycled aggregates used in substitution of natural ones; the water contents per unit volume; the quantities per unit volume of both natural and recycled aggregates for each

sieve fraction; two different water-binder ratios.

Table 4.2: Mix design for RCA+FA concrete mixtures.

Aggregates and Cement																
Sand	Sand_IT					RCA _{6,Sand}										
Class1	NA _{C1_IT}					RCA _{6,C1}										
Class2	NA _{C2_IT}					RCA _{6,C2}										
Class3	NA _{C3_IT}					RCA _{6,C3}										
Cement type	CEM I 42.5 R															
Mix composition																
Mix	CEM	FA	FA/C	RCA	W	w _{add}	NA_IT				RCA ₆				w _{tot} /b ₀	w _{tot} /b
	[kg/m ³]			[%]	[kg/m ³]			C3	C2	C1	Sand	C3	C2	C1		
							[kg/m ³]									
N	280	0	0	0	150	14.02	505	470	165	830	-	-	-	-	0.59	0.59
LN	250	80	0.32	0	150	14.02	505	470	165	750	-	-	-	-	0.58	0.58
LR30	250	80	0.32	30	150	21.86	-	408	165	750	445	55	-	-	0.61	0.61
LR60	250	80	0.32	60	150	38.16	-	-	-	750	445	415	145	-	0.67	0.67
LR100	250	80	0.32	100	150	109.65	-	-	-	-	445	415	145	660	0.92	0.92
MN	250	220	0.88	0	150	11.28	545	490	170	500	-	-	-	-	0.48	0.57
MR30	250	220	0.88	30	150	17.85	35	490	170	500	450	-	-	-	0.50	0.59
MR60	250	220	0.88	60	150	28.99	-	-	185	500	455	450	-	-	0.53	0.63
MR100	250	220	0.88	100	150	98.84	-	-	-	-	400	375	130	595	0.74	0.88
HN	200	255	1.27	0	150	11.28	545	490	170	500	-	-	-	-	0.53	0.71
HR30	200	255	1.27	30	150	17.85	35	490	170	500	450	-	-	-	0.56	0.74
HR60	200	255	1.27	60	150	28.68	-	-	175	500	455	445	-	-	0.59	0.79
HR100	200	255	1.27	100	150	98.84	-	-	-	-	400	375	130	595	0.82	1.10

As regards the water content, the authors aimed at keeping unchanged the water available for the chemical reaction (i.e. $w=150 \text{ kg/m}^3$). Therefore, an “extra” quantity of water (w_{add}) has been added to the various mixes depending on the water absorption capacity of the employed aggregates (see Table 2.2). This additional water content has been estimated assuming that aggregates were initially dry and considering the actual amount of NA and RCA for each sieve fraction.

The composition of the “control mixture” (label “N”) is shown at the first row of the table; such a mixture meets the requirements of the EN 206:2013 for the exposure class XC2, for which the maximum water-cement ratio is 0.60, the minimum cement content (C_{min}) is 280 kg/m^3 , and the minimum compressive strength class is C25/30.

The control mixture only contains NAs and Portland cement and presents a total water content of about 164 kg/m^3 . Therefore, the water-cement ratio

($w_{tot}/C=164.02/280=0.59$) is within the range given by the European code.

According to the abovementioned European Standard, the minimum cement content C_{min} may be reduced by the maximum amount:

$$\Delta C = (C_{min} - 200) \cdot k \quad (4.2)$$

if fly ash is added in the mixture, so that the following relationship is satisfied:

$$C + FA = (C_{min} - \Delta C) + FA \geq C_{min} \quad (4.3)$$

Coefficient k is a sort of “*cementing efficiency index*” of fly ash, and the following “ k -value” can be used for a concrete containing CEM-I conforming to EN 197-1:2011:

- $k=0.2$ in case of CEM-I 32.5;
- $k=0.4$ in case of CEM-I 42.5 and higher.

The maximum amount of FA that can be used has to meet the following code requirement:

$$\frac{FA}{C} \leq 0.33 \text{ (by mass)} \quad (4.4)$$

According to the EN 206:2013, if a greater amount of fly ash is used, the excess cannot be taken into account for the calculation of the water-binder ratio:

$$\frac{w}{b} = \frac{w}{C + k \cdot FA} \quad (4.5)$$

Two values of this ratio have been evaluated herein by:

$$\frac{w_{tot}}{b} = \frac{w + w_{add}}{C + k \cdot FA} \quad (4.6)$$

and considering once the total amount of FA ($b=b_0=C+k \cdot FA_{tot}$), then computing the total binder content, “ b ”, by limiting the amount of FA as request by the European Standard (see eq. (4.4)).

The two values of the ratio calculated for each mix are reported in the last two columns of Table 4.2. Four mixes (in Table 4.2 identified by “L” as first letter of the label), fully in agreement with the abovementioned code provisions, have been obtained by the “control mix” adding FA and substituting given amounts of NA with as many of RCA. Particularly, according to eq. (4.2), the cement content was reduced to $C=250 \text{ kg/m}^3$ and, correspondingly, 80 kg/m^3 of FA were added; therefore, the limitation given by eq. (4.4) has been respected. It has to be underlined that in evaluating ΔC we assumed a k -value of 0.40, since a cement type

CEM I 42.5 R has been used.

The first of the four mixes – labelled as “LN” – differs from the “control one” only for the mentioned reduction of cement and the consequent addition of FA. Instead, the other ones are characterised by the RCA replacement by 30% (mix “LR30”), 60% (“LR60”) and 100% (“LR100”) of NAs.

A second group of four mixes (mixtures with first letter “M”) have been produced using 220 kg/m³ of FA and 250 kg/m³ of cement. Therefore, these mixes contain about 140 kg/m³ of FA that cannot be considered as binder. The content of aggregates has been changed as reported in Table 4.2 in order to balance the volumes. As for the previous group of mixes, labels “MN”, “MR30”, “MR60” and “MR100” correspond to mixtures having different content of NAs and RCAs.

Moreover, a third group of four mixes has been considered (first letter “H”). These mixes have been obtained by further reducing the content of cement down to 200 kg/m³, i.e. well beyond the limits allowed by eq. (4.2). In order to keep the total volume of binder equal to the one of the second group of mixes, 255 kg/m³ of coal FA have been used.

Table 4.2 highlights that not all the mixes comply with the limit value of the water-binder ratio given by the EN 206:2013 Standard for the exposure class XC2 (see the last column of the table). Concretes above described were prepared by using a small mixer available in the Materials and Structures Testing Laboratory of the University of Salerno.

First of all, both coarse and fine aggregates have been saturated and mixed; subsequently, cement and fly ash and, finally, a super-plasticizer have been added and the mixing operation has continued for about 10 minutes.

Then, slump tests have been performed to evaluate the workability of the various concrete mixes, and also the density of the fresh concrete has been measured.

Finally, concretes have been cast in cubic and cylindrical polyurethane moulds, and duly vibrated. After 36 hours the concrete samples have been removed from the moulds and cured at about 20°C with 100% humidity (i.e. in water) (EN 12390-3:2009). Particularly, the time evolution of the compressive strength has been monitored by testing twelve cubic specimens for each type of concrete: compression tests have been carried out at 2, 7, 28, 60 and 90 days (EN 12390-3:2009), (Figure 4.6a). Tensile splitting tests, instead, have been performed only at 28 days, according to EN 12390-6:2009 (Figure 4.6b).

Pull-out tests have been conducted for estimating the bond behaviour of deformed steel rebars embedded in recycled aggregate concretes (Figure 4.6c-d-e). For this purpose, four 150x150x150 mm³ RAC specimens for each mix have been casted with a 10 mm diameter bars located in the centre. According to the RILEM

standard (1994b), pull-out tests were performed at 28-days and a bond length equal to 5 bar diameters has been assumed.

Table 4.3 outlines the experimental programme and reports the shape and the geometric dimension of the concrete samples.

Table 4.3: Experimental programme for RCA+FA mixtures.


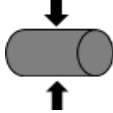
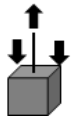
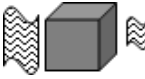
Type of test and geometry of specimens		Days	Number of tests
Compression Cube $150 \times 150 \times 150 \text{ mm}^3$		2	2
		7	1
		28	6
		60	2
		90	1
Tensile Cylinder $\Phi 150 \text{ mm. } h=300 \text{ mm}$		28	2
Pullout Cube $150 \times 150 \times 150 \text{ mm}^3$ $\Phi 10$ steel bar		28	4
Permeability Cube $150 \times 150 \times 150 \text{ mm}^3$		90	1



Figure 4.6: Specimens for investigating mechanical properties of RAC.

The water permeability (or hydraulic conductivity) of the considered concrete mixtures has been also evaluated. Permeability tests were carried out according to the EN 12390-8:2009: one cubic specimen for each mix was tested by injecting water at a constant pressure, P_i , equal to 5 bar (Figure 4.7a).

Finally, the resistance of concrete samples to the chloride ion penetration has been evaluated according to the ASTM C1202-12 specifications. Particularly, two cylindrical specimens for each mix, having 100 mm diameter and 50 mm height (Figure 4.7b), have been tested at 90 days of curing.

A potential difference of 60V of discontinuous current has been maintained between the two ends of the specimens, one of which was immersed in a sodium chloride solution and the other one in a sodium hydroxide solution (Figure 4.7c). The amount of electricity passed through the cylinders in 6 hours has been measured; the resistance to this flow can be interpreted as an indirect measure of durability.

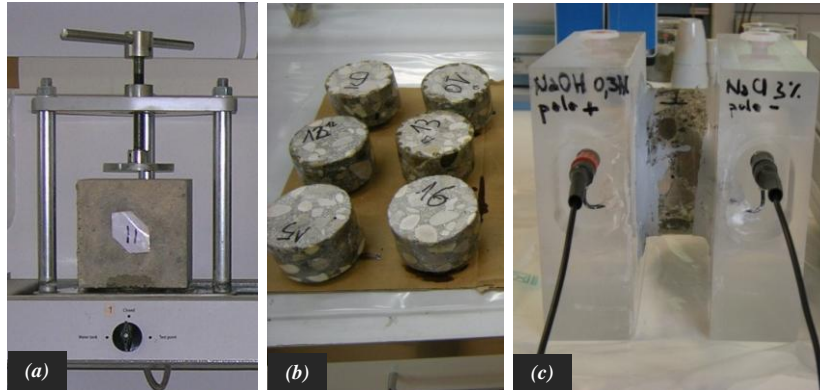


Figure 4.7: Specimens for investigating the durability properties of the considered concretes.

4.2.2 Analysis of the results

Results obtained from tests described in the previous section are reported and discussed in what follows. Presenting the experimental results particular emphasis will be given to the actual influence of the combined use of RCAs and FA on the physical and mechanical properties of concrete.

Workability

Slump tests have been performed for determining the consistency of all the produced concrete batches, thus evaluating the influence of the combined use of FA and RCA on the workability of fresh concretes.

It has to be underlined that the control mixture “N” has been designed to achieve a consistency class “S4”, which correspond to slump values ranging from 160 mm to 210 mm (EN 206:2013). For this reason, a small quantity of a super-plasticizer (0.22%) was added in that mix. Larger amounts of the same super-plasticizer were added in the other mixes trying to achieve comparable slumps. Results from slump tests are shown in Figure 4.8.

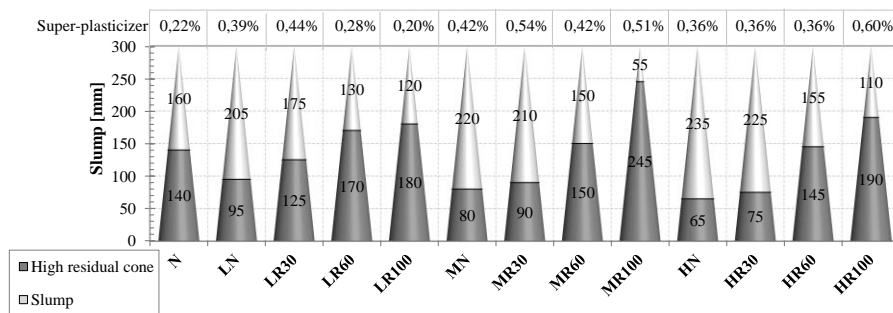


Figure 4.8: Results of the slump tests.

The following observation can be drawn out by examining the diagram:

- the desired slump has been obtained for the control mix (160 mm);
- due to the rougher surfaces and to the more irregular shapes of the recycled concrete aggregates with respect to the normal ones, the replacement of NAs with RCAs has caused a significant reduction of workability;
- on the contrary, the addition of fly ash in the mixture has produced a clear increase in the workability;
- although “green” concretes made with 100% of recycled concrete aggregates (RAC100%) were prepared with higher amounts of superplasticizer (up to 0.6%) a sensible reduction in their workability has been observed.

Finally, the percentage increase of recycled aggregates has been detrimental in terms of workability, thus confirming results already published by other Authors (Corinaldesi & Moriconi, 2010).

Mass density

A normal concrete weighs about 2400 kg/m³, but the unit mass of concrete (density) varies depending on the amount and density of the aggregate, the amount of entrained air (and entrapped air), and the water and cement contents.

A reduced density of normal concrete almost always corresponds to a higher water content, which, in turn, results in lower strength concrete. In the case of RAC, density values also depend on the content of coarse and fine recycled aggregate.

Figure 4.9 reports the mean values of the density deduced by weighting several 150x150x150 mm³ cubic samples made using the thirteen concrete mixes under investigation; one hundred fifty-six specimens have been weighted at different days: twenty-six samples at 2; thirteen at 7; seventy-eight at 28; twenty-six at 60; and thirteen at 90 days.

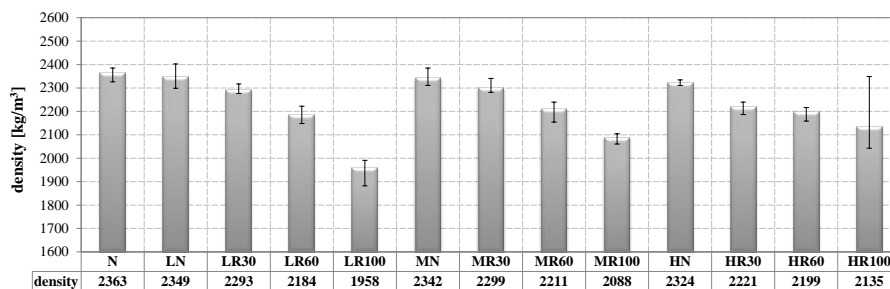


Figure 4.9: Density of the concrete samples.

Figure 4.9 also reports the minimum and maximum values of the density obtained for each mix. Table 4.4, instead, shows the theoretical value of the fresh concrete density calculated for each mix.

Table 4.4: Mix proportions and densities for RCA+FA concrete mixtures.

Mix	NA [%]	RCA [%]	C [kg/m ³]	FA [kg/m ³]	w _{tot} [kg/m ³]	NA [kg/m ³]	RCA [kg/m ³]	D [kg/m ³]
N	100	0	280	0	164.02	1970	0	2414
LN	100	0	250	80	164.02	1890	0	2384
LR30	70	30	250	80	171.86	1323	500	2325
LR60	40	60	250	80	188.16	750	1005	2273
LR100	0	100	250	80	259.65	0	1665	2255
MN	100	0	250	220	161.28	1705	0	2336
MR30	70	30	250	220	167.85	1195	450	2283
MR60	40	60	250	220	178.99	685	905	2239
MR100	0	100	250	220	248.84	0	1500	2219
HN	100	0	200	255	161.28	1705	0	2321
HR30	70	30	200	255	167.85	1195	450	2268
HR60	40	60	200	255	178.68	675	900	2209
HR100	0	100	200	255	248.84	0	1500	2204

Both Table 4.4 and Figure 4.9 indicate that the presence and the amount of RCA affects the concrete density. Particularly, the higher the percentage of substitution of natural aggregates with recycled ones, the lower the mean value of the concrete density; such a reduction in density is almost negligible in the case of concretes with only 30% of RCAs, whereas, the scatters between the minimum and maximum value increase with the amount of RCAs.

Compressive strength

Figure 4.10 reports the mean values of the compressive strength evaluated by testing several cubic samples made of the thirteen concrete mixes under consideration; tests have been performed at different curing times, ranging between 2 and 90 days. The error bars used in the chart were drawn using one standard deviation (positive and negative) from the samples.

Figure 4.10 highlights that the compressive strength determined for samples made with the mix “LN” (i.e. the natural aggregate concrete realised with the lowest amount of FA) is very similar to the one obtained for those samples made with the control mix “N”. Therefore, in terms of compression strength, the 80 kg/m³ of fly ash added to the control mix produces, more or less, the same effect

respect to the replaced 30 kg/m³ of Portland cement. Particularly, at short curing times - namely, up to 7 days - the strength measured on samples made of mix “LN” is slightly lower than the one determined on samples made of mix “N”, while for curing times equal or longer than 28 days is even higher (at 90 days is significantly higher). The late achievement of a target strength shown by concrete samples made of the "LN" mix is due to the delayed binding action of FA, which occurs in longer times with respect to those required for the Portland cement.

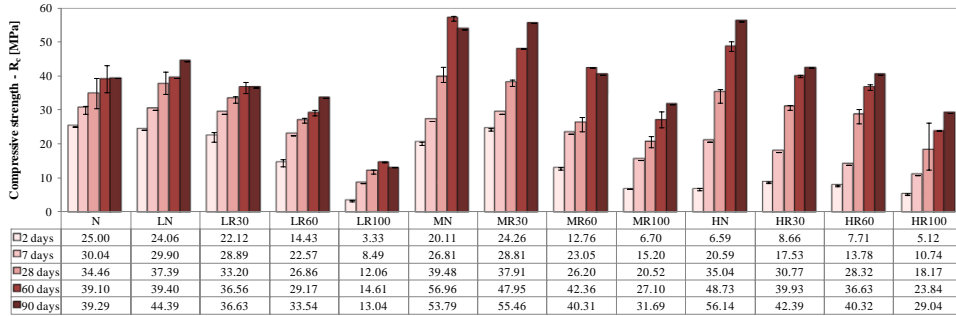


Figure 4.10: Cube compressive strength of concrete for each curing time.

This phenomenon is even more evident for concretes with higher fly ash contents, i.e. for those made with "MN" and "HN" mixes. Particularly, after 60 days of curing, samples made of these two mixtures have exhibited average values of the compressive strength about 40% higher than those resulting from tests on samples made of "N" and "LN" mixtures. This means that:

- the amount of fly ash exceeding the 33% C (see eq. (4.4)), did not behave as inert as it has produced a non-negligible increase of strength, although at longer curing times;
- even reducing the content of cement well beyond the limits allowed by the European Standard (see eq. (4.2)) is still possible to reach optimal levels of the compressive strength after 60 days (see values obtained for all the “H” mixes).

The experimental results also show that the replacement of natural aggregates with recycled ones produces a substantial change in the compressive strength of the concrete. Particularly, by examining the experimental results for RAC specimens the following observations can be drawn:

- a progressive reduction of the concrete compressive strength has been observed as a result of an increased percentage of recycled aggregates in the mix (compare the strength values obtained for the three mixtures “LR”, the three “MR” and the three “HR” reported in the bar diagram of Figure 4.10);
- nevertheless, acceptable performances have been obtained for times of

curing longer than 28 days, in case of RAC60% when high amounts of FA have been added to the concrete mix (see strength values of mixes "MR60" and "HR60");

- the replacement of 30% of NAs with RCAs together with the addition of a low amount of FA (namely, the mix "LR30") has led to a concrete having compressive strength comparable to that of the mixture taken as reference (i.e. the mix "N"); in fact, regardless the curing times, a difference not larger than 10% between the mean strength values of these two types of concrete has been observed;
- the concrete strength of mixes with high content of RCA can be improved by partially substituting the finest portion of aggregates with FA (compare the strengths of RAC100% samples, i.e. mixes "LR100", "MR100" and "HR100").

Splitting tensile strength

The values of the tensile strength of the studied concretes have been obtained by performing splitting tests at 28 day; two tests for each mix have been carried out and the mean values are shown in Figure 4.11. Only the value of the reference concrete is based on a single measure, because of the premature failure of one of the two specimens; this result is indicated by the horizontal dashed line shown in the figure.

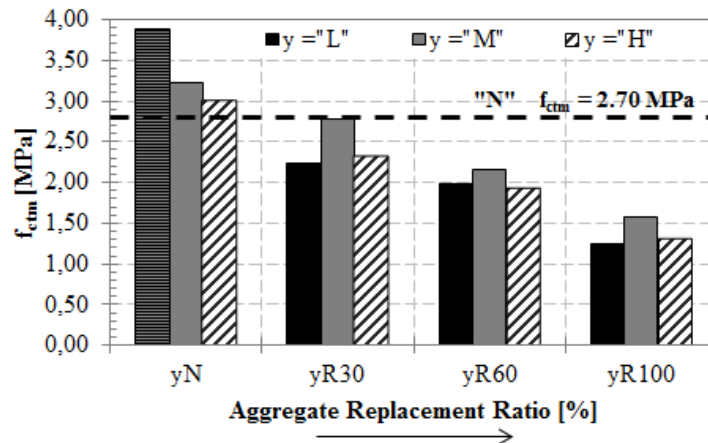


Figure 4.11: Tensile strength of concrete mixes.

The following remarks can be outlined:

- specimens only made with natural aggregate concrete (NAC100%), whose results are represented by the first three bars of the histogram, have exhibited a splitting strength higher than RACs;

- as for the compression tests, also from splitting ones a progressive reduction of strength has been observed by increasing the percentage of recycled aggregates in the mix;
- with the exception of the mix “MR30”, a not negligible reduction of strength has been noted already for RAC30%;
- specimens having the 60% or 100% of RCAs content have shown a very strong reduction of the tensile strength at 28 days.

Since the studied RACs always contain fly ash, and as fly ash gives rise to a delayed binding action, further splitting tests should have to be performed at different curing times in order to better investigate their behaviour under tension.

Finally, several contributions available in the scientific literature point out that the compressive and splitting tensile strengths of a RAC are mainly affected by the quality of the recycled aggregate, rather than by its quantity (Tavakoli & Soroushian, 1996; Malešev et al., 2010). However, the experimental results reported in this study do not allow focusing on this topic, since only one type of RCA has been used in producing concretes. Nevertheless, the obtained results are in agreement with other previous studies, which already observed that the level of reduction in RAC compressive and tensile strength increases with the RCA content (Hansen & Narud, 1983; Thomas et al., 2013), and this is the reason for which the aggregate replacement ratio is often limited to approximately 30%.

Bond strength

Fifty-two concrete specimens (i.e. four for each of the thirteen mixes) have been realised with a deformed steel bar embedded in the centre, in order to perform pull-out tests (see the geometric scheme depicted in Figure 4.12). Steel rebars having diameter $D_b=10$ mm and an anchorage length L_b of 50 mm were employed.

Therefore, four pull-out tests for each mixture have been performed after 28 days of concrete curing (few tests unexpectedly gave results patently incorrect and will not be considered in the following). The bond strength values have been calculated assuming a uniform stress distribution along the length L_b :

$$f_b = \frac{P}{\pi \cdot D_b \cdot L_b} \quad (4.7)$$

where P is the applied pull-out load.

The bond strengths, f_b , calculated with eq. (4.7) and the average values evaluated for each type of concrete, are reported in Table 4.5. The best bond behaviour has been exhibited in the concrete specimens prepared by using the “control” mix “N”, whereas the worst one has been observed in those made with

100% of RCAs.

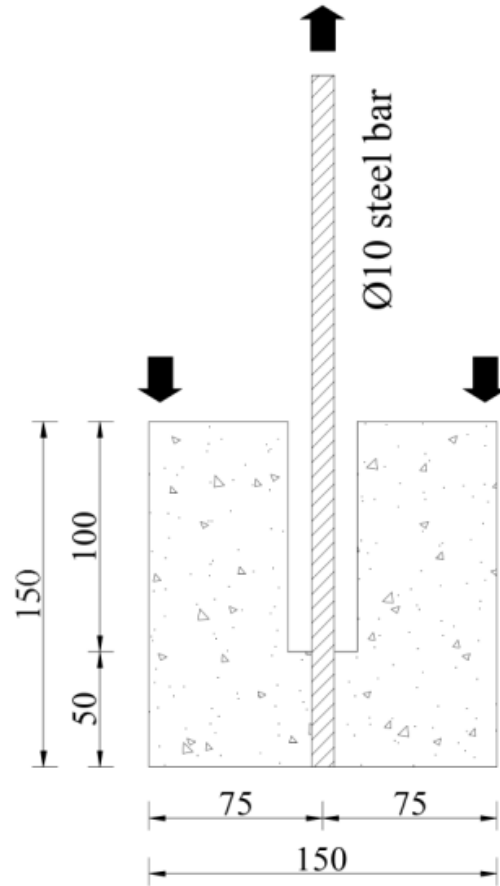


Figure 4.12: Sketch of the pull-out specimen.

In the case of specimens with only natural aggregates, the use of FA seems to yield to a deterioration of the steel-concrete bond interaction. The use of the 30% of RCAs in the mix, instead, plays a positive role on bond behaviour; finally, the use of a cement content less than the minimum required by the European Standard (i.e. less than 250 kg/m^3) has provided a significant decrease of bond strength. The authors' opinion is that further experimental tests on the bond behaviour of deformed steel rebars embedded in recycled aggregate concrete, with or without fly ash, have to be performed: a) in the same test conditions, in order to check the reliability of the abovementioned results; b) by changing the test set-up, because the one used herein (suggested by RILEM, 1994b) introduces a sort of confinement effect which can lead to overestimate the actual bond strength (ACI 408R-03; Mazaheripour et al., 2013).

Table 4.5: Average values of pull-out strengths (in MPa).

Mix	Test #1	Test #2	Test #3	Test #4	f_{bm}
N	25.56	21.57	29.22	27.45	25.95
LN	22.43	-	18.75	15.34	18.84
LR30	18.41	20.17	19.06	18.72	19.09
LR60	14.92	18.76	10.95	13.00	14.41
LR100	11.93	11.09	11.71	11.20	11.48
MN	21.28	-	19.69	16.14	19.04
MR30	20.64	22.31	22.20	22.36	21.88
MR60	27.11	17.05	24.36	-	22.84
MR100	14.10	12.70	13.40	-	13.40
HN	13.46	-	14.05	13.57	13.69
HR30	16.99	22.26	19.19	20.39	19.71
HR60	21.90	14.83	16.23	-	17.65
HR100	7.76	-	7.39	7.38	7.51

Permeability

Permeability is defined as the property that governs the rate of flow of a fluid into a porous solid. The overall permeability of concrete to water is a function of the permeability of the paste, the permeability and gradation of the aggregate, and the relative proportion of paste to aggregate.

A recent study on the durability of RAC has shown that water permeability increases with the water-cement ratio and with the RCA content (Thomas et al., 2013). The durability of concrete significantly depends on its permeability: increased water tightness improves concrete resistance to re-saturation, sulphate and other chemical attack, and chloride ion penetration. Moreover, permeability also affects the destructiveness of saturated freezing.

Permeability tests, have been performed according to EN 12390-8:2009 on thirteen concrete cubes (one for each mix). They were finalised at measuring the depth of penetration of water in concrete specimens under pressure of 5 bar; in order to do this concrete cubes have been split into two parts after 72 hours of this “treatment” and the wet profile has been measured (see Figure 4.13).

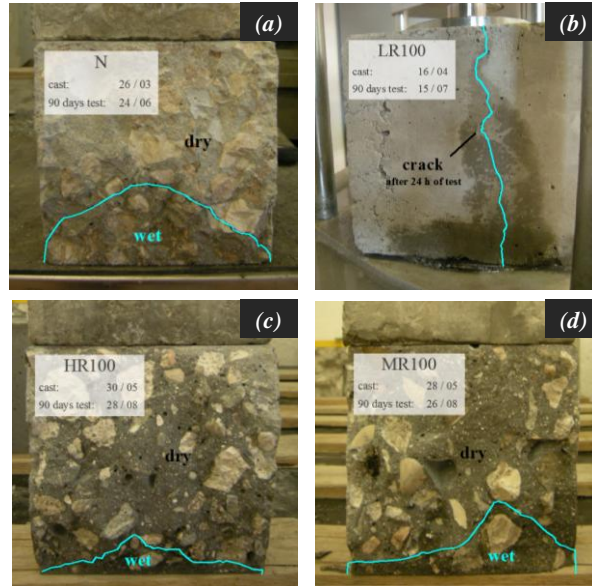


Figure 4.13: Wet profiles derived by permeability tests.

Figure 4.14 outlines the results of all the permeability tests in terms of height of the water penetration h_m . Higher values of h_m indicate less watertight concretes, i.e. concretes more easily affected by degradation phenomena.

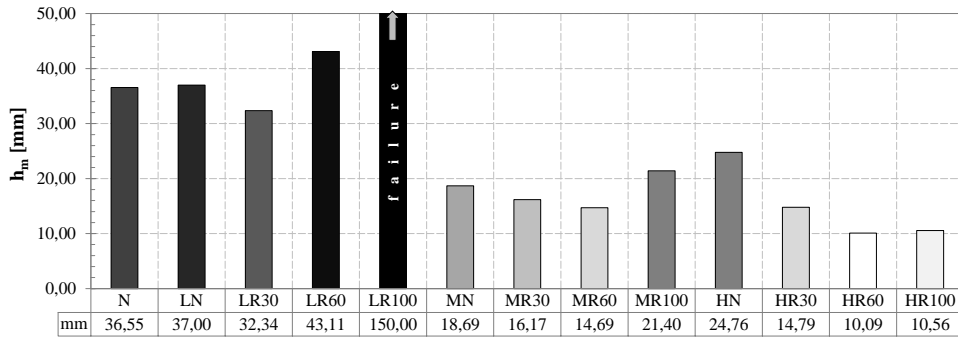


Figure 4.14: Results of permeability tests.

Observing the experimental data reported in that figure can be noted as the use of fly ash enhances the water tightness of the concrete, also counterbalancing the negative effect produced by the recycled concrete aggregates.

It has to be noticed that the test performed on the specimen made of the “LR100” mixture is failed, since the water has passed through the specimen from side to side; this is probably happened because of a pre-existing micro-crack which has been further enlarged by the action of the water under pressure (see Figure 4.13b). This test was stopped after 24 hours because of the fracture of the concrete

sample.

Resistance to chlorides

Chloride ion penetration is one of the major problems that affect the durability of reinforced concrete structures. Although chloride ions in concrete do not directly cause important damage to the concrete, they contribute to the corrosion of steel rebars embedded in the structures.

Rapid Chloride Penetration Tests (ASTM C1202-12) have been performed on twenty-six concrete cylinders at 90 days. Particularly, the amount of electric charge passing through each cylinder in six hours, from side to side, has been measured.

A qualitative correlation between the electric charge and the expected sensitivity to chloride diffusion is shown in Table 4.6.

Table 4.6: Electric charge vs diffusion of chloride according to ASTM C1202-12.

Electric charge [C]	Diffusion of Chloride
>4000	High
2000 – 4000	Moderate
1000 – 2000	Low
100 – 1000	Very Low
< 1000	Negligible

Figure 4.15 reports the quantity of charge, measured in Coulombs, passing through all the concrete specimens under investigation.

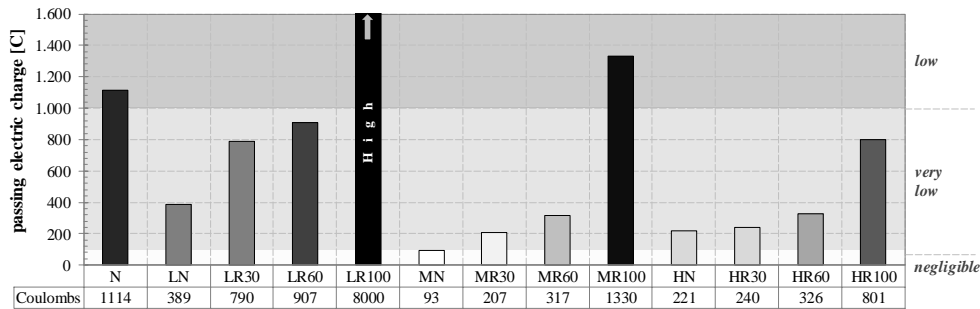


Figure 4.15: Results of chloride diffusion tests.

Looking at such figure, as a low value of the electric charge corresponds to a high resistance of concrete to chloride penetration, it is clear that:

- adding fly ash in the concrete mix produces a significant improvement of the anti-chloride performance of concrete;

- on the contrary the use of recycled aggregates causes a worsening of such performance; higher is the percentage of recycled aggregates, smaller is the resistance to chlorides penetration.

The obtained results fully agree with the literature (Kou & Poon, 2013).

4.3 Empirical relationships for compressive strength of RAC+fly ash

An empirical formulation, intended at interpreting the time evolution of the compressive strength in a recycled aggregate concrete, has been recently proposed by Malešev et al. (2010):

$$R_{cm} = \frac{a \cdot t}{b + t} \quad (4.8)$$

where t is the curing time, while a and b are two coefficients that should be calibrated on the basis of experimental test results. Particularly, the coefficient a represents the target value of the compressive strength (i.e. the concrete strength achievable per $t \rightarrow \infty$).

The least-square method has been used herein to calibrate values of these two coefficients by means of a best fitting of the experimental data shown in Figure 6 (see Section 3.3); the couple of values of a and b obtained for each of the mixes under investigation are listed in Table 4.7, along with the corresponding value of the “coefficient of determination”, R^2 , which qualifies the accuracy of the predictive model (i.e. the model given by eq. (4.8)).

Table 4.7: Values of the a and b coefficients and of R^2 .

MIX	a [MPa]	b [days]	R^2
N	39.70	2.42	0.862
LN	41.47	1.79	0.880
LR30	36.33	1.42	0.959
LR60	31.57	2.63	0.934
LR100	14.86	5.82	0.971
MN	58.88	7.05	0.870
MR30	50.59	3.63	0.786
MR60	41.69	6.20	0.854
MR100	32.05	9.30	0.943
HN	65.86	19.80	0.983
HR30	47.29	12.17	0.991
HR60	46.73	16.32	0.993
HR100	31.98	16.46	0.970

The curves representing the time evolution of strength during curing are shown in Figure 4.16 to Figure 4.19 together with the experimental strength values. The corresponding numerical curves have been evaluated for all the mixes except for the control one, by using eq. (4.8) and the values of coefficients a and b reported in Table 4.7. A very good agreement between the experimental measures and the analytical predictions has been observed; this highlights the effectiveness of the predictive model given by eq. (4.8).

Particularly, Figure 4.16 shows the time evolution of the compressive strength for samples made with the four concretes containing only natural aggregates (namely, N, LN, MN and HN).

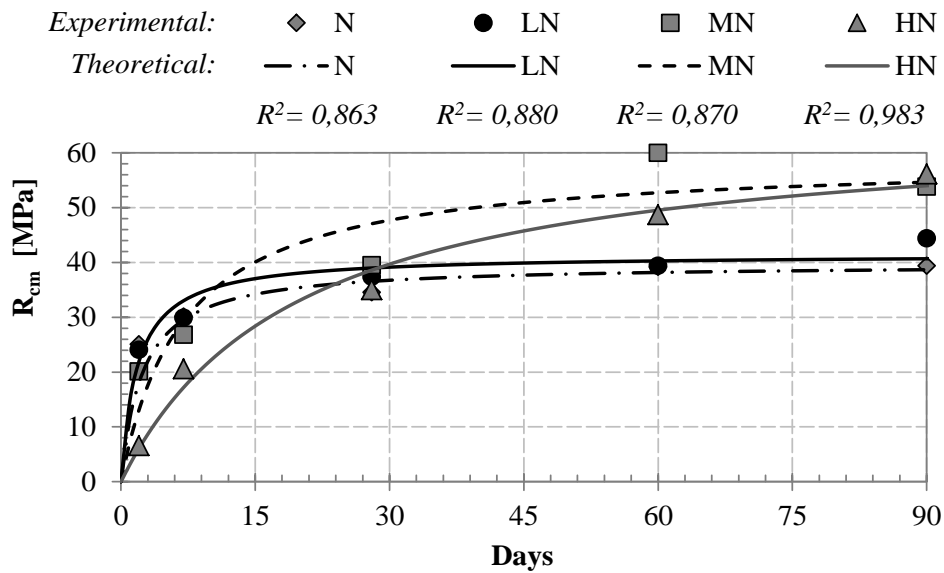


Figure 4.16: Time evolution of the compressive strength for NAC.

These curves confirm that NACs containing fly ash can reach compression strengths higher than the those of NACs without FA, but for longer curing times (generally, longer than 28 days). This is probably due both to the different time of chemical reaction of the fly ash with respect to the Portland cement, and to the reduction of the cement content consequent to the addition of fly ash in the mix. Figure 4.17, Figure 4.18 and Figure 4.19 show the same curves for RAC30%, RAC60% and RAC100%, respectively. It can be observed that the trend of all the analytical curves is always more or less the same. All the curves tend to a horizontal asymptote that represents the attainable maximum strength; the lower the percentage of recycled aggregates, the higher the strength threshold.

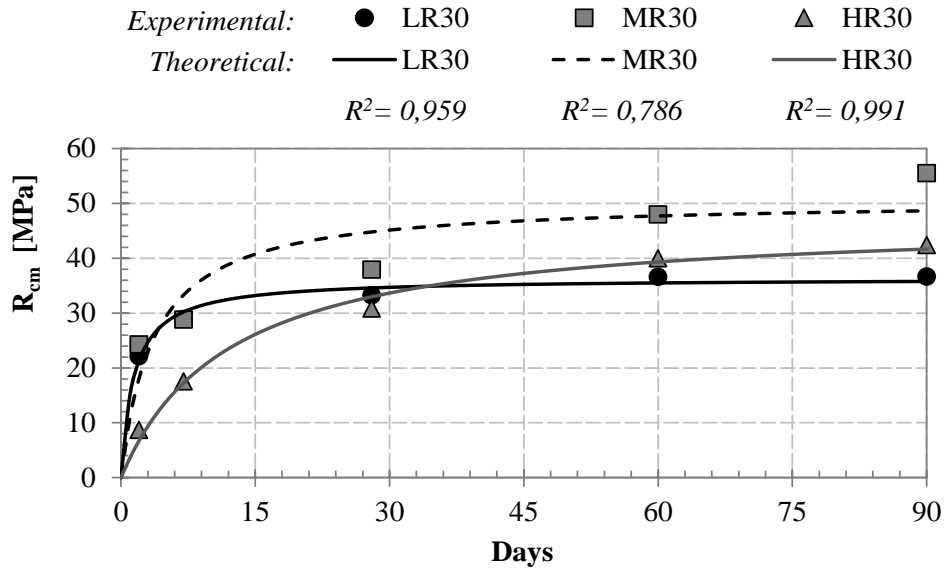


Figure 4.17: Time evolution of the compressive strength for RAC30.

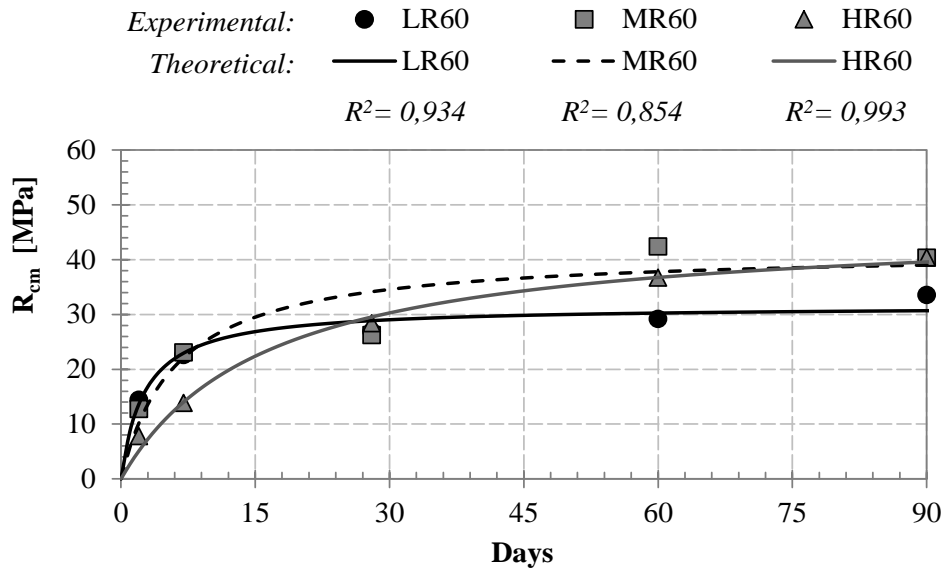


Figure 4.18: Time evolution of the compressive strength for RAC60.

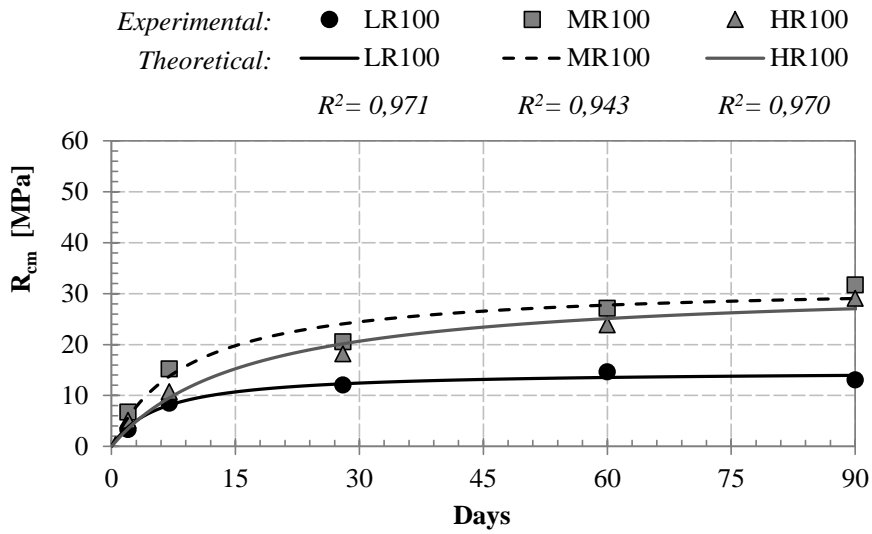


Figure 4.19: Time evolution of the compressive strength for RAC100.

Figure 4.20 depicts values of coefficient a in function of the RCAs content (from 0% to 100%). The graphs show that, for all the considered content of fly ash, a linear correlations always exists that well fits the actual variation of parameter a with the percentage of RCAs.

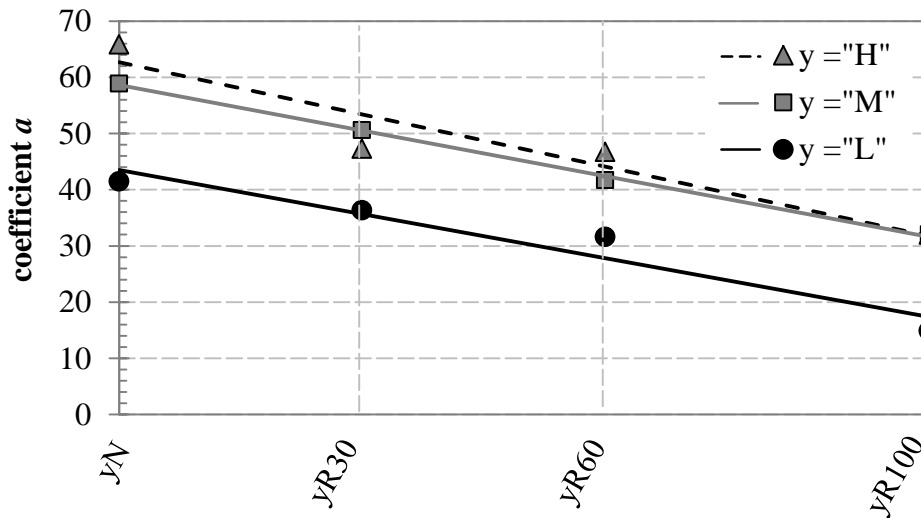


Figure 4.20: Values of the a coefficient vs the content of RCA in concrete mixes.

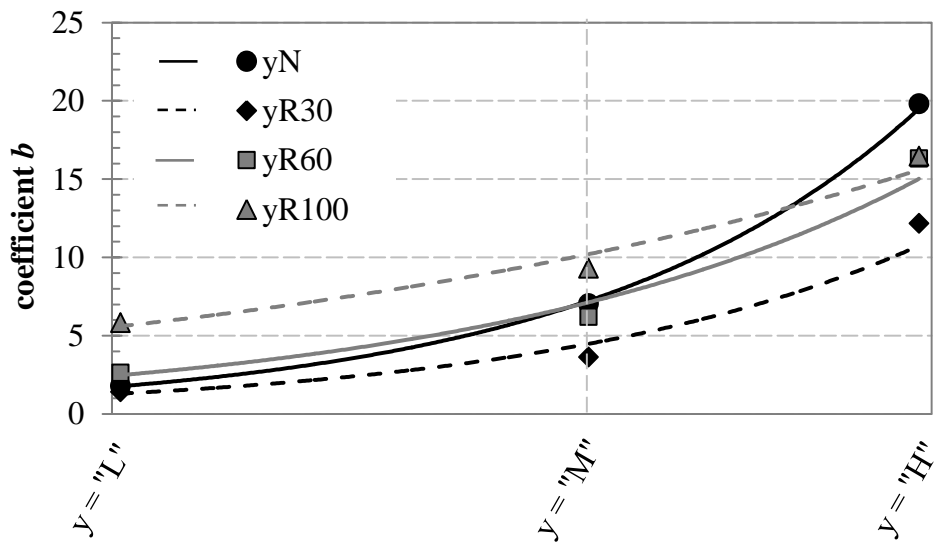


Figure 4.21: Values of the b coefficient vs the content of FA in concrete mixes.

Finally, Figure 4.21 shows the trend of values assumed by parameter b in function of the FA content. It is worth highlighting that higher are the values of b slower is the hardening processes; therefore, as expected, larger contents of FA lead to higher values of coefficient b .

4.4 Conclusions

The results of a wide experimental campaign carried out for evaluating the most important physical and mechanical properties of “green concretes” have been presented and discussed in this study. Several concretes deriving by a “control” one, made only of normal aggregates and Portland cement, have been studied.

These concretes have been produced by replacing given amounts of natural aggregates with recycled concrete aggregates and by adding fly ash in partial replacement of cement. Since one type of RCA has been used, this study focused on the effect of the quantity rather than the quality of RCAs on the concrete performances.

The following conclusions can be summarised.

Replacing normal aggregates with recycled ones generally leads to a decay in the concrete performance; in fact, tests performed on RAC specimens have shown:

- a significant reduction of workability;

- a progressive reduction both of compressive and tensile strength by increasing the percentage of recycled aggregates in the mix;
- a higher permeability and, consequently, a smaller resistance to chlorides penetration;
- a reduction of the bond strength of deformed steel reinforcing rebars to concrete.

Nevertheless, the addition of fly ash in the mixture enhances the mechanical properties and durability performance of the concrete, thus mitigating the worsening effects of RCAs.

Particularly, it has been observed that:

- the addition of fly ash in the mixture produces an improvement of the workability;
- both compressive and tensile strengths increase by increasing the fly ash content;
- adding fly ash in the concrete mix produces a significant improvement of the resistance to chlorides penetration.

It is worth highlighting that fly ash produces a delayed binding action; therefore, the higher the content of fly ash, the longer the time needed to achieve the maximum strength.

Finally, also concrete samples obtained by reducing the content of cement (and, correspondingly adding fly ash) far beyond the limits allowed by the current European Standards have been investigated: although these concretes have shown lower mechanical and physical properties, a possible enhancement of such limits is still possible and could be implemented in the future versions of European Standards as a further driver towards the production of more sustainable structural concretes.

5. Modelling the hydration process and predicting the cement paste properties

The use of alternative binders and recycled aggregates intended at enhancing the sustainability of concrete industry can significantly affect the fundamental material properties change the performance of structural systems (Naik, 2005). Partial replacing of classical binders such as Portland cement with less impactful alternatives like slag, fly-ashes, rice husk ash, sugarcane baggasse, and others, will change the fundamental chemical/physical/mechanical properties of the cementitious microstructure (Aitcin, 2007). Moreover, the use of recycled aggregates, such as for example aggregates received from recycled concrete, for replacing of ordinary ones can lead to concretes characterised by significantly different structural performance (Caggiano et al., 2011).

A way to evaluate the altered performance of a sustainable concrete is by scrutinising its hardening behaviour in more detail (van Breugel, 1991). Particularly, the key aspects of the resulting hydration mechanisms (Bullard et al., 2011) can be observed by measuring the so-called degree of hydration of concrete (Koenders, 1997; Pane & Hansen, 2005) and investigating its possible correlations with the development of the relevant material properties, such as compressive strength and elastic modulus (Laube, 1991; Lokhorst, 1999; Gutsh, 2002). As a matter of fact, the degree of hydration can be easily measured only in the case of adiabatic conditions, as in that case it is directly related to the temperature development (Koenders, 1997). On the contrary, in more general conditions, advanced techniques are generally required to obtain a direct estimate the degree of hydration of concrete during setting and hardening (Livesey et al., 1991; Brandstet et al., 2001; Feng et al., 2004).

In principle, modern modelling techniques, such as the Finite Element Method (FEM), can be employed for simulating the time development of temperature and the hydration process during hardening, within the borders that these software provide (Bentz, 1997; Jeong & Zollinger, 2006).

However, a more fundamental approach that can be employed to analyse the early age behaviour of concretes with (partial) replacement of cement and/or aggregates would be to go back to the basic analytical formulations for temperature development and hydration, and to use this as input for the evaluation of the (prevailing) formulae for the development of the material properties (de Schutter &

Tearwe, 1996; Schindler & Folliard, 2005). This approach gives an enormous insight into the dependency of the material properties on the basic parameters that control the progress of the hydration process. In this way, the direct correlation between the degree of hydration and the outcome of the formulae for the development of the material properties can be envisioned systematically (Lokhorst, 1999). Moreover, the possible correlation between the degree of hydration and a simpler parameter, such as the concrete “Maturity” can be also proposed.

This chapter presents the complete theoretical formulation and a consistent numerical implementation of a model aimed at simulating the cement hydration process and its consequences on the relevant mechanical properties of concrete. Particularly, based on the widely-accepted Arrhenius model of hydration kinetics (van Breugel, 1991; Koenders, 1997) and the well-established theory of heat flow (Narasimhan, 1999), the proposed model is a general and handy tool for estimating the degree of hydration from simple temperature measurements carried out during the setting and hardening phases in general non-adiabatic situation. Thus, it could be employed in calibrating sound correlations between material properties, taking into account the effect of concrete mixtures and the possible replacement of Portland cement and aggregates with the by-products mentioned at the beginning of this section.

In this framework, Section 5.1 outlines the theoretical formulation of the physical/chemical problem under consideration. For the sake of simplicity, and to comply with the aim of the present proposal, such a model is formulated in a 1D space domain and its validity field is clearly bordered with reference to the current state of scientific knowledge. Then, a consistent numerical solution based on the Finite Difference (FD) technique is developed in section 5.2 with the declared aim of pointing out all the mathematical details needed by Readers who are possibly interested in writing their own numerical code: in this regard, the numerical solution is explained like in a ready-made “recipe” and is particularly fit for a spreadsheet-based solution. The experimental results obtained on two concrete mixes are reported in subsection 5.3.1. Since temperature measurements are available for each one of such mixtures in both adiabatic and non-adiabatic conditions, the same experimental results are considered in subsection 5.3.2 to validate the proposed model and demonstrate its ability in simulating the behaviour of hardening concrete in both conditions. Then, Section 5.4 shows a relevant application of the proposed model aimed at unveiling the possible correlation between concrete compressive strength and hydration-related parameters such as degree of hydration and maturity.

5.1 Theoretical formulation

This section describes the main physical phenomena that occur during concrete setting and hardening and outlines the key theoretical assumptions and the mathematical models currently available to simulate the temperature development and associated degree of hydration. The main aspects are related to the liberation of heat due to the exothermal nature of the cement hydration reaction. Moreover, the heat-flow generated throughout the hardening concrete specimen as a result of non-adiabatic boundary conditions is analysed to simulate the effect of the variable (semi-adiabatic) temperature development on the cement hydration process and the resulting concrete maturity. Then, the correlations between the hydration process and the progressive development of the relevant mechanical properties of concrete, i.e. the compressive strength and the elastic modulus, are reported.

5.1.1 Adiabatic heat development of concrete

The chemical reactions which take place during concrete setting and hardening are mainly driven by the hydration process of the cement grains within the concrete mix. The hydration reaction of cement is exothermic in nature and results in a significant production of heat inside the hardening concrete.

The status of the cement hydration reaction can be described in terms of the so-called degree of hydration $\alpha_h(t)$ which is defined as the ratio between the amount of hydrated cement at time t relative to the original amount of cement in the mix. Since the amount of hydrated cement at time t is proportional to the total amount of heat $Q(t)$, the degree of hydration can be analytically defined as follows:

$$\alpha_h(t) = \frac{Q(t)}{Q_{\max}} \quad (5.1)$$

where Q_{\max} is the amount of heat potentially liberated by the hydration of all the amount of cement actually present in the concrete mix under consideration. According to Bogue's equations (1955), the value of Q_{\max} can be evaluated as follow:

$$\frac{A}{F} < 0.64 \left\{ \begin{array}{l} C_3S = 4.071 \cdot c - (7.6 \cdot S + 4.479 \cdot A + 2.859 \cdot F + 2.852 \cdot s) \\ C_2S = 2.867 \cdot S - 0.7544 \cdot C_3S \\ C_3A = 0 \\ C_4AF = 2.1 \cdot A + 1.702 \cdot F \end{array} \right. \quad (5.2)$$

$$\frac{A}{F} \geq 0.64 \left\{ \begin{array}{l} C_3 S = 4.071 \cdot c - (7.6 \cdot S + 6.718 \cdot A + 1.43 \cdot F + 2.852 \cdot s) \\ C_2 S = 2.867 \cdot S - 0.7544 \cdot C_3 S; \\ C_3 A = 2.65 \cdot A - 1.69 \cdot F \\ C_4 A F = 3.043 \cdot F \end{array} \right. \quad (5.3)$$

where:

- C= CaO;
- S= SiO₂;
- A= Al₂O₃;
- F= Fe₂O₃;
- s= SO₃;
- fl= Free Lime;
- c=C-fl.

The heat produced by the hydration reaction is significantly influenced by the temperature which depends on the sample dimensions, boundary conditions and, then, is controlled, in turn, by the produced heat itself. Particularly, a simple analytical relationship can be written between the degree of hydration α_h (or the heat $Q_a(t)$ produced in the same conditions) and the corresponding temperature variation ΔT_a in the ideal case of adiabatic conditions (Koenders, 2005):

$$\Delta T_a(t) = \frac{C}{\rho_c c_c} \cdot Q_a(t) = \frac{C \cdot Q_{\max}}{\rho_c c_c} \cdot \alpha_h(t) \quad (5.4)$$

where

- C is the cement content per unit volume [kg/m³];
- c_c specific heat of concrete [J/gK];
- ρ_c specific mass of concrete [g/m³].

Therefore, the current temperature developed within the hardening concrete can be expressed by introducing in equation (5.1) the definition of α_h reported in equation (5.4):

$$T_a(t) = T_R + \Delta T_a(t) = T_R + \frac{C \cdot Q_{\max}}{\rho_c c_c} \cdot \alpha_h(t) \quad (5.5)$$

where T_R is the room temperature.

Since the hydration process results in a partial reaction of cement grains which produces the reaction heat denoted as Q_{\max}^* the following relationship can be

introduced between Q_{\max}^* and Q_{\max} by considering the definition of α_h reported in equation(5.1):

$$Q_{\max}^* = Q_{\max} \cdot \left[\lim_{t \rightarrow \infty} \alpha_h(t) \right] = Q_{\max} \cdot \alpha_{h,\max} \quad (5.6)$$

where $\alpha_{h,\max}$ is the degree of hydration theoretically achieved at the end of the hydration process (namely, in the limit for $t \rightarrow \infty$). Thus, the degree of hydration in adiabatic conditions (consistently denoted as $\alpha_{a,h}$) can also be expressed in terms of temperature increase:

$$\alpha_{a,h}(t) = \frac{Q_a(t)}{Q_{\max}} = \frac{\Delta T_a(t)}{\Delta T_{a,\max}} \alpha_{h,\max} \quad (5.7)$$

where $\Delta T_{a,\max}$ is the asymptotic value achieved by the temperature in adiabatic conditions.

Finally, based on the results of experimental tests on hardening concrete samples in adiabatic conditions, two possible analytical expressions were proposed to approximate the observed time evolution of heat $Q_a(t)$ (van Breugel, 1991):

$$Q_a(t) = Q_{\max}^* \cdot (1 - e^{-rt}) \quad (5.8)$$

$$Q_a(t) = Q_{\max}^* \cdot e^{-\left(\frac{\tau}{t}\right)^\beta} \quad (5.9)$$

where Q_{\max}^* is the total heat produced by the hydration reaction in adiabatic conditions and r , τ and β control the shape of the functions introduced to describe the heat evolution in time.

5.1.2 Heat flow and degree of hydration during setting and hardening

Since concrete is generally cured in non-adiabatic conditions, heat-flow occurs throughout the concrete body during setting and hardening phases and results in a transient temperature field.

As a matter of principle, the non-stationary heat conduction problem characterising the thermal behaviour of concrete during setting and hardening can be described by the well-known Fourier equation (Narasimhan, 1999).

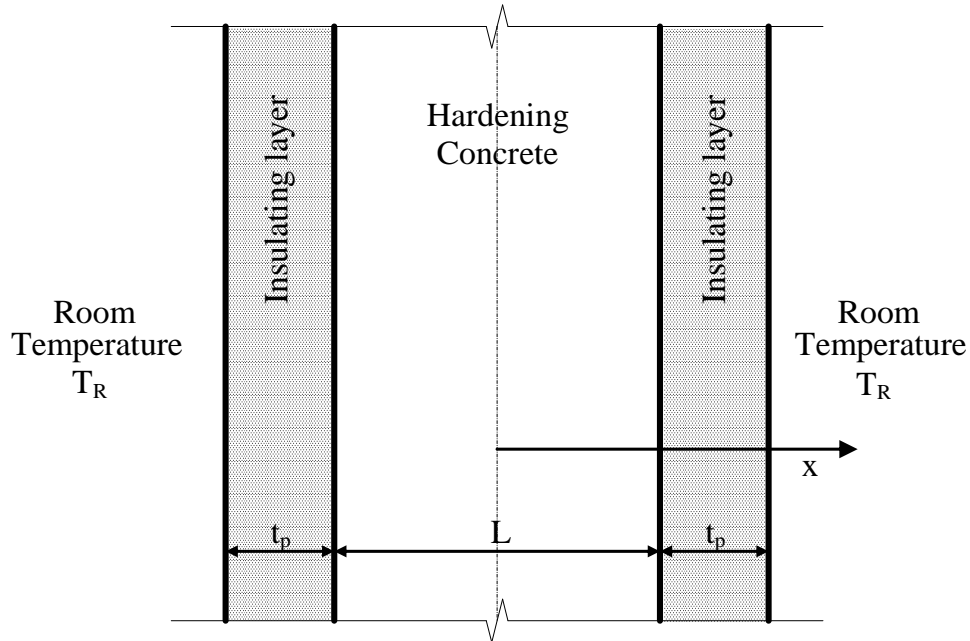


Figure 5.1: Geometrical description of the 1D problem.

In the case of the 1D geometry considered in the present study (Figure 5.1), such a Partial Differential Equation (PDE) has the following analytical expression:

$$\rho_c c_c \frac{\partial T}{\partial t} = \lambda_c \cdot \frac{\partial^2 T}{\partial x^2} + q_c(x, t) \quad (5.10)$$

where

λ_c is the heat conduction coefficient [W/mK];

T is the temperature field in concrete [K];

t time [s];

q_c is the rate of heat source [J/m³s].

and

$$q_c(x, t) = C \cdot \frac{dQ_c}{dt} \quad (5.11)$$

where Q_c is the function describing the heat produced by the hydration reaction per unit mass of cement in general (non-adiabatic) conditions.

As already mentioned in subsection 5.1.1, the rate of heat generation q_c is significantly affected by the actual values of the temperature developed inside the concrete sample. Then, since temperature itself depends on the produced heat, a clear feedback effect can be recognised between q_c and T . Therefore, the effect of

absolute temperature T on the rate $V(T)$ of chemical reaction can be generally expressed through the well-known Arrhenius equation which can be analytically described by the following relationship (van Breugel, 1991):

$$V(T) = A_V \cdot e^{-\frac{E_A}{R \cdot T}} \quad (5.12)$$

where A_V is a reference rate value, E_A is the apparent activation energy (usually expressed in J/mol) and R is the universal gas constant ($R \approx 8.3145$ J/molK). In principle, the values of A_V and E_A can be determined by measuring the rate V under two different temperature values. However, the following applications will be based on assuming $E_A = 33000$ J/mol for hardening concrete, according to experimental results currently available in the scientific literature (Kada-Benameur et al. 2000; D'Aloia & Chanvillard, 2002; van Breugel, 2004).

The Arrhenius equation (5.12) is useful to express the relationship between the actual heat production rate $q_c(T)$ and the corresponding one $q_a(T_a)$ which should have been measured under adiabatic conditions at the same stage of the hydration reaction (Figure 5.2). Thus, if the semi-adiabatic process has achieved the degree of hydration $\alpha_h(t)$ at the time t , an equivalent time t_{eq} can be defined to identify the corresponding status of the hydration reaction in adiabatic conditions:

$$Q_a(t_{eq}) = \alpha_h(t) \cdot Q_{max} \quad (5.13)$$

The actual analytical expression of t_{eq} depends on the analytical form chosen for describing the function $Q_a(t_{eq})$. For instance the following two expressions correspond to the two functions reported in equations (5.8) and (5.9), respectively:

$$\left(1 - e^{-rt_{eq}}\right) = \frac{\alpha_h(t)}{\alpha_{h,max}} \Rightarrow e^{-rt_{eq}} = 1 - \frac{\alpha_h(t)}{\alpha_{h,max}} \Rightarrow t_{eq} = -\frac{1}{r} \cdot \ln \left[1 - \frac{\alpha_h(t)}{\alpha_{h,max}} \right] \quad (5.14)$$

$$e^{-\left(\frac{\tau}{t_{eq}}\right)^\beta} = \frac{\alpha_h(t)}{\alpha_{h,max}} \Rightarrow t_{eq} = \frac{\tau}{\left\{ -\ln \left[\frac{\alpha_h(t)}{\alpha_{h,max}} \right] \right\}^{\frac{1}{\beta}}} \quad (5.15)$$

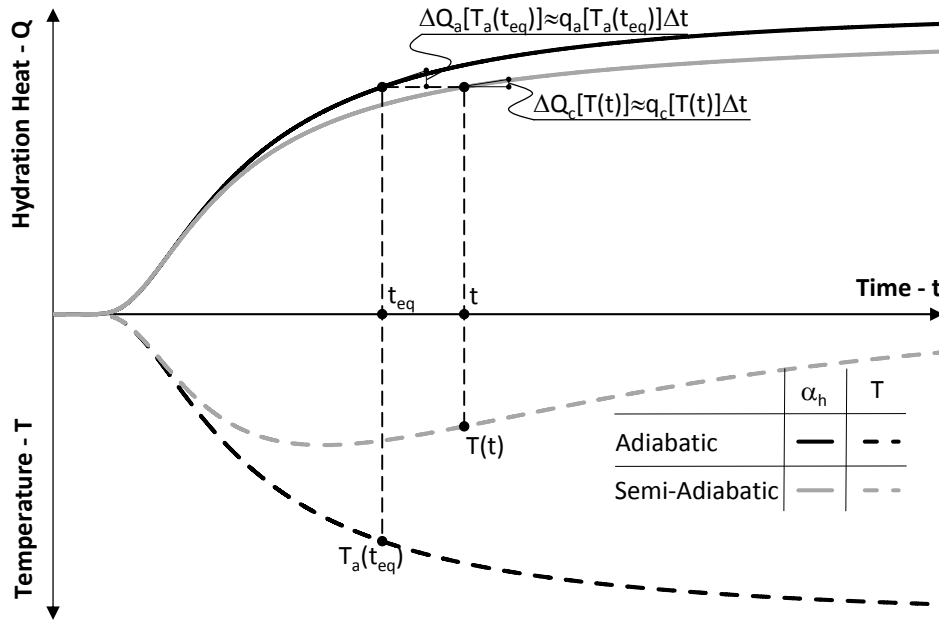


Figure 5.2: Hydration heat produced and temperature developed in adiabatic and non-adiabatic conditions.

Although, in principle, the amount of heat $Q_c(T)$ produced by the general hydration process is equal to that correspondingly generated in the ideal adiabatic process up to the time t_{eq} , the two temperatures T and T_a developed in the two systems at time t and t_{eq} are not equal, as a result of the heat transfer phenomena taking place in this respect. Having pointed out this, a clear relationship can be stated through equation (5.12) between the rate of heat production in the two above mentioned conditions:

$$\frac{q_c[T(t)]}{q_a[T_a(t_{eq})]} = \frac{e^{-\frac{E_A}{R \cdot T(t)}}}{e^{-\frac{E_A}{R \cdot T_a(t_{eq})}}} = e^{\frac{E_A}{R} \cdot \frac{T_a(t_{eq}) - T(t)}{T_a(t_{eq}) \cdot T(t)}} \quad (5.16)$$

As clearly demonstrated in de Schutter & Tearwe (1996), the Arrhenius approach is most accurate for concretes whose binder is mainly made of Portland Cement (e.g., CEM I and CEM II according to the European Classification, EN 197-1:2011), as a unique dominant reaction phase, i.e. C3S, can be recognised in such materials. Under this limitation, the following analytical expression can be determined for the PDE describing the heat flow in hardening concrete by introducing in equation (5.10) the expression of $q_c[T(t)]$ derived by equation (5.16):

$$\rho_c c_c \frac{\partial T}{\partial t} = \lambda_c \cdot \frac{\partial^2 T}{\partial x^2} + q_a [T_a(t_{eq})] \cdot e^{-\frac{E_A}{R} \frac{T_a(t_{eq}) - T(t)}{T_a(t_{eq}) T(t)}} \quad (5.17)$$

where the flow source in adiabatic conditions can be determined as follows:

$$q_a [T_a(t_{eq})] = C \cdot \left. \frac{dQ_a}{dt} \right|_{t=t_{eq}} \quad (5.18)$$

Equation (5.17) can be solved numerically, as explained in section 5.2, once initial and boundary conditions are defined. Initial conditions are rather simple, as room temperature T_R has to be imposed to the entire space domain at $t=0$:

$$T(x, t = 0) = T_R \quad (5.19)$$

Boundary condition at the two external sides can be directly imposed if the time evolution of temperatures $T_{left}(t)$ and $T_{right}(t)$ measured there during the hydration process are actually available:

$$T\left(x = -\frac{L}{2}, t\right) = T_{left}(t) \quad T\left(x = +\frac{L}{2}, t\right) = T_{right}(t) \quad (5.20)$$

where L is the characteristic length of the 1D system under consideration. More often, an insulating layer bounds the two external surfaces of the concrete specimen (Figure 5.1). If t_p is the thickness of such a layer, and λ_p is its heat conduction coefficient, the boundary conditions can be derived by expressing the continuity of the heat flows $q_{left}(t)$ and $q_{right}(t)$ throughout the insulation-concrete interfaces:

$$q_{left}(t) = \lambda_p \cdot \frac{T_{left}(t) - T_R}{t_p} = \lambda_p \cdot \left. \frac{\partial T}{\partial x} \right|_{x=-\frac{L}{2}} \quad (5.21)$$

$$q_{right}(t) = \lambda_p \cdot \frac{T_{right}(t) - T_R}{t_p} = \lambda_p \cdot \left. \frac{\partial T}{\partial x} \right|_{x=+\frac{L}{2}} \quad (5.22)$$

Thus, equation (5.17), initial conditions (5.19) and boundary ones (5.21) and (5.22), describe completely the 1D heat-flow occurring within the hardening concrete element describing in Figure 5.1.

5.1.3 Development of the relevant mechanical properties

It is widely recognised that the degree of hydration α_h controls the key relevant mechanical properties of concrete during the hardening phase (van Breugel, 1991; de Schutter & Tearwe, 1996; Bentz, 1997). Particularly, for the sake of brevity, only two main properties, such as compressive strength f_c and Young Modulus E_c , are considered in the present study.

The former was investigated in-depth and the following linear relationship between f_c and α_h was proposed (Lokhorst, 1999):

$$f_c = f_{c,\max} \frac{\alpha_h - \alpha_0}{1 - \alpha_0} \quad (5.23)$$

where $f_{c,\max}$ is the fictitious maximum strength in the ideal case of complete hydration ($\alpha_h=1.0$) and α_0 is the so-called critical hydration below which no relevant strength gain is achieved. It is worth reporting that a similar correlation between tensile strength $f_{c,t}$ and degree of hydration of concrete was proposed (Lokhorst, 1999).

As far as the Young modulus E_c is of concern, the following non-linear expression was proposed to describe its relationship with α_h (Gutsch & Rostasy, 1994):

$$E_c = E_{c,0} \cdot \sqrt{\frac{\alpha_h - \alpha_0}{1 - \alpha_0}} \quad (5.24)$$

in which $E_{c,0}$ is the fictitious elastic modulus potentially achieved for $\alpha_h = 1.0$ and α_0 has the same meaning defined in equation (5.23).

5.1.4 The “Maturity” concept

As mentioned in subsection 5.1.1 the degree of hydration can be determined from the actual temperature profile and the adiabatic temperature curve. Therefore, in more general conditions, the solution of a heat-flow problem described by the PDEs outlined in subsection 5.1.2 is required to determine $a_h(t)$. However, a possible definition for an alternative parameter that characterises the state of the hydration process, but is easier to measure in both laboratory and field application, would be worthwhile to provide to designers. This would make it more feasible to apply equations (5.23)-(5.24) and predict the actual evolution of the relevant mechanical properties during the concrete hydration process. The so-called “maturity” is a parameter which can possibly be considered to describe the status of the hydration reaction, though its definition is less fundamental than α_h (de

Schutter, 2004). The Nurse-Saul definition of maturity $M(t)$ represents the measure of the area below the temperature-time curve measured on concrete during setting and hardening (Figure 5.3):

$$M(t) = \int_0^t T(\tau) \cdot d\tau \quad (5.25)$$

An alternative formulation was also proposed for the Maturity concept that takes into account the influence of temperature variation on the hydration reaction rate. Particularly, the definition proposed in Freiesleben-Hansen & Pedersen (1977) is among the most well-established one and is also recognised in Han (2005):

$$M(t) = \int_0^t T(\tau) \cdot e^{-\left[\frac{E_A}{R} \left(\frac{1}{T_{ref}} - \frac{1}{T(\tau)} \right) \right]} \cdot d\tau \quad (5.26)$$

where T_{ref} is an (absolute) reference temperature ($T_{ref} = T_R$ is assumed in this study).

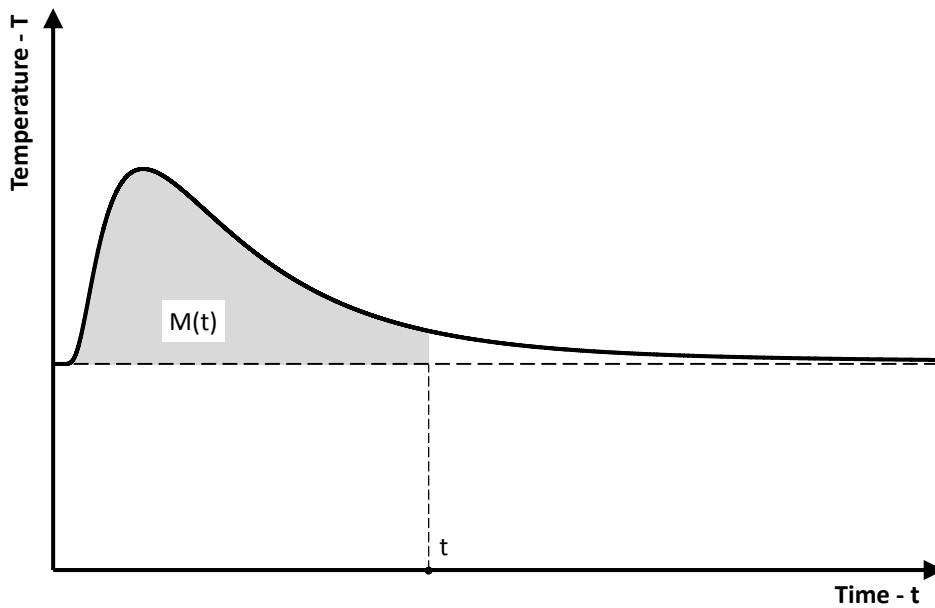


Figure 5.3: The graphical interpretation of the Maturity concept.

5.2 Numerical implementation

The PDE outlined in section 5.1 can be solved numerically through a Finite Difference (FD) approach which is described in subsection 5.2.1. Furthermore,

such a solution for the heat-flow problem and the further calculations needed to determine the degree of hydration and associated mechanical properties of concrete is described in details like in a “recipe” described in subsection 5.2.2.

5.2.1 Finite difference solution of PDEs

The PDE (5.17) which describes the heat-diffusion process throughout the hardening concrete can be turned to a convenient FD expression in each node of a time-space mesh. Particularly, the space domain is subdivided in n_s spaces and (n_s+1) nodes whose distance is

$$\Delta x = \frac{L}{n_s} \tag{5.27}$$

Moreover, a time increment Δt is assumed to develop a time-explicit solution scheme. Figure 5.4 shows the FD discretisation of the space-time domain and the relevance for the problem under consideration.

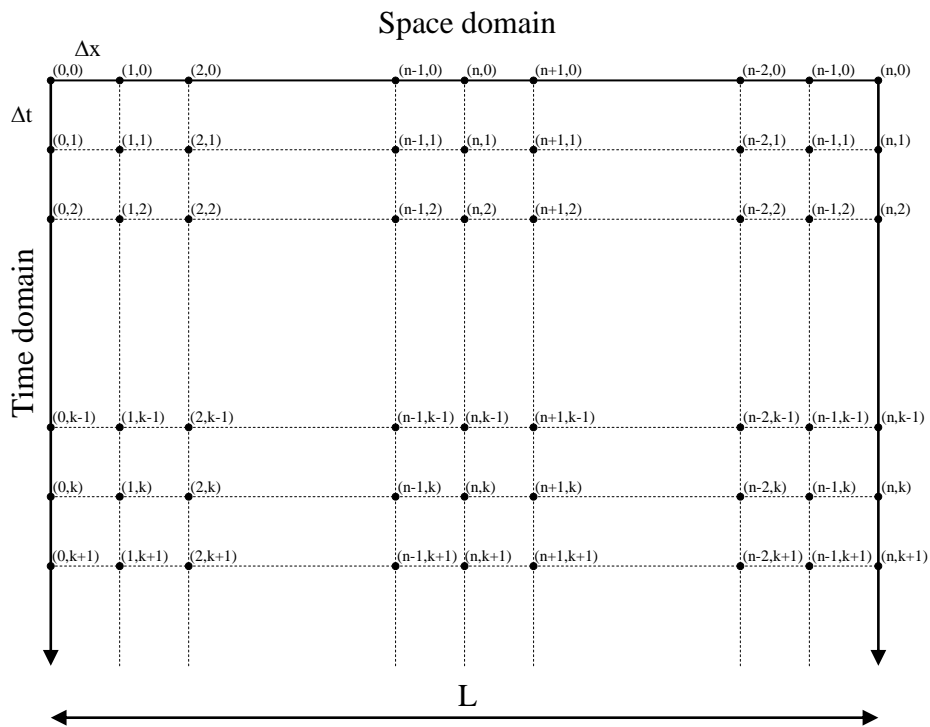


Figure 5.4: Finite Difference scheme integration in time and space.

Then, the FD expression of equation (5.17) is obtained by introducing the central-difference scheme for the space derivative and the forward or backward scheme for the time one. Particularly, the following FD expressions are adopted herein to approximate the second space derivative and the first time derivative of the temperature field $T(x,t)$ in the (n,k) -node of the space-time domain:

$$\left[\frac{\partial^2 T}{\partial x^2} \right]_{n,k} \approx \frac{T_{n+1,k} - 2 \cdot T_{n,k} + T_{n-1,k}}{\Delta x^2} \quad (5.28)$$

$$\left[\frac{\partial T}{\partial t} \right]_{n,k} \approx \frac{T_{n,k+1} - T_{n,k-1}}{\Delta t} \quad (5.29)$$

where a forward scheme is assumed for the latter, which leads to an explicit numerically integration scheme. Thus, the following FD algebraic equation can be determined by introducing equations (5.28) and (5.29) in (5.17) in order to express the value $T_{n,k+1}$ of the temperature field in the $(n,k+1)$ -node:

$$T_{n,k+1} = T_{n,k} + a_c \cdot \frac{\Delta t}{\Delta x^2} \cdot (T_{n+1,k} - 2 \cdot T_{n,k} + T_{n-1,k}) + \frac{\Delta Q_a [T_a(t_{eq,n,k})]}{\rho_c c_c} \cdot e^{-\frac{E_A}{R} \left(\frac{T_{a,eq,n,k} - T_{n,k}}{T_{a,eq,n,k} \cdot T_{n,k}} \right)} \quad (5.30)$$

where n ranges from 1 to (n_s-1) and

$$a_c = \frac{\lambda_c}{\rho_c c_c} \quad (5.31)$$

and then $T_{a,eq,n,k}$ is the temperature which would have been developed in adiabatic conditions at the time $t_{eq,n,k}$ defined in equation (5.13), through the analytical expression described by equations (5.14) and (5.15) corresponding to the heat production functions (5.8) and (5.9), respectively. In fact, it can be determined through equation (5.5) which can be finally expressed as follows, taking into account the equations (5.8) and (5.6):

$$T_{a,eq,n,k} = T_a(t_{eq,n,k}) = T_R + \frac{C}{\rho_c c_c} \cdot Q_a(t_{eq,n,k}) \quad (5.32)$$

Particularly, the definition of $t_{eq,n,k}$ is based in the degree of hydration $\alpha_{h,n,k}$ developed up to the end of the k -th step of the forward time integration. It can be evaluated as follows:

$$q_{c,n,k+1} = q_c(T_{n,k+1}) = q_a(T_{a,eq,n,k+1}) \cdot e^{-\frac{E_A}{R} \frac{T_{a,eq,n,k+1} - T_{n,k+1}}{T_{a,eq,n,k+1} \cdot T_{n,k+1}}} \quad (5.33)$$

$$Q_{c,n,k+1} = \sum_{i=1}^{k+1} \frac{q_{c,n,i} + q_{c,n,i-1}}{2} \cdot \Delta t \quad (5.34)$$

$$Q_{c,k+1} = \frac{1}{L} \cdot \sum_{n=1}^{n_s} \frac{Q_{c,n,k+1} + Q_{c,n-1,k+1}}{2} \cdot \Delta x \quad (5.35)$$

$$\alpha_{h,n,k+1} = \frac{Q_{c,n,k+1}}{Q_{max}}; \quad (5.36)$$

$$\alpha_{h,k+1} = \frac{Q_{c,k+1}}{Q_{max}}$$

Initial conditions can be easily imposed as follows according to equation (5.19):

$$T_{n,0} = T_R \quad \text{for } n=0, \dots, n_s \quad (5.37)$$

Moreover, boundary conditions in space can be turned into a convenient FD form by transforming the analytical expressions reported in equations (5.21)-(5.22):

$$\lambda_p \cdot \frac{T_R - T_{0,k+1}}{t_p} = \lambda_c \cdot \frac{T_{1,k+1} - T_{0,k+1}}{\Delta x} \Rightarrow T_{0,k+1} = \frac{\frac{\lambda_p}{t_p} \cdot T_R + \frac{\lambda_c}{\Delta x} \cdot T_{1,k+1}}{\frac{\lambda_p}{t_p} + \frac{\lambda_c}{\Delta x}} \quad (5.38)$$

$$\lambda_p \cdot \frac{T_{n_s,k+1} - T_R}{t_p} = \lambda_c \cdot \frac{T_{n_s,k+1} - T_{n_s,-1k+1}}{\Delta x} \Rightarrow T_{n_s,k+1} = \frac{\frac{\lambda_p}{t_p} \cdot T_R + \frac{\lambda_c}{\Delta x} \cdot T_{n_s}}{\frac{\lambda_p}{t_p} + \frac{\lambda_c}{\Delta x}} \quad (5.39)$$

Equation (5.30) demonstrates that the outlined numerical procedure is explicit in space and time, as the value $T_{n,k}$ depends on values of the temperature field at both time t_{k+1} and t_k . However, for each instant t_k the value of the temperature field in (n_s+1) nodes should be determined. In fact, (n_s-1) field

equations (5.30) along with the boundary conditions (5.38) and (5.39) balance the number of unknowns.

In order to achieve a stable solution for the explicit numerical integration scheme considered in this approach, equation (5.30), a convergence criterion has to be considered. For a steady state 1D schematisation for time integration, the following criterion holds (Laube, 1991; Van Kan et al., 2008):

$$\frac{a_c \cdot \Delta t}{\Delta x^2} \leq \frac{1}{2} \quad (5.40)$$

Finally, the two definitions of concrete maturity reported in equations (5.25) and (5.26) can be easily calculated in the general node n of the space domain on the basis of the numerical values of the time evolution of temperature field $T_{n,k}$:

$$M_n(t) = \sum_{i=1}^k \frac{T_{n,i} + T_{n,i-1}}{2} \cdot \Delta t \quad (5.41)$$

$$M_n(t) = \frac{\sum_{i=1}^k T_{n,i} \cdot e^{-\left[\frac{E_A}{R} \left(\frac{1}{T_{ref}} - \frac{1}{T_{n,i}}\right)\right]} + T_{n,i-1} \cdot e^{-\left[\frac{E_A}{R} \left(\frac{1}{T_{ref}} - \frac{1}{T_{n,i-1}}\right)\right]}}{2} \quad (5.42)$$

Then, a global value of such parameter for the whole specimen can be calculated through a space average:

$$M_n(t_k) = \sum_{i=1}^{n_s} \frac{M_n(t_k) + M_{n,i-1}(t_k)}{2} \quad (5.43)$$

5.2.2 Details about the proposed numerical “recipe”

The proposed numerical solution of the heat-flow problem (subsection 5.2) can be easily implemented in either a high-level programming language or a spreadsheet tool. In this second case each node of the space-time domain represented in Figure 5.4 can correspond to a cell of the spreadsheet and the equations can be solved iteratively for each time step. The numerical scheme described by equation (5.30) can be copied in all cells corresponding to the internal nodes of the FD mesh represented in Figure 5.4. The boundary conditions in space are created by considering at each time step the equations (5.38) and (5.39) on the left and right lateral borders, respectively. The starting conditions of the PDE represent the actual temperature of the concrete mix: This is the temperature after mixing and is representing the initial condition of the elements $T(x,t=0)=T_R$. As long as hydration proceeds ($Q_a(t)>0$), heat will be generated by the adiabatic curve reported in

equation (5.9) and the temperature will be transferred to the boundaries according to the heat flow equation (5.30). The continuous increase of heat will lead to an increase of the temperature while the associated temperature field is solved by the spreadsheet solver. From the calculated temperature field the distribution of the degree of hydration can be calculated at the end of the current time step through equations (5.33)-(5.36). The degree of hydration will depend on the development of the temperature in the different cells and indicate the amount of hydration products that have been formed in the concrete during hydration. Therefore, based on this, the equations (5.23) and (5.24) for strength and elastic modulus are implemented, and relate the development of these mechanical properties to the degree of hydration.

Finally, Figure 5.5. depicts a flow-chart of the proposed numerical “recipe”. It describes the sequence of operations possibly needed to implement the proposed numerical simulation whose time integration ends when the amount of heat produced in the last iteration falls below a given user-defined tolerance represented by the parameter ε_Q reported in the last “diamond” block of the flow-chart in Figure 5.5.

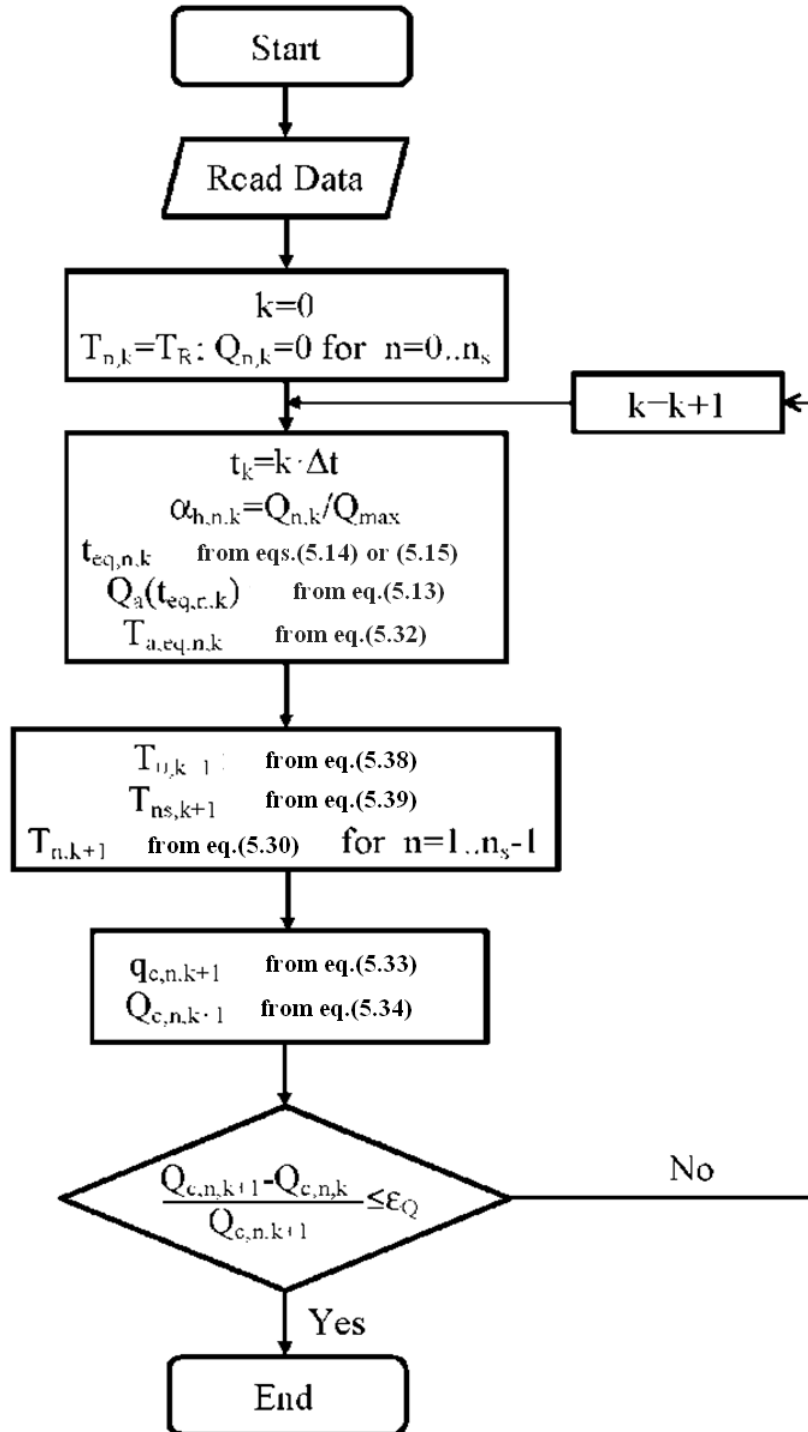


Figure 5.5: Flow-chart of the proposed numerical procedure.

5.3 Validation of the proposed heat-flow and hydration model

This section summarises the experimental results considered as a benchmark and proposes the comparison between such results and the corresponding numerical simulations whose agreement leads to the validation of the proposed model.

5.3.1 Outline of experimental test setups

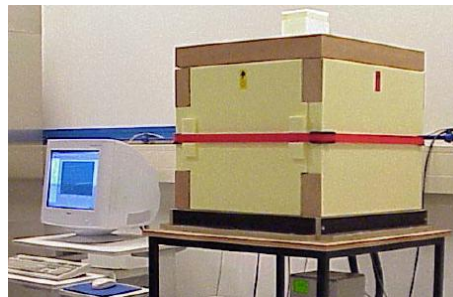
The model presented in sections 5.1 and 5.2 needs to be validated in its capability to simulate the hydration process under both adiabatic and non-adiabatic conditions. Experimental data, characterizing the hydration process of four concrete mixtures for a water-cement ratio $w/c=0.4$, was obtained from temperature measurements conducted at Delft University of Technology (The Netherlands) and reported in (Koenders, 2005). However, since the proposed model relies upon the Arrhenius function for controlling the rate of the hydration heat mentioned in subsection 5.1.2, and is, therefore, most accurate for applications with Portland Cement-based concretes (Voglis et al., 2005; Wang et al., 2010), only the specimens indicated as “Mixture 3” and “Mixture 4” are considered in the present study. Particularly, Mixture 3 contains 450 kg/m^3 of CEM I 32.5 with addition of 5% of silica-fume, whereas 450 kg/m^3 of CEM II/A was employed in Mixture 4. From the experimental data, a set of temperature measurements carried out on different concrete samples cured at both adiabatic and non-adiabatic conditions was available (Koenders, 2005). Figure 5.6 depicts the experimental equipment employed in the experimental tests.

The adiabatic hydration curve is measured from a freshly cast concrete cube for which the thermal boundary conditions are controlled in such a way that heat liberation to the surrounding is prevented. This means that all heat generated inside the concrete cube will be used in favour of the rate of the chemical reaction process. It is a method to calculate the maximum heat generated by a concrete mixture. At Delft University of Technology, the test set-up to determine the adiabatic hydration curve consists of an insulated mould of which the thermal boundary conditions are controlled by computer and a cryostat unit (Figure 5.6a).

To measure the semi-adiabatic temperature evolution, the dummy setup is used (Figure 5.6b), which is part of the Thermal Stress Testing Machine (TSTM), and is generally used to measure temperature developments and free deformations. The temperature evolution is measured in the centre of the specimen, at half of the specimen height; the thickness of the specimen is 100 mm and the width 150 mm

(Figure 5.6b). The mould is thermally insulated which leads to the increased temperature evolution during hardening (semi-adiabatic).

Compressive strength measurements were obtained from cubic specimen of $150 \times 150 \times 150 \text{ mm}^3$ (EN 12390-3:2009) tested at 1, 3, 7 and 28 days (3 for each age). After casting, the cubes were vibrated and covered with a plastic foil. The semi-adiabatic temperature evolution measured from the test setup (Figure 5.6b) was imposed to the compressive strength cubes by means of thermally adaptive cubes to which copper water tubes mounted, at the side panels of the steel moulds (Figure 5.6c).



(a) Adiabatic conditions



(b) Non-adiabatic conditions



(c) Thermal adaptive moulds for measuring the compressive strength

Figure 5.6: Experimental equipment (Koenders, 2005).

5.3.2 Temperature experiments and numerical predictions

To validate the proposed flow and hydration model, both adiabatic and semi-adiabatic temperature evolution measurements are simulated. Figure 5.7 describes the time evolution of the temperatures measured in the specimens made of the Mixtures 3 and 4 under the conditions described above. The adiabatic temperature

curves show the upper boundaries of the temperature evolution whereas temperature measurements under semi-adiabatic conditions show a maximum after which the temperature turns back to the room temperature, being the result of the heat flow. Moreover, Figure 5.8 reports the time evolution of cubic compressive strength measured from the concrete specimens made of the same mixtures and cured under the same semi-adiabatic conditions.

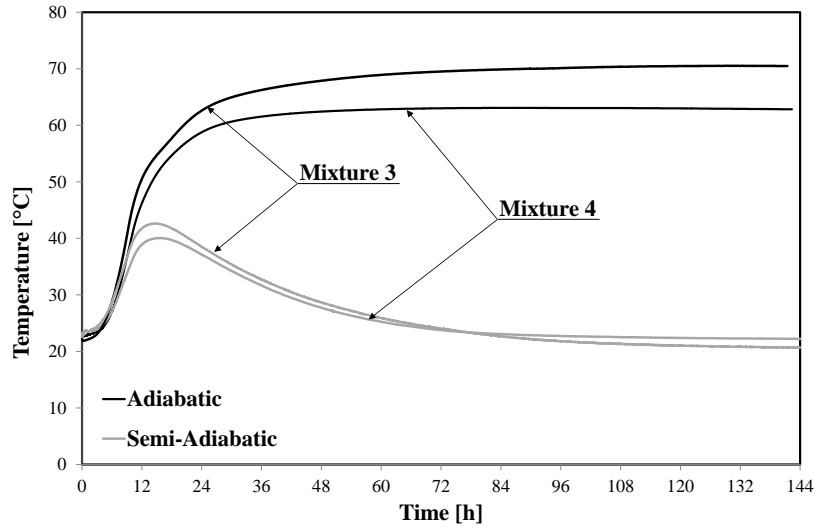


Figure 5.7: Experimental results: time evolution of temperature (Koenders, 2005).

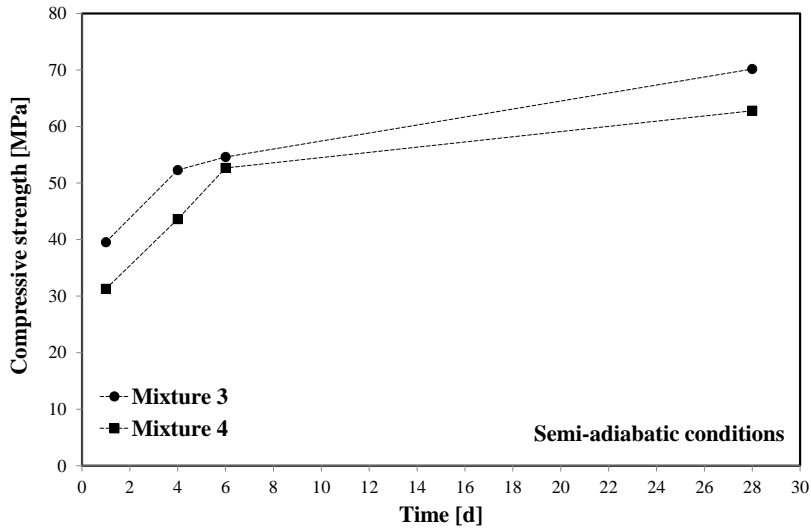


Figure 5.8: Experimental results: time evolution of the compressive strength (Koenders, 2005).

Both the adiabatic and semi-adiabatic temperature mixtures are simulated with the proposed flow model using the input values given in Table 5.1.

Table 5.1: Overview of input values used to simulate Mixture 3 and 4.

Input value flow model	Symbol	Mix.3	Mix.4
Maximum degree of hydration [-]	$\alpha_{h,max}$	0.78	0.77
Maximum potential heat [kJ/kg]	Q_{max}	350	300
Cement content [kg/m ³]	C	450	450
Density times specific heat [kJ/m ³ K]	$\rho_c c_c$	2500	2500
Heat conduction coefficient [W/mK]	λ_c	2.5	2.5
Heat diffusion coefficient [m ² /sK]	a_c	1E-6	1E-6
Time increment [s]	Δt	20	20
Space increment [m]	Δx	0.0075	0.0075
Insulation thickness [m]	t_p	0.04	0.04
Heat conduction coefficient of insulation layer [W/mK]	λ_p	0.125	0.125
Apparent activation energy [J/mol]	E_A	33000	33000
Universal gas constant [J/molK]	R	8.31	8.31
Coefficient for adiabatic function [h] acc. to equation (5.8)	τ	8.5	9
Coefficient for adiabatic function [-] acc. to equation (5.8)	β	1.6	2.1

Particularly, the simulation has been carried out by fine-tuning the values of τ and β according to an Inverse Identification Procedure (Faella et al., 2009). The results are plotted in Figure 5.9 and Figure 5.10 and the model shows similar temperature evolution as measured experimentally. In the simulations the adiabatic temperature evolution acts as the heat source (equations (5.8) and (5.9)) whereas the semi-adiabatic temperature evolution represents the respond of the model.

The potential of the model to simulate in a single run the temperature evolution in both adiabatic and semi-adiabatic conditions is very promising. From the semi-adiabatic temperature evolution and the adiabatic curve the actual heat development can be calculated. For this, the actual rate of hydration can be attained by applying the Arrhenius function. This approach enables the calculation of the actual rate of hydration for a (semi-adiabatic) temperature, which is always lower than the adiabatic temperature evolution. From the actual heat development and the maximum heat that can be generated under adiabatic conditions, both degree of hydration and maturity. This approach can also be easily implemented in the numerical solutions (e.g. developed in a spreadsheet) and the evolution of the degree of hydration with time is simulated for both Mixture 3 and 4.

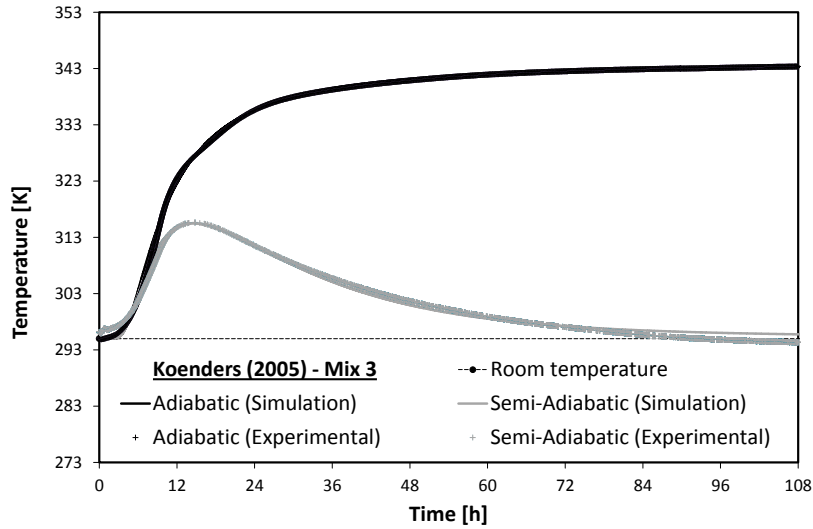


Figure 5.9: Time evolution of Temperature (adiabatic heat production according to equation (5.9)): Mixture 3.

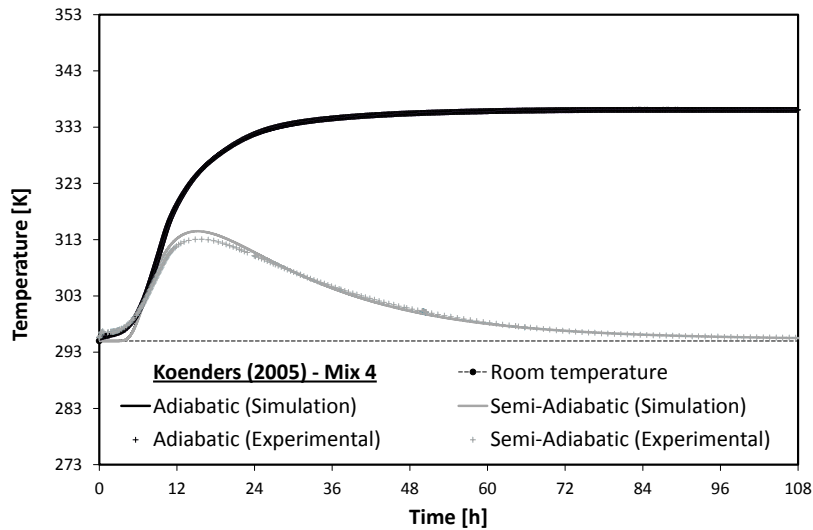


Figure 5.10: Time evolution of Temperature (adiabatic heat production according to equation (5.9)): Mixture 4.

The results of this calculation are depicted in Figure 5.11 and Figure 5.12. It can be observed that the degree of hydration for both mixtures starts to deviate from hydration under adiabatic conditions at the moment that the temperature evolution is deviating significantly from the adiabatic conditions.

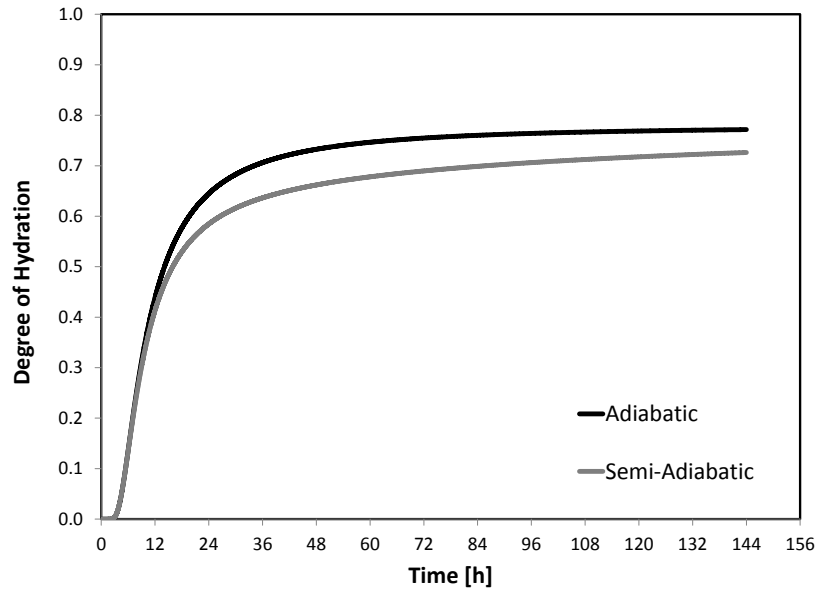


Figure 5.11: Time evolution of degree of hydration: Mixture 3.

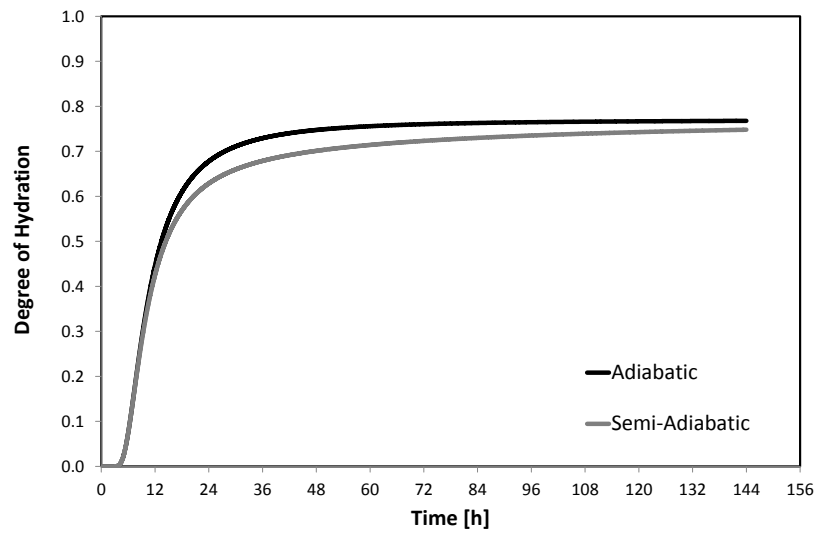


Figure 5.12: Time evolution of degree of hydration: Mixture 4.

The reduced temperature leads to a reduction of the rate of hydration according to Arrhenius that finally leads to a lower degree of hydration. However, for the given temperature conditions, the degree of hydration of both mixtures tend to approach the maximum degree of hydration under adiabatic conditions closely.

5.4 Hydration process and material properties

This section outlines a relevant application of the proposed model aimed at investigating the possible correlation between the development of compressive strength in the hardening stage and the corresponding status of the hydration reaction which can be described through degree of hydration and maturity

5.4.1 Correlation between degree of hydration and compressive strength

As the degree of hydration reflects the amount of cement that has reacted and the progressive formation of a load bearing microstructure that is built up from hydration products, a correlation with the material properties can be expected. In Lokhorst (1999) reported a strong relationship between the degree of hydration and the compressive strength, the tensile splitting strength and the elastic modulus. In order to evaluate the performance of the flow model and to examine the relationship between the concrete compressive strength and the degree of hydration, the compressive strength tests (Figure 5.8) were correlated to the associating degree of hydration for both Mixture 3 and 4.

The results of this correlation are depicted in Figure 5.13 and it can be observed that the number of available data points is not sufficient to be able to confirm the correlation between the compressive strength and the degree of hydration for the Mixtures 3 and 4. Therefore, the relation proposed by Lokhorst (equation(5.23)) is not considered in this figure, but instead, a linear trend line was fitted through the available data points. The results show a linear impression with the compressive strength.

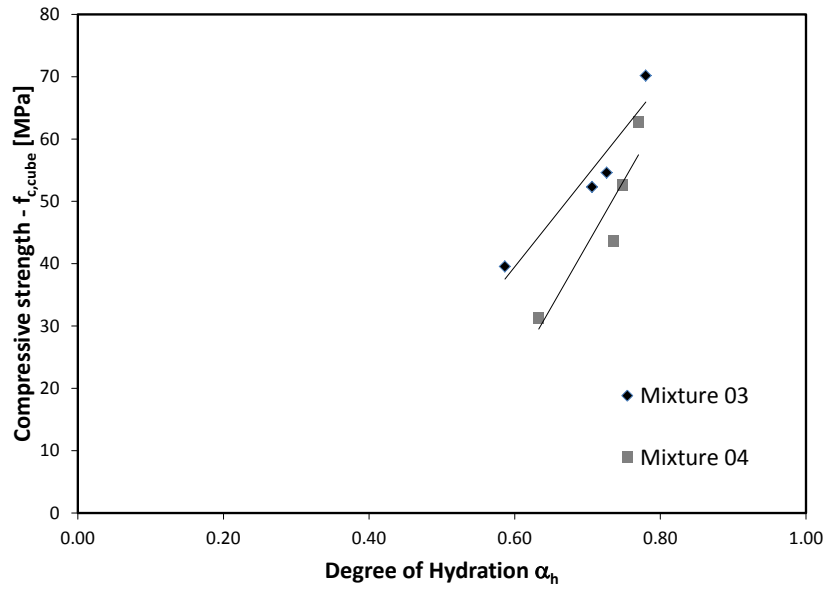


Figure 5.13: Evolution of compressive strength versus degree of hydration: Mixture 3 and 4.

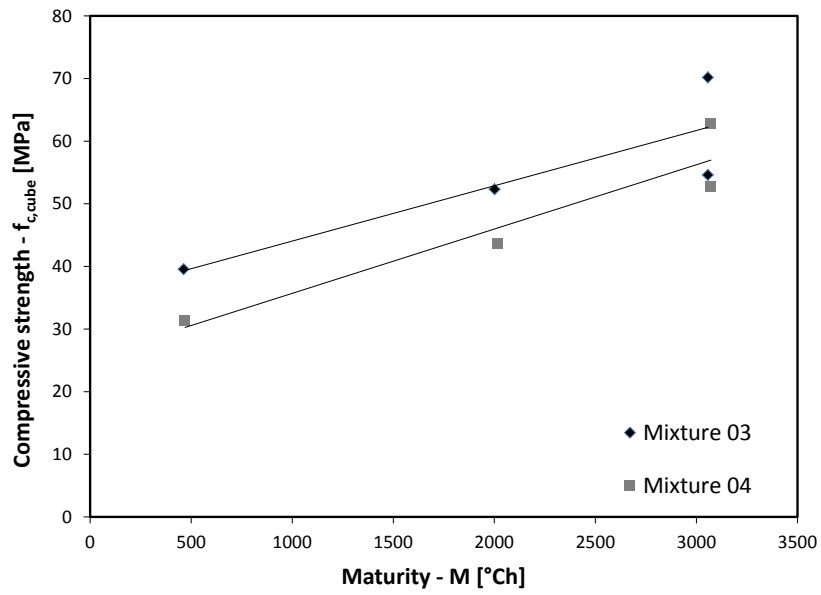


Figure 5.14: Evolution of compressive strength versus maturity: Mixtures 3 and 4.

5.4.2 Correlation between maturity and compressive strength

A more practical parameter that can be applied to indicate the evolution of the material properties is the maturity (see subsection 5.1.4). When considering the maturity to reflect the state of the hydration process, a correlation between the evolution of the maturity and the compressive strength is also to be expected.

In Figure 5.14, the evolution of the compressive strength is shown as a function of the maturity. In order to evaluate the linearity of the dependency with the maturity, a trend line was drawn through the available data points as well. The results show a linear correlation where only at the end of hydration the trend becomes more irregular. However, it worth noting that, also for these results, the number of available data points is insufficient to confirm the validity of the proposed trend of this research.

5.5 Conclusions

This chapter proposed a theoretical model for simulating hydration process and the resulting heat production (and temperature development) occurring in concrete during the hardening phase.

A step-by-step “recipe” was presented to make reasonably feasible the numerical implementation of the complex theoretical formulations needed to accurately analyse the above mentioned phenomena. Thus, the model can be easily employed for analysing the evolution of mechanical properties such as the compressive strength, the tensile strength and the elastic modulus, and enables the possibility to relate the development of these material properties to one fundamental parameter, called the degree of hydration.

Furthermore, the model was validated by means of temperature curves measured from two different hardening concretes under adiabatic and semi-adiabatic conditions. Main aim of this validation is to demonstrate the potential of the model to compare both the adiabatic hydration curve (heat source) and the semi-adiabatic temperature response (output), for given boundary and starting conditions, during one single run. For the two selected mixtures, good agreement could be found between measured and simulated temperatures. Based on the assumptions of applicability of the Arrhenius function for concrete, the heat of hydration could also be simulated under general semi-adiabatic conditions, and from this the degree of hydration. The following conclusions can be drawn:

- The proposed numerical model accurately simulates the temperature evolution of hardening concrete;

- The model simulates the degree of hydration of a hardening concrete sample under adiabatic and semi-adiabatic conditions;
- A correlation between the experimentally obtained compressive strength data and the simulated degree of hydration show a linear trend. However, more data is needed to confirm this observation;
- The correlation between the maturity and the experimentally obtained compressive strength data shows a linear trend. Also here, more data is needed to strengthen this correlation.
- The proposed 1D flow and hydration model turns out to be a useful tool for researchers to analyse the data obtained from early age concrete problems.

The proposed flow model is developed within the framework of the “EnCoRe” Project and should be considered as a first approach towards the design of an analysis tool for concretes with recycled aggregates and binders. The model will be further developed in this respect with emphasis on the mechanical performance of the natural and recycled aggregates partly in combination with replaced binders such as fly-ash. Of particular attention will be the correlation between the evolution of the degree of hydration and the development of the material properties. For this the formulation for the material properties evolution as well as dependency of the hydration kinetics for different temperature conditions (Arrhenius) will be considered.

6. Predicting the mechanical properties of RAC

This chapter describes some of the possible modelling approaches for both prediction and controlling the key mechanical properties of Recycled Aggregate Concretes. The chapter is organised in three sections in which the different models applied during the research are described.

The first modelling approach was performed through the Compressible Packing Model (CPM) developed by de Larrard (1999) This is a semi-empirical model and is validated for several kind of concrete families (i.e., ordinary concrete, high performance concrete, concrete with lightweight aggregates etc.). The aim of this simulation was to understand if this CPM can be easily extendible in the case of RACs. In particular, the main focus of this research was on the prediction of the compressive strength for RAC.

Then, a FEM analysis was performed with lattice model simulation. In fact, the Delft Lattice model was used (Schlangen & Van Mier, 1992). The aim of this other simulation was to unveiling the rule of each phases in the failure mechanism for the case of RACs.

Moreover, based on the application of the Hydration Model described in chapter 5 to some of the experimental results illustrated in chapter 3, an innovative modelling approach is proposed for the case of RAC. Particularly, the proposed formulations should be considered as a novel conceptual approach capable of considering the key physical and mechanical features characterising the structural behaviour of resulting concrete made out with Recycled Concrete Aggregates.

The first two sections are divided in two subsections in which both the theoretical approach and then the RAC application are reported, respectively. Moreover, the modelling approach is described in the last section and then the novel conceptual formulation is calibrated and validated.

6.1 Compressible packing model

The compressible packing model (CPM) was developed by de Larrard (1999) to describe the packing density achieved by a granular mixture. The main principle of the model is that all size classes in the mixture interact with all other size classes by affecting the overall density. The CPM models the actual packing density which can be achieved using a mixture of actual aggregates and is a refined version of a previous model, the linear packing model for grain mixtures (Stovall et al., 1986). In this section, a brief overview of the model is given by focusing on the modelling approach for the compressive strength of the concrete mixture. Subsequently, the results of some applications of the CPM model to the case of RAC are reported.

6.1.1 Theoretical formulation

Virtual Packing Density

The virtual packing density concept, defined as the maximum packing density reachable for a given mixture, is particularly relevant for the following theoretical formulation. For example, the virtual packing density of a mix composed by mono-size spheres is equal to 0.74 the packing density of a face-centred cubic lattice of touching spheres (Figure 6.1). The virtual packing density of a single component mixture is denoted β_i .

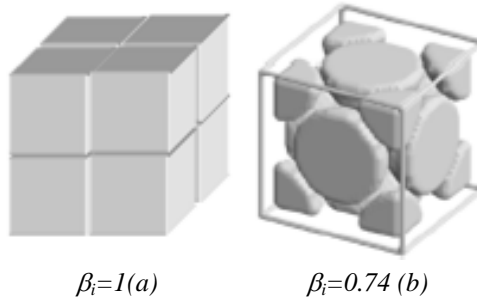


Figure 6.1: Virtual packing density for: cubes (a) and spheres (b).

It should be noted that the virtual packing density is a theoretical concept that is only a component of the achievable density of an real mixture: in fact, the physical packing density is also influenced by the compaction of the granular particles. Moreover, when different particle sizes are involved in the mixtures, the particles can interact with each others. Particle without interaction, means that the local arrangement of an assembly of grains of a certain size in not perturbed by the vicinity of a grain of the second size. Based on that concept, it is possible to define

the effect of a dominant class. A class of large grains is dominant when it fills all space available such that adding a smaller grains would merely fill interstitials without forcing the large particles apart (Figure 6.2a). On the contrary, a class of small grains is dominant when it consumes more space than the interstitials available between the large particles (Figure 6.2b).

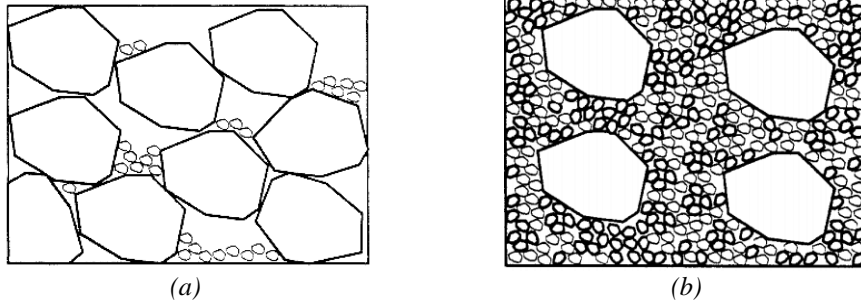


Figure 6.2: Binary mixture without interaction, Coarse (a) and fine (b) grains dominant (de Larrard, 1999).

For these reasons, if, for example, a class j grain is inserted in the porosity of a coarse grain packing (dominant), and if it is no longer able to fit in a void, there is locally a decrease of volume of class i grains (loosing effect, Figure 6.3).

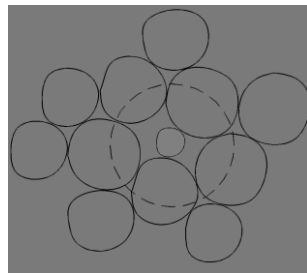


Figure 6.3: Loosening effect.

Moreover, if some isolated coarse grains are immersed in a sea of fine grains (dominant), there is a further amount of voids in the packing of class j in the interface vicinity (wall effect, Figure 6.4).

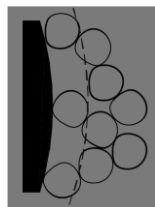


Figure 6.4: Wall effect.

The following equation defines the packing density γ_i when class i is dominant and represents the most general formulation for the virtual packing density γ of a granular mix:

$$\gamma_i = \frac{\beta_i}{1 - \sum_{i=1}^{i-1} \left[1 - \beta_i + b_{ij} \cdot \beta_i \cdot \left(1 - \frac{1}{\beta_i} \right) \right] \cdot y_i - \sum_{j=i+1}^n \left[1 - a_{ij} \cdot \frac{\beta_i}{\beta_j} \right] \cdot y_j} \quad (6.1)$$

$$\gamma = \min\{\gamma_i\} \quad (6.2)$$

where the value y_i represents the volume fraction of the i -th size class, while a_{ij} and b_{ij} are the two parameters defining loosening and wall effects, respectively.

As mentioned, the loosening effect describes the phenomenon observed when the introduction of small particles forces apart larger particles. When $d_i \gg d_j$ (no interaction), $a_{ij}=0$, while when $d_i=d_j$ (total interaction), $a_{ij}=1$.

The analytical expression for the parameter a_{ij} is:

$$a_{ij} = \sqrt{1 - \left(1 - \frac{d_j}{d_i} \right)^{1.02}} \quad (6.3)$$

The wall effect describes an effect whereby larger particles cause interstitials in the mixture which are too small to be filled by other particle classes. When $d_i \gg d_j$ (no interaction), $b_{ji}=0$, while when $d_i=d_j$ (total interaction), $b_{ji}=1$.

The analytical expression of the parameter b_{ji} is:

$$b_{ji} = 1 - \left(1 - \frac{d_j}{d_i} \right)^{1.50} \quad (6.4)$$

The Compressible Packing Model Equations

Once having introduced the virtual packing density of a granular mixture, the real (or “actual”) packing density should be defined. In order to evaluate the actual packing density, it is necessary to introduce a scalar index K that establishes a relationship between the real and the virtual packing density. The K parameter depends on the process of building the particles. de Larrard (1999) assumes the following expression for the parameter K :

$$K = \sum_{i=1}^n K_i = \sum_{i=1}^n \frac{\frac{y_i}{\beta_i}}{\frac{1}{\phi} - \frac{1}{\gamma}} \quad (6.5)$$

where ϕ represents the percentage solids of the mixture ($\phi < \gamma$). The scalar K depends on the manner in which the mixture is compacted. The Table 6.1 reports the value assumed for K as a function of the compaction process.

Table 6.1: Experimental values for the parameter K .

Process of building the particles	K
Simple release	4.1
With a stick	4.5
Vibration	4.75
Water demand	6.7
Vibration + compaction	9
Virtual packing	∞

To obtain a mixture of maximal density, one must optimise K in equation (6.5) with respect to ϕ . A theoretical result for a simplified model presented elsewhere (de Larrard, 1999) indicates that an optimal mixture with size classes of the form $d_n = \lambda d_n^{\max}$ with $n = 0$ for the largest and $n = i$ for the i -th size class should have equal values of K_i when the density is maximised. Moreover, in order to consider the effect of segregation possibly occurring in the granular mixtures, the following formula is introduced:

$$S = 1 - \min \frac{K_i}{1 + K_i} \quad (6.6)$$

Finally, to find out the optimal mixture, the CPM equation should be solved by maximising the ϕ value and minimising the segregation. It can be observed from the segregation potential equation (6.6) that the minimum value for K_i is achieved when all K_i are equal since $9.0 = K$. This condition minimises both the segregation potential and maximises the density. The calculation can be conducted by optimizing ϕ without optimizing S but the mixture will have a larger tendency to segregate. Then, the final solution is based on optimising the compressible packing model equation for $K_i = K_{i+1} = \dots$

Residual packing density

The residual packing density (virtual packing density of a monosize class) is governed by the shape and surface texture of aggregate particles. In a given aggregate fraction it depends on the particle size. In fact, it is deduced from the actual packing density, which is measured with a given packing process.

Following the CPM theory, the actual packing density can be measured using a variety of procedures, all characterised by a compaction index. However, experience has shown that methods producing high packing values (corresponding to high compaction index) are preferable, because their variability is less.

In the method proposed by Sedran and de Larrard (1994) a mass M_D of dry aggregate is put in a cylinder having a diameter D , which is more than five times the maximum size of aggregate. A piston is introduced in the cylinder, and a pressure of 10 kPa is applied on the surface of the specimen. Then, the cylinder is fixed on a vibrating table, and submitted to vibration for 2 min. The actual packing density is calculated from the final height, h , of the sample:

$$\phi = \frac{4 \cdot M_D}{\pi \cdot D \cdot h \cdot \rho_D} \quad (6.7)$$

If the aggregate is monosized (which means that it passes entirely through a sieve of size d_i , and is fully retained by a sieve of size d_{i+1} , with $d_i / d_{i+1} < 1.26$) we have:

$$\bar{\beta} = \left(1 + \frac{1}{K}\right) \cdot \phi \quad (6.8)$$

where $\bar{\beta}$ is the mean residual packing density, affected by the wall effect due to the cylinder. The residual packing density in infinite volume β is then:

$$\beta = \frac{\bar{\beta}}{1 - (1 - k_w) \cdot \left[1 - \left(1 - \frac{d}{D}\right)^2 \cdot \left(1 - \frac{d}{h}\right)\right]} \quad (6.9)$$

where k_w is the wall effect coefficient that takes into account of the boundary conditions, d is the average diameter of the aggregate and h is the height in the cylinder. The value of k_w was measured by de Larrard for round and crushed grains in 30 widely varying cases. For round grains, $k_w=0.88$ and for crushed grains, $k_w=0.73$.

Concrete compressive strength

As the concrete is a composite in which the cement paste represents the matrix and the aggregates (both fine and coarse) are the inclusions, every compounds plays an important rule for the definition of the strength related to final concrete performance.

First, the time evolution of strength in the cement paste, influenced by the cement type, water to cement ratio and curing condition, should be determined. The approach followed in the CPM is to model the hardened cement paste characteristics through micro-structural models. Particularly, the microstructure of hardened cement paste is compared with a lattice structure and the CSH gel between two pores may form either rods or plates. By following this approach, the compressive strength of the cement paste f_{cp} become a function of the actual volume of the cement v_c , the volume of water v_w and the volume of the entrapped air v_a :

$$f_{cp} = \alpha \cdot \left(\frac{v_c}{v_c + v_w + v_a} \right)^2 \quad (6.10)$$

The above formula is the well know Féret equation (1892) where α is a scalar representing the direct proportion between the cement paste strength and the volumetric fractions of cement, water and air.

The equation (6.10) furnishes the value of the cement paste strength, but it does not take into account of the presence of granular inclusion such us sand and coarse aggregates. In principle, it is possible to define the matrix strength f_{cm} that represents the compressive strength of the cement paste f_{cp} when granular inclusion are mixed with cement paste. Obviously, f_{cm} is a function of f_{cp} , but it is also influenced by the “geometrical parameters” of the inclusions, such us grading, shape of the grains and concentration in the composite (i.e., mortar or concrete).

In fact, in a dry packing of particles loaded in compression, the coarse particles tends to carry the maximum stresses and represents the “hard points” while, the fine aggregates in between these particles are the soft medium. When the particles are distributed randomly, two of the coarse particles can be in touch and the maximum stress of the dry mixture is reached (Figure 6.5a). Now, if the cement paste is the soft medium, the area in between these two coarse particles will be highly stressed compared with the other points of the mixtures (Figure 6.5b).

For taking into account of this effect, the CPM introduce a parameter defined as Maximum Paste Thickness (MPT) and physically represents the distance in between the coarse aggregates (Figure 6.5b).

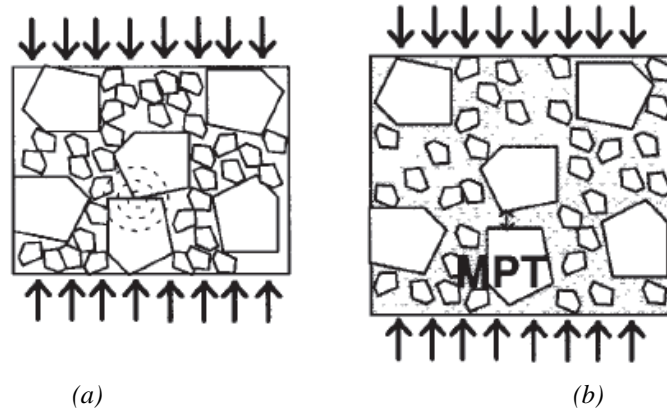


Figure 6.5: The MPT concept (de Larrard, 1999).

The MPT is calculated by considering the total amount of the aggregates, their maximum size, their shape and distribution inside the mixture. Consequently, the cement matrix strength is equal to:

$$f_{cm} = f_{cp} \cdot \text{MPT}^{-0.13} \quad (6.11)$$

Finally, the development of concrete strength is strictly proportional to the one of the matrix. In the CPM model, the following formulation is proposed for taking into account of the rule of the aggregates on the compressive strength of the concrete composite:

$$f_c = \frac{p \cdot f_{cm}}{q \cdot f_{cm} + 1} \quad (6.12)$$

where f_{cm} is the compressive strength of the cement matrix (in MPa) and f_c is the resulting concrete strength (in MPa). Meanwhile, p and q are two empirical constants depending on the aggregates. Physically, p represents the bond between the aggregate and the paste, while q identifies the intrinsic strength of the aggregates.

No direct measurement is possible for determining the values of p and q . It is necessary to produce at least two concretes (1 and 2) of very different strength (e.g., a normal-strength concrete and a high-performance concrete), with a cement of known strength. For each concrete batch produced, the aggregate packing density must be evaluated, so that the MPT and the matrix strength can be calculated. Then, a system of two equations with two unknown parameters, leads to the calculation of both coefficients p and q :

$$f_{c,1} = \frac{p \cdot f_{cm,1}}{q \cdot f_{cm,1} + 1} \quad (6.13)$$

$$f_{c,2} = \frac{p \cdot f_{cm,2}}{q \cdot f_{cm,2} + 1} \quad (6.14)$$

6.2 Application

In this section an example relative to the application of the CPM performed on the case of RAC is given. The material employed for the application are:

- Cement: CP V ARI RS;
- Natural Sand: SAND_BR (see Table 2.2);
- Natural Aggregates: NA_BR (see Table 2.2);
- Recycle concrete aggregates: RCA1 (See Table 2.2);
- Superplasticizer (SP in the following tables): Glenium 51.

First of all, it is necessary to define all the input parameters for running the simulation using the BétonlabPro 3 software in which de Larrard & Sedran (2007) developed the CPM.

As mentioned in the previous section, the input parameters necessary for the concrete mixture optimization through CPM are the main physical and geometrical characteristic of both coarse and fine aggregates, together with some chemical-mechanical information related to the cement employed in the mixture (Figure 6.6).

Classe vraie à 1 jour	15,16
Classe vraie à 2 jours	
Classe vraie à 3 jours	25,08
Classe vraie à 7 jours	35,28
Classe vraie à 28 jours	50,08
Classe vraie à 90 jours	55,83
Classe vraie à 360 jours	
Masse volumique (kg/m ³)	3100
Capacité thermique (kJ/K.Kg)	0,73
Dosage de saturation (%)	0,2

Figure 6.6: CPM input data for CP V ARI RS, BetonLab Pro 3 (de Larrard & Sedran, 2007).

As a matter of fact, the input parameters with regards the aggregate particles are :

- Particle density (see Table 2.2);
- Water absorption (see Table 2.2);
- Grain size distribution (Figure 6.7);
- Compaction index.

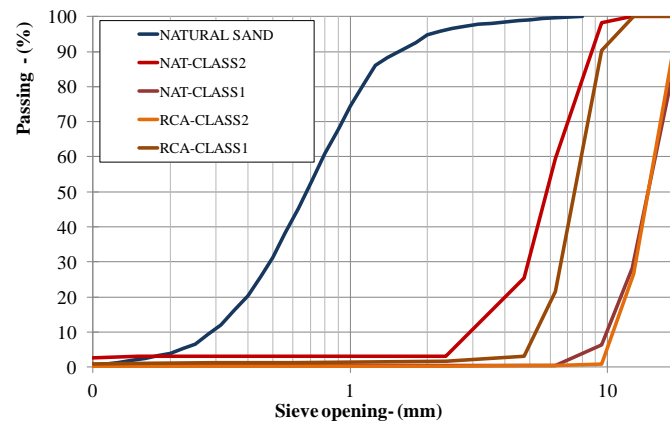


Figure 6.7: Grain size distribution as input for CPM.

The compaction index, both for natural and recycled aggregates was determined by using the method proposed by Sedran and de Larrard (1994), in which a cylinder is filled of aggregates (Figure 6.8a) and then by a piston, 10 kPa of pressure are applied for 2 minutes while the cylinder is fixed to a vibrating table (Figure 6.8b).



(a)



(b)

Figure 6.8: Determination of the compaction index.

The compaction index is then calculated with the equation (6.7). Table 6.2 reports the experimental values obtained for coarse natural and recycled aggregates.

Table 6.2: Experimental results for compaction index.

Value	NA_BR _{C2}	NA_BR _{C1}	RCA _{1,C2}	RCA _{1,C1}
M _D [kg]	7.5	7.5	7.5	7.5
D [mm]	160	160	160	160
ρ _D [kg/m]	2634	2464	2268	1946
h ₀ [mm]	198.8	196.3	198.7	197.4
h _f - test1 [mm]	439.0	459.8	478.2	477.9
h _f - test2 [mm]	443.1	442.3	481.9	478.6
φ test 1	0.590	0.575	0.588	0.683
φ test 2	0.580	0.615	0.581	0.682
φ	0.585	0.595	0.585	0.682

Other fundamental parameters are needed for predicting of the compressive strength of the concrete with CPM: particularly, p and q can be determined by casting two concrete mixture of different strength. The formulation for this calculation was reported in the previous subsection. As an example, Table 6.3 reports the two concrete batches produced for determining the p and q values for the recycled aggregates.

Table 6.3: Mix design of concrete batches for calibration of parameters p and q (RCA).

MIX	CP V ARI RS kg/m ³	Free water kg/m ³	w/c	SP kg/m ³	Sand_BR kg/m ³	RCA _{1,C2} kg/m ³	RCA _{1,C1} kg/m ³
1	420	168	0.4	4.2	923	460	280
2	233	168	0.8	2.1	1016	506	308

Then, the p and q values can be obtained by solving the linear system of the two equations (6.13) and (6.14). The same procedure was applied for the natural aggregates and Table 6.4 summarise the results obtained.

Table 6.4: Determination of parameters p and q, both for natural and recycled aggregates.

Parameter	Sand_BR	NA_BR	RCA ₁
p	1.15375	1.36725	1.2083
q	0.00805	0.00828	0.01444

Once having defined all the input parameters for CPM, it is possible to optimise some concrete mixtures by applying the theory reported in the previous section. In this research, two concrete batches were optimised for verifying if the CPM can be easily applied in the case of Recycled Aggregate Concrete. Table 6.5 summarises the optimisation performed in this research. The optimisation criteria was to maximise the granular packing density and at same time reaching a

compressive strength of 45 MPa and 37 MPa at 28 days. The first mixture was produced with both natural coarse (class 1) and recycled (class 2) aggregates, while the second with only recycled coarse ones. For both mixtures, the natural sand was employed.

Table 6.5: Mix design optimised by the CPM.

MIX	CEM kg/m ³	Water kg/m ³	w/c	SP kg/m ³	Sand_BR kg/m ³	RCA _{1,C2} kg/m ³	RCA _{1,C1} kg/m ³	NA_BR _{C1} kg/m ³
RAC45MPa	315.9	126.6	0.401	3.17	696.6	1025.75	-	161.5
RAC37MPa	300	136.8	0.456	4.02	980.1	416.6	357.5	-

Table 6.6 reports the comparison between the compressive strength values predicted by the CPM and the experimental data.

Table 6.6: Comparison between CPM prediction and experimental results.

MIX	Compressive strength	
	CPM prediction	Experimental value
RAC45MPa	44.9 MPa	46.45 MPa
RAC37MPa	37.1 MPa	36.3 MPa

The analysis of those results, highlights as the CPM can be easily extended for the prediction of the compressive strength of RAC, even if further research are necessary to verify the above consideration and analyse also the influence of the recycled aggregate on the fresh properties of concrete.

Finally, it is worth to mention that, as already explained in the previous chapters the recycled aggregates are generally characterised by an higher absorption capacity with respect to the natural ones of the same size class. For this reason, their initial moisture condition plays a key rule on the definition of the effective water to cement ratio. It should be clarified that, in this application, the coarse aggregates were employed in saturate (with dry surface) condition. Even if this condition it is not easy to apply when a real concrete structure have to be realised, it represents the moisture condition that less can alter the free water inside the mixture as also reported by the formula (3.10) proposed in chapter 3. Moreover, in the last section of this chapter a conceptual model will be presented for taking into account of the aggregates moisture condition influence in the concrete strength evolution.

6.3 Lattice Model

In this section one application for RAC of the Delft Lattice Model developed by Schlangen & Van Mier (1992) is illustrated.

6.3.1 Theoretical formulation

The fracture processes in multiphase materials can be simulated by lattice fracture model (Schlangen & Garboczi, 1997). The model can be used at a small scale, where the particles in the grain structure are generated and aggregate, matrix and bond properties are assigned to the lattice elements. Simulations at this scale are useful for studying the influence of material composition. Different researches demonstrate that realistic crack patterns are found compared with experiments on laboratory-scale specimens (Lilliu & van Mier, 2003). Cracks generally propagate in a direction which is perpendicular to the maximum tensile stress. In heterogeneous materials like concrete they also follow the weakest links in the material. The crack patterns in this kind of material will therefore never be straight and continuous. Due to the heterogeneity of the material cracks are tortuous and there are overlaps or so-called crack face bridges. The crack propagation in structures is often simulated with finite element methods (FEM) based on continuum theories.

Following these procedures, satisfying predictions are only found if homogeneous materials are concerned or if the disorder is weak. For studying fracture of materials in the cases where disorder is important, lattice models are preferred. In lattice models the medium is discretised such that all sites are equivalent, i.e. the grid is not made finer in regions of higher stress as often done for FEM: each site has the same number of neighbours so that the lattice is regular.

Different procedures for crack growth through the medium can be used. The disorder of the medium is in most cases implemented by randomly assigning chosen material properties to the elements in the lattice. In the present research such a (triangular) lattice model is used for simulating fracture in concrete prepared with recycled aggregates (Figure 6.9).

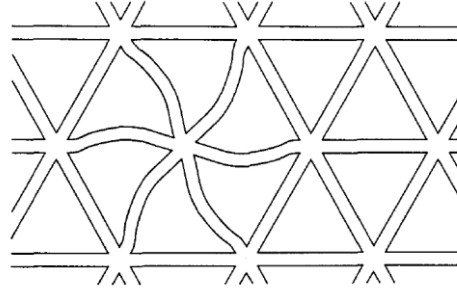


Figure 6.9: Triangular lattice mesh (Schlangen & Van Mier, 1992).

Different material properties that are assigned to the respective bar elements in matrix, aggregates and bond zone, i.e. the elements between matrix and aggregates, were introduced for representing the effect of disorder within the concrete structure. In the model, the material is schematised as a lattice of brittle-breaking beam elements. This type of lattice gives the least chance for preferential crack directions, which is essential for the model under consideration. Therefore, it is based on a linear elastic finite-element code.

In the Delft Lattice Model, the material is discretised as a lattice consisting of small beam elements (Figure 6.10).

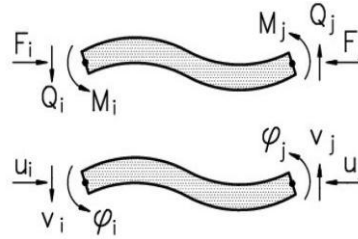


Figure 6.10: Nodal forces and displacement in beams (Schlangen & Van Mier, 1992).

Each of the beams in the lattice can transfer, in general, normal force (F), shear force (Q) and bending moment (M). The relation among these forces and corresponding displacements for the endpoints (i and j) of a beam can be expressed as follows (Figure 6.10):

$$F_i = \frac{EA}{l} \cdot (u_i - u_j) \quad (6.15)$$

$$Q_i = \frac{12EI}{l^3} \cdot (v_i - v_j) - \frac{6EI}{l^3} \cdot (\phi_i - \phi_j) \quad (6.16)$$

$$M_i = \frac{6EI}{l^2} \cdot (v_j - v_i) - \frac{4EI}{l} \cdot \left(\phi_i - \frac{\phi_j}{2} \right) \quad (6.17)$$

in which E is Young's modulus, l is the length, A is the cross-sectional area and I is the moment of inertia of a beam element, (u, v) are the translational displacements and ϕ is the nodal rotation. For a lattice with a regular geometry, the quantities E , A , l and I are in principle, equal for all elements.

However, these parameters can be varied, either element by element or according to a superimposed microstructure, in order to implement heterogeneity.

The simulation of fracture is realised by performing a linear elastic analysis of the lattice under loading and removing an element from the mesh that exceeds a certain threshold. In the present simulations a combination of normal and bending moment forming a tensile stress in each element is compared to its strength. More details on the elastic equations and the solver that is used as well as the fracture procedure of the model are explained in Schlangen & Van Mier (1992).

The nonlinearities are introduced through the fracture law, which states that a bar element is removed from the mesh as soon as a combination of normal force and bending moment, caused by either an external load on the lattice or by boundary displacements, is exceeded:

$$\sigma_t = \frac{N}{A} + \alpha \cdot \frac{\left(|M_i|, |M_j| \right)_{\max}}{W} \quad (6.18)$$

where N is the normal force in the bar element, M_i and M_j are the bending moments in nodes i and j of the bar element, respectively, A is the cross-sectional area of the bars, and W the section modulus. The coefficient α is introduced in order to select a failure mode where bending plays either a dominant or a limited role. The exact magnitude of this coefficient should be determined from a parameter study and comparison with experimental measurements. After removal of a bar element the linear analysis is repeated.

The procedures for lattice fracture analysis can be divided into three sequential modules, namely pre-processing, kernel solver and post-processing. In the pre-processing stage, a network of lattice is constructed and local mechanical properties are assigned to every lattice element depending on which phase it represents. Approximate boundary conditions must be defined as the fracture processes are dependent on both the material itself and its boundary conditions (Schlangen & Garboczi, 1997).

The kernel solver handles the simulation of fracture processes by removing critical lattice elements from the system step by step. On the basis of the information obtained from the previous two stages, load displacement diagram can be plotted and cracks propagation be animated in the post-processing stage.

Finally, it is important highlighting that the above described simulation approach can be applied both for 2D or 3D cases. In the present research the 2D simulation was performed.

6.3.2 Application

In this research, the lattice model simulation was applied for the case of Recycled Aggregate Concrete. The aim of the simulation was to determine the mechanical properties of each phases inside concrete when recycled aggregate are used. As described in chapter 2 the RCA is a bi-phases material in which both old natural aggregates and Attached Mortar are present. For this reason, when RCAs are used in concrete different phases in the concrete can be found. In fact not only the natural aggregate (NA), the cement paste (CP) and the Interfacial Transition Zone (ITZ NA-CP) between them is present, but also the AM and other two ITZs: between attached mortar and cement paste (ITZ AM-CP) and the “old” transition zone in between the natural aggregate and the attached mortar (ITZ AM-NA). For this reason the analysis of the failure mechanism and, consequently, the crack propagation inside the composite become more difficult.



Figure 6.11: Multi-phases characteristic for RACs.

Figure 6.11 shows a picture of the transverse section of a RAC cylinder sample in which the various above mentioned phases are clearly visible: the darker spots are the natural aggregates, the gray ones are related to the cement paste and the light-brown spots to the AM, while the various ITZs are in between the NA, AM and CP spots.

The analysis performed in this research is aimed at unveiling the weakest part of the composite and better understanding the physical and mechanical mechanisms which mobilise when RAC is loaded up the failure.

First of all, a concrete batch with both natural and coarse aggregates was produced. The mix design of the produced concrete mixture is fully reported in Table 6.7, while the details concerning the relevant aggregate properties are listed in Table 2.2.

Table 6.7: Mix design prepared for lattice model simulation.

Aggregates and Cement								
Sand	Sand_BR							
Class1	NA _{C1} _BR				-			
Class2	-				RCA _{1,C2}			
Cement type	CP V ARI RS							
Mix composition								
Mix	CEM	w	Add.w	SP	w/c	Sand_BR	NA _{C1} BR	RCA _{1,C2}
	[kg/m ³]					[kg/m ³]		
RAC	315.9	126.6	34.7	3.17	0.40	696.6	156.8	976.90

Several cylindrical concrete samples (d=100 mm and h=200 mm) were cast and tested at 28 days both in tension (splitting test) and compression. During the test also the E modulus was measured.

An average value of compressive strength equal to 50.6 MPa (average of five specimens) was reached such as a splitting strength of around 4.2 MPa (average of three specimens) and an elastic modulus of around 31 GPa.

As know in the literature, the splitting (or Brazilian) strength represents an indirect measure of the direct tensile strength and several guidelines highlight as the splitting test (more easy to perform with respect to the direct tensile test) overestimates the tensile strength of around 20%. For this reason, in order to correlate the splitting strength with the tensile one a factor equal to 1.20 should be applied for determining the tensile strength of the concrete In this case, the tensile strength results equal to 3.5 MPa (being the splitting strength equal to 4.2 MPa).

As mentioned in the previous section, a 2D simulation was performed on RAC. Several studies demonstrated as the 2D simulation of the compressive

strength test is not reliable as too many effect are neglected, meanwhile the splitting test such us the direct tensile one are less influenced by the 3D geometry.

Numerical analyses based on the Delft Lattice model were carried out for simulating the behaviour observed in both splitting and direct tensile tests. First of all, a geometric triangular mesh network was implemented, also considering the boundary conditions for the loading case. Particularly, for both splitting and tensile tests, the boundary condition were simulating by loading the upper and the lower nodes of the specimens. Moreover, in order to avoid local failures (due to applied load in the nodes) the beam elements of the loaded nodes were defined as “unbreakable”.

Once defined the geometrical grid of the triangular meshes, the heterogeneity of the composite was introduced by defining the several phases present in the RAC concrete.

For determining the distribution of the AM, NA, CP and the corresponding ITZs, an image analysis (with Image J software) was conducted. The starting point was the image of a cylindrical sample (Figure 6.12a) of the casted concrete (described in Table 6.7), then, the main 3 phases were identified:

- Cement mortar Paste, (including both natural sand and Cement paste), CP in Figure 6.12b;
- Attached Mortar, AM in Figure 6.12c;
- Natural Aggregates, NA in Figure 6.12d;

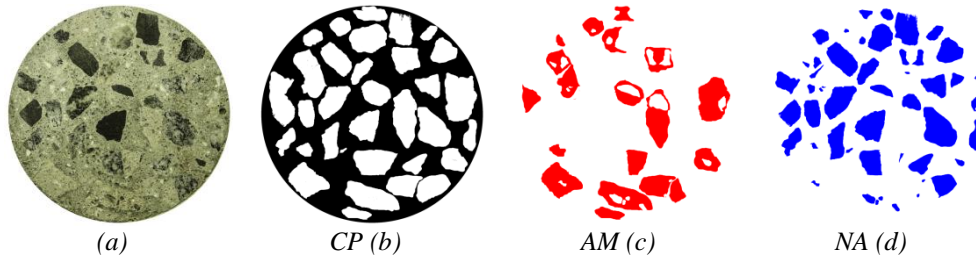


Figure 6.12: Lattice model simulation, introduction of heterogeneity.

In this research the lattice analysis was conducted on this image with cylinder (diameter of 100 mm) for the splitting test while a rectangular specimen ($b=75$ mm and $h=150$ mm) was considered for the tensile test. Both samples were geometrically schematised with a thickness of 1 mm. The shape of each lattice beam was cylindrical. The mean length of the beam was equal to 1 mm. The radius of the beam was calibrated by performing a preliminary analysis of the rectangular sample with homogenous mechanical properties. Particularly, a direct tensile test was simulated with all the frames characterised by a constant value of 3 MPa

strength in tension. The radius was calibrated up to reaching a value of 3 MPa also for the concrete composite.

Then, by using the GLAK software developed at TU Delft (Qian et al., 2011), the random triangular mesh lattices were tagged on the specimen as shown in Figure 6.13. It is worth highlighting that, depending on the position of the phases in the mixture, each type of beam element is coloured. In fact there are six types of beam elements: NA, CP, AM and the corresponding ITZs.

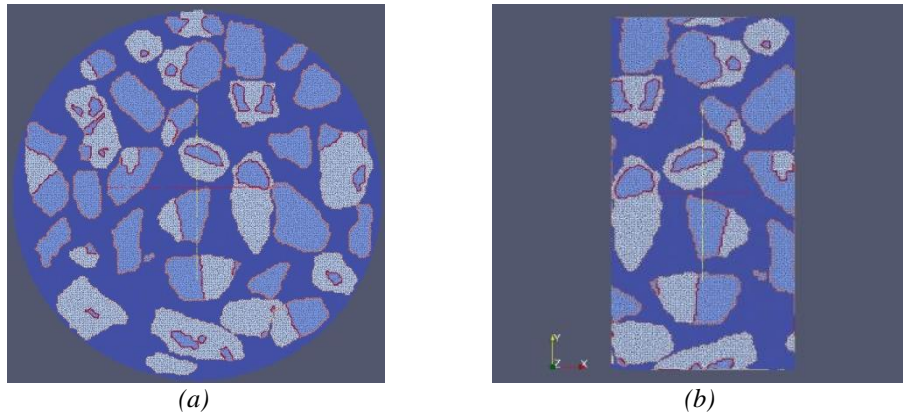


Figure 6.13: Triangular mesh discretisation for RAC lattice simulation.

The simulation was conducted after having calibrated the mechanical properties of each phases up to that the simulating strength reached the experimental values measured for the recycled concrete aggregate described in this section. The results of the above calibration are summarised in Table 6.8 while the resulting load-displacement curves for both splitting and tensile test, are reported in Figure 6.14 and Figure 6.15, respectively. The analysis of the calibrated mechanical properties of the different phases present in RAC confirms that the weakest element is represented by the AM mortar content and, consequently, the critical ITZs in between it and the other phases.

Table 6.8: Mechanical properties of the phases in RACs.

Element	E [GPa]	G [GPa]	Tensile Strength [MPa]	Compressive Strength [MPa]
Cement Paste (CP)	30	12	4.3	55
Aggregates (AGG)	50	20	6.5	100
Attached mortar (AM)	25	10	2.9	30
ITZ AM-CP	28	11	3.2	35
ITZ NA-CP	30	12	3.8	45
ITZ AM-AGG	25	10	2.9	30

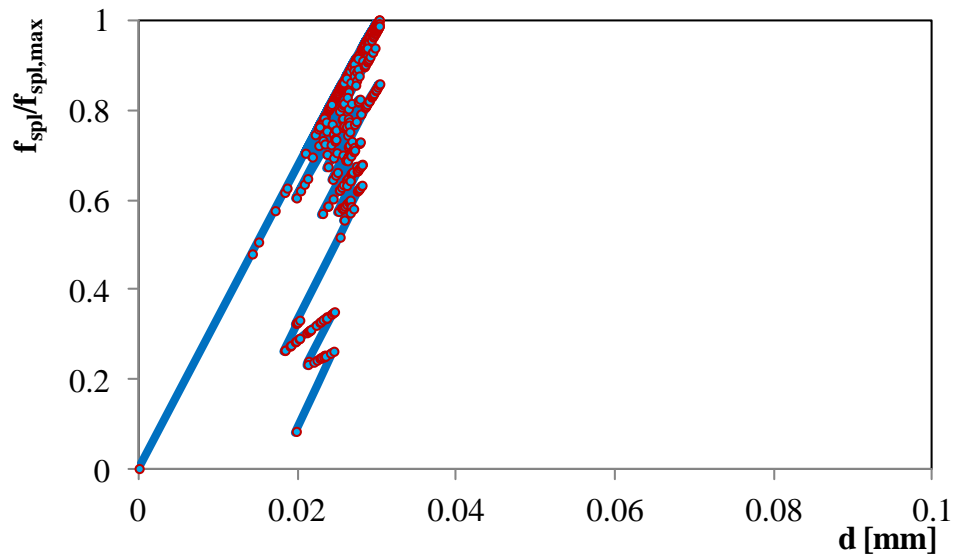


Figure 6.14: Lattice model simulation, results of splitting test.

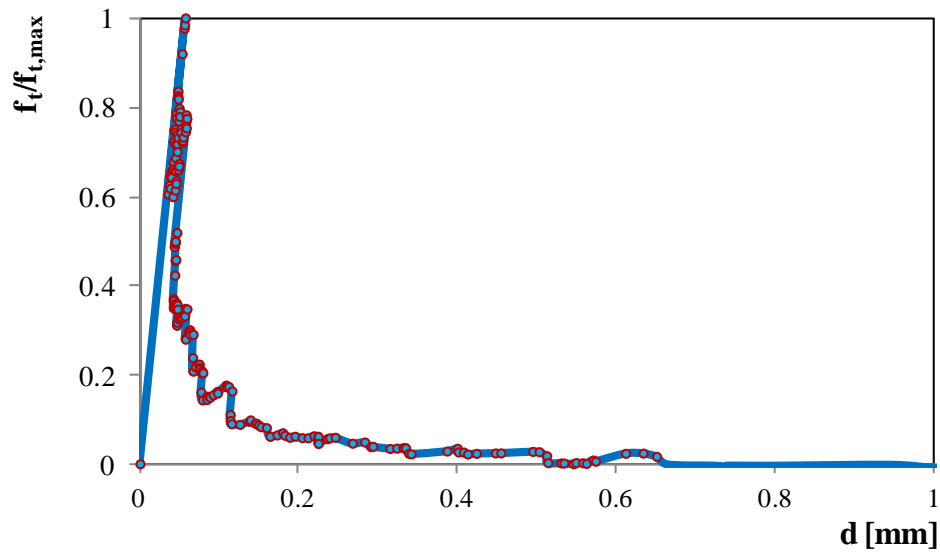


Figure 6.15: Lattice model simulation, results of direct tensile strength test.

The resulting crack propagation for the above simulations are reported in Figure 6.16.

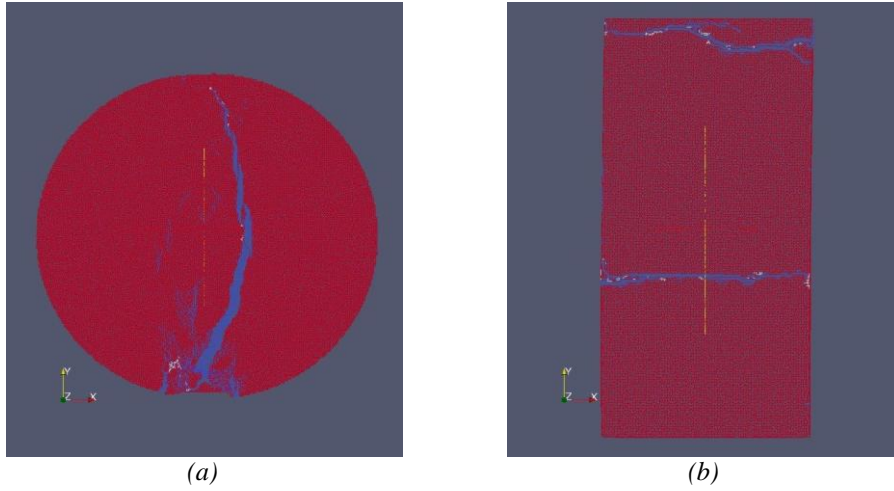


Figure 6.16: crack propagation for RAC lattice simulations.

The agreement between the simulations and the experimental results, in terms of tensile strength, splitting strength and elastic modulus, can be appreciated with the analysis of the output data reported in Table 6.9. In fact, the gap between the simulations and the experimental data is negligible, especially for a concrete composite characterised by a high heterogeneity of the constituents. Particularly, in the case of RAC this factor is higher as the RCA were derived from demolition waste. Moreover, by coupling the resulting Figure 6.13 and Figure 6.16 it is possible to understand that the AM is responsible for the lower strength that generally characterise the RAC performance compared with ordinary concrete mixtures. In fact the crack propagation occurs mainly in the AM phase or the corresponding ITZs.

Table 6.9: Results of the lattice model simulation.

Test	Experiment [MPa]	Lattice [MPa]
Tensile strength	3.5	3.4
Splitting strength	4.2	4.1
E	31000	32000

Once having clarified that AM is the main factor affecting the mechanical performance of RCA, a conceptual model will be presented in the following section for controlling and predicting the RAC compressive strength by taking into account of the AM, indirectly measured through the water absorption of RCAs (eq. (2.1)).

6.4 A proposed conceptual model for RACs

The proposed model described in this section represents a novel conceptual approach through which the compressive strength of Recycled Aggregate Concrete becomes predictable once defined the concrete mixture composition and the physical properties of Recycled Concrete Aggregates.

The main concept upon which the model is based is that the higher porosity that characterises the RCAs plays a fundamental role in defining of the free water available for the mixture and, consequently, it influences the time evolution of the compressive strength. For this reason, the hydration processes that can be simulated by the model proposed in chapter 5 is further considered. Then, a correlation between the degree of hydration and the corresponding concrete strength is proposed as also function of the mixture composition and casting procedures for RACs.

The analysis of these simulation led to propose some design formulations calibrated on the experimental results reported in section 3.3.3 and validated with some other concrete mixtures.

6.4.1 Theoretical approach

This section aims at presenting the theoretical models employed in this study used for evaluating the time evolution of both the degree of hydration and the compressive strength of concrete.

Due to their high porosity and water absorption capacity, RCAs can affect the hydration process of cementitious composites significantly, as they modify the actual amount of water which is available for the hydration reaction. The time evolution of the hydration reaction can be monitored by observing the progress of the so-called degree of hydration α which, in principle, is defined as the ratio between the amount of cement that has already reacted at the time t and the total amount of cement available in the mixture under consideration (van Breugel, 1991). In principle, the degree of hydration of cement based mixtures can be determined by the following methods:

- temperature measurement, either adiabatic (maximum heat development), or semi-adiabatic, partial developed heat, (Lokhorst, 1999);
- chemical bounded water measurements, measuring from concrete samples, representing the amount of water that has actually reacted with cement;
- numerical models, simulating the chemical reaction process between cement and water systems (van Breugel, 1991).

Based on the above considerations, chapter 5 proposed a theoretical model for predicting the time evolution of the degree of hydration from temperature measurements performed on concrete cubic samples cured under semi-adiabatic boundary conditions (Martinelli et al., 2013). Therefore, that proposed model enables the calculation of the time evolution of the degree of hydration based on semi-adiabatic temperature measurements and, based on this, simulate hydration reactions for different thermal boundary conditions. Particularly, isothermal conditions generally imposed for curing concrete samples tested for measuring the compressive strength development: an example of the hydration model output is proposed in Figure 6.17.

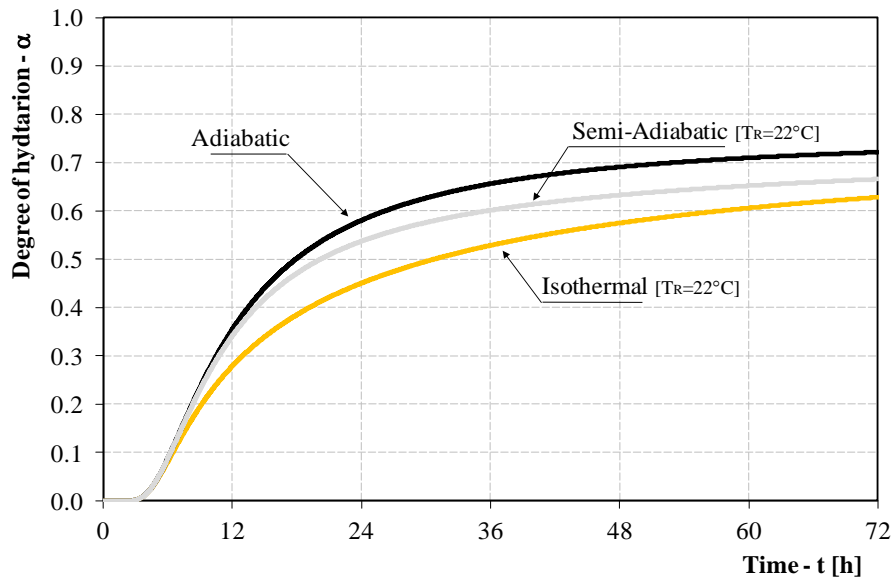


Figure 6.17: Time evolution of the degree of hydration with different curing boundary conditions.

Once the time evolution of the degree of hydration has been calculated, the experimental results obtained in the compressive tests carried out at different curing times and the corresponding values of the degree of hydration can be correlated. Moreover, in literature the following conceptual formula was proposed for the correlation between the degree of hydration (α) and the cubic compressive strength R_c (Lokhorst, 1999):

$$R_c = R_{c,\max} \cdot \frac{\alpha - \alpha_0}{1 - \alpha_0} \quad (6.19)$$

where α_0 is, in principle, the minimum degree of hydration representing the moment that the strength in the mixture is starting to build up (i.e. end of setting phase), and $R_{c,max}$ the maximum cubic compressive strength, ideally corresponding to a degree of hydration equal to 1. Then, the correlation between the mechanical properties and the degree of hydration may show the impact of RCAs on the resulting RAC properties. Particularly, it may express the influence of the residual anhydrous cement fractions, the porosity and the moisture conditions of the attached mortar on the overall hydration process that controls the formation of the concrete microstructure and associated strength.

6.4.2 Proposed formulations for predicting the strength of RAC

The analysis reported in this section is based on the results achieved from the experimental campaign described in section 3.3.3.

The experimental data obtained from temperature measurements were employed for scrutinising the hydration process which took place in the concrete specimens tested in compression. Then, the hydration model described in chapter 5 was employed while taking care of the under semi-adiabatic conditions applied during temperature measurement and the isothermal conditions applied to the concrete specimens during the 28 day hardening period. Once having determined the time evolution of the degree of hydration, a possible correlation was figured out with the experimental results of compressive tests. As a matter of fact, this correlation can be represented in the form of a proposed equation (6.19), where the best fit values of the couples ($R_{c,max} - \alpha_0$) are determined through a least-square regression method for each of the ten concrete mixtures under consideration.

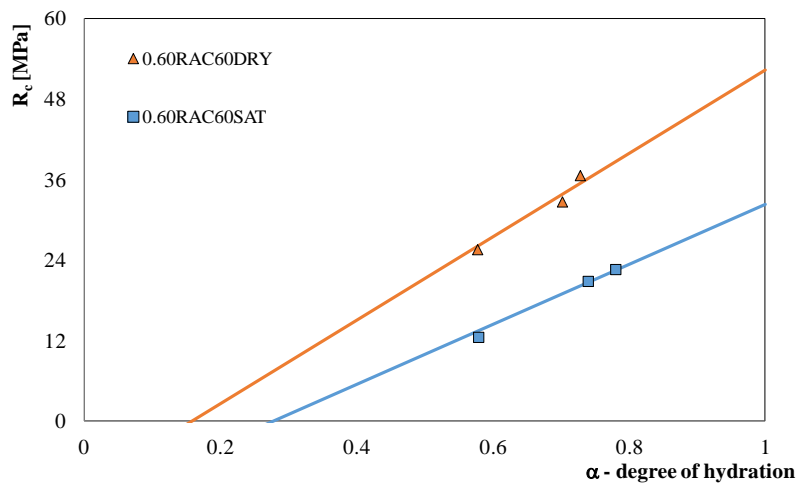


Figure 6.18: Degree of hydration-Compressive strength.

One example is given in Figure 6.18 where a proposed linear correlation for the concrete mixture RAC60 and w/c=0.60 (both DRY and SAT) is reported together with the intersecting data points determined from the compressive strength (x-axis) results and the hydration model (y-axis). The resulting calibrated values of α_0 and $R_{c,max}$ for all the mixtures are reported in Table 6.10.

Table 6.10: α_0 and $R_{c,max}$ values.

Mix		α_0	$R_{c,max}$
0.50NAT	DRY	0.42	84.0
	SAT	0.46	82.0
0.50RAC30	DRY	0.20	76.0
	SAT	0.27	74.0
0.50RAC60	DRY	0.08	55.0
	SAT	0.17	45.0
0.40RAC60	DRY	0.03	67.0
	SAT	0.10	64.0
0.60RAC60	DRY	0.16	52.3
	SAT	0.28	32.2

The first step in formulating a model capable of predicting the mechanical strength development and evolution of other RAC properties, based on both the mixture composition and the main parameters characterizing RCAs, consists on considering a possible correlation between the values reported in Table 6.10, and the relevant parameters and aspects defining the concrete mixtures, such as the initial moisture conditions of the coarse aggregates, the recycled-to-natural aggregate replacement ratio and the water-to-cement ratio of a mixture.

A first possible correlation can be elaborated between the two parameters α_0 and $R_{c,max}$, and the effective water-to-cement ratio defined by equation (3.10), which takes into account the amount of free water available into the mix based on the aggregates absorption capacity and their initial moisture condition. Figure 6.19 and Figure 6.20 show the results of the aforementioned parameters with respect to the effective water-to-cement ratio defined by equation (3.10): it can be seen that both parameters tend to decrease for higher aggregate replacement ratios (i.e., moving from NAT to RAC30 to RAC60).

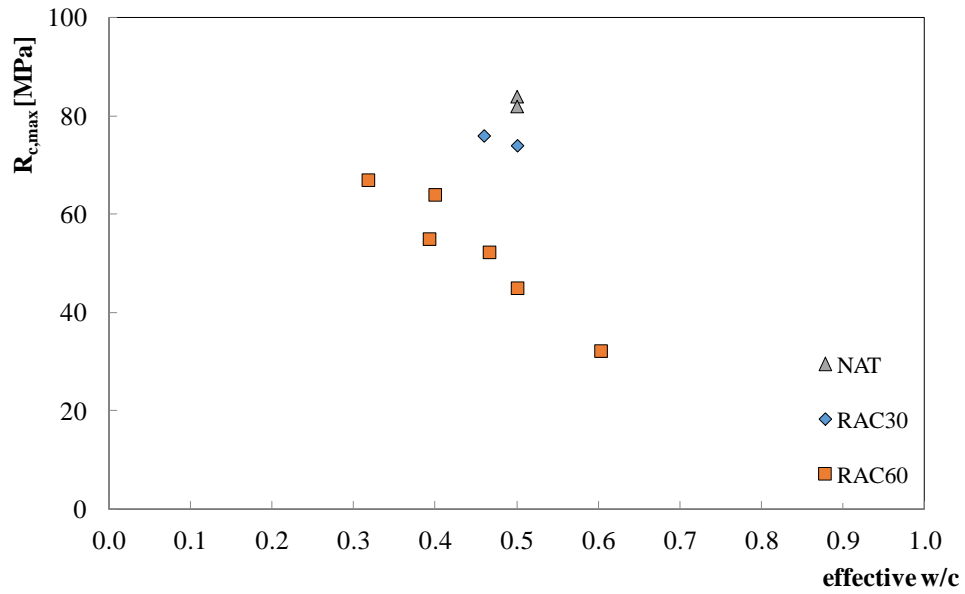


Figure 6.19: $w/c_{eff} - R_{c,max}$.

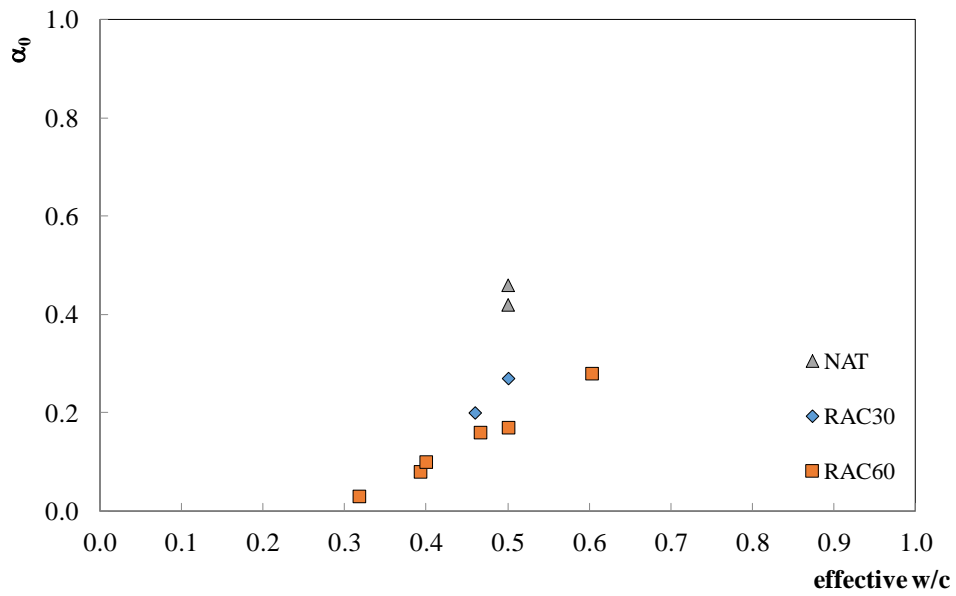


Figure 6.20: $w/c_{eff} - \alpha_0$.

However, the concrete strength is also affected by the aggregate replacement ratio which is not explicitly considered in the definition of $(w/c)_{eff}$. Therefore, a

further parameter is introduced that accounts for the average porosity of the coarse aggregates employed in the mixture, and is defined as follows:

$$A_{MIX} = \sum_{i=1}^n p_i \cdot V_i \quad (6.20)$$

where p_i is the open porosity characterising the i -th fraction of the coarse aggregates and V_i is the corresponding fraction volume in the mixture. The values of A_{MIX} for the ten concrete mixtures under investigation are reported in Table 6.11.

Table 6.11: A_{MIX} values.

Mix	Replacement ratio [%]	Aggregates type		Abs _i		V _i		A _{MIX}	A _{NAT} /A _{MIX}
		C1	C2	C1 [%]	C2 [%]	C1 [%]	C2 [%]		
0.50NATDRY	0	NA _{C1}	NA _{C2}	0.50	0.40	50	50	0.45	1
0.50NATSAT	0	NA _{C1}	NA _{C2}	0.50	0.40	50	50	0.45	1
0.50RAC30DRY	30	NA _{C1}	RCA _{3,C2}	0.50	6.60	50	50	3.55	0.13
0.50RAC30SAT	30	NA _{C1}	RCA _{3,C2}	0.50	6.60	50	50	3.55	0.13
0.50RAC60DRY	60	RCA _{3,C1}	RCA _{3,C2}	8.70	6.60	50	50	7.65	0.06
0.50RAC60SAT	60	RCA _{3,C1}	RCA _{3,C2}	8.70	6.60	50	50	7.65	0.06
0.40RAC60DRY	60	RCA _{3,C1}	RCA _{3,C2}	8.70	6.60	50	50	7.65	0.06
0.40RAC60SAT	60	RCA _{3,C1}	RCA _{3,C2}	8.70	6.60	50	50	7.65	0.06
0.60RAC60DRY	60	RCA _{3,C1}	RCA _{3,C2}	8.70	6.60	50	50	7.65	0.06
0.60RAC60SAT	60	RCA _{3,C1}	RCA _{3,C2}	8.70	6.60	50	50	7.65	0.06

This parameter can be useful for describing the reduction in compressive strength due to the replacement of NAs by RCAs. Particularly, it can physically explain the decrease of α_0 and $R_{c,max}$ that characterises the evolution of the compressive strength of RACs with respect to $\alpha_{0,NAT}$ and $R_{c,max,NAT}$, which represents the compressive strength of a reference concrete made of only natural aggregates (and keeping the grain size distribution constant). Therefore, it is possible to define the ratios of r^* and α^* for expressing the reduction in strength and its rate development in terms of $R_{c,max}$ and α_0 , respectively:

$$r^* = \frac{R_{c,max}}{R_{c,max,NAT}} \quad (6.21)$$

$$\alpha^* = \frac{\alpha_0}{\alpha_{0,NAT}} \quad (6.22)$$

Moreover, the following analytical formulations are introduced for describing the existing relation between the above described parameters r^* and a^* and the A_{NAT} -to- A_{MIX} ratio:

$$r^* = \frac{a_R \cdot \frac{A_{\text{NAT}}}{A_{\text{MIX}}}}{b_R + \frac{A_{\text{NAT}}}{A_{\text{MIX}}}} \quad (6.23)$$

$$\alpha^* = \frac{a_\alpha \cdot \frac{A_{\text{NAT}}}{A_{\text{MIX}}}}{b_\alpha + \frac{A_{\text{NAT}}}{A_{\text{MIX}}}} \quad (6.24)$$

where, A_{NAT} is the corresponding A_{MIX} value for an ordinary concrete mixture (i.e., RAC0) and a_R , b_R , a_α and b_α are constants which should, in principle, be calibrated on experimental results. Based on tested mixtures described in section 3.3.3, the values of a_R and b_R can be approximated to be 1.06 and 0.06 (Figure 6.21), respectively, while a_α and b_α are equal to 1.05 and 0.05 (Figure 6.22).

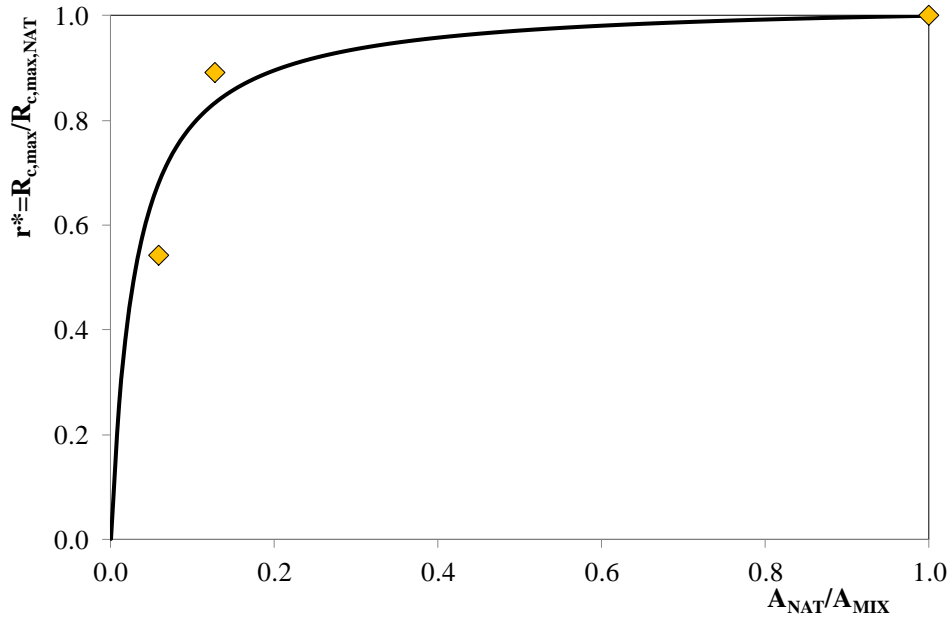


Figure 6.21: Proposed formulation for r^* .

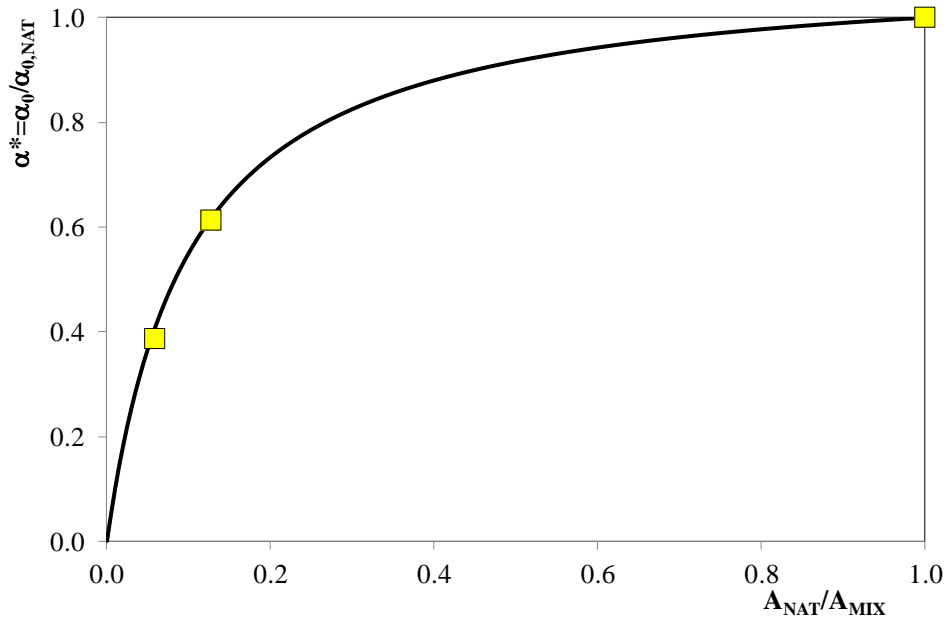


Figure 6.22: Proposed formulation for α^* .

The accuracy of these calibrations can be assessed if the individual pairs of $R_{c,max}$ and α_0 (reported in Table 6.10) are divided by the corresponding values of r^* and α^* and, then, represented with respect to the effective water-to-cement ratio (see section 3.3.3). Figure 6.23 shows that all the points ($w/c_{eff} \cdot R_{c,max}/r^*$) can be aligned on a curve that can be analytically expressed by the well know Abram's law (Neville, 1981) and, particularly, it assumes the following expression:

$$\frac{R_{c,max}}{r^*} = \frac{A_R}{B_R^{(w/c)_{eff}}} \quad (6.25)$$

in which the values of A_R and B_R can be assumed to be equal to 265 and 9.5, respectively, based on the aforementioned experimental data.

Similarly, Figure 6.24 reports a possible linear correlation existing between w/c_{eff} and α_0/α^* that can be expressed by the following analytical formulation:

$$\frac{\alpha_0}{\alpha^*} = A_\alpha \cdot \left[\left(\frac{w}{c} \right)_{eff} - B_\alpha \right] \quad (6.26)$$

where A_α is equal to 1.62 and B_α is equal to 0.28.

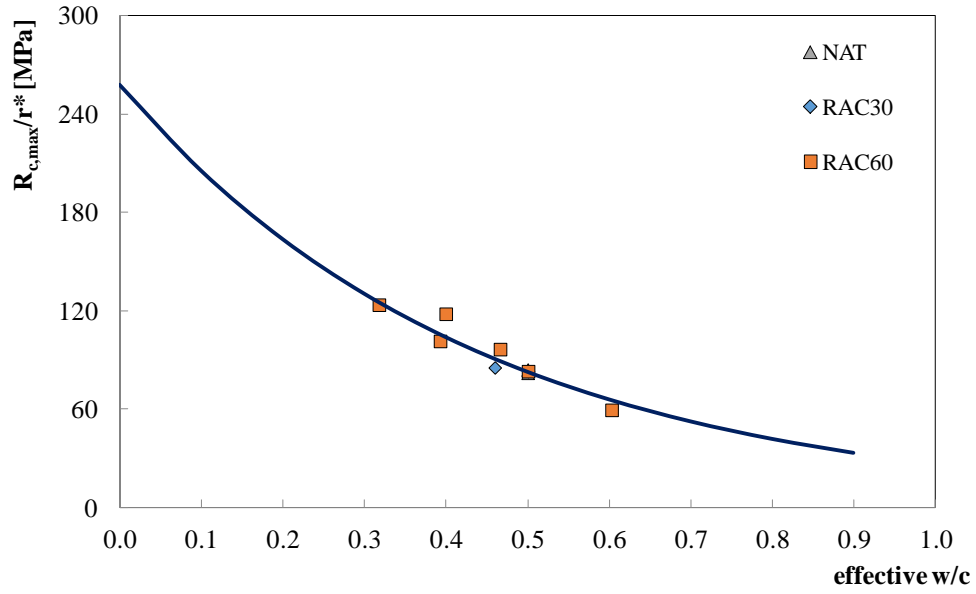


Figure 6.23: Proposed formulation for $R_{c,max}$.

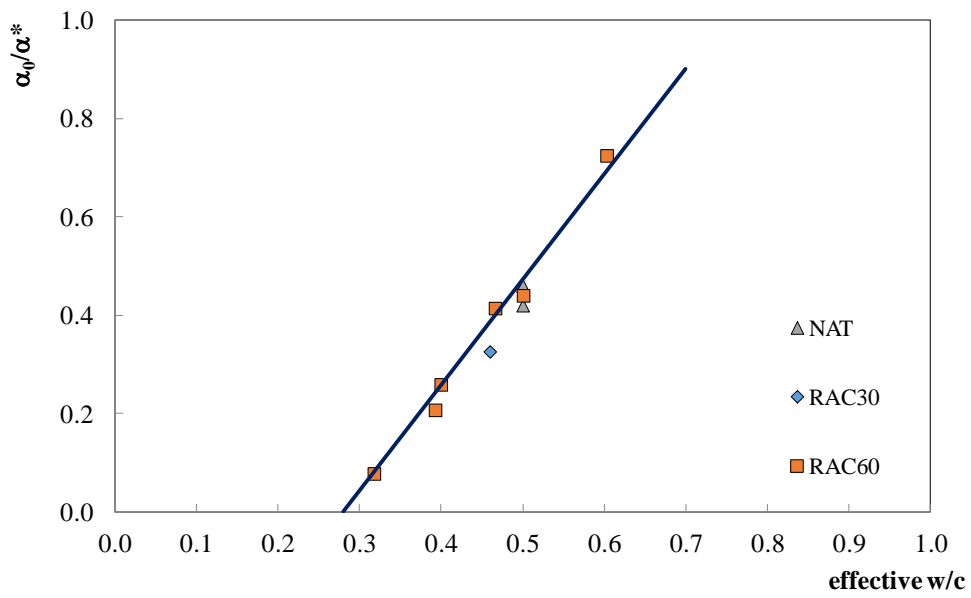


Figure 6.24: Proposed formulation for α_0 .

6.4.3 Model validation

Three additional concrete mixtures were produced according to the composition reported in Table 6.12, in order to validate the proposed rational mix design method for RACs. They were designed by keeping constant the nominal value of water-to-cement ratio (i.e., equal to 0.50), the aggregate replacement ratio (i.e., RAC30) and initial moisture condition of the coarse aggregates were dry (i.e., DRY). Therefore, the extra amount of water added during mixing is the only variable parameter for this group of mixtures and is defined as a percentage of the total amount of water potentially absorbed by aggregates in 24 hours. Particularly, the concrete mixtures designed for the validation of the proposed model were prepared by considering the 33%, 66% and 100% of the coarse aggregate absorption capacity at 24 hours, respectively.

Therefore, the aforementioned moisture situations (i.e., dry + added water) represent some intermediate conditions between the DRY and SAT ones presented in this study.

Table 6.12: Aggregate and mix design of concrete batches (validation).

Aggregates						
Sand						
Class1	NA _{C1}					
Class2	RCA _{4,C2}					
Mix Composition						
Mix	CEM I	Free water	w/c	Sand	NA _{C1}	RCA _{4,C2}
	[kg]	[kg]		[kg]	[kg]	[kg]
0.50RAC30DRY+33%	380	190	0.5	814	696	588
0.50RAC30DRY+66%	380	190	0.5	814	696	588
0.50RAC30DRY+100%	380	190	0.5	814	696	588
Mix Properties						
Aggregate replacement ratio					30%	
Aggregate Absorption for class C1					0.50 %	
Aggregate Absorption for class C2					8.29 %	
A _{MIX}					4.40 %	
A _{NAT} /A _{MIX}					0.10	

The compressive strength of the three mixtures was measured on cubic samples (15x15x15 cm³) at 1, 2, 7 and 28 days and isothermal curing. Moreover, the temperature evolution of the hydration process was monitored on an insulated cubic sample (20x20x20 cm³) cured for three days in semi-adiabatic conditions. Also in this case, the time evolution of the degree of hydration was simulated by

using the hydration model mentioned in chapter 5. Based on the mixture composition and initial moisture conditions, the value of the effective water-to-cement ratio was evaluated by using equation (3.10), and the values of A_{MIX} , r^* and α^* by equations (6.20), (6.23) and (6.24), respectively. Then, $R_{c,max}$ and α_0 were estimated by using equations (6.25) and (6.26) for defining the relation between degree of hydration and cubic compressive strength.

The results of such a validation are proposed in Figure 6.25 where the blue points come out by coupling the experimental data of compressive strength and the hydration model, while in orange the curve determined from the proposed design formulation (namely, equation (6.19)).

The aforementioned graphs highlight that the proposed rational method is capable of assessing the evolution of compressive strength, while taking into account the mix composition and the key characteristics of RCAs.

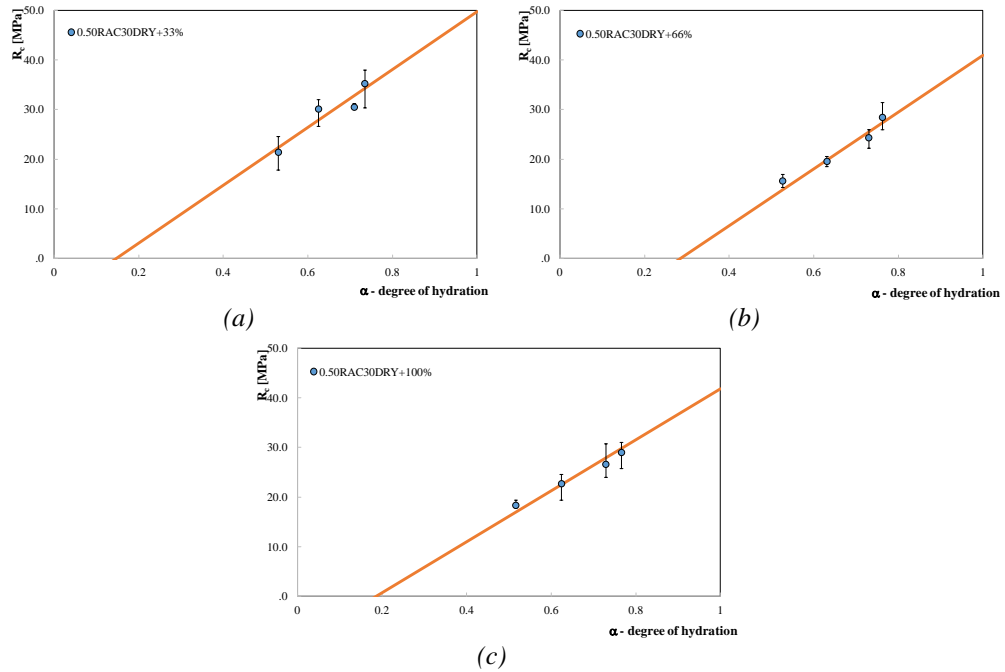


Figure 6.25: Results of the validation.

7. Mix design formulation for RAC

This chapter summarises the main aspects investigated in the previous ones and, based on their contents, proposes a comprehensive physically-based conceptual approach for designing RAC mixtures for a given target compressive strength.

As a matter of fact, based on the information derived from the experimental campaigns performed on recycled concrete aggregates (chapter 2), some analytical formulations were proposed for determining the physical relationships between the AM content and the key engineering properties of RCAs, such as open porosity, water absorption capacity (and rate) and particle density. Moreover, chapter 2 proposed an alternative processing procedure for RCA based on the so-called autogenous cleaning process which can be implemented to directly modify the open porosity of RCAs and consequently, their key engineering properties.

Therefore, an innovative modelling approach was proposed in chapter 6 for predicting the time evolution of compressive strength. Particularly, the proposed method is based on the analysis of the hydration processes that were simulated by applying the model described in chapter 5. The formulation of this novel approach for predicting the compressive strength of RACs is calibrated on the data available from the experimental campaign reported in chapter 3.

In the following section, the complete application of the aforementioned formulations is reported. In fact, starting from the aggregates characterisation, such formulations are recalled and utilised for predicting the time evolution of the compressive strength for a given mixture containing RCAs, and, in other words, formulating a rational mix-design approach for concrete containing RCAs.

7.1 Conceptual Model flow chart

As a matter of fact, the possible application of the entire formulation presented in this thesis is schematically highlighted in Figure 7.1.

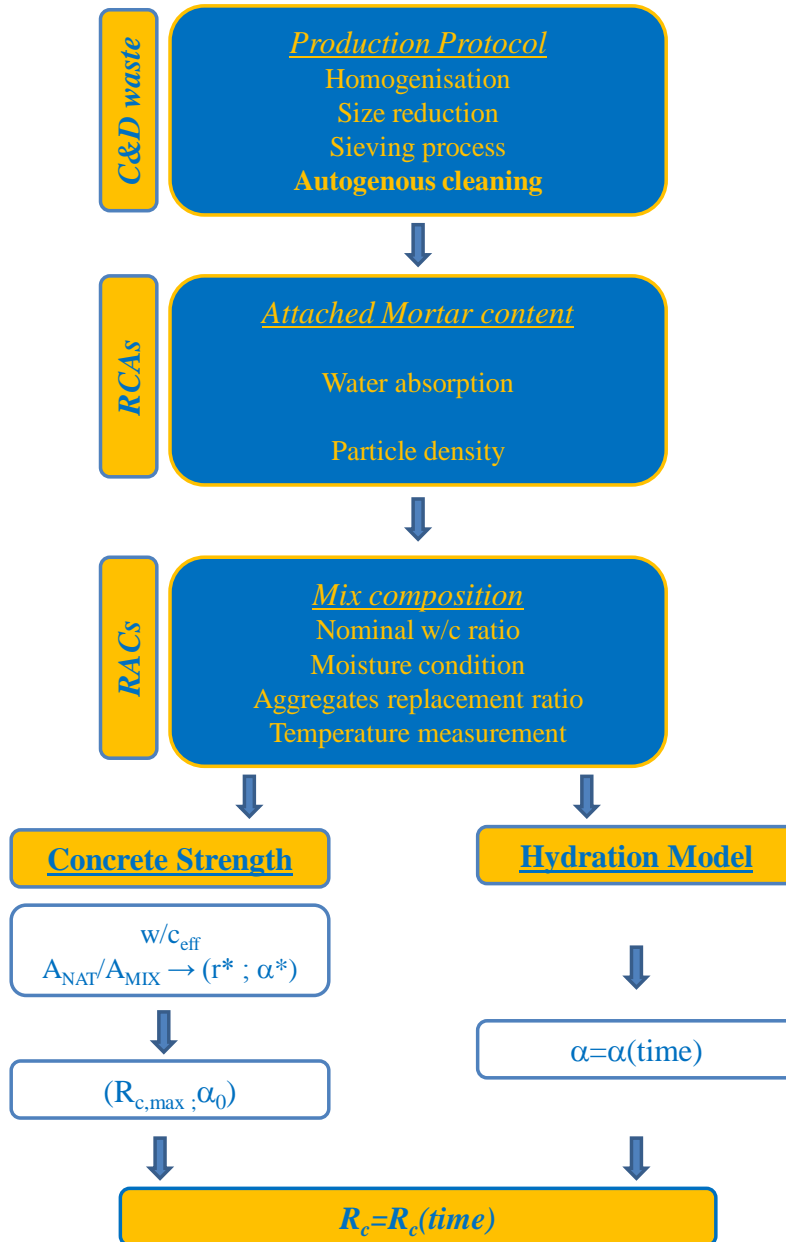


Figure 7.1: Flow chart of the conceptual model for RCAs.

The scheme reported therein encompasses various boxes summarising the contents of the previous chapters. Particularly, the “*C&D waste and RCAs*” box reported refers to the production protocol and the physical and mechanical characterisation of RCAs described in chapter 2. Moreover, the “*RACs*” box deals with the influence of the RCAs in concrete mixtures investigated in chapter 3. Thus, the proposed formulation aimed at simulating the hydration processes, described in chapter 5, is reported in the “*Hydration model*” box.

Finally, the Recycled Aggregate Concrete strength (predictable with the novel method proposed in chapter 6) is represented in the “Concrete strength” box.

Therefore, Figure 7.1 proposes a rational combination of the various aspects addressed in this thesis and shows that they can contribute to a comprehensive approach for predicting the time evolution of the resulting compressive strength of concrete made out with recycled concrete aggregates.

C&D waste: Production protocol

First of all, the production protocol for RCAs has to be defined. In chapter 2 the possible alternative processing procedures for RCAs were reported (i.e., demolition, homogenisation, size reduction and sieving) and, specifically, the “autogenous cleaning process” was investigated as a procedure capable of improving the physical properties of RCAs. Particularly, equation (2.7) proposed a possible correlation between the target open porosity (easily measurable with the water absorption test) of recycled aggregates with the time needed by autogenous cleaning to achieve such a target value.

Figure 7.2, reports the complete scheme of the production protocol steps aimed at transforming concrete waste into recycled concrete aggregates. Particularly, the quality control box can be identified as a measurement of the physical properties of RCA that could affect the mechanical performance of resulting RAC.

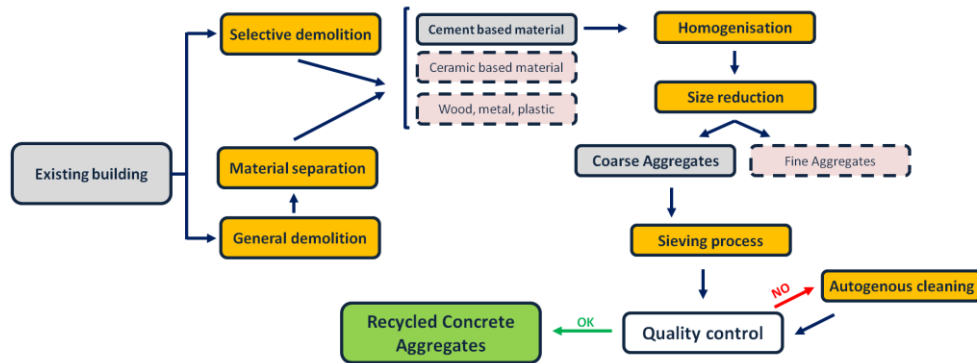


Figure 7.2: Schematic representation of the production protocol.

Engineering properties of Recycled Concrete Aggregates

Once having defined the production protocol for RCAs, it is fundamental to determine their physical and mechanical properties. As described in chapter 2, the RCAs are composed of natural aggregates and attached mortar (AM) that represents the key characterising parameter for RCAs.

As the direct measurement of the AM content is not straightforward, the proposed formula (2.1), whose linear trend is reported in Figure 7.3, highlights the conceptual relationship for quantifying AM content as a function of open porosity.

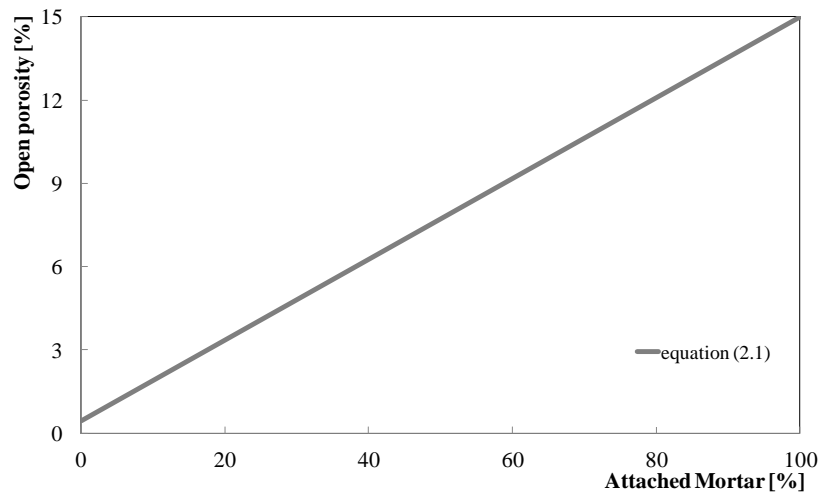


Figure 7.3: Typical correlation between open porosity and attached mortar.

Then, equations (2.2) and (2.3) define the analytical expressions that correlate the open porosity with the water absorption rate capacity and the particle density, respectively (see Figure 7.4 and Figure 7.5).

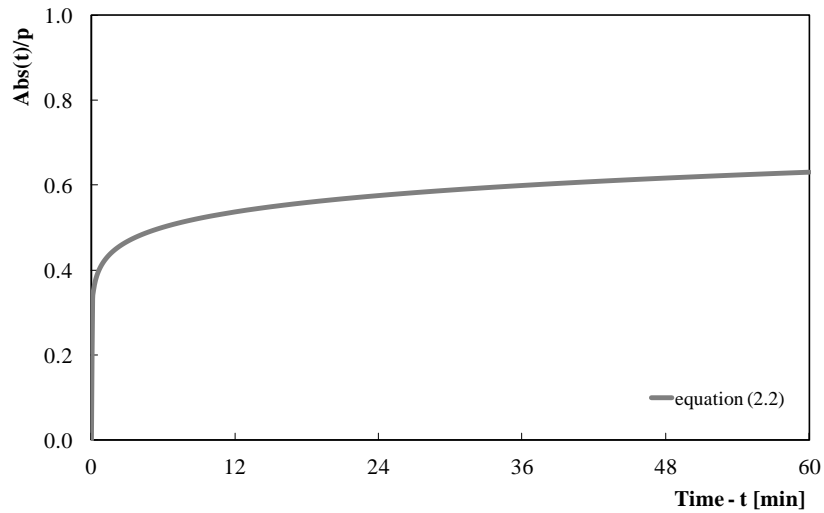


Figure 7.4: Typical correlation between water absorption rate and time.

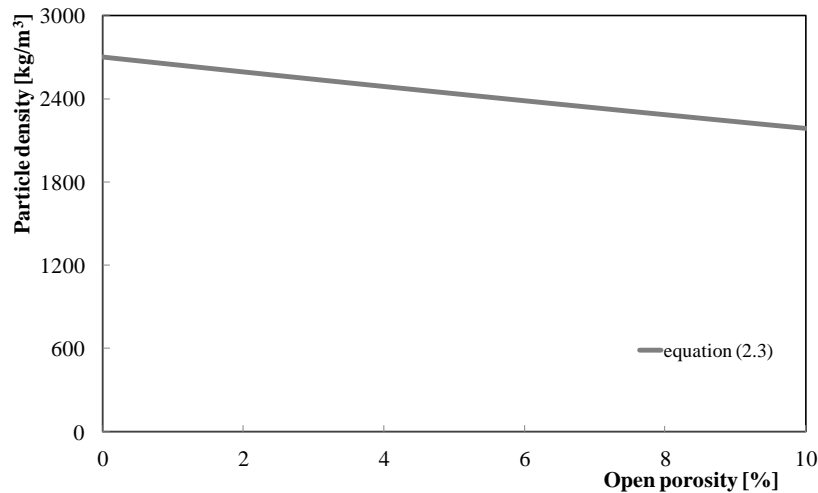


Figure 7.5: Typical correlation between open porosity and particle density.

The application of the aforementioned formulations allows determining the main engineering properties of RCAs as a function of the open porosity.

It is worth highlighting that the open porosity can be directly measured by performing the water absorption capacity test of the aggregates already defined in

various standards and regulations (EN 1097-6:2013; ASTM C127-12). As a consequence, the application of the formulae proposed in chapter 2 allows to estimate the full set of physical parameters characterising the RCAs that can be used as the input data for the mix design of resulting concrete batches: AM content, water absorption capacity and particle density.

Recycled Aggregate Concretes: composition

As reported in the conceptual scheme of Figure 7.1, when all the physical properties of RCAs are determined, it is possible to define a mix composition of structural concrete produced with them. Particularly, the analysis of the experimental results reported in chapter 3 highlighted that the mechanical performance of RAC is mainly influenced by the following three parameters:

- Nominal water to cement ratio;
- Initial moisture condition of aggregates;
- Aggregate replacement ratio.

As a matter of fact, the higher porosity of the RCAs and their initial moisture condition during the mixing phase, tend to modify the free water available for the cement and, for this reason, the equation (3.10) defines an effective water to cement ratio (w/c_{eff}) related to the above listed parameters and the rate of the water absorption capacity, that can be estimated with the formula presented in chapter 2 (i.e., equation 2.2).

Concrete strength and degree of hydration

The novel approach methodology proposed in chapter 6 for predicting of the mechanical behaviour of RACs is based on the existing linear correlation, i.e., equation (6.19), between the cubic compressive strength R_c and the degree of hydration α .

In order to determine the aforementioned relationship the $R_{c,\text{max}}$ and α_0 values should be defined. These two values can be estimated by applying the analytical formulation proposed in chapter 6.

As a matter of fact, the novel approach methodology is based on the definition of the parameter A_{MIX} that represents the average porosity of the concrete mixture made out with recycled concrete aggregates. Once defined the mix composition of the concrete batch, by applying the formula (6.20), the parameter A_{MIX} is evaluable and consequently, the ratio $A_{\text{NAT}}/A_{\text{MIX}}$ is defined. Moreover, the r^* and α^* parameters can be determined by applying equation (6.23) and equation (6.24), respectively.

The above numerical parameters leads to determining the values of $R_{c,\text{max}}$ and α_0 by applying equations (6.25) and (6.26).

Figure 7.6 and Figure 7.7 show the trend of $R_{c,max}$ and α_0 values related to the A_{NAT}/A_{MIX} parameter that represents the amount of recycled concrete aggregates or particularly the amount of the AM inside the resulting concrete mixture. In fact, the main difference in composition between ordinary concrete mixture and RACs is the presence of the AM content into the RCAs composed of AM and natural aggregates.

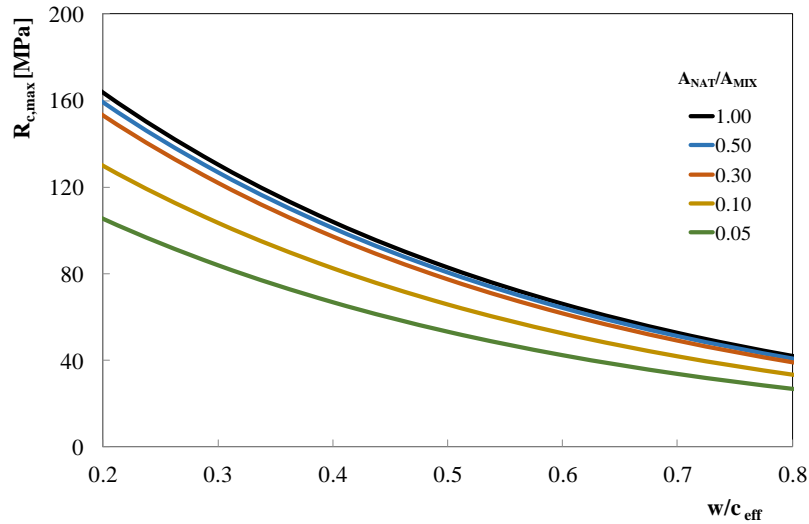


Figure 7.6: Influence of A_{NAT}/A_{MIX} on $R_{c,max}$.

The analysis of the curves reported in Figure 7.6 highlights that the presence of RCAs in concrete tends to reduce the values of $R_{c,max}$ for a fixed value of the w/c_{eff} determined through the equation (3.10). It is clear that the influence of RCAs in concrete is more evident for low values of w/c_{eff} . In fact, the concrete mixtures with a low value of w/c_{eff} presents a stronger cement matrix than in the case of high values of w/c_{eff} . This evidence clearly demonstrates that for lower values of w/c_{eff} , the failure of the composite is governed by the strength of the aggregates, while, for high values of w/c_{eff} the failure of the concrete can be attribute to a lower strength of the cement matrix.

In the same way, the analysis of the curves reported in Figure 7.7 highlights the influence of RCAs on the parameter α_0 . In fact, when RCAs are used in concrete, the α_0 value is lower than ordinary mixtures. This effects is evident for higher values of w/c_{eff} but it is null for its minimum value of w/c_{eff} . As a matter of the fact, the setting time is governed by the water available for the cement matrix and the presence of RCAs in concrete introduce the additional porosity in the mixture and as a consequence the available water is modified.

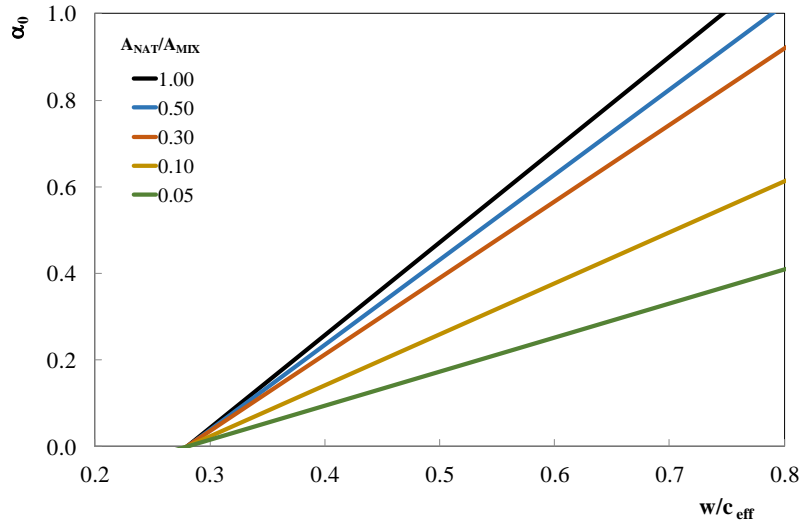


Figure 7.7: Influence of A_{NAT}/A_{MIX} on α_0 .

Finally, as mentioned above, the $R_{c,max}$ and α_0 values allow to define the existing relation between the degree of hydration (α) and the cubic compressive strength R_c through the use of formula (6.19), as reported in Figure 7.8.

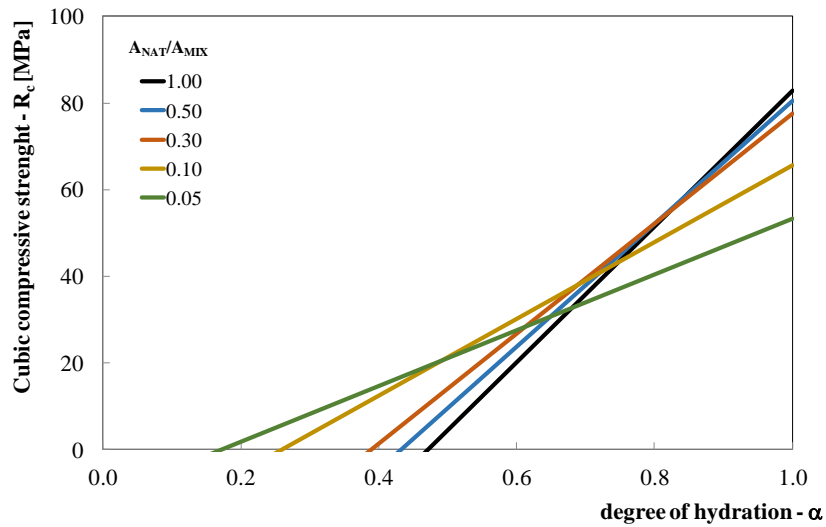


Figure 7.8: Influence of A_{NAT}/A_{MIX} on cubic compressive strength evolution.

Time evolution of the compressive strength

The presented conceptual methodology is aimed at predicting the time evolution of the compressive strength in the case of RACs. With this aim, the application of the

hydration model proposed in chapter 5 allows to estimate the time evolution of the degree of hydration as a function of the mixture composition and the curing conditions the concrete mixture (Figure 7.9).

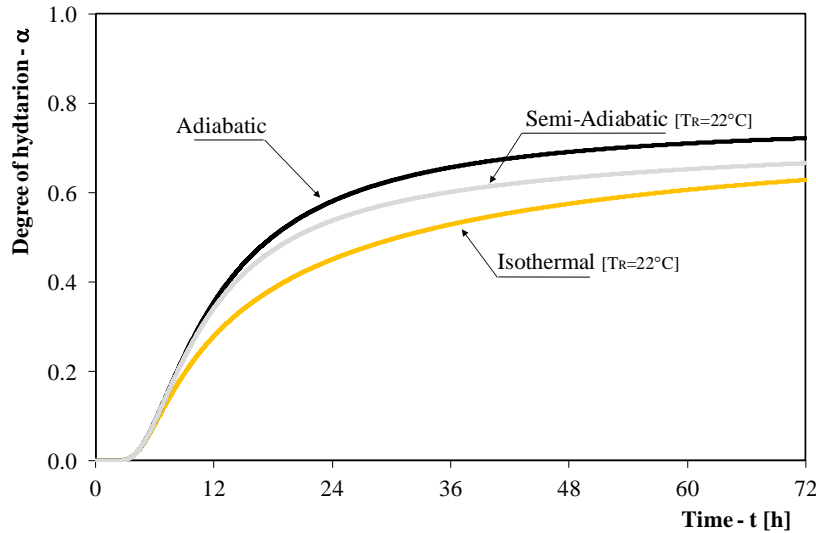


Figure 7.9: Time evolution of the degree of hydration.

The application of the proposed hydration model is based on using as input data the experimental curve of the temperature evolution of a RAC sample cured in semi-adiabatic or adiabatic conditions. The hydration model leads to determine the time evolution of the degree of hydration, while formula (6.19) defines the exiting relation between degree of hydration and cubic compressive strength. With these information, the time evolution of the cubic compressive strength of RACs can be finally obtained.

Alternatively, in the absence of temperature measurements, the compressive strength at 28 days can be determined by calculating the maximum degree of hydration through the following formulation which is available in literature (Hansen, 1986b):

$$\alpha_{\max} = \frac{1.031 \cdot \frac{w}{c_{\text{eff}}}}{0.194 + \frac{w}{c_{\text{eff}}}} \quad (7.1)$$

However, the application of the above formula (7.1) is only valid if Portland cement type I is used into the concrete mixture.

Finally, it may be worth highlighting that the formulations proposed for predicting the time evolution of the compressive strength could also be used in an inverse way, by fixing the desired concrete strength and determining the mix composition of the concrete batch. For these reasons, the proposed formulations represent a rational mix design method for recycled aggregate concretes. A schematic representation of the proposed method is drawn up in Figure 7.10.

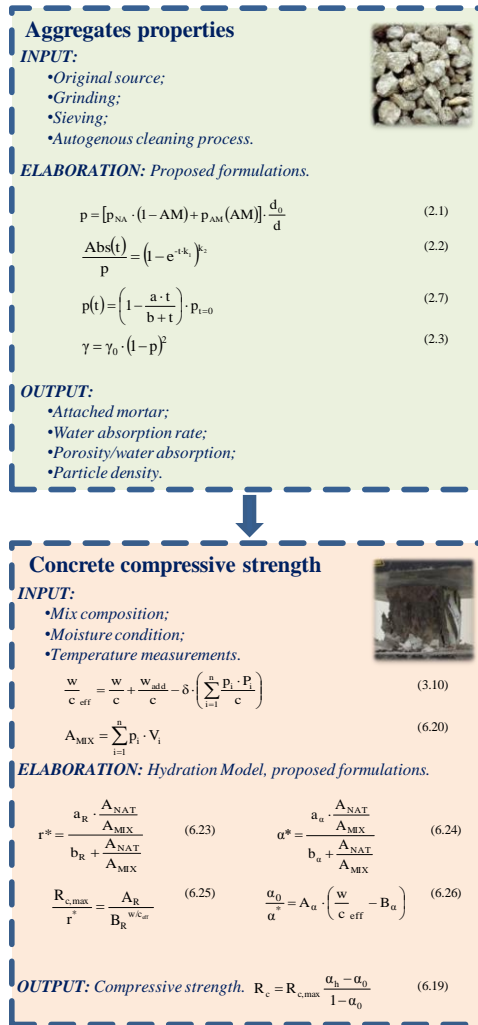


Figure 7.10: Summary of the proposed formulations.

7.2 Conclusions

This thesis proposes a rational approach to control and possibly predict the compressive strength development of concretes made with recycled concrete aggregates (RCAs) driven by the hydration reaction as a fundamental process directly affected by the concrete mixture composition and RCAs characteristics. Particularly, the following conclusions can be drawn out:

- the attached mortar content (AM) of RCAs results in higher open porosity than in NAs and, consequently, and influences properties, such as water absorption capacity and particle density;
- due to the higher porosity of RCAs, the resulting concrete performance is significantly affected by the following parameters: the initial moisture condition of RCAs, aggregates replacement ratio and water-to-cement ratio;
- the definition of an effective water-to-cement ratio was proposed to take into account the water transfer phenomena from/to coarse RCAs, whose higher porosity and water absorption capacity exhibited an enhanced influence on RACs than in ordinary concrete mixtures;
- modelling the hydration process showed a linear correlation between the concrete compressive strength and degree of hydration;
- the time evolution of the compressive strength of RACs can be estimated by considering the parameters that characterise the recycled aggregates, i.e. attached mortar as an indirect measure to identify the water absorption capacity.

Finally, it may be worth highlighting that, although the proposed conceptual formulation are nonetheless based on a firm experimental basis, a wider set of experimental results is needed to confirm its applicability to RAC mixtures with variable composition and constituents properties.

7.3 Future developments

Even if remarkable results are achieved in this thesis for predicting the mechanical behaviour of structural concrete made out with recycled concrete aggregates, further aspects should be investigated for the reliable use of RCAs in concrete.

First, further modelling work is necessary for defining completely the mechanical behaviour of RACs and, particularly their stress-strain relationships. In fact, a possible schematisation already applied for composites materials (Ahmed & Jones, 1990) could be extended in the case of RACs. Particularly, the possible composite models that can be applied for RACs are schematically illustrated in

Figure 7.11. In order to use these models, it is necessary to define the mechanical behaviour of each phase that compounds the concrete composite. With this aim, the experimental campaign presented in chapter 3 aimed at unveiling the mechanical behaviour of RCAs, could be extended. Meanwhile, the cement matrix properties could be related to the time evolution of the degree of hydration, by extending the hydration model proposed in chapter 5.

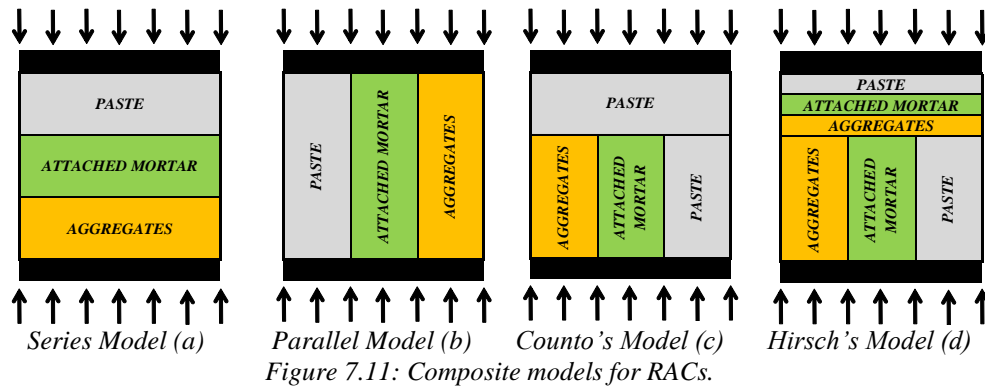


Figure 7.11: Composite models for RCAs.

moreover, since the use of RCAs modifies the free water available in the concrete mixtures, as clearly demonstrated in this thesis, further analysis are necessary in order to control also the rheology (e.g., the workability) of the resulting concrete mixtures produced with RCAs. In fact, starting from the formula (3.10) proposed in chapter 3 for the definition of the effective water-to-cement ratio, the amount of free water available in the fresh concrete mixture could be determined. Thus, a possible extension for RCAs of some models and formulations already available in literature for the case of ordinary mixtures, e.g., the Lyse's rule for workability at the fresh state (Neville, 1981), could be performed.

Finally, since the chemical and physical compositions of RCAs differ from ordinary natural aggregates, it is essential to analyse and model the effect of using durability response of RCAs.

References

- Abbas A., Fathifazl G., Isgor O.B., Razaqpur A.G., Fournier B., Foo S. (2008). Proposed method for determining the residual mortar content of recycled concrete aggregates. *Journal of ASTM International*, 5(1), 12.
- Abbas A., Fathifazl G., Fournier B., Isgor O.B., Zavadil R., Razaqpur A.G., Foo S. (2009). Quantification of the residual mortar content in recycled concrete aggregates by image analysis. *Materials characterization*, 60(7), 716-728.
- ACF (2008). *Proceedings of papers of the 3rd ACF International conference: Sustainable Concrete Technology and Structures in Local Climate and Environmental Conditions*. November 11-13, 2008, Ho Chi Minh city (Vietnam). Asian Concrete Federation.
- ACI 308R-01. *Guide to Curing Concrete*. American Concrete Institute.
- ACI 318-11. *Building Code Requirements for Structural Concrete and Commentary*. American Concrete Institute.
- ACI 408R-03. *Bond and development of straight reinforcing bars in tension*. American Concrete Institute.
- ACI 555R-01. *Removal and Reuse of Hardened Concrete*. American Concrete Institute.
- ACI E-701 (2007). Aggregates for Concrete. *ACI Education Bulletin E1-07*, , *Materials for Concrete Construction*.
- Ahmed S., Jones F.R. (1990). A review of particulate reinforcement theories for polymer composites. *Journal of Materials Science*, 25(12), 4933-4942.
- Aïtcin, P. C. (2007). *Binders for durable and sustainable concrete*. CRC Press.
- AITEC (2011). *Relazione Annuale 2010*. Associazione Italiana Tecnico Economica Cemento.
- Ajdukiewicz, A., Kliszczewicz, A. (2002). Influence of recycled aggregates on mechanical properties of HS/HPC. *Cement and concrete composites*, 24(2), 269-279.
- Alexander M., Mindess S. (2010), *Aggregates in concrete*, CRC Press.
- ASTM C1202-12. *Standard test method for electrical indication of concrete's ability to resist chloride ion penetration*. American Society for Testing and Materials.
- ASTM C127-12. *Standard test method for density, relative density (specific gravity), and absorption of coarse aggregate*. American Society for Testing and Materials.

- ASTM C128-12. *Standard test method for density, relative density (specific gravity), and absorption of fine aggregate*. American Society for Testing and Materials.
- ASTM C150/C150M-12. *Standard Specification for Portland Cement*. American Society for Testing and Materials.
- ASTM C33/C33M-13. *Standard Specification for Concrete Aggregates*. American Society for Testing and Materials.
- ASTM C496 / C496M-1. *Standard Test Method for Splitting Tensile Strength of Cylindrical Concrete Specimens*. American Society for Testing and Materials.
- ASTM C618-05. *Standard specification for coal Fly Ash and raw or calcinated natural pozzolan for use in concrete*. American Society for Testing and Materials.
- ASTM C88-13. *Standard Test Method for Soundness of Aggregates by Use of Sodium Sulfate or Magnesium Sulfate*. American Society for Testing and Materials,.
- ASTM D4404-10. *Standard Test Method for Determination of Pore Volume and Pore Volume Distribution of Soil and Rock by Mercury Intrusion Porosimetry*. American Society for Testing and Materials, USA.
- ASTM E1570-11. *Standard Practice for Computed Tomographic (CT) Examination*. American Society for Testing and Materials.
- Barreto Santos M., de Brito J., Santos Silva A. (2009). Métodos de evaluación de las reacciones álcali-sílice en hormigones con áridos reciclados. *Revista ingeniería de construcción*, 24(2), 141-152.
- Behera M., Bhattacharyya S.K., Minocha A.K., Deoliya R., Maiti S. (2014). Recycled aggregate from CD waste its use in concrete—A breakthrough towards sustainability in construction sector: A review. *Construction and building materials*, 68, 501-516.
- Belin P., Habert G., Thiery M., Roussel N. (2014). Cement paste content and water absorption of recycled concrete coarse aggregates. *Materials and Structures*, 47(9), 1451-1465.
- Beltz G. (2009). *L'impiego delle ceneri di carbone nel calcestruzzo*. ENEL ricerca. Available at www.enel.it [Accessed on 25th September 2013].
- Bentz D.P. (1997). Three-Dimensional Computer Simulation of Portland Cement Hydration and Microstructure Development. *Journal of the American Ceramic Society*, 80(1), 3-21.
- Berndt M.L. (2009). Properties of sustainable concrete containing fly ash, slag and recycled concrete aggregate. *Construction and Building Materials*, 23(7), 2606-2613.
- Bogue R.H. (1955). The chemistry of Portland cement. *Soil Science*, 79(4), 322.
- Böhmer S., Moser G., Neubauer C., Peltoniemi M., Schachermayer E., Tesar M., ... Winter B. (2008). *Aggregates case study*. Deutsch Umweltbundesamt, Germany.

- Bolomey J. (1947). The grading of aggregate and its influence on the characteristics of concrete. *Revue des Matériaux de Construction et Travaux Publiques*, 147-149.
- Brandštettr J., Polcer J., Krátký J., Holešinský R., Havlica J. (2001). Possibilities of the use of isoperibolic calorimetry for assessing the hydration behavior of cementitious systems. *Cement and Concrete Research*, 31(6), 941-947.
- BS 6187 (2011). *Code of practice for full and partial demolition*. British Standards Institution, London (UK).
- BS 8500-2. (2006). *Concrete. Complementary British Standard to BS EN 206-1. Specification for constituent materials and concrete*. British Standards Institution, London (UK).
- Bullard J.W., Jennings H.M., Livingston R.A., Nonat A., Scherer G.W., Schweitzer J.S., ... Thomas J.J. (2011). Mechanisms of cement hydration. *Cement and Concrete Research*, 41(12), 1208-1223.
- Butler L., West J.S., Tighe S.L. (2011). The effect of recycled concrete aggregate properties on the bond strength between RCA concrete and steel reinforcement. *Cement and Concrete Research*, 41(10), 1037-1049.
- Butler L. (2012). Evaluation of recycled concrete aggregate performance in structural concrete. *PhD Thesis*. University of Waterloo, Canada.
- Caggiano A., Faella C., Lima C., Martinelli E., Mele M., Pasqualini A., Valente, M. (2011). Mechanical behavior of concrete with recycled aggregate. In *2nd Workshop on "The new boundaries of structural concrete"*, Università Politecnica delle Marche-ACI Italy Chapter, Ancona (Italy) (pp. 18-16).
- CCAA (2008). *Use of Recycled Aggregates in Construction*. Cement Concrete Aggregates Australia.
- Chalmin P., Gaillochet C. (2009). From Waste to Resource. An Abstract of World Waste Survey, 2009. Paris: Cyclope and Veolia Environmental Services.
- Choong W.K., Lau T.L., Sin C.S., Ali Mohamed A. (2013). Effects of Recycled Aggregates on Water-Cement Ratio for Concrete. *Applied Mechanics and Materials*, 423, 1010-1013.
- Colleparidi M., Colleparidi S., Troli R. (2009). *Il nuovo calcestruzzo*. Tintoretto.
- Corinaldesi V., Moriconi G. (2009). Influence of mineral additions on the performance of 100% recycled aggregate concrete. *Construction and Building Materials*, 23(8), 2869-2876.
- Corinaldesi V. (2010). Mechanical and elastic behaviour of concretes made of recycled-concrete coarse aggregates. *Construction and Building Materials*, 24(9), 1616-1620.
- Corinaldesi V., Moriconi G. (2010). Recycling of rubble from building demolition for low-shrinkage concretes. *Waste management*, 30(4), 655-659.
- Crow J.M. (2008). The concrete conundrum. *Chemistry World*, 5(3), 62-66.
- CSIRO (2002). *Guide to the use of recycled concrete and masonry materials (HB 155)*. Commonwealth Scientific and Industrial Research Organisation. Standards Australia.

- D.lgs. 156/2006 Art. 185 *Norme in materia ambientale*. Gazzetta Ufficiale n. 88 del 14 aprile 2006, Italy (in Italian).
- DAfStb (1998). *Guideline of the German Committee for Reinforced Concrete*. Deutscher Ausschuss für Stahlbeton, Germany.
- D'Aloia L., Chanvillard G. (2002). Determining the “apparent” activation energy of concrete: E_a —numerical simulations of the heat of hydration of cement. *Cement and Concrete Research*, 32(8), 1277-1289.
- de Juan M.S., Gutiérrez P.A. (2004). Influence of recycled aggregate quality on concrete properties. In *Conference on use of recycled materials in building and structures* (pp. 9-11).
- de Juan M.S., Gutiérrez P.A. (2009). Study on the influence of attached mortar content on the properties of recycled concrete aggregate. *Construction and Building Materials*, 23(2), 872-877.
- de Larrard F. (1999). *Concrete mixture proportioning: a scientific approach*. CRC Press.
- de Larrard F., Sedran T. (2007). Le logiciel BétonlabPro 3. *Bulletin des laboratoires des ponts et chaussées*, (270-271), pp-75.
- De Pauw I.C. (1981). Fragmentation and recycling of reinforced concrete some research results. In *Adhesion Problems in the Recycling of Concrete* (pp. 311-319). Springer US.
- de Schutter G., Taerwe L. (1996). Degree of hydration-based description of mechanical properties of early age concrete. *Materials and Structures*, 29(6), 335-344.
- de Schutter G. (2004). Applicability of degree of hydration concept and maturity method for thermo-visco-elastic behaviour of early age concrete. *Cement and Concrete Composites*, 26(5), 437-443.
- DIN 4226-100: 2002. *Aggregates for concrete and mortar - Part100: Recycled aggregates*. Deutsches Institut für Normung, Germany.
- Domingo-Cabo A., Lázaro C., López-Gayarre F., Serrano-López M.A., Serna P., Castaño-Tabares J.O. (2009). Creep and shrinkage of recycled aggregate concrete. *Construction and Building Materials*, 23(7), 2545-2553.
- Duan Z.H., Poon C.S. (2014). Properties of recycled aggregate concrete made with recycled aggregates with different amounts of old adhered mortars. *Materials Design*, 58, 19-29.
- EC (2000). 532/200/CE. *Construction and demolition waste*. Commission Of The European Communities. Official Journal Of The European Communities.
- EC (2008). *Directive 2008/98/CE of the European Parliament and of the Council of 19 November 2008 on waste and repealing certain Directives*. Official Journal of the European Union.
- EDCW (2014). *Environmental Data Centre on Waste*. Available online at <http://epp.eurostat.ec.europa.eu/> [accessed on 01/09/2014].
- EEA (2007). *Europe's environment - The fourth assessment*. European Environment Agency. Available at www.eea.europa.eu [Accessed on 31st January 2015].

- EN 1097-6:2013. *Tests for mechanical and physical properties of aggregates - Part 6: Determination of particle density and water absorption*. CEN, European Committee for Standardization.
- EN 12350-2:2009. *Testing fresh concrete - Part 2: Slump-test*. CEN, European Committee for Standardization.
- EN 12390-3:2009. *Testing hardened concrete - Part 3: Compressive strength of test specimens*. CEN, European Committee for Standardization.
- EN 12390-6:2009. *Testing hardened concrete – Part 6: Tensile splitting strength of test specimens*. CEN, European Committee for Standardization
- EN 12390-8:2009. *Testing hardened concrete - Part 8: Depth of penetration of water under pressure*. CEN, European Committee for Standardization.
- EN 12620:2013. *Aggregates for concrete*. CEN, European Committee for Standardization.
- EN 13242:2013. *Aggregates for unbound and hydraulically bound materials for use in civil engineering work and road construction*. CEN, European Committee for Standardization.
- EN 197-1:2011. *Cement - Part 1: Composition, specifications and conformity criteria for common cements*. CEN, European Committee for Standardization.
- EN 1992-1-1:2004. *Eurocode 2: Design of concrete structures - Part 1-1: General rules and rules for buildings*. CEN, European Committee for Standardization.
- EN 206:2013. *Concrete. Specification, performance, production and conformity*. CEN, European Committee for Standardization.
- EN 450-1:2012. *Fly ash for concrete. Definition, specifications and conformity criteria*. European Committee for Standardization.
- Etxeberria M., Vázquez E., Marí A., Barra M. (2007). Influence of amount of recycled coarse aggregates and production process on properties of recycled aggregate concrete. *Cement and concrete research*, 37(5), 735-742.
- Evangelista L., de Brito J. (2007). Mechanical behaviour of concrete made with fine recycled concrete aggregates. *Cement and Concrete Composites*, 29(5), 397-401.
- Faella C., Martinelli E., Nigro E. (2009). Direct versus indirect method for identifying FRP-to-concrete interface relationships. *Journal of Composites for Construction*, 13(3), 226-233.
- Fathifazl G.(2008). Structural performance of steel reinforced recycled concrete members. *PhD Thesis*. University of Ottawa, Canada.
- Fathifazl G., Abbas A., Razaqpur A.G., Isgor O.B., Fournier B., Foo S. (2009). New mixture proportioning method for concrete made with coarse recycled concrete aggregate. *Journal of materials in civil engineering*, 21(10), 601-611.
- Feng X., Garboczi E.J., Bentz D.P., Stutzman P.E., Mason T.O. (2004). Estimation of the degree of hydration of blended cement pastes by a scanning electron microscope point-counting procedure. *Cement and Concrete Research*, 34(10), 1787-1793.
- Feret R. (1892). On the compactness of the mortars. In *Annales des Ponts et Chaussées, Série*, 7(4), 5-164.

- fib (2013). *Model Code for Concrete Structures 2010*. fédération international du beton. Ernst Sohn Verlag, Berlin, Germany.
- Fischer C., Werge M. (2009). *EU as a Recycling Society: present recycling levels of municipal waste and construction demolition waste in the EU. ETC*. SCP working paper 2/2009. European Topic Centre on Sustainable Consumption and Production, Copenhagen.
- Florea M.V.A., Brouwers H.J.H. (2013). Properties of various size fractions of crushed concrete related to process conditions and re-use. *Cement and Concrete Research*, 52, 11-21.
- Folino P., Xargay H. (2014). Recycled aggregate concrete–Mechanical behavior under uniaxial and triaxial compression. *Construction and Building Materials*, 56, 21-31.
- Fonseca N., de Brito J., Evangelista L. (2011). The influence of curing conditions on the mechanical performance of concrete made with recycled concrete waste. *Cement and Concrete Composites*, 33(6), 637-643.
- Fuller W.B., Thompson S.E. (1906). The laws of proportioning concrete. *Transactions of the American Society of Civil Engineers*, 57(2), 67-143.
- Glanville W.H., Collins A.R., Matthews D.D. (1947). *The grading of aggregates and workability of concrete*. HM Stationery Office.
- Gokce A., Nagataki S., Saeki T., Hisada M. (2004). Freezing and thawing resistance of air-entrained concrete incorporating recycled coarse aggregate: The role of air content in demolished concrete. *Cement and Concrete Research*, 34(5), 799-806.
- Gomez-Soberon J.M. (2002). Porosity of recycled concrete with substitution of recycled concrete aggregate: an experimental study. *Cement and concrete research*, 32(8), 1301-1311.
- González-Fonteboa B., Martínez-Abella F., Eiras-López J., Seara-Paz S. (2011). Effect of recycled coarse aggregate on damage of recycled concrete. *Materials and structures*, 44(10), 1759-1771.
- Guedes M., Evangelista L., de Brito J., Ferro A.C. (2013). Microstructural characterization of concrete prepared with recycled aggregates. *Microscopy and Microanalysis*, 19(05), 1222-1230.
- Gutsch A., Rostasy F.S. (1994). Young concrete under high tensile stresses –Creep, Relaxation and Cracking. *Proceedings of the RILEM Symp. Thermal Cracking in Concrete at Early Ages*, Munich, 111-118.
- Gutsch A.W. (2002). Properties of early age concrete-Experiments and modelling. *Materials and Structures*, 35(2), 76-79.
- Han N. (2005). Maturity method, in *Advanced Testing of Cement-Based Materials during Setting and Hardening. Final Report of RILEM TC 185-ATC*, Editors Reinhardt H.W. and Grosse C.U., RILEM Publications SARL, 277-296.
- Hansen P.F., Pedersen E.J. (1977). *Maturity computer for controlled curing and hardening of concrete*.

- Hansen T.C. (1986a). Recycled aggregates and recycled aggregate concrete second state-of-the-art report developments 1945–1985. *Materials and structures*, 19(3), 201-246.
- Hansen, T.C. (1986b). Physical structure of hardened cement paste. A classical approach. *Materials and Structures*, 19(6), 423-436.
- Hansen T.C., Narud H. (1983). Strength of recycled concrete made from crushed concrete coarse aggregate. *Concrete International*, 5(1), 79-83.
- Hansen T.C. (1992). Recycling of demolition concrete and masonry. *RILEM Report*, 6. CRC Press.
- HKBD (2004). *Code of practice for demolition of buildings*. Hong Kong Buildings Department.
- HKBD (2009). *Use of Recycled Aggregates in Concrete*. Hong Kong Buildings Department.
- IEA (2011). *CO₂ Emissions from Fuel Combustion 2011 Edition*. International Energy Agency.
- Isaia G.C., Gastaldini A.L.G., Moraes R. (2003). Physical and pozzolanic action of mineral additions on the mechanical strength of high-performance concrete. *Cement and concrete composites*, 25(1), 69-76.
- James M.N., Choi W., Abu-Lebdeh T. (2011). Use of recycled aggregate and fly ash in concrete pavement. *Am. J. Eng. Applied Sci*, 4, 201-208.
- Jeong J.H., Zollinger D.G. (2006). Finite-element modeling and calibration of temperature prediction of hydrating Portland cement concrete pavements. *Journal of materials in civil engineering*, 18(3), 317-324.
- Kada-Benameur H., Wirquin E., Duthoit B. (2000). Determination of apparent activation energy of concrete by isothermal calorimetry. *Cement and concrete research*, 30(2), 301-305.
- Katz A. (2003). Properties of concrete made with recycled aggregate from partially hydrated old concrete. *Cement and concrete research*, 33(5), 703-711.
- Khalaf F.M., DeVenny A.S. (2004). Recycling of demolished masonry rubble as coarse aggregate in concrete: review. *Journal of materials in civil engineering*, 16(4), 331-340.
- Koenders E.A.B. (1997). Simulation of Volume Changes in Hardening Cement-Based Materials. *Ph.D. Thesis*, Delft University of Technology (The Netherlands).
- Koenders E.A.B. (2005). Mix Design for Venice Barriers. *Report Nr. 15.5-05-08*, Confidential communication.
- Koenders E.A., Pepe M., Martinelli E. (2014). Compressive strength and hydration processes of concrete with recycled aggregates. *Cement and Concrete Research*, 56, 203-212.
- Kou S.C., Poon C.S., Chan, D. (2004). Properties of steam cured recycled aggregate fly ash concrete. In *International RILEM conference on the use of recycled materials in buildings and structures, Barcelona* (pp. 590-599).

- Kou S.C., Poon C.S., Chan D. (2007). Influence of fly ash as cement replacement on the properties of recycled aggregate concrete. *Journal of Materials in Civil Engineering*, 19(9), 709-717.
- Kou S.C., Poon C.S., Chan D. (2008). Influence of fly ash as a cement addition on the hardened properties of recycled aggregate concrete. *Materials and Structures*, 41(7), 1191-1201.
- Kou S.C., Poon, C.S. (2013). Long-term mechanical and durability properties of recycled aggregate concrete prepared with the incorporation of fly ash. *Cement and Concrete Composites*, 37, 12-19.
- Kwan W.H., Ramli M., Kam K.J., Sulieman M.Z. (2012). Influence of the amount of recycled coarse aggregate in concrete design and durability properties. *Construction and Building Materials*, 26(1), 565-573.
- Laube M. (1991). Werkstoffmodell zur Berechnung von Temperaturspannungen in massigen Betonbauteilen im jungem Alter. *PhD-thesis*, Braunschweig (Germany).
- Legambiente (2011). *Rapporto Cave 2011 – I numeri, il quadro normative, il punto sull'impatto economico e ambientale dell'attività estrattiva nel territorio italiano*.
- Levy S.M., Helene P. (2004). Durability of recycled aggregates concrete: a safe way to sustainable development. *Cement and concrete research*, 34(11), 1975-1980.
- Li X. (2008). Recycling and reuse of waste concrete in China: Part I. Material behaviour of recycled aggregate concrete. *Resources, Conservation and Recycling*, 53(1), 36-44.
- Lilliu G., van Mier, J. G. (2003). 3D lattice type fracture model for concrete. *Engineering Fracture Mechanics*, 70(7), 927-941.
- Lima C., Caggiano A., Faella C., Martinelli E., Pepe M., Realfonzo R. (2013). Physical properties and mechanical behaviour of concrete made with recycled aggregates and fly ash. *Construction and Building Materials*, 47, 547-559.
- Limbachiya M.C., Leelawat T., Dhir R.K. (2000). Use of recycled concrete aggregate in high-strength concrete. *Materials and structures*, 33(9), 574-580.
- Limbachiya M., Meddah M.S., Ouchagour Y. (2012). Use of recycled concrete aggregate in fly-ash concrete. *Construction and Building Materials*, 27(1), 439-449.
- Lin Y.H., Tyan Y.Y., Chang, T. P., Chang, C. Y. (2004). An assessment of optimal mixture for concrete made with recycled concrete aggregates. *Cement and concrete research*, 34(8), 1373-1380.
- Liu Q., Xiao J., Sun Z. (2011). Experimental study on the failure mechanism of recycled concrete. *Cement and Concrete Research*, 41(10), 1050-1057.
- Livesey P., Donnelly A., Tomlinson C. (1991). Measurement of the heat of hydration of cement, *Cement and Concrete Composites*, 13(3) 177-185.
- Lokhorst S.J. (1999), Deformation behavior of concrete influenced by hydration related changes of the microstructure. *Internal Report Nr. 5-99-05*, Delft University of Technology (The Netherlands).

- López-Gayarre F., Serna P., Domingo-Cabo A., Serrano-López M.A., López-Colina C. (2009). Influence of recycled aggregate quality and proportioning criteria on recycled concrete properties. *Waste Management*, 29(12), 3022-3028.
- LS-614 (2001). *Freezing and Thawing of Coarse Aggregate*. Ministry of Transportation, Ontario, Canada.
- Luz A., Almeida S. (2012). Manual de Agregados para a Construção Civil–2ª edição. *Centro de Tecnologia Mineral–CETEM. Rio de Janeiro*. (in Portuguese).
- Malešev M., Radonjanin V., Marinković S. (2010). Recycled concrete as aggregate for structural concrete production. *Sustainability*, 2(5), 1204-1225.
- Martinelli E., Koenders E.A., Caggiano A. (2013). A numerical recipe for modelling hydration and heat flow in hardening concrete. *Cement and Concrete Composites*, 40, 48-58.
- Mazaheripour H., Barros J.A., Sena-Cruz J.M., Pepe M., Martinelli E. (2013). Experimental study on bond performance of GFRP bars in self-compacting steel fiber reinforced concrete. *Composite Structures*, 95, 202-212.
- McNeil K., Kang T.H.K. (2013). Recycled concrete aggregates: A review. *International Journal of Concrete Structures and Materials*, 7(1), 61-69.
- Mefteh H., Kebaïli O., Oucief H., Berredjem L., Arabi N. (2013). Influence of moisture conditioning of recycled aggregates on the properties of fresh and hardened concrete. *Journal of Cleaner Production*, 54, 282-288.
- Mehta P.K. (1986). *Concrete. Structure, properties and materials*.
- Meyer C. (2009). The greening of the concrete industry. *Cement and Concrete Composites*, 31(8), 601-605.
- Movassaghi R. (2006). Durability of reinforced concrete incorporating recycled concrete as aggregate (RCA).
- Müller N., Harnisch J. (2008). *A blueprint for a climate friendly cement industry*. Report for the WWF–Lafarge Conservation Partnership. Gland, Switzerland.
- Nagataki S., Gokce A., Saeki T., Hisada M. (2004). Assessment of recycling process induced damage sensitivity of recycled concrete aggregates. *Cement and concrete research*, 34(6), 965-971.
- Naik T.R. (2005). Sustainability of cement and concrete industries. In *Proceedings of the International Conference on Achieving Sustainability in Construction*, 141-150.
- Narasimhan T.N. (1999). Fourier's heat conduction equation: History, influence, and connections. *Reviews of Geophysics*, 37(1), 151-172.
- Nassar R.U.D., Soroushian, P. (2012). Strength and durability of recycled aggregate concrete containing milled glass as partial replacement for cement. *Construction and Building Materials*, 29, 368-377.
- NBR 5733:1991. *High early strength Portland cement – Specification*. ABNT, Associação Brasileira de Normas Técnicas.
- NBR 5739:2007. *Concrete - Compression test of cylindrical specimens - method of test*. ABNT, Associação Brasileira de Normas Técnicas.

- NBR 8522:2008. *Concrete - Determination of the elasticity modulus by compression*. ABNT, Associação Brasileira de Normas Técnicas.
- NBR NM 248:2003. *Aggregates - Sieve analysis of fine and coarse aggregates*. ABNT, Associação Brasileira de Normas Técnicas.
- NBR NM 53:2009. *Coarse aggregate - Determination of the bulk specific gravity, apparent specific gravity and water absorption*. ABNT, Associação Brasileira de Normas Técnicas.
- Neville A.M. (1981). *Properties of concrete*.
- NRMCA (2008). *Specifying Fly Ash for Use in Concrete*. National Ready Mixed Concrete Association.
- NTC (2008). *DM 14.01. 2008: Norme Tecniche per le Costruzioni*. Italian Ministry of Infrastructures and Transportation (in Italian).
- Padmini A.K., Ramamurthy K., Mathews M.S. (2009). Influence of parent concrete on the properties of recycled aggregate concrete. *Construction and Building Materials*, 23(2), 829-836.
- Pane I., Hansen W. (2005). Investigation of blended cement hydration by isothermal calorimetry and thermal analysis. *Cement and concrete research*, 35(6), 1155-1164.
- Pepe M., Toledo Filho R.D., Koenders E.A., Martinelli, E. (2014). Alternative processing procedures for recycled aggregates in structural concrete. *Construction and Building Materials*, 69, 124-132.
- Poon C.S., Shui Z.H., Lam L., Fok H., Kou, S.C. (2004a). Influence of moisture states of natural and recycled aggregates on the slump and compressive strength of concrete. *Cement and Concrete Research*, 34(1), 31-36.
- Poon C.S., Shui Z.H., Lam L. (2004b). Effect of microstructure of ITZ on compressive strength of concrete prepared with recycled aggregates. *Construction and Building Materials*, 18(6), 461-468.
- Qian Z., Schlangen E., Ye G., van Breugel K. (2011). 3D lattice fracture model: theory and computer implementation. *Key Engineering Materials*, 452, 69-72.
- Quist J. (2012). Cone crusher modelling and simulation. *Master of Science Thesis*. Chalemer University of Technology, Göteborg, Sweden.
- Ravindrarajah R.S., Tam C.T. (1985). Properties of concrete made with crushed concrete as coarse aggregate. *Magazine of Concrete Research*, 37(130), 29-38.
- RILEM (1994a). Specification for concrete with recycled aggregates. *Materials and Structures*, 27(173), 557.
- RILEM (1994b). *Bond Test for Reinforcing Steel. 2. Pull-Out Test*. Recommendations for the Testing and Use of Constructions Materials.
- RRL (1950). *Design of Concrete mixes*. Road Research Laboratory, London (UK).
- Ryu J.S. (2002). An experimental study on the effect of recycled aggregate on concrete properties. *Magazine of Concrete Research*, 54(1), 7-12.
- Sagoe-Crentsil K.K., Brown T., Taylor A.H. (2001). Performance of concrete made with commercially produced coarse recycled concrete aggregate. *Cement and concrete research*, 31(5), 707-712.

- Sakai K. (2005). Environmental design for concrete structures. *Journal of Advanced Concrete Technology*, 3(1), 17-28.
- Schindler A.K., Folliard K.J. (2005). Heat of hydration models for cementitious materials. *ACI Materials Journal*, 102(1), 24-33.
- Schlangen E., Van Mier J.G.M. (1992). Simple lattice model for numerical simulation of fracture of concrete materials and structures. *Materials and Structures*, 25(9), 534-542.
- Schlangen E., Garboczi, E.J. (1997). Fracture simulations of concrete using lattice models: computational aspects. *Engineering fracture mechanics*, 57(2), 319-332.
- Schneider M., Romer M., Tschudin M., Bolio H. (2011). Sustainable cement production—present and future. *Cement and Concrete Research*, 41(7), 642-650.
- Scrivener K.L., Crumbie A.K., Laugesen P. (2004). The interfacial transition zone (ITZ) between cement paste and aggregate in concrete. *Interface Science*, 12(4), 411-421.
- Sedran T., de Larrard F. (1994). RENE-LCPC—Un logiciel pour optimiser la granularité des matériaux de Génie Civil. *Bulletin des Laboratoires des Ponts et Chaussées*, 194, 87-93.
- Silva R.V., de Brito J., Dhir R.K. (2014). Properties and composition of recycled aggregates from construction and demolition waste suitable for concrete production. *Construction and Building Materials*, 65, 201-217.
- Sim J., Park C. (2011). Compressive strength and resistance to chloride ion penetration and carbonation of recycled aggregate concrete with varying amount of fly ash and fine recycled aggregate. *Waste management*, 31(11), 2352-2360.
- Stovall T., de Larrard F., Buil M. (1986). Linear packing density model of grain mixtures. *Powder Technology*, 48(1), 1-12.
- Struble L., Skalny J., Mindess S. (1980). A review of the cement-aggregate bond. *Cement and Concrete Research*, 10(2), 277-286.
- Tam V.W., Gao X.F., Tam C.M. (2005). Microstructural analysis of recycled aggregate concrete produced from two-stage mixing approach. *Cement and Concrete Research*, 35(6), 1195-1203.
- Tavakoli M., Soroushian P. (1996). Strengths of recycled aggregate concrete made using field-demolished concrete as aggregate. *ACI Materials Journal*, 93(2).
- Tavares L.M. (2007). Breakage of single particles: quasi-static. *Handbook of powder technology*, 12, 3-68.
- Thomas C., Setién J., Polanco J.A., Alaejos P., de Juan M.S. (2013). Durability of recycled aggregate concrete. *Construction and Building Materials*, 40, 1054-1065.
- Toledo Filho R.D., Koenders E., Pepe M., Cordeiro G.C., Fairbairn E., Martinelli E. (2013). Rio 2016 sustainable construction commitments lead to new developments in recycled aggregate concrete. In *Proceedings of the ICE-Civil Engineering* (Vol. 166, No. 6, pp. 28-35). Thomas Telford.

- Tu T.Y., Chen Y.Y., Hwang C.L. (2006). Properties of HPC with recycled aggregates. *Cement and Concrete Research*, 36(5), 943-950.
- USGS (2011). *USGS Mineral Program Cement Report*. United States Geological Survey, USA.
- Valente M., Bressan M., Pasqualini A., Liberatore F.M, Vivaldi S. (2011). Fattori di efficienza k della cenere volante relativi alla penetrazione dei cloruri ed alla permeabilità all'acqua nell'ottica dell'incremento della vita utile delle strutture in C.A. *General Admixtures s.p.a. Studi e Ricerche*. Available at www.gageneral.com [Accessed on 1st March 2012].
- van Breugel K. (1991). Simulation of hydration and formation of structure in hardening cement-based materials. *Ph.D. Thesis*, Delft University of Technology (The Netherlands).
- van Breugel, K. (2004). Concrete structures under temperature and shrinkage deformations. *Lecture notes CT5120*, Delft University of Technology, The Netherlands.
- Van Kan J., Segal A., Vermolen F. (2008). Numerical Methods in Scientific Computing. Department of Applied Mathematics, Delft University of Technology, The Netherlands.
- Voglis N., Kakali G., Chaniotakis E., Tsivilis S. (2005). Portland-limestone cements. Their properties and hydration compared to those of other composite cements. *Cement and Concrete Composites*, 27(2), 191-196.
- Wang X.Y., Lee H.S., Park K.B., Kim J.J., Golden, J. S. (2010). A multi-phase kinetic model to simulate hydration of slag-cement blends. *Cement and Concrete Composites*, 32(6), 468-477.
- Washington Post (2009). *The Climate Agenda – Global Emissions*. USA.
- WBCSD (2012). *The Cement Sustainability Initiative Progress Report*. World Business Council For Sustainable Development.
- www.basf-cc.com.br [Accessed on 2nd April 2014].
- www.boeingitaly.it [Accessed on 24th September 2014].
- www.vegedry.com.br [Accessed on 21st May 2014].
- Xiao J., Li J., Zhang C. (2005). Mechanical properties of recycled aggregate concrete under uniaxial loading. *Cement and concrete research*, 35(6), 1187-1194.
- Yang K.H., Chung H.S., Ashour A.F. (2008). Influence of type and replacement level of recycled aggregates on concrete properties. *ACI Materials Journal*, 105(3).
- Yong P.C., Teo D.C.L. (2009). Utilisation of recycled aggregate as coarse aggregate in concrete. *UNIMAS E-Journal of civil engineering*, 1(1), 1-6.
- Zhang M.H., Gjørsv O.E. (1991). Permeability of high-strength lightweight concrete. *ACI Materials Journal*, 88(5).